UNIVERSITAT POLITÈCNICA DE VALÈNCIA

Toxicological assessment of silica particles functionalised with essential oil components and their constituents

Doctoral Thesis presented by:
Cristina Fuentes López

Supervised by:
José Manuel Barat Baviera
María José Ruiz Leal
Ana Fuentes López

Valencia, December 2021

José Manuel Barat Baviera, PhD in Food Technology and Professor at the *Universitat Politècnica de València*, **María José Ruiz Leal**, PhD in Pharmacy and Professor at the *Universitat de València*, and **Ana Fuentes López,** PhD in Food Technology and Lecturer at the *Universitat Politècnica de València*

CERTIFY:

That the work **"Toxicological assessment of silica particles functionalised with essential oil components and their constituents"** has been developed by Cristina Fuentes López under their supervision in the Food Technology Department of the *Universitat Politècnica de València* and the Laboratory of Toxicology of *the Universitat de València*, and is eligible to be defended by its author for opting for the PhD degree in Biotechnology at the *Universitat Politècnica de València*

Valencia, December 2021

José Manuel Barat Baviera María José Ruiz Leal Ana Fuentes López

Acknowledgements

Agradecimientos

En primer lugar, quiero agradecer a mis directores todo el apoyo recibido durante el desarrollo de esta tesis. A José Manuel Barat, por darme la oportunidad de formar parte de su grupo de investigación y de llevar a cabo en él la tesis doctoral. A María José Ruiz, por acogerme como una más de su grupo y estar siempre dispuesta a enseñarme y ayudarme en todo lo que he necesitado. A Ana, nunca te agradeceré suficiente todo tu esfuerzo y dedicación, gracias por ayudarme en todo siempre desde siempre.

A todos los investigadores y compañeros con los que he compartido este periodo: Ana, Alberto, Alejandro, Arantxa, Cris, Damián, David, Édgar, Esteban, Francisco, Héctor, Marta, María, Mila, Nataly, Patri, Raúl, Samu, Sergio, Susana… gracias por vuestro apoyo y compañía a lo largo de estos años. Gracias Isa por tu ayuda incondicional tanto en lo científico como en lo personal, es una suerte para mí poder tener cerca a alguien como tú. Muchas gracias Eli y Sara, por ayudarme tanto de una forma tan generosa cuando lo he necesitado, os estaré siempre agradecida.

Gracias al Laboratorio de Toxicología de la Facultad de Farmacia de la Universidad de Valencia por su cálido acogimiento, en especial a Vero y Mercedes, muchas gracias por vuestra amabilidad y generosidad infinita, vuestra ayuda ha sido incalculable para mí.

Thanks to Prof. Hugh J. Byrne for receiving me in the FOCAS Research Institute from the Technological University of Dublin during my stay. Thank you for your time and support, it was such an honor for me to meet such an exceptional researcher. Many thanks to all lab members too, Qasim, Aseez, Awatif, Mahmud, Francesca… for helping me in so honest and generous way.

Gracias a mis amigos, en especial a los que mejor habéis comprendido lo que significa pasar por esto. Gracias a los *despojos biotecnológicos*: Alberto, Elena, Jose, Merche, Julia, Pablo y Sara. A todos gracias por vuestra ayuda y

ánimo y por los momentos tan divertidos que he pasado con vosotros. Es una suerte haberos conocido.

A Nacho y mi familia, por vuestro cariño y apoyo incondicional, por vuestro espíritu crítico, por ser capaces de ir a la contra, por ser lo mejor.

Abstract

Functionalisation of silica particles with essential oils components (EOCs) has emerged as a useful tool for enhancing EOCs' antimicrobial activity and stability. Given these new materials' promising applications for the food industry, toxicological studies must be performed to identify possible hazards for human health. In the present doctoral thesis, the potential risk deriving from oral exposure to three types of silica particles (SAS, MCM-41 microparticles, MCM-41 nanoparticles) functionalised with four different EOCs (carvacrol, eugenol, thymol, vanillin) was investigated and compared to free EOCs and pristine particles. For this purpose, three different replacement methods were used as a strategy to carry out the toxicological assessment of these new materials: simulated physiological conditions, HepG2 culture cells and the non-mammalian organism model *Caenorhabditis elegans*.

As the expected human exposure to these materials was the oral route, the first step in the toxicological assessment of the silica particles was to study their degradation behaviour in acellular physiological fluids that mimic oral exposure conditions. The results showed that functionalisation of silica with EOCs increases particles' biodurability under conditions representing the human gastrointestinal tract and lysosomal fluid, as observed by both, the lower dissolution rates in the different functionalised particle types and the preservation of the EOCs-functionalised MCM-41 nanoparticles structure. However, the agglomeration state of the particles did not change under the physiological conditions, which remained within the micro-sized range in all cases. Therefore, given their large size, these materials present a low risk of accumulation after oral ingestion.

The *in vitro* toxicity study showed that the EOCs-functionalised particles displayed stronger cytotoxic effect than the free EOCs and pristine silica.

Independently of EOC type, the EOCs-functionalised MCM-41 microparticles were the most cytotoxic materials from the different silica particle types analysed. Our results suggest that the EOCs-functionalised particles induce toxicity on HepG2 cells by an oxidative stress-related mechanism that causes mitochondrial dysfunction and apoptosis activation via the mitochondrial pathway. This cytotoxic effect was caused by direct cell-particle interactions, and not by degradation products released to culture media.

Acute exposure to moderate and high concentrations of EOCs reduced HepG2 viability and nematode survival. The toxicity ranking was maintained between culture cells and nematodes, being carvacrol the most toxic compound followed by thymol, eugenol, and lastly by vanillin. Moreover, sublethal concentrations to these components induced reproductive toxicity in *C. elegans*, which suggests that they may present toxic effects at the concentrations required for their bioactive properties.

The *in vivo* toxicity study of the particles showed that both the bare and EOCs-functionalised particles cause acute reproductive toxicity and inhibition in nematode growth and reproduction after long-term exposure. The vanillin-functionalised particles displayed milder acute toxic effects, but severer long-term exposure toxicological responses. However, the eugenol-functionalised particles exhibited stronger effects than the bare and vanillin-functionalised silica.

According to both, the *in vitro* and *in vivo* assays, the type of EOC anchored to silica surfaces and the functionalisation yield were the most important factors to determine the toxicological effects of these new antimicrobial systems. Alternatives to synthetic preservatives for food applications are not free from potential toxicological hazards and thus, toxicity

studies are necessary for the understanding of the interactions of new materials with biological systems and to guarantee their safety for human health.

Resumen

La funcionalización de partículas de sílice con componentes de aceites esenciales (EOCs) se ha propuesto como una estrategia prometedora para mejorar la actividad antimicrobiana y la estabilidad de estos compuestos. Sin embargo, debido a la potencial aplicación de estas partículas en la industria alimentaria, es necesario llevar a cabo estudios toxicológicos que permitan identificar los posibles efectos sobre la salud que puede conllevar el uso de estos nuevos materiales. En esta tesis doctoral, se ha evaluado el riesgo derivado de la exposición oral a tres tipos de partículas de sílice (SAS, micropartículas MCM-41 y nanopartículas MCM-41) funcionalizadas con cuatro tipos de EOCs (carvacrol, eugenol, timol y vainillina) y se ha comparado con el efecto de los EOCs libres y las partículas sin funcionalizar. La evaluación toxicológica de estos nuevos materiales se llevó a cabo a través de una estrategia formada por 3 tipos de estudios diferentes como son: la simulación de condiciones fisiológicas, el uso de la línea celular HepG2 y el organismo modelo *Caenorhabditis elegans*.

El primer paso en la evaluación toxicológica de las partículas consistió en estudiar su estabilidad en fluidos fisiológicos que simulan las condiciones de exposición por vía oral. Los resultados mostraron que la funcionalización con EOCs aumenta la biodurabilidad de las partículas en condiciones que representan el tracto gastrointestinal humano y el fluido lisosomal, como se observa tanto por la menor disolución de los diferentes tipos de partículas funcionalizadas como por la conservación de la estructura de las nanopartículas MCM-41. Sin embargo, el estado de aglomeración de las partículas no cambió en condiciones fisiológicas, y todas ellas se mantuvieron dentro del rango de tamaño de las micropartículas. Por tanto, dado su gran tamaño, estos materiales presentan un bajo riesgo de acumulación tras ingestión oral.

El estudio *in vitro* de la toxicidad de los materiales demostró que las partículas funcionalizadas con EOCs presentan un efecto citotóxico mayor que los EOCs libres y la sílice sin funcionalizar. Además, independientemente del tipo de EOC, las micropartículas MCM-41 funcionalizadas fueron los materiales más citotóxicos. Los resultados sugieren que las partículas funcionalizadas con EOCs inducen toxicidad en las células HepG2 mediante un mecanismo relacionado con el estrés oxidativo, el cual provoca daño mitocondrial y la consecuente activación de procesos de apoptosis. Por otra parte, se demostró que este efecto citotóxico está causado por interacciones directas entre las células y las partículas, y no por productos de degradación liberados al medio de cultivo.

La exposición aguda a concentraciones moderadas y altas de EOCs redujo la viabilidad de las células HepG2 y la supervivencia de *C. elegans*. La jerarquía de la toxicidad se mantuvo entre células y nemátodos, siendo el carvacrol el compuesto más tóxico, seguido del timol, el eugenol y, por último, la vainillina. Además, concentraciones subletales de estos componentes indujeron toxicidad reproductiva en *C. elegans*, lo que sugiere que pueden presentar efectos tóxicos a las concentraciones requeridas para ejercer sus propiedades bioactivas.

El estudio *in vivo* de la toxicidad de las partículas mostró que tanto las partículas sin funcionalizar como las funcionalizadas con eugenol causan toxicidad reproductiva en *C. elegans* tras la exposición aguda, e inhibición en el crecimiento y la reproducción de los nematodos tras la exposición a largo plazo. Las partículas funcionalizadas con vainillina mostraron efectos tóxicos agudos leves, pero un mayor efecto tras la exposición a largo plazo. En líneas generales, los resultados obtenidos muestran que las partículas funcionalizadas con eugenol presentan mayores efectos sobre *C. elegans* que la sílice sin funcionalizar y las partículas funcionalizadas con vainillina.

De acuerdo con los resultados obtenidos tanto en los ensayos *in vitro* como *in vivo*, los principales factores que determinan los efectos toxicológicos de estos nuevos sistemas antimicrobianos son; el tipo de EOC inmovilizado en la superficie de las partículas de sílice y el rendimiento de la reacción de funcionalización. Las alternativas a los conservantes sintéticos en aplicaciones de la industria alimentaria no están exentas de posibles riesgos toxicológicos, por lo que es necesario llevar a cabo estudios de toxicidad exhaustivos que permitan comprender las interacciones de los nuevos materiales con los sistemas biológicos y garantizar así su seguridad para la salud humana.

Resum

La funcionalització de partícules de sílice amb components d'olis essencials (EOCs) s'ha proposat com una estratègia prometedora per a millorar l'activitat antimicrobiana i l'estabilitat d'aquests compostos. No obstant això, a causa de la potencial aplicació d'aquestes partícules en la indústria alimentària, és necessari dur a terme estudis toxicològics que permeten identificar els possibles efectes sobre la salut que pot comportar l'ús d'aquests nous materials. En aquesta tesi doctoral, s'ha avaluat el risc derivat de l'exposició oral a tres tipus de partícules de sílice (SAS, micropartícules MCM-41 i nanopartícules MCM-41) funcionalitzades amb quatre tipus de EOCs diferents (carvacrol, eugenol, timol i vanil·lina) i s'ha comparat amb l'efecte dels EOCs lliures i les partícules sense funcionalitzar. L'avaluació toxicològica d'aquests nous materials es va dur a terme a través d'una estratègia formada per 3 tipus d'estudis diferents com són la simulació de condicions fisiològiques, l'ús de la línia cel·lular HepG2 i l'organisme model *Caenorhabditis elegans*.

El primer pas en l'avaluació toxicològica de les partícules va consistir a estudiar la seua estabilitat en fluids fisiològics que simulen les condicions d'exposició per via oral. Els resultats van mostrar que la funcionalització amb EOCs augmenta la biodurabilidad de les partícules en condicions que representen el tracte gastrointestinal humà i el fluid lisosomal, com s'observa tant per la menor dissolució dels diferents tipus de partícules funcionalitzades com per la conservació de l'estructura de les nanopartícules MCM-41. No obstant això, l'estat d'aglomeració de les partícules no va canviar en condicions fisiològiques, i totes elles es van mantindre dins del rang de grandària de les micropartícules. Per tant, donat la seua grandària, aquests materials presenten un baix risc d'acumulació rere ingestió oral.

L'estudi *in vitro* de la toxicitat dels materials va demostrar que les partícules funcionalitzades amb EOCs presenten un efecte citotòxic major que els EOCs lliures i la sílice sense funcionalitzar. A més, independentment del tipus d'EOC, les micropartícules MCM-41 funcionalitzades van ser els materials més citotòxics. Els resultats suggereixen que les partícules funcionalitzades amb EOCs indueixen toxicitat en les cèl·lules HepG2 mitjançant un mecanisme relacionat amb l'estrés oxidatiu, el qual provoca dany mitocondrial i la conseqüent activació de processos d'apoptosis. D'altra banda, es va demostrar que aquest efecte citotòxic és causat per interaccions directes entre les cèl·lules i les partícules, i no per productes de degradació alliberats al mitjà de cultiu.

L'exposició aguda a concentracions moderades i altes de EOCs va reduir la viabilitat de les cèl·lules HepG2 i la supervivència de *C. elegans*. La jerarquia de la toxicitat es va mantindre entre cèl·lules i nemàtodes, sent el carvacrol el compost més tòxic, seguit del timol, el eugenol i, finalment, la vanil·lina. A més, concentracions subletals d'aquests components van induir toxicitat reproductiva en *C. elegans*, la qual cosa suggereix que poden presentar efectes tòxics a les concentracions requerides per les seues propietats bioactives.

L'estudi *in vivo* de la toxicitat de les partícules va mostrar que tant les partícules sense funcionalitzar com les funcionalitzades amb eugenol causen toxicitat reproductiva en *C. elegans* després de l'exposició aguda, i inhibició en el creixement i la reproducció dels nematodes després de l'exposició a llarg termini. Les partícules funcionalitzades amb vanil·lina van mostrar efectes tòxics aguts lleus, però un major efecte després de l'exposició a llarg termini. En línies generals, els resultats obtinguts mostren que les partícules funcionalitzades amb eugenol utilitzades en l'estudi presenten majors efectes sobre *C. elegans* que la sílice sense funcionalitzar i les partícules funcionalitzades amb vanil·lina.

D'acord amb els resultats obtinguts tant en els assajos *in vitro* com *in vivo*, els principals factors que determinen els efectes toxicològics d'aquests nous sistemes antimicrobians són; el tipus d'EOC immobilitzat en la superfície de les partícules de sílice i el rendiment de la reacció de funcionalizatció. Les alternatives als conservants sintètics en aplicacions de la indústria alimentària no estan exemptes de possibles riscos toxicològics, per la qual cosa és necessari dur a terme estudis de toxicitat exhaustius que permeten comprendre les interaccions dels nous materials amb els sistemes biològics i garantir així la seua seguretat per a la salut humana.

Dissemination of results

List of publications included in this thesis

This thesis is based on the following papers:

Fuentes, C., Ruiz-Rico, M., Fuentes, A., Ruiz, M. J., & Barat, J. M. (2020). Degradation of silica particles functionalised with essential oil components under simulated physiological conditions. *Journal of Hazardous Materials*, 123120.

Fuentes, C., Ruiz-Rico, M., Fuentes, A., Barat, J. M., & Ruiz, M. J. (2021). Comparative cytotoxic study of silica materials functionalised with essential oil components in HepG2 cells. *Food and Chemical Toxicology*, 147, 111858.

Fuentes, C., Fuentes, A., Barat, J. M., & Ruiz, M. J. (2021). Relevant essential oil components: a minireview on increasing applications and potential toxicity. *Toxicology Mechanisms and Methods*, 1-27.

Fuentes, C., Verdú, S., Fuentes, A., Ruiz, M. J., & Barat, J. M. (2022). Effects of essential oil components exposure on biological parameters of *Caenorhabditis elegans*. *Food and Chemical Toxicology,* 159, 112763.

Fuentes, C., Fuentes, A., Byrne, H.J., Barat, J. M., & Ruiz, M. J. *In vitro* toxicological evaluation of mesoporous silica microparticles functionalised with carvacrol and thymol. *Food and Chemical Toxicology,* 160, 112778.

Fuentes, C., Verdú, S., Fuentes, A., Ruiz, M. J., & Barat, J. M. *In vivo* toxicity assessment of eugenol and vanillin-functionalised silica particles using *Caenorhabditis elegans*. Under review in *Ecotoxicology and Environmental Safety.*

Other scientific contributions

Oral communications:

C. Fuentes, M. Ruiz-Rico, A. Fuentes, J.M. Barat, M.J. Ruiz, H.J. Byrne. Estudio de citotoxicidad de micropartículas de sílice MCM-41 funcionalizadas con carvacrol. VII Jornadas de Formación en Toxicología. Valencia, April of 2019.

C. Fuentes, S. Verdú, R. Grau, A. Fuentes, M.J. Ruiz, J.M. Barat. *Caenorhabditis elegans* como modelo *in vivo* para evaluar la toxicidad de nuevos materiales de aplicación en la industria alimentaria. X Jornadas de Calidad y Seguridad Alimentaria. Grupo Analiza Calidad 2020 "Salud" en la Cadena Alimentaria. Valencia, November of 2020.

C. Fuentes. Uso del nemátodo *Caenorhabditis elegans* para evaluar la toxicidad de compuestos bioactivos en alimentos. VI Seminario Internacional de Investigación: Biotecnología y Sostenibilidad en la Industria de Alimentos y XVI Semana Alimentaria. Florencia (Colombia, *on-line*), October of 2021.

Poster communications:

C. Fuentes, M. Ruiz-Rico, A. Fuentes, A. Juan, M.J. Ruiz, J.M. Barat. Toxicity evaluation of vanillin functionalised silica particles used as antimicrobial agents. XII International Workshop on Sensor and Molecular Recognition. Valencia, July of 2018.

C. Fuentes, M. Ruiz-Rico, A. Fuentes, L. Manyes, J.M. Barat, M.J. Ruiz. XIII Citotoxicidad de partículas de sílice amorfa funcionalizadas con eugenol. Congreso Español de Toxicología y VII Iberoamericano. Sevilla, June of 2019.

C. Fuentes, M. Ruiz-Rico, A. Fuentes, M.J. Ruiz, J.M. Barat. Cytotoxic effect of the immobilisation of thymol on micro and nanoparticles MCM-41 on HepG2 cells. XIII International Workshop on Sensors and Molecular Recognition. Valencia, July of 2019.

C. Fuentes, M. Ruiz-Rico, A. Fuentes, M.J. Ruiz, J.M. Barat. Estudio de estabilidad en fluido lisosomal de partículas de sílice funcionalizadas con vainillina. II Congreso de Jóvenes Investigadores en Ciencias Agroalimentarias. Almería, October of 2019.

C. Fuentes, S. Verdú, A. Fuentes, J.M. Barat, M.J. Ruiz. Correlation between HepG2 cells and *Caenorhabditis elegans* exposed to essential oil components. XIV International Workshop on Sensors and Molecular Recognition. Valencia, July of 2021.

Predoctoral stage at a foreign institution

FOCAS Research Institute, Dublin Institute of Technology, Dublin, Ireland. From September to December 2018, under the supervision of Hugh J. Byrne.

Table of contents

Abbreviations

ΔΨm	Mitochondrial membrane potential
AB	Alamar blue
ADI	Acceptable daily intake
AESAN	Agencia Española de Seguridad Alimentaria y Nutrición
ALF	Artificial lysosomal fluid
APTES	(3-aminopropyl)triethoxysilane
ATP	Adenosine triphosphate
BHT	Di-ter-butyl- methylphenol
CGC	Caenorhabditis Genetics Center
CI	Chemotaxis index
CTAB	Hexadecyltrimethylammonium bromide
DFA	Deferoxamine mesylate salt
DCFH-DA	Dichlorofluorescein diacetate
DLS	Dynamic light scattering
DMEM	Dulbecco's modified eagle medium
DMSO	Dimethyl sulfoxide
DNA	Deoxyribonucleic acid
ECHA	European Chemicals Agency
EDTA	Ethylenediaminetetraacetic acid
EFSA	European food safety authority
EOC	Essential oil component
EU	European Union
FADH	Flavin adenine dinucleotide semiquinone
FAU	Formazin attenuation units
FDA	US Food and Drug Administration
FMNH	Flavin mononucleotide semiquinone

GFP	Green fluorescent protein
GI	Growth inhibition
GRAS	Generally Recognized as Safe
GSH	Glutathione
H_2-DCFDA	2′,7′-dichlorodihydrofluorescein diacetate
IC_{50}	Half maximal inhibitory concentration
ICCVAM	Interagency Coordinating Committee on the Validation of Alternative Methods
IPA	Isopropyl alcohol
LC_{50}	Lethal concentration 50
LD_{50}	Lethal dose 50
LDH	Lactate dehydrogenase
LPO	Lipid peroxidation
MCM-41	Mobile crystalline material-41
MDA	Malondialdehyde
MTT	Thiazolyl blue tetrazolium bromide
NADH	Nicotinamide adenine dinucleotide reduced form
NADPH	Nicotinamide adenine dinucleotide phosphate reduced form
NaN_3	Sodium azide
NBCS	Newborn calf serum
NGM	Nematode growth medium
NO	Nitric oxide
NOAEL	No-observed-adverse-effect level
OECD	Organisation for Economic Co-operation and Development
PBS	Phosphate buffer saline
PCA	Principal component analysis
PI	Propidium iodide

RI	Reproduction inhibition
ROS	Reactive oxygen species
SAS	Synthetic amorphous silica
SBF	Simulated body fluid
SEM	Standard error of the mean
SGF	Simulated gastric fluid
SID	Simulated *in vitro* digestion process
SIG	Simulated intestinal fluid
SSF	Simulated salivary fluid
TBA	Thiobarbituric acid
TBARS	Thiobarbituric acid reactive substances
$TEAH_3$	Triethanolamine
TEM,	Transmission electron microscopy
TEOS	Tetraethylorthosilicate
TGA	Thermogravimetric analysis

Preamble

This doctoral thesis forms part of research projects "*Hybrid systems based on biocompatible supports for development of antimicrobials based on natural substances and controlled release (AGL2015-70235-C2-1-R)"*, funded by the 2015-2018 Ministerio de Economía y Competitividad, and *"Development and application of antimicrobial systems for the food industry based on functionalized surfaces and controlled release systems (RTI2018-101599-B-C21-AR)"*, funded by the Ministerio de Ciencia, Innovación y Universidades, the Agencia Estatal de Investigación and FEDER-EU.

As part of the above-mentioned projects, new antimicrobial systems have been designed to be applied to the food industry. These innovative devices consist in the covalent immobilisation of natural antimicrobials, such as essential oil components (EOCs) carvacrol, thymol, eugenol or vanillin, on the surface of different types of amorphous silica particles. This strategy has been demonstrated to increase EOCs' antimicrobial activity and to overcome some of the limitations of their application to foods, such as high volatility, low solubility in aqueous solutions or marked sensory properties. EOCs-functionalised silica particles have been proven to be effective preservatives when added to different food matrices (Ribes et al., 2019, 2017; Ruiz-Rico et al., 2017). Their successful application as filtering materials for the cold pasteurisation of beverages like wine (García-Ríos et al., 2018), drinking water (Peña-Gómez et al., 2019b; Ribes et al., 2020), apple juice (Peña-Gómez et al., 2019a) or craft beer (Peña-Gómez et al., 2020) has also been demonstrated.

Amorphous silica particles are stable and biocompatible, and exhibit low toxicity. However, the functionalisation of silica particles by the binding on their surface organic molecules like EOCs modifies these materials' physico-chemical characteristics, which could lead to alter their biological behaviour and toxicological properties. Therefore, a toxicological evaluation on a case-by-case basis needs to be performed for any modified material designed for

food or food contact applications. In this context, toxicity testing is essential for identifying and characterising potential hazards that derive from exposure to these new materials for consumer health.

Multiple toxicity endpoints are required for the accurate prediction of new materials' toxicological properties on human health and to elucidate their mechanism of action. In this thesis, three different replacement methods have been followed as a strategy for the toxicological assessment of different types of EOCs-functionalised silica particles and their constituents; EOCs and pristine silica materials. These methods are: simulated physiological conditions; HepG2 culture cells; the non-mammalian organism model *Caenorhabditis elegans*.

General introduction

Review article

The first part of the general introduction is based on the review article: Fuentes, C., Fuentes, A., Barat, J. M., & Ruiz, M. J. (2021). Relevant essential oil components: a minireview on increasing applications and potential toxicity. Toxicology Mechanisms and Methods, 1-27.

1. General introduction

1.1. Essential oils and their main components

In recent decades, consumers' rejection to the use of additives in food and the demand for more 'natural' products have both increased (Abbaszadeh et al., 2014). As a consequence, the food industry has search for alternative compounds to synthetic preservatives to extend the shelf life of their products (Ribes et al., 2018). Among these compounds, essential oils have been one of the most studied natural antimicrobials mainly due to their high antimicrobial activity against a wide spectrum of microorganisms and their low toxicity (Burt, 2004; Calo et al., 2015).

Essential oils are oily aromatic liquids obtained from different plant material structures (Hyldgaard et al., 2012) that consist in a complex mixture of compounds including terpenoids, esters, aldehydes, ketones, acids and alcohols (Ramos et al., 2013). The biological functions of essential oils have been related to their content in phenolic components. Among these, the two isomeric monoterpenoids carvacrol and thymol, and the phenylpropenes eugenol, and vanillin (Fig. 1) are of the most commonly used and studied compounds due to their relevant biological properties (Hyldgaard et al., 2012).

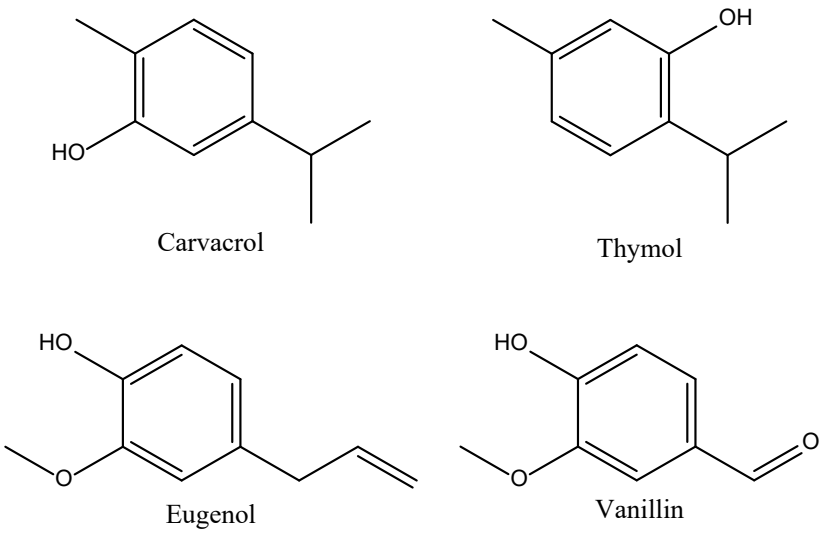

Figure 1. Molecular structure of the EOCs carvacrol, thymol, eugenol, and vanillin.

All four components have been used in a wide range of both food and non-food applications (Al-Naqeb et al., 2010; Kachur and Suntres, 2020; Memar et al., 2017; Nejad et al., 2017) and are authorised as flavouring agents without any specific restriction of use in the EU according to Regulation (EC) 1334/2008 (EC, 2008). They are also approved as Generally Recognized as Safe (GRAS) compounds by the U.S. Food and Drug Administration (FDA) (FDA, 2020) and are considered safe by the Joint FAO/WHO Expert Committee on Food Additives since "No safety concern at current levels of intake when used as a flavouring agent" has been stablished for these components (JECFA, 2021).

1.1.1. Carvacrol and thymol

Carvacrol (5-isopropyl-2-methylphenol) and thymol (2-isopropyl-5-methylphenol) are two isomeric monoterpene phenols that are found in origanum, thyme, marjoram and other aromatic plants and their essential oil fractions as major components (De Vincenzi et al. 2004). Both these components are used as flavorings in foods, beverages, perfumes, fragrances and cosmetics (Memar et al. 2017). Other applications include their use as disinfectant, insecticide, antiseptic in mouthwash and for dental practice (Suntres et al. 2015; Kachur and Suntres 2020).

Carvacrol and thymol are two of the most extensively studied EOCs because they have been identified as the most active monoterpenoids against a broad spectrum of microorganisms (Hyldgaard et al. 2012). These components are potent antibacterial agents against Gram-positive and Gram-negative bacteria (Dorman and Deans 2000; Tippayatum and Chonhenchob 2007), food spoilage or pathogenic yeast and fungi (Abbaszadeh et al. 2014; Marchese et al. 2016), and have demonstrated the inhibition of toxins production by food-relevant bacteria (Ultee and Smid 2001). These effects have been proven *in vitro*, and also in different food matrices like meat, fish, dairy products, vegetables, rice, fruit and fruit juice (Burt 2004; Calo et al. 2015). The antimicrobial activity of carvacrol and thymol has been related to their hydrophobicity and chemical structure, characterised by a hydroxyl group and the presence of a system of delocalised electrons in the phenol aromatic ring (Ultee et al. 1999; Ben Arfa et al. 2006). These elements are responsible for producing significant effects on the structural and functional properties of the cytoplasmic membrane. The main reported antimicrobial mechanism consists in cytoplasmic membrane disruption, which increases its permeability and depolarises its potential, and leads to intracellular content leakage and bacteria lysis (Xu et al. 2008). Other proposed mechanisms consist in the inhibition of efflux pumps, bacterial motility or membrane

bound ATPases, and in the reduction of biofilm formation (Kachur and Suntres 2020).

These compounds also present a wide range of other beneficial effects. Given their antioxidant activity, they have been proposed as 'natural' replacements for 'synthetic' antioxidant food additives as they minimise oxidation of the lipid components in food (Yanishlieva et al. 1999). Other reported properties include analgesic, anti-inflammatory, anti-mutagenic and anti-carcinogenic effects, as well as a modulator role in different central neurotransmitter pathways and the immune system (Deb et al. 2011; Salehi et al. 2018; Sharifi-Rad et al. 2018). The protective effects of these components in metabolic disorders like diabetes mellitus, obesity, renal diseases or gastrointestinal disorders, among others, have also been documented (Nagoor Meeran et al. 2017).

Although carvacrol and thymol are generally considered safe for consumption, some studies indicate that they may cause potential toxicological effects and allergic reactions. Table 1 summarises some of the most relevant *in vitro* and *in vivo* studies performed in the past few years. *In vitro* studies show that both carvacrol and the carvacrol and thymol mixture induce toxic effects on Caco-2 cells when measured by different basal cytotoxicity endpoints. Llana-Ruiz-Cabello et al. (2014) did not observe cytotoxic effects for thymol when administered alone, but the morphological analysis of exposed cells showed cellular damage that comes in the form of lipid degeneration, mitochondrial damage, nucleolar segregation and apoptosis. Other authors have reported an IC_{50} value for thymol of approximately 400 μM using V79 and HepG2 cells, while Caco-2 cells prove more resistant to thymol exposure with an IC_{50} value of 700 μM (Slamenová et al. 2007). Oxidative stress seems to play a crucial role in damage induced by carvacrol and its mixture with thymol, as demonstrated by higher ROS levels and lower GSH levels. At low concentrations, both components play a

protective role in Caco-2 cells against H_2O_2-induced damage (Llana-Ruiz-Cabello et al., 2015). Indeed, research suggests that the cytotoxic effect of these components on eukaryotic cells consists in induced apoptosis by the direct activation of the mitochondrial pathway (Bakkali et al. 2008; Yin et al. 2012). These components would affect inner cell membranes and organelles like mitochondria by provoking their permeabilisation and depolarisation. Changes in membrane fluidity may then result in the leakage of radicals, cytochrome c, calcium ions and proteins by acting as pro-oxidants. The intracellular redox potential and mitochondrial dysfunction would lead to cell death by apoptosis and necrosis (Bakkali et al. 2008).

Very few studies have investigated the mutagenic and genotoxic potential of carvacrol and thymol, but results are sometimes contradictory. Llana-Ruiz-Cabello et al. (2014) evaluated the potential mutagenic activity of the current usage concentrations of carvacrol and thymol by the bacterial reverse-mutation assay (Ames test), and their genotoxic activity using the comet assay on intestinal cell line Caco-2. These authors found that carvacrol exhibited mutagenic activity at 115-230 µM concentrations and genotoxic potential at a concentration of 460 µM. Thymol, on the contrary, showed no mutagenic or genotoxic effects at any tested concentration (0-250 µM). However, other works have reported no or low levels of genotoxicity and mutagenicity for carvacrol (Ündeğer et al. 2009; Maisanaba et al. 2015).

In vivo studies report adverse effects of acute and prolonged oral exposure to carvacrol and thymol in mice, rats and rabbits (Andersen 2006). The LD_{50} for oral exposure to carvacrol and thymol in rats is 810 mg/kg bw and 980 mg/kg bw, respectively. For chronic exposure, no repeated dose toxicity data are available for carvacrol, while the thymol NOAEL value determined after subchronic exposure in rats is 667 mg/kg bw/day (ECHA 2021).

Moreover, exposure to these compounds may cause allergic reactions in humans like dermatitis and skin inflammation (Salehi et al., 2018). Indeed, carvacrol is classified as skin corrosive category 1B/C via acute inhalation and dermal exposure (ECHA 2021).

1.1.2. Eugenol

Eugenol (4-allyl-2-methoxyphenol) is a phenylpropene extracted from certain essential oils. It is the main component of clove oil and is also present in essential oils or extracts of many other plants, including cinnamon, basil and nutmeg (Kamatou et al. 2012). Eugenol is applied as a flavoring to food products, fragrances, cosmetics and personal care products (Nejad et al. 2017). In dentistry, it is widely used during the manufacture of dental plasters, fillings and cements for its analgesic and anti-inflammatory properties (Rojo et al. 2006). Other uses include anesthetic in aquaculture (Palić et al. 2006) and a substrate for vanillin production (Kaur and Chakraborty 2013).

Eugenol has been well-studied for its antimicrobial properties in the food industry. Antimicrobial effects have been reported against a wide variety of foodborne and food spoilage bacteria, yeasts and fungi (Tippayatum and Chonhenchob 2007; De Souza et al. 2014). Eugenol antimicrobial activity has been associated with the ability of its hydroxyl group to disrupt the cytoplasmic membrane and the cell wall, and to interact with proteins, to result in intracellular content leakage and the disruption of the proton motive force (Hyldgaard et al. 2012).

Besides its antimicrobial role, and its analgesic and anesthetic action, eugenol exhibits other important pharmacological properties. It has anti-oxidant and anti-inflammatory effects at low concentrations (Fujisawa et al. 2002), a neuroprotective potential and offers hypolipidemic and anti-diabetic effectiveness. Moreover, eugenol has demonstrated anti-cancer activity by inhibiting propagation of different cancer cell types, an anti-mutagenic

potential against different genotoxic compounds, and its use in regenerative medicine has been proposed since the proliferation and migration promotion of stem cells *in vitro* has been demonstrated (Khalil et al. 2017; Sisakhtnezhad et al. 2018).

On the toxicological profile of eugenol, *in vitro* studies have demonstrated its cytotoxic potential against different cell types in a dose-, frequency- and duration-dependent manner (Babich et al. 1993; Ho et al. 2006; Prashar et al. 2006). Intracellular glutathione depletion levels have been described as one of the mechanisms that underlie eugenol-induced cytotoxicity (Ho et al., 2006). This is because, despite its anti-oxidant activity at low concentrations, eugenol acts as a pro-oxidant agent at high concentrations, which enhances the generation of free radicals and results in tissue damage (Fujisawa et al. 2002). The *in vitro* genotoxic potential of eugenol has also been described. Maralhas et al. (2006) found that eugenol induces chromosomal aberrations and endoreduplication in V79 Chinese hamster fibroblasts in a concentration-dependent manner. Similarly, Martins et al. (2011) found that a 1-hour exposure to eugenol produces both DNA single strand and double strand breaks in Chinese hamster ovary (CHO-K1) cells, and apoptosis was also observed after a 24-hour incubation period to the 750 μM concentration.

Eugenol is considered not acutely toxic and has an LD50 value over 2,000 mg/kg bw for rats, and between 1,500 and 3,000 mg/kg bw for mice, while chronic studies establish a NOAEL value of 300 mg/kg bw/day (ECHA 2021). However, acute *in vivo* studies found that eugenol causes respiratory distress with hemorrhagic pulmonary edema after injection in rats (Wright et al. 1995), kidney damage, apoptosis and morphological alteration in renal cells of exposed frogs at aesthetic doses (Goulet et al. 2011), and genotoxic effects on *Drosophila melanogaster* (Munerato et al. 2005).

In humans, the use of eugenol in fragrance ingredients and dental products has been associated with different adverse reactions, including skin irritation, ulcer formation, dermatitis and slow healing. A case study has also revealed adverse side effects after unintentional ingestion of eugenol that results in similar hepatoxic effects to paracetamol poisoning (Kamatou et al. 2012).

1.1.3. Vanillin

Vanillin (4-hydroxy-3-methoxybenzaldehyde) is a phenolic aldehyde and the main component of the extract of the bean and pod of the vanilla orchid. It is one of the most widely used flavor compounds in foods, pharmaceuticals, fragrances and personal care products (Al-Naqeb et al., 2010). In the food industry, it is often employed in processed foods as a flavoring agent, and as a sweetener in dairy, bakery and confectionary products, and also in beverages. Vanillin is also used in aromatherapy and is an ingredient of perfumes, toothpastes, soaps, cosmetics, and other personal and household products. In the chemical and pharmaceutical industry, vanillin is involved in the manufacture of herbicides, antifoaming agents or drugs like L-dopa. Other products that may also contain vanillin include cigarettes, cattle feed or pharmaceuticals, paints and plastics where it is used as an odor-masking agent (Cheng et al. 2007).

Albeit less studied than carvacrol, thymol or eugenol, the antimicrobial action of vanillin has also been demonstrated *in vitro* against different food-related bacteria, yeasts and molds (Hyldgaard et al. 2012). Vanillin's antimicrobial mode of action has not been completely elucidated, but it has a demonstrated deleterious effect on cytoplasmic membrane integrity, with the resulting loss of pH homeostasis and respiratory activity inhibition (Fitzgerald et al. 2004).

Besides, vanillin and its analogues have also shown different beneficial properties, such as antioxidant (Oliveira et al. 2014), antimutagenic (Lee et al.

2014), anticarcinogenic (Ho et al. 2009; Pereira et al. 2016) and hypolipidemic activity (Al-Naqeb et al. 2010).

The toxicological effects of vanillin are reported less than those of other EOCs. It is considered to have a low cytotoxic potential as only high concentrations (mM range) reduce cell viability in a dose- and time-dependent manner (Oliveira et al. 2014; Fuentes et al. 2020). Additionally, vanillin is not considered harmful by ingestion, with an LD_{50} of 3,978 mg/kg bw for acute oral exposure and a NOAEL value of 650 mg/kg/day, as determined by a subchronic study in rats (ECHA 2021).

The use of essential oils and their main components has considerably increased in recent years and the market is predicted to grow because of rising consumer demand for natural products and their potential use in multiple applications. Therefore, prolonged consumer exposure to these compounds is expected in the foreseeable future. Carvacrol, thymol, eugenol and vanillin are four of the most used and investigated EOCs for their relevant biological properties. Different studies describe adverse effects after exposure to medium and high concentrations of these components, although information remains limited. Thus, more toxicological research, including chronic exposure studies and combined exposures to different components, is necessary to not only elucidate the possible risks deriving from increased exposure to these components, but to also guarantee their safety for human health and the environment.

Table 1. *In vitro* and *in vivo* toxicological effects described for carvacrol, thymol, eugenol and vanillin.

EOC	Toxicological effects	References
Carvacrol	***In vitro***	
	Cytotoxic effects on Caco-2 cells	Llana-Ruiz-Cabello et al. (2014)
	Mutagenic effect on Caco-2 cells in the Ames test and genotoxic activity in the comet assay	Llana-Ruiz-Cabello et al. (2014)
	Weak genotoxic effects on mouse lymphoma cells in the micronucleus test	Maisanaba et al. (2015); Ündeğer et al. (2009)
	No genotoxic potential for Chinese hamster lung fibroblast (V79) cells in the comet assay	Ündeğer et al. (2009)
	In vivo	
	Acute toxic effects after oral exposure in mice, rats and rabbits. Skin irritation after acute dermal exposure in mice	Andersen (2006)
Thymol	***In vitro***	
	No cytotoxic effects (250 µM) but lipid degeneration, mitochondrial damage, nucleolar segregation and apoptosis	Llana-Ruiz-Cabello et al. (2014)
	No cytotoxic effects on peripheral blood mononuclear cells (100 µM)	Deb et al. (2011)
	Cytotoxic activity against V79, HepG2 and Caco-2 cells	Slamenová et al. (2007)
	No mutagenic or genotoxic effects at any tested concentration (0-250 µM)	Llana-Ruiz-Cabello et al. (2014)
	Genotoxic effects on V79 cells (25 µM) in the comet assay	Ündeğer et al. (2009)
	In vivo	
	Toxic effects after acute, short-term and prolonged oral exposure at high doses in *in vivo* studies	Andersen (2006)
	Allergic reactions in human	Salehi et al. (2018)
Eugenol	***In vitro***	
	Cytotoxicity in human HFF fibroblasts and HepG2 cells	Babich et al. (1993)
	Cytotoxic effects on the human osteoblastic (U2OS) cell line	Ho et al. (2006)
	Cytotoxic effects on human fibroblasts and endothelial cells	Prashar et al. (2006)

EOC	Toxicological effects	References
	Genotoxicity in V79 cells by the chromosomal aberrations test	Maralhas et al. (2006)
	Genotoxic effects on Chinese hamster ovary (AA8) cells	Martins et al. (2011)
	In vivo	
	Respiratory problems after exposure in rats.	Wright et al. (1995)
	Kidney and renal damage in frogs at anesthetic doses	Goulet et al. (2011)
	Genotoxic effects on *Drosophila melanogaster*	Munerato et al. (2005)
	Adverse reactions in humans (skin irritation, ulcer formation, dermatitis and slow healing)	Kamatou et al. (2012)
Vanillin	***In vitro***	
	Low *in vitro* toxic effects on murine macrophage cells	Oliveira et al. (2014)
	Cytotoxic effects on HepG2 cells at high concentrations	Fuentes et al. (2020)

1.2. Synthetic amorphous silica

1.2.1. Classification of silicon dioxide materials

There are mainly three types of silicon dioxide that come under the same CAS number: crystalline silica, amorphous silica (naturally occurring or as by-products) and ynthetic amorphous silica (SAS) (Fig. 2). Of the three, SAS is the only authorised form of silica as a food additive (E 551) (Fruijtier-Pölloth, 2012). SAS is an amorphous, crystalline-free type of silicon dioxide that is intentionally manufactured in the form of white dry hygroscopic powers or dispersions.

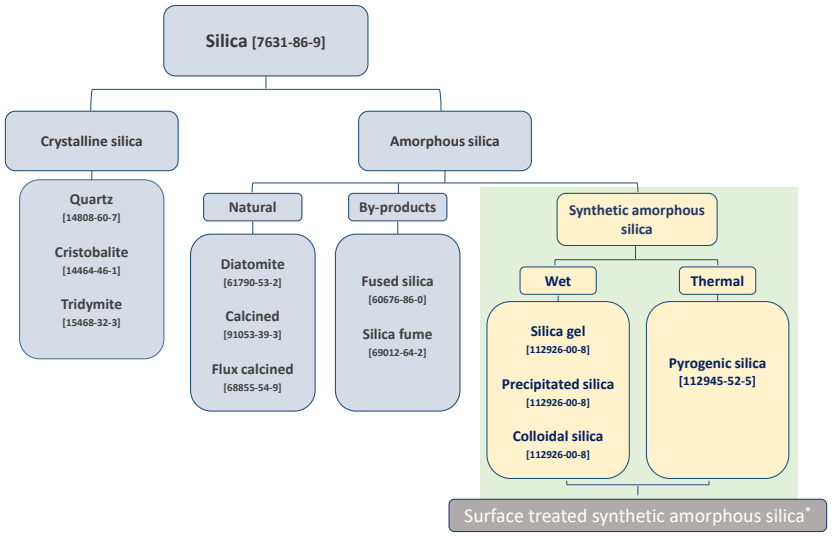

Figure 2. Different types of silica forms with their corresponding CAS numbers. *All forms of SAS can be surface-treated physically or chemically. Adapted from Fruijtier-Pölloth (2012).

SAS can be produced by two different processes: by a thermal route to yield pyrogenic silica (also known as fumed silica); by a wet route to yield silica gel, precipitated or colloidal silica. The manufacturing process of pyrogenic SAS consists in the vapour-phase hydrolysis of volatile chlorosilanes in an oxygen-hydrogen burner at temperatures over 1,000 ºC. After agglomeration in a cooling system, silica particles are filtered and the adsorbed hydrochloric acid is removed in a deacidification step. High temperature yields a fluffy amorphous substance with low water content in the form of white dry powder or granules (Harrison, 2009). SAS production by the wet process consists in the precipitation of silica particles from an aqueous solution of sodium silicate by acid neutralisation. The following manufacturing steps include filtration, washing, drying and milling to achieve a defined particle size distribution. The wet route produces SAS powders with

a high bound water content in the form of hydrates or surface absorbed water products. Depending on the solution's final pH, precipitated silica (alkaline pH) or silica gel (acidic pH) is obtained (EFSA., 2018a). Although chemically identical, both show some differences in their physico-chemical properties, of which the most important is pore size distribution (Otterstedt and Brandreth, 2013). Colloidal silica preparations consist in stable dispersions of SAS nanoparticles in liquids, usually water. They can be directly produced by the wet process or indirectly obtained by re-dispersion of silica particles in a liquid, typically water (Harrison, 2009). Finally, as shown in Figure 2, all SAS forms can be surface-modified by either physical or chemical treatment. The commonest chemical SAS modification includes treatment with organosilicon compounds to increase SAS hydrophobicity by, for example, silylation with dimethyl dichlorosilane (ECETOC, 2006).

Some of SAS' physical characteristics, such surface composition, depend on their manufacture mode (USDA, 2010). However, other properties are common to the different SAS product types. SAS particles are characterised by being hydrophilic due to the silanol groups (Si—OH) present on their surface, insoluble or slightly soluble in water and organic solvents, hygroscopic, optically transparent, chemically inert, and resistant to mechanical and thermal stress and to microbial attack (ECETOC, 2006). SAS is composed of nanosized primary particles that covalently bind to form aggregates that are, on average, bigger than 100 nm. These aggregates come together via hydrogen bonding and Van der Waals interactions to form agglomerates, which results in larger structures with a mean diameter within the micrometre range (Murugadoss et al., 2020).

1.2.2. Mesoporous silica: MCM-41 materials

By adjusting the conditions used during the synthesis process, different SAS types can be obtained according to physical properties like morphology, surface area or pore size distribution (Fruijtier-Pölloth, 2012). M41S are a family of ordered mesoporous materials discovered by the Mobil Corporation in 1992, and characterised by a large specific surface area and ordered pore distribution (Kresge et al., 2004). Mesoporous silica is synthesised by the hydrolysis and condensation of an inorganic precursor, such as tetraethylorthosilicate (TEOS), around long-chain surfactant molecules as the structure-directing agent, and under basic or acidic conditions. Then the surfactant used as a template is removed by calcination or solvent extraction to result in mesoscopically ordered materials (Maleki et al., 2017).

Mobil Composition of Matter (MCM)-41 is the most widely studied member of the M41S family for its simple and easy preparation and its thermal stability (Chaudhary and Sharma, 2017). MCM-41 has a surface area of up to 1,200 m^2/g and large pore volumes within the 2–10 nm range, and is uniformly ordered in a hexagonal structure of empty channels (Meynen et al., 2009). These materials are characterised by their chemical stability, biocompatibility and easy surface modification (Jaganathan and Godin, 2012; Shi et al., 2004).

1.2.3. Synthetic amorphous silica applications

Given SAS products' outstanding properties, they are used in a wide range of industrial and consumer applications. Indeed, more than 500,000 tonnes of SAS are produced in Europe per year by the Association of Synthetic Amorphous Silica Producers in the form of silica gel, precipitated and pyrogenic silica (ASAP, 2021).

Industrial SAS applications include being employed as a reinforcement agent in silicones and rubber (i.e. car tyres or footwear), as a matting agent or rheological additive in varnishes, paints, lacquers, vinyl coatings, adhesives,

printing inks and glues, and as corrosion-resistant coatings in various types of cans and moisture-impermeable films. Other applications consist in preventing plastic films from sticking, thermal insulations, as a precursor to manufacture different catalyst systems or as a desiccant for packaged goods in the case of silica gel. SAS is also frequently used as a biocide for insect control in stored grain, an inert carrier in dry pesticides, a soil conditioner and a turf soil supplement (IARC, 1987; SIDS, 2004; USDA, 2010).

In cosmetics, SAS is employed to thicken pastes and creams, to preserve flow properties in powder products, as a carrier for fragrances and as an abrasion additive in toothpaste (SIDS, 2004). In medicine, SAS is utilised mainly as an excipient in the formulation of solid dosage forms of pharmaceuticals, and is also being increasingly used as an oral delivery system for drugs, biological molecules or cells in different areas like cancer therapy or DNA transfection (Barik et al., 2008; Diab et al., 2017).

As previously mentioned, SAS is the only type of silicon dioxide authorised as a food additive. Additive E 551 includes the SAS forms of silica gel, precipitated and pyrogenic silica, while colloidal silica does not meet EU specifications for being authorised as a food additive as its suspensions may contain isolated primary nanoparticles (EFSA., 2018a). The main functions of E 551 are: anticaking agent, a filtering aid for clarifying beverages, a stabiliser in beer production, a defoaming agent or a carrier (USDA, 2010). According to Regulation (EC) No. 1333/2008 of the European Parliament and the Council, E 551 is permitted in all food categories, except for foods intended for infants and young children. In foods in tablet and coated tablet forms, SAS can be employed *quantum satis.* In dried powered foods, it may be used at a maximum level. Products containing SAS include sugar, top-table sweeteners, salt, salt substitutes, seasonings, food supplements and the surface treatment of different confectionary products. As a carrier, it is authorised for preparing nutrients and different categories of food additives, such as emulsifiers and

colour preparations, food enzymes and food flavourings. Moreover, it is utilised as an anticaking agent and as an authorised carrier in vitamins and mineral premixes for animal feed (Regulation (EC) No. 1333/2008 of the European Parliament and of the Council of 16 December 2008 on Food Additives (Text with EEA Relevance), 2008). Similarly, the FDA has classified silicon dioxide as GRAS, whose use as a food is approved additive in amounts up to 2% per food product weight (FDA, 2021).

In turn, the outstanding properties of MCM-41 particles have made these materials suitable to be applied in catalysis, adsorption, separations or as chemical sensors (Chaudhary and Sharma, 2017), and they have also drawn considerable research interest for a variety of biomedical and biological applications (Moritz and Geszke-Moritz, 2015).

1.2.4. Synthetic amorphous silica functionalisation

The presence of silanol groups on silica particles' surface enables a wide variety of surface modifications by the covalent attachment of specific functional groups and organic molecules (Diab et al., 2017).

SAS particles' surface can be made up of two different functional groups: siloxane and silanol groups. Siloxane groups consist of covalently bound oxygen and silicon, and are hydrophobic and scarcely reactive. In silanol groups, oxygen is bond to silicon and hydrogen, and they are hydrophilic and more reactive than siloxane groups. Silanol groups exist in three different spatial arrangements: isolated or free silanol (the most reactive); vicinal groups (hydrogen bonded silanol groups); germinal groups (two hydroxyl groups linked with one silicon atom) (Fig. 3). SAS reactivity depends on the degree and accessibility of silanol groups, especially in the free silanol form. This, in turn, depends on the silica type and the synthesis method (OECD, 2016).

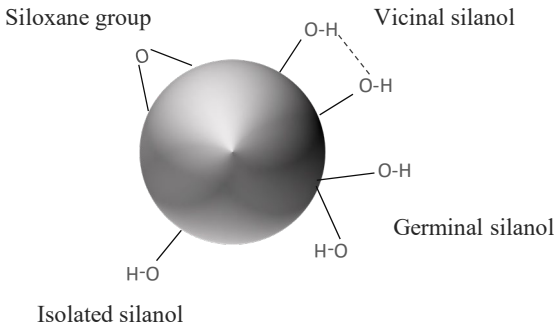

Figure 3. Siloxane bonds and different types of silanol groups on SAS particles' surface. Adapted from Bikiaris and Vasileiou (2009).

A major form of modifying silica particles' physico-chemical properties consists in incorporating organic and inorganic components into their surface by a process known as functionalisation (Alothman, 2012). Functionalisation of silica materials can be carried out with the silanol groups present on their surface via two main general approaches: co-condensation synthesis and post-synthetic grafting. In co-condensation, the functionalisation of silica's surface directly occurs during the synthesis process by mixing the components for silica manufacture together with a precursor of the functional group to be incorporated. Conversely in the most widely used method in grafting, the desired functional groups are post-synthetically introduced into surfactant-removed silica particles using non-polar anhydrous solvents (Brühwiler, 2010; Trewyn et al., 2007).

With mesoporous silica particles, functionalisation is possible in three separated topological areas: within the silica framework, on the internal pore and on the particle's surface (Bagheri et al., 2018). By the co-condensation method, organic groups are mainly incorporated into mesopores to yield homogeneous distribution (Maleki et al., 2017), but leads to alterations to the

mesoporous structure (Brühwiler, 2010). During the post-synthetic grafting process, although mesoporosity is retained, a higher density of organic groups can be found in pore openings and on particles' surface, but with less efficiency within the interior silica framework, which leads to heterogeneous surface chemistry (Bagheri et al., 2018; Trewyn et al., 2007).

Different compounds have been used to react with silanol groups on silica surfaces to give rise to a wide variety of functional groups, including phenyl, amine, carboxyl and thiol groups, among others (Alothman, 2012). Quite frequently, silica particles have been functionalised with polyethylene glycol-silanes to enhance particles' biocompatibility and stability (Brown et al., 2007; Hao et al., 2012; He et al., 2011), and with chlorosilanes or alkoxysilanes as a linker for other functional molecules (Liberman et al., 2014). Additionally, by the grafting method, not only small molecules, but also macromolecules like polymers and lipids, can be covalently attached to silica particles' surface (Maleki et al., 2017).

The wide range of possible chemical modifications allows numerous functional silica-based hybrid structures to be designed with potential applications in many areas, including catalysis, chromatography, controlled drug delivery, bioimaging or biosensing (Alothman, 2012; Diab et al., 2017; Gañán et al., 2014; Liberman et al., 2014; Lu et al., 2019).

In the food industry sector, silica-based hybrid materials with new functionalities have been proposed for many applications, which range from the encapsulation and delivery of food ingredients and nutraceuticals to the development of a new generation of sensors and antimicrobial systems to guarantee food quality and safety (Ros-Lis et al., 2018). Some examples include: encapsulation of garlic extracts in the MCM-41 microparticles functionalised with polyamines or hydrolysed starch to increase stability and to reduce sensorial perception (Acosta et al., 2014); encapsulation of nisin A

in organic-inorganic hybrid mesoporous silica matrices to improve their stability (Flynn et al., 2019); folic acid or vitamin B2 encapsulation in amine functionalised mesoporous silica to control its release along the digestive tract (Bernardos et al., 2008; Pérez-Esteve et al., 2016b); fumed silica modification with isonicotinic acid hydrazide for the preconcentration and determination of Hg (II) ions from fish samples by solid-phase extraction (Ahmadi et al., 2019); immobilisation of EOCs on different silica particles' surface to improve their antimicrobial activity (Ribes et al., 2017; Ruiz-Rico et al., 2018).

1.2.5. Toxicological evaluation of synthetic amorphous silica as a food additive

Synthetic amorphous silica materials have been used for decades in a wide variety of applications, and provide no evidence for adverse health effects. The oral route is an important exposure form. SAS may be naturally present in large amounts in different foods, mainly vegetables (Fruijtier-Pölloth, 2016) and, as previously mentioned, can be added as a food additive for different technological purposes. As SAS is a component employed for manufacturing adhesives, coatings, paper, paperboard and polymers, SAS particles can be indirectly added to food products by migration from food-packaging materials (EFSA, 2018a). Finally, it can also be ingested through other sources, such as pharmaceuticals, toothpaste or dietary supplements (Fruijtier-Pölloth, 2016).

In 2018, the EFSA Panel on Food Additives and Nutrient Sources added to Food (ANS) published a scientific opinion on the re-evaluation of the safety of SAS as a food additive based on the data submitted by interested parties after EFSA public calls, and information from previous evaluations and the available literature (EFSA, 2018a). According to this information, the EFSA Panel considered low acute and long-term toxicity for SAS products when specified for use as food additive E 551. Indeed, the highest exposure (50

mg/kg bw per day) was substantially lower than the NOAELs determined in different toxicological studies. Yet despite limitations in some *in vitro* and *in vivo* studies, no evidence for biopersistence or bioaccumulation, genotoxic, carcinogenic, reproductive or developmental adverse effects was observed. Therefore, the re-evaluation report concluded that SAS forms used as E 551 in currently authorised uses and use levels do not pose a safety concern for consumers.

As discussed above, food additive E 551 is formed by aggregates of primary nanosized silica particles with a mean diameter over 100 nm (Murugadoss et al., 2020). However, depending on the starting material or the manufacturing process, differences in aggregate size may be found and the presence of aggregates smaller than 100 nm cannot be excluded (Fruijtier-Pölloth, 2016). Regarding concerns about the presence of nanosized SAS particles in food products, the Panel considered that EU specifications for correct E 551 characterisation were not sufficient and urged to include the characterisation of particle size distribution with appropriate statistical descriptors, such as range, median and quartiles, and the percentage of nanoparticles present in the food additive.

It is worth mentioning that the EFSA re-evaluation did not include chemically modified SAS particles as these materials differ from the silicon dioxide used as food additive E 551. Surface properties of particles are crucial for affecting biological responses and must, therefore, be considered for ecotoxicological and toxicological testing (Fruijtier-Pölloth, 2012; Kyriakidou et al., 2020; Puerari et al., 2019; Yoshida et al., 2012). Accordingly, and as stated by Fruijtier-Pölloth (2016), “Any new or novel forms of silicon dioxide that do not comply with established specifications, or are produced to perform a new technological function in food, would require specific safety and risk assessments”.

1.3. Toxicological assessment for food-regulated products

According to EU legislation, any new substances developed for being used in the food chain must be subjected to a safety evaluation by the EFSA (EFSA, 2012). Application forms for the authorisation of a new food additive or a modification of an already authorised food additive must be accompanied by a technical dossier containing information on the substance's chemical composition and specifications, proposed uses and estimated exposure, and toxicological studies. This information will be used by the EFSA Panel for the risk assessment of any new substance. Based on the EFSA safety opinion, the European Commission, together with other general criteria like technological and consumer aspects, will consider the authorisation of the proposed food- and feed-related product or application for the EU market.

During the risk assessment process, information deriving from toxicological studies is crucial to fulfil different aims (WHO, 2009):

- Identification of potential adverse effects
- Definition of the exposure conditions needed to produce effects
- Assessment of concentration-response relations
- Investigation of mechanisms of toxicity

Toxicological studies and other data requirements needed for the safety evaluation of new products are specified by the EFSA Panel on Food Additives and Flavourings in different guidances depending on the product or food application, including:

- Guidance for submission for food additive evaluations (EFSA, 2012).
- Guidance on the risk assessment of the application of nanoscience and nanotechnologies in the food and feed chain (EFSA, 2018b).

Or by the national agencies of the Member States concerned about food security:

- Guidelines indicating the necessary documentation for the assessment of processing aids intended for use in human food (AESAN, 2010).

1.3.1. Guidance for submission for food additive evaluations

Regulation (EC) No. 1331/2008 of the European Parliament and the Council establishes a common procedure for the evaluation and authorisation of food additives, food enzymes and food flavourings (EC, 2008). The toxicological evaluation proposed by the EFSA for these substances consists of a tiered approach designed to evaluate four core toxicological areas: toxicokinetics, genotoxicity, toxicity (including subchronic and chronic toxicity, and carcinogenicity), and reproductive and developmental toxicity. Together with these main areas, other toxicological studies are also considered for the adequate evaluation of certain substances; e.g., immunotoxicity, hypersensitivity and food intolerance, neurotoxicity, endocrine activity and mechanisms and modes of action. The Panel also emphasises the need to comprehensively analyse the composition, structure and metabolic fate of the tested substance before toxicity testing.

The tiered toxicological approach comprises three different levels (Fig. 4), whereby available information from lower testing tiers determines the requirements for further risk assessment steps. Accordingly, less complex assays are firstly performed to obtain the substance's hazard information. If the obtained data are insufficient for risk assessments, further studies from a higher tier are then conducted. Thus, all the substances are evaluated at Tier 1, but only for those absorbed compounds or compounds presenting toxic or genotoxic effects is more extensive toxicological information needed and, therefore, Tier 2 testing is performed. Similarly, results indicating concern from Tier 2 are further evaluated at Tier 3 using specific endpoints on a case-by-case basis (EFSA, 2012).

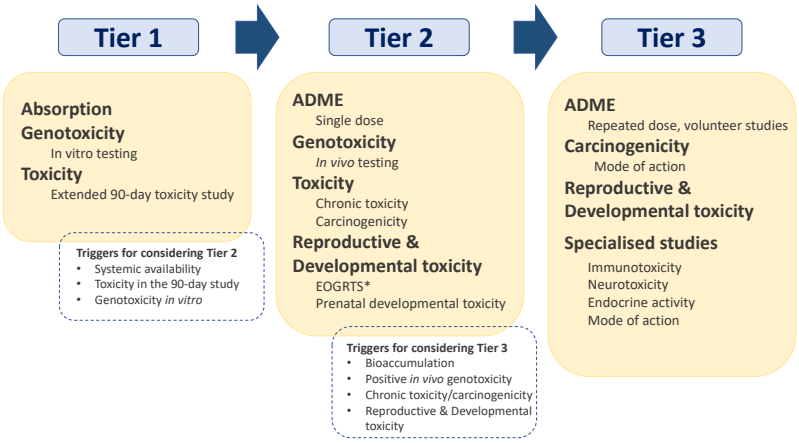

Figure 4. Diagram of the tiered approach for the toxicity testing of food additives (adapted from EFSA (2012)). *Extended One-Generation Reproductive Toxicity Study.

1.3.2. Guidance on risk assessment of applying nanoscience and nanotechnologies in the food and feed chain

Reducing particle size to the nanoscale can affect materials' properties and biokinetics behaviour by leading to altered toxicological effects compared to their bulk. For this reason, the safety of engineered nanomaterials for food and feed applications cannot be necessarily comparable to their corresponding non-nanoforms and need their own risk assessment, regardless of their intended use as food additives, enzymes, flavourings, food contact materials, novel foods, feed additives or pesticides.

The "Guidance on risk assessment of the application of nanoscience and nanotechnologies in the food and feed chain" document is an overview on information requirements and how to perform risk assessments of engineered nanomaterials in the food and feed areas (EFSA, 2018b). This Guidance is applicable to particles that meet the criteria for engineered nanomaterials

according to the European Commission's recommended definition: 50% of particles with a particle size within the 1-100 nm range (European Parliament, 2015), materials larger than 100 nm, but retain properties on the nanoscale, non-engineered nanomaterials that contain a fraction of particles within the 1-100 nm size range, nanomaterials with the same elemental composition, but with different morphological shapes, sizes, crystalline forms and/or surface properties or a nanoscale entity made of natural materials that has been deliberately produced to obtain nano-enabled properties, or has been modified to be used to develop other nanoscale materials.

This Guidance describes a stepwise approach for the safety assessment of nanomaterials' exposure, and includes appropriate *in vitro* and *in vivo* tests that can be used to identify and characterise toxicological hazards. A nanomaterial's risk is determined by its chemical composition, physico-chemical properties, its interactions with tissues and its potential exposure levels.

The schematic procedure for the risk assessment of ingested engineered nanomaterials is shown in Figure 5. The material's detailed physico-chemical characterisation must firstly be performed. This will help applicants to determine if the Guidance for engineered nanomaterials is applicable and to provide information about a nanomaterial's potential toxicity and the appropriate testing strategy. Then the materials that meet the requirements for being considered a nanomaterial are tested in three different steps, which are preceded by an initial degradation study under conditions that represent the gastrointestinal tract (Step 0). The nanomaterials that demonstrate a high degradation rate to ions or molecules under physiological conditions are not expected to exhibit nano-related behaviour and, thus, a standard risk assessment on conventional non-nanomaterials must be applied. In contrast, the nanomaterials that do not quickly degrade are considered for further testing in Step 1, where a compilation of the available information, a battery

of relevant *in vitro* toxicity and genotoxicity tests, and a degradation test under simulated lysosomal conditions come into play. If the information from Step 1 indicates that the nanomaterial is non-persistent and there is no indication of any toxic and genotoxic potential, a decision can be made to dismiss further nanomaterials' specific testing in Step 2, but a safety assessment for conventional non-nanomaterials is still needed. However, in most cases, testing in Step 2 is required as *in vitro* testing alone is not considered to provide conclusive evidence for toxicity.

In step 2, a modified 90-day oral toxicity test in rodents (OECD TG 408 with extended parameters from OECD TG 407) (OECD Guideline, 2018) should be performed to identify the nanomaterial potential to cause immunological, proliferative, neurotoxic, reproductive or endocrine-mediated effects. Evidence for nanomaterial absorption and toxicity is further determined by toxicological research in Step 3.

In Step 3, specialised and in-depth testing should be performed to obtain additional toxicological information to refine the risk assessment. This step may include toxicokinetic studies to evaluate nanomaterial accumulation during long-term exposure and differences between species, in-depth testing for reproductive and developmental toxicity neurotoxicity, immunotoxicity, carcinogenicity or endocrine-mediated effects, or specialised assays to evaluate the effects of nanomaterials on the gut microbiome.

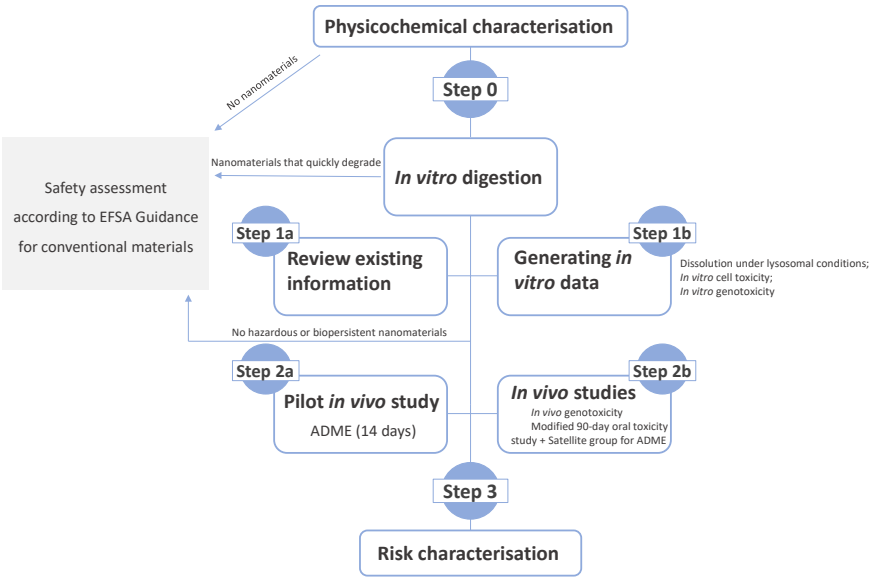

Figure 5. Schematic procedure for human and animal health risk assessments of ingested nanomaterials (adapted from EFSA (2018b)).

1.3.3. Guidelines indicating the necessary documentation for assessing the processing aids intended for use in human food

According to Regulation (EC) No. 1333/2008 on food additives, processing aids are substances not consumed as food itself, but intentionally used while processing foods, which in the final product do not have any technological effect and only remain as residue. The unintentional presence of the residue of the substance or its derivatives in the final product is allowed, provided that it does not pose any consumer safety risk.

As they are absent in the final product, they are not considered food ingredients and, save certain specific cases, are excluded from the scope of Regulation (EC) No. 1333/2008 and only need to be included on the list of ingredients if they are considered to potentially cause allergies or food

intolerances. As a result, EU Member States should develop their own legislation on processing aids (AESAN, 2021).

In Spain, the Spanish Agency of Food Safety and Nutrition (AESAN) published the "Guidelines indicating the necessary documentation for assessing processing aids intended for use in human food", which includes the information required by the AESAN Scientific Committee to perform the safety assessment of food processing aids (AESAN, 2010).

The Guidance identifies different situations according to the "status" of the processing aid for which the required data are adapted on a case-by-case basis. This information varies depending on whether or not the substance has been previously authorised for human consumption, if an acceptable daily intake (ADI) has been established by a recognised scientific institution (*quantum satis* or specified ADI) and if there inevitable and detectable residues are present in the final product. For all these situations, it is necessary to provide information on administrative data, physico-chemical properties and the processing aid's technological function. When its use results in technically unavoidable residue being present, information must also be provided about the detection method in the food product and its validation. If substances are authorised, but for which no ADI has been established, or substances have not been previously authorised for use in human nutrition, safety studies must be carried out at different levels depending on the processing aid condition:

- **Level A**: substance already used for human consumption with no specified ADI that results in technically unavoidable residue
- **Level B**: substance not previously used for human consumption and does not produce detectable residue
- **Level C**: substance not previously employed for human consumption and results in technically unavoidable residue

All these levels require information on the toxicokinetics and toxicology of these compounds. Level B also needs an oral toxicity study at repeated doses for 28 days in rodents, *in vitro* and *in vivo* genotoxic and mutagenic tests and an evaluation of the potential to cause allergy or intolerance reactions. Further studies on carcinogenesis, reproductive and developmental toxicity, and immunotoxicity may be required in some cases. At level C, a subchronic 90-day toxicity study in rodents and a reproductive toxicity evaluation (including teratogenesis) must be provided (Fig. 6).

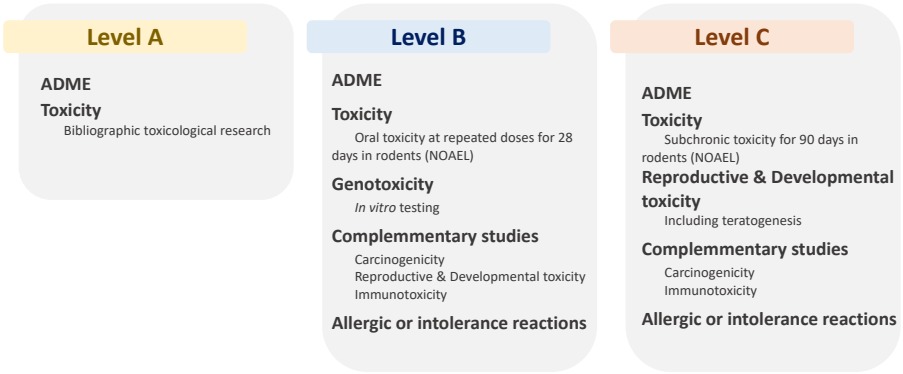

Figure 6. Toxicological studies for the assessment of processing aids according to the three requirement levels (AESAN, 2010).

In all cases, the different guidelines recommend, wherever possible, the use of alternative methods to animal testing during the toxicological evaluation of food-related compounds to meet the 3Rs strategy requirements.

1.4. The 3Rs strategy for toxicity testing

In the European Union, all industrial sectors, including the agro-food industry, are obliged to apply available methods to guarantee the 3Rs principles during the safety assessment of their products (European Parliament, 2010).

The 3Rs strategy was proposed by William Rusell and Rex Burch in 1959 to perform more humane animal research (Rusell and Burch, 1959). In the last few decades, the enforcement of this approach has considerably intensified given animal welfare concerns of scientists working with animals, environmental groups and the general public. Moreover, a shift from animal testing to 3Rs methods is expected in the future, thanks mainly to scientific developments and technological innovations, societal changes in the form of revised animal research regulations and test guidelines for approved *in vitro* methodologies, and economic aspects (Daneshian et al., 2011).

Specifically, the 3Rs strategy proposes the reduction, refinement and replacement of animal use whenever possible, and without compromising scientific rigour (Stephens and Mak, 2013).

Reduction refers to using the minimum number of animals during experiments while still obtaining statistically valid and robust results. This may be achieved by, for instance, reducing the number of variables with a good experimental design, by rigorously controlling experimental conditions or by employing genetically homogeneous animals (Erkekoglu et al., 2011).

Refinement consists in adopting techniques and approaches that minimise animal pain and suffering during experimentation and in enhancing animal welfare. Examples of refinement include using appropriate analgesia, anaesthesia and euthanasia techniques, housing social animals in groups or improving housing conditions with larger cages or toys (Stephens and Mak, 2013).

Replacement involves the partial or full substitution of animals for non-sentient systems. Replacement systems include the use of human volunteers, *ex vivo* methods through isolated animal tissues and organs, *in vitro* methods employing primary or continuous cell lines, *in silico* approaches that simulate chemical structure-activity relationships, or employing non-mammalian models, such as zebrafish eggs, insects like *Drosophila melanogaster*, nematodes like *C. elegans*, and plants or unicellular organisms (Daneshian et al., 2011; Kandárová and Letaáiová, 2011).

Objectives

2. Objectives

This PhD thesis aims to identify and characterise the potential risk deriving from oral exposure to different silica particle types functionalised with essential oil components (EOCs) and designed to be used as antimicrobial devices for the food industry. We investigated three silica particle types (SAS, MCM-41 microparticles, MCM-41 nanoparticles) functionalised with four EOCs (carvacrol, eugenol, thymol, vanillin).

This general goal is pursued by the following specific objectives to:

- Determine the stability of the different bare and EOCs-functionalised silica particles after oral exposure under simulated physiological conditions: an *in vitro* digestion process and representative conditions of lysosomal fluid
- Evaluate the cytotoxic effect of the different types of EOCs-functionalised silica particles and their constituents (EOCs and bare silica particles) in HepG2 cells
- Elucidate the toxicological mechanism of action of the EOCs-functionalised silica particles at the cellular and molecular levels by studying specific metabolic endpoints
- Evaluate the *in vivo* toxic effects of the different types of functionalised silica particles and their constituents (EOCs and bare silica particles) using the biological model system *C. elegans*
- Establish a relation between particles' physico-chemical properties and *in vitro* and *in vivo* toxicological effects

Experimental outline

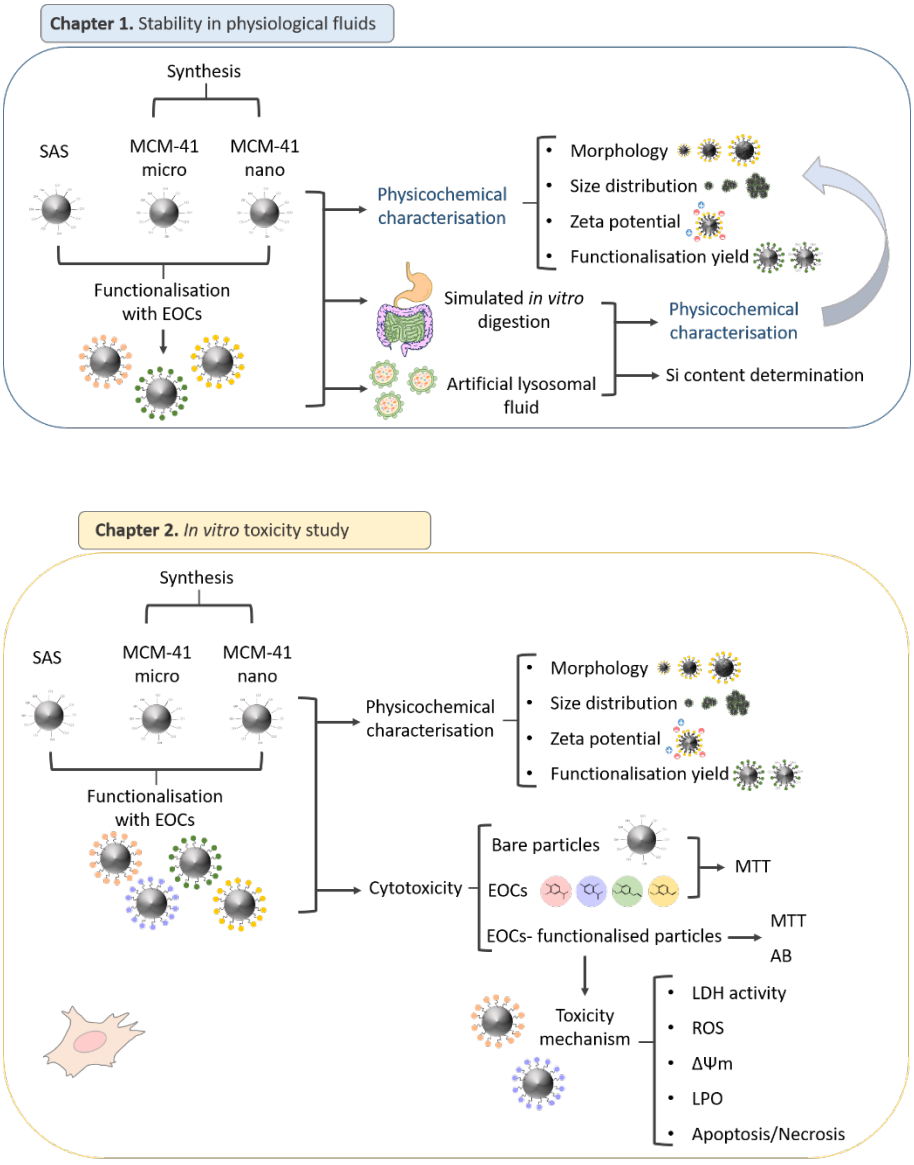

Figure 7. General outline of the experimental work (chapters 1 and 2).

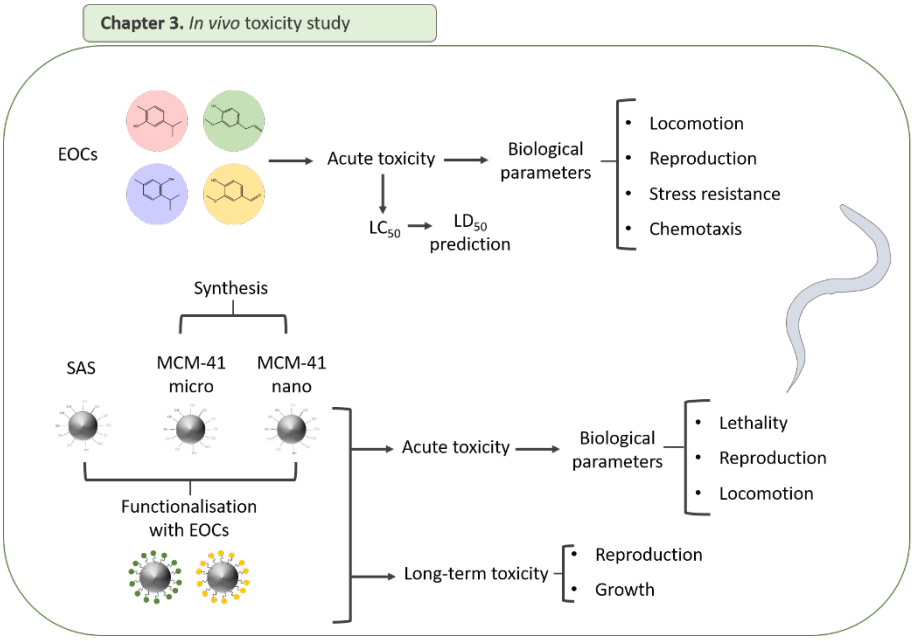

Figure 8. General outline of the experimental work (chapter 3).

Chapter 1

Stability in physiological fluids

Article 1

Fuentes, C., Ruiz-Rico, M., Fuentes, A., Ruiz, M. J., & Barat, J. M. (2020). Degradation of silica particles functionalised with essential oil components under simulated physiological conditions. *Journal of Hazardous Materials*, 123120.

A first step to evaluate the potential toxicity of new materials' exposure is to investigate the physico-chemical transformations that they can undergo under physiological conditions. An important parameter associated with the possible health hazards of materials is biopersistence (De Meringo et al., 1994). Biopersistence is the capacity of particles and fibres to withstand physiological clearance mechanisms and to remain inside the organism. A crucial material property that determines biopersistence is biodurability, which consists in exogenous particles' ability to resist chemical and biochemical alterations through dissolution and enzymatic biodegradation or chemical disintegration (OECD, 2018).

It is generally assumed that particles with low biodurability (e.g. they rapidly dissolve under physiological conditions) present low biopersistence and are, therefore, less toxic than particles with high biodurability, which tend to accumulate inside the organism and produce tissue injury (Di Giuseppe, 2020). Indeed, materials with low biodurability can cause short term toxicity and health effects, while materials with high biodurability can produce both short- and long-term health effects and show high environmental persistency (OECD, 2018). Therefore, the study of materials' biopersistence and biodurability provides useful information to predict their long-term toxicity during risk assessments (De Meringo et al., 1994; OECD, 2018).

Biopersistence is evaluated using *in vivo* animal experiments, while biodurability is measured by *in vitro* cellular and acellular tests (OECD, 2018). Although *in vitro* experiments do not completely mimic *in vivo* conditions and cannot fully substitute *in vivo* experiments, they help to predict biopersistence in a fast cost-effective and controlled manner (Gualtieri et al., 2018; Utembe et al., 2015). *In vitro* cellular tests investigate the dissolution rates of materials in different cell lines cultures, frequently macrophage cultures. For these experiments, cultured cells are exposed to particles, and the microscopic examination of intracellular materials is performed to determine

changes in their diameter and composition (Utembe et al., 2015). The acellular *in vitro* assessment of particles' biodurability is conducted by measuring particles' stability after exposure to experimental physiological solutions that simulate the conditions that they can encounter once inside the body. These artificial extracellular and intracellular physiological fluids vary under solution composition and pH conditions. Some of the most widely used solutions include: Gamble's solution as a surrogate for the interstitial fluid deep inside lungs; artificial lysosomal fluid that mimics the intracellular fluid within lysosomes after phagocytosis into cells; simulated gastric and intestinal fluids that simulate conditions occurring during the digestion process and phosphate buffer saline (PBS) and different cell culture media as standard physiological solutions (Calas et al., 2017; Stebounova et al., 2011; Stopford et al., 2003). Dissolution experiments are performed at 37 ºC to simulate human body temperature by either static or dynamic methods. In both methods, dissolution can be determined by measuring the total ion concentration released to the simulated body fluids and/or the change in sample mass or particles' diameter. Dynamic protocols use a continuous flow model in which particles are exposed to a large volume of biological fluid, and the concentration of the dissolved particle constituents is very low. In contrast with the static protocol, particles are exposed to a limited volume of simulated biological fluids in a beaker. Although dynamic tests better simulate *in vivo* conditions, static tests allow to more easily control experimental conditions and involve a slighter internal variation in the results (De Meringo et al., 1994).

Biodurability depends on not only the physico-chemical properties of particles and fibres, but also on the properties of biological media, such as ionic strength, pH or temperature (Braun et al., 2016; Stopford et al., 2003). Clear differences are seen in the dissolution rates of distinct amorphous silica particle types (Braun et al., 2016; He et al., 2010). Together with the nature of

the bulk material, other physico-chemical properties of particles, such as morphology, surface area, pore size, aggregation state or surface charge, have also demonstrated to influence the dissolution of silica particles (Croissant et al., 2018; Larson, 2010; Pérez-Esteve et al., 2016a). Moreover, as particles' surface directly interacts with biological media, surface modifications markedly determine their dissolution behaviour. Indeed, several studies have demonstrated that particle functionalisation with different functional groups results in a lower dissolution rate and, therefore, in these materials' increased stability in distinct simulated physiological fluids (Fashina et al., 2013; Izquierdo-Barba et al., 2010; Lin et al., 2011; Pérez-Esteve et al., 2016a). Hence studying the biodurability of modified silica particles seems mandatory to evaluate their potential toxicity and pathogenicity.

Degradation of silica particles functionalised with essential oil components under simulated physiological conditions

Cristina Fuentes[a], María Ruiz-Rico[a], Ana Fuentes[a], María José Ruiz[b], José Manuel Barat[a]

[a]Department of Food Technology, Universitat Politècnica de València. Camino de Vera s/n, 46022, Valencia, Spain: crifuelp@upvnet.upv.es

[b]Laboratory of Toxicology, Faculty of Pharmacy, Universitat de València, Av. Vicent Andrés Estellés s/n, 46100 Burjassot, Valencia, Spain

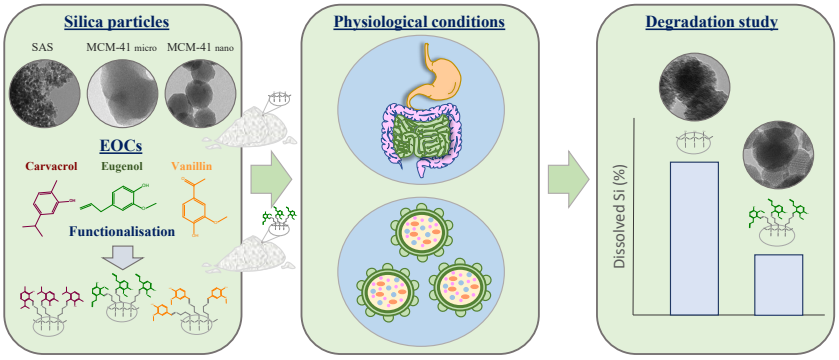

Abstract

In this work, the biodurability of three silica particle types (synthetic amourphous silica, MCM-41 microparticles, MCM-41 nanoparticles) functionalised with three different essential oil components (carvacrol, eugenol, vanillin) was studied under conditions that represented the human gastrointestinal tract and lysosomal fluid. The effect of particle type, surface immobilised component and mass quantity on the physico-chemical properties of particles and silicon dissolution was determined. Exposure to biological fluids did not bring about changes in the zeta potential values or particle size distribution of the bare or functionalised materials, but the *in vitro* digestion process partially degraded the structure of the MCM-41 nanoparticles. Functionalisation preserved the structure of the MCM-41 nanoparticles after simulating an *in vitro* digestion process, and significantly decreased the amount of silicon dissolved after exposing different particles to both physiological conditions, independently of the essential oil component anchored to their surface. The MCM-41 microparticles showed the highest solubility, while synthetic amorphous silica presented the lowest levels of dissolved silicon. The study of these modified silica particles under physiological conditions could help to predict the toxicological behaviour of these new materials.

Keywords: Silica; MCM-41; Functionalisation; *In vitro* digestion; Artificial lysosomal fluid

1. Introduction

Particle biodurability is defined as its ability to resist enzymatic biodegradation or chemical disintegration through dissolution, and is considered an important property that should be investigated to evaluate particles' toxicity (Utembe et al., 2015). Biodurability can be studied by the dissolution of materials in acellular physiological fluids that mimic intracellular or extracellular conditions. Of these, the degradation rate under conditions that represented the human gastrointestinal tract and lysosomal fluid is considered key information in the structured approach to identify and characterise toxicological hazards after oral exposure (Hardy et al., 2018). A simulated *in vitro* digestion process (SID) can be used to investigate the stability of particles under conditions that mimic the gastrointestinal tract. Once in the body, if the material does not quickly degrade, it may not be easily eliminated and can accumulate over time. The lysosome is the commonest intracellular compartment for particles sequestration and degradation. For this reason, artificial lysosomal fluid (ALF) that simulates the inorganic acidic environment within lysosomes has been widely used to study the durability of different materials after phagocytosis into cells (Cho et al. 2012; Henderson et al. 2014; Stebounova, Guio, and Grassian 2011).

Synthetic amorphous silica (SAS) has been used in a variety of oral applications, including foodstuffs (Pennington, 1991; Villota and Hawkes, 1986), pharmaceuticals (Colas and Rafidison, 2005) or dentistry materials (Lührs and Geurtsen, 2009). The presence of silanol groups (Si-OH) on the inner and outer surfaces of silica materials facilitates its chemical functionalisation by specific groups to increase their applicability (Diab et al., 2017). In the last few decades, mobile crystalline material 41 (MCM-41), an amorphous porous silica material, has been proposed for a wide range of new biotechnological applications (Flynn et al., 2019; Manzano et al., 2008; Pérez-Esteve et al., 2016b; Wang et al., 2009) due to its unique properties, such as

ordered structure, large surface area and big pore volume (Alothman, 2012). The dissolution behaviour of different types of SAS under biological-like conditions has been demonstrated to differ depending on the nature of the bulk material (He et al., 2011; Roelofs and Vogelsberger, 2004). Moreover, physico-chemical properties like size, morphology, surface area, pore size and surface modification influence the degradability of silica particles (Croissant et al., 2018). These changes may lead to altered toxicological effects compared to the corresponding bare materials (Lin et al., 2011), which indicates the need to develop a case-by-case study of the behaviour of modified materials under physiological conditions and their specific risk assessment.

The aim of the present work was to study the stability of different silica particles under simulated physiological conditions after oral exposure. In particular, we investigated the degradation behaviour of three types of silica particles (SAS, MCM-41 microparticles, MCM-41 nanoparticles) functionalised with three different essential oil components (EOCs: carvacrol, eugenol, vanillin) which were designed to be used as antimicrobial devices against food-borne pathogens and spoilage microorganisms (Ribes et al., 2017, 2019; Ruiz-Rico et al., 2017). For this purpose, the physico-chemical properties of the materials and the concentration of the dissolved silicon after an *in vitro* digestion process and under conditions representing lysosomal fluid, were determined.

2. Materials and Methods

2.1. Chemicals

Triethanolamine ($TEAH_3$), sodium hydroxide (NaOH), tetraethylorthosilicate (TEOS), *N*-cetyltrimethylammonium bromide (CTAB), paraformaldehyde, (3-aminopropyl) triethoxysilane (APTES), carvacrol (98% w/w), eugenol (99% w/w), hydrochloridric acid (HCl), pepsin,

bile extract and pancreatine (all three of porcine origin), and all the other reagents used to prepare SID solutions and ALF, were supplied by Sigma-Aldrich (Madrid, Spain). Vanillin was acquired from Ventós (Barcelona, Spain). Amorphous silica microparticles (SYLYSIA® SY350/FCP; 4 (0.1) μm) were purchased from Silysiamont (Milano, Italy). All the employed materials were of standard analytical grade.

2.2. Mesoporous silica particles synthesis

Mesoporous MCM-41 microparticles. The synthesis of the MCM-41 microparticles was carried out via the 'atrane route' using a molar ratio of reagents: 7 $TEAH_3$: 2 TEOS: 0.52 CTAB: 0.5 NaOH: 180 H_2O. To perform this reaction, a solution of NaOH and $TEAH_3$ was heated to 120 ºC and stirred at 300 rpm. The mixture was cooled to 70 ºC. After adding TEOS, temperature was increased to 118 ºC. CTAB was added to the solution, temperature was lowered again to 70 ºC and then 180 mL of distilled water were added by increasing the stirring speed to 600 rpm. A white precipitate formed and the solution was stirred for 1 h at room temperature. After this time, the suspension was placed in a Teflon container at 100 ºC and kept for 24 h to then be vacuum-filtered and the solid was washed with distilled water to a neutral pH. The obtained material was dried at 72 ºC for 24 h and calcined at 550 ºC in an oxidant atmosphere for 5 h to remove the organic template (MCM-41 micro).

Synthesis of mesoporous MCM-41 nanoparticles. For the synthesis of the MCM-41 nanoparticles, CTAB (2.74 mM) was dissolved in distilled water at 500 rpm and the NaOH solution (7 mM) was added. The mixture was kept at 80 ºC and stirring increased to 1,200 rpm. Then 22.39 mM of TEOS were added drop-wise and a white suspension formed. The reaction was left stirring at 80 ºC for 30 min. After this time, heat was turned off and the reaction was neutralised with 4 mL of the HCl 1M solution (pH~7). Finally, the solid

product was centrifuged at 9,500 rpm for 20 min, washed with deionised water and dried at 70 ºC. After drying, and like the MCM-41 microparticles, the resulting nanoparticles were calcined (MCM-41 nano).

2.3. Immobilisation of EOCs on the surface of particles and quantification

The functionalisation process of the silica particles with EOCs was done by a three-stage reaction (Fig. 1). First of all, the synthesis of aldehyde derivatives of carvacrol by direct formylation using paraformaldehyde and eugenol was performed according to the Reimer-Tiemann reaction. The presence of an aldehyde group in the vanillin structure allowed this stage to be avoided. In a second stage, the EOC-alkoxysilane derivatives were synthesised by the reaction of APTES with the aldehyde forms of carvacrol and eugenol or pure vanillin. Finally, the alkoxysilane derivatives were covalently anchored to the silanol groups present on the surface of the three different studied silica particles. The functionalisation process is fully described by García-Ríos et al. (2018).

The content of the EOCs grafted on the silica particle's surface was determined by the thermogravimetric analysis (TGA) and the elemental analysis. A TGA/SDTA 851e Mettler Toledo scale (Mettler Toledo Inc., Schwarzenbach, Switzerland) was used for the TGA analysis done with the samples in an oxidising atmosphere (air, 80 mL/min) with a heating programme (heating ramp of 10 ºC/min from 25 ºC to 1,000 ºC) and a heating stage. The elemental analysis for C, H and N was performed by a combustion analysis run in a CHNOS Vario EL III model (Elemental Analyses System GMHB, Langenselbold, Germany).

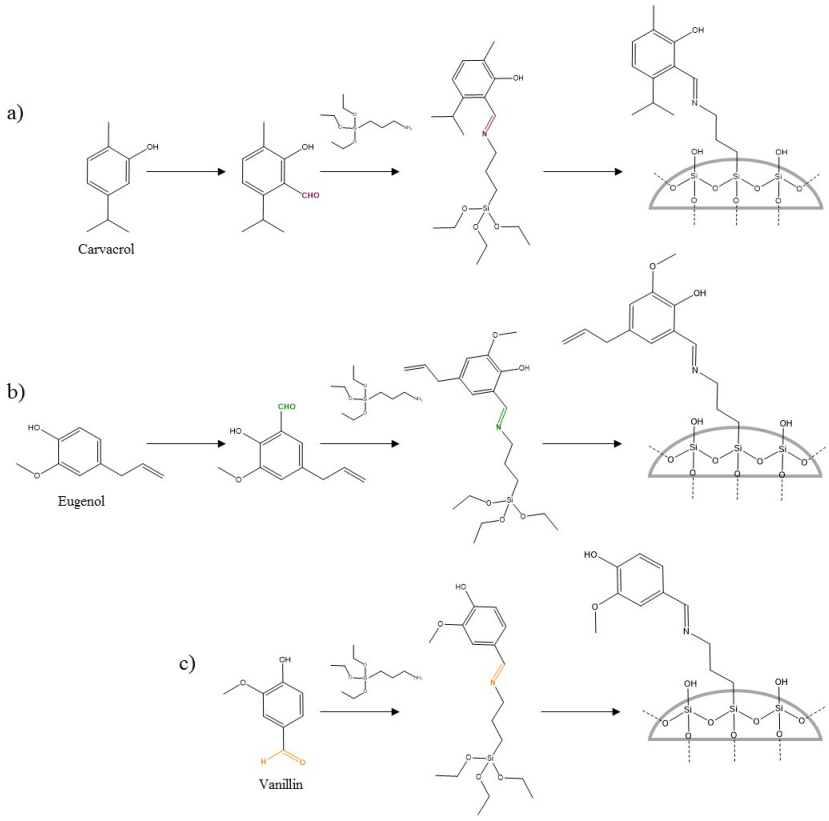

Fig. 1. Synthetic route for the formation of the carvacrol (a), eugenol (b) and vanillin (c) functionalised silica particles. Firstly, aldehyde derivatives of carvacrol and eugenol were synthesised (substitution at the ortho position provided as an example). Secondly the aldehydes of carvacrol and eugenol or pure vanillin were transformed into the corresponding alkoxysilane derivatives by a reaction with APTES. Finally, alkoxysilane derivatives were anchored to the surface of the three studied types of silica particles (SAS, MCM-41 micro, MCM-41 nano).

2.4. In vitro degradation tests

The stability of the different silica particles under two physiological conditions was investigated as an important factor that would influence the toxicity of these materials. Firstly, a stability study under the simulated gastrointestinal tract conditions was conducted to evaluate the degradation of particles after oral ingestion. Secondly, a degradation test under the simulated lysosomal conditions was performed to study the durability of particles after phagocytosis in cells. Dissolution studies were conducted with 11 different particle types: SAS microparticles without mesoporous structure, MCM-41 micro and MCM-41 nano, bare or functionalised with all three EOCs (carvacrol, eugenol, vanillin). Two different mass of particles were studied for each sample: 50 mg (C1) and 100 mg (C2). Each condition was tested in duplicate. A scheme of the experimental procedure herein followed is shown in Figure 2.

2.4.1. In vitro gastrointestinal digestion

A static *in vitro* digestion model was used to simulate the digestion of silica particles by the gastrointestinal tract. The *in vitro* digestion model consisted of three steps to simulate the physiological conditions of the human gastrointestinal tract: saliva, gastric, small intestine digestion. The standardised protocol based on an international consensus developed by the COST INFOGEST network (Brodkorb et al., 2019; Minekus et al., 2014) was employed with minor modifications. Briefly, particles were diluted in 5 mL of simulated salivary fluid (SSF) with 1.5 mM of $CaCl_2$. The mixture was stirred for 2 min and, due to small particle size, mastication was ignored. Subsequently, 5 mL of simulated gastric fluid (SGF) with 0.15 mM of $CaCl_2$ and the pepsin enzyme were added and incubated under agitation at pH 3.0 for 2 h. Finally, 10 mL of simulated intestinal fluid (SIG) with 0.6 mM of $CaCl_2$, bile salts and pancreatic enzymes were added and incubated at pH 7

for another 2-hour period. At the end of the digestion process, samples were adjusted to pH 5 to stop the digestion reaction and were then kept at -40 ºC until the analysis. Throughout the procedure, digestion tubes were orbitally stirred (100 rpm) at 37 ºC and the pH values of the digestive fluids were readjusted, if necessary, with NaOH (1 M) or HCl (6 M). The SID procedure is summarised in Figure S1. An *in vitro* digestion assay without enzymes and bile extracts was run in parallel to avoid the organic components interfering with the measurements of the particles' physico-chemical properties.

Digestive juices were prepared the day before and heated to 37 ºC before the experiment. The constituents and concentrations of the different simulated digestion fluids are fully described by Brodkorb et al. (2019).

2.4.2. Stability in lysosomal fluid

In order to assess the stability of the different silica particles under lysosomal conditions, dissolution in ALF was evaluated. The ALF solution was prepared in advance using the chemical composition and concentrations described by Stopford et al. (2003). The solution was heated to 37 ºC. Then 50 mL were added to each sample tube. Samples were continuously stirred at 100 rpm on an orbital shaker for the time that the experiment took. Solutions were monitored to note any pH changes occurring during the experiment. The control blanks, consisting solely of ALF, were sampled and continuously stirred in the same way as the test solutions. Three different time points were investigated: exposures of 24, 48 and 72 h. At each sampling point, samples were centrifuged at 9,500 rpm for 10 min and 5 mL of each supernatant were collected, while an equal volume of fresh ALF solution was added to each tube. At the end of the SID assay and after 72 h of the ALF treatment, particles were recovered by centrifugation (9,500 rpm; 10 min) for their characterisation. Supernatants were stored at -40 ºC until the analysis.

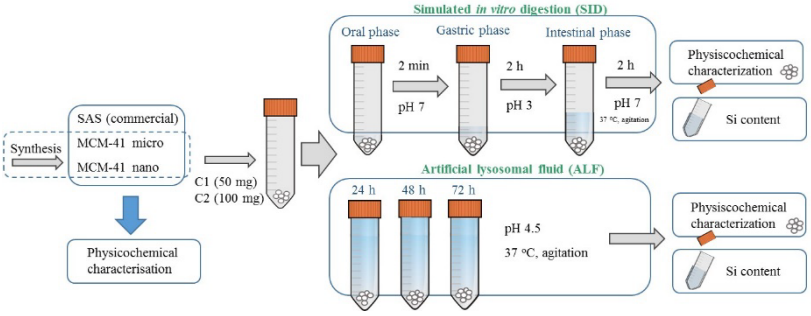

Fig. 2. Schematic representation of the experimental procedure.

2.5. Characterisation of silica particles

Materials were characterised before and at the end of the degradation tests (SID and 72 h of ALF) by three different techniques: transmission electron microscopy (TEM); zeta potential; dynamic light scattering (DLS). The TEM images were acquired by a Philips CM 10 microscope (Koninklijke Philips Electronics N.V., Eindhoven, the Netherlands) operating at an acceleration voltage of 80 kV. The zeta potential (ζ-potential) of the particles was measured by a Zetasizer Nano ZS (Malvern Instruments Ltd., Worcestershire, UK). Smoluchowski's mathematical model was used to convert the electrophoretic mobility measurements into ζ-potential values. Particle size distribution was studied by DLS using a laser diffractometer (Mastersizer 2000, Malvern Instruments Ltd., Worcestershire, UK). The Mie theory was applied by considering a refractive index of 1.45 for all the particles, and absorption indices of 0.01 and 0.1 for the SAS particles and the MCM-41 particles, respectively. For the zeta potential and particle size distribution measurements, samples were diluted in distilled water and sonicated in an ultrasonic bath for 2 min to prevent the agglomeration of particles. All the determinations were made in triplicate.

2.6. Quantification of the silicon content in biological fluids

Supernatants were analysed to determine the total concentration of free silicon in each sample. In the SID study, due to the organic matter content of samples, aliquots were previously subjected to an acid digestion process in a microwave oven at 180 ºC. Then the SID- and ALF-treated samples were all filtered and analysed by Inductively Coupled Plasma Mass Spectrometry (ICP-MS). An Agilent 7900 ICP-MS (Agilent Technologies LTd., CA, US) was used, equipped with a MicroMist nebulizer and a Scott spray chamber. The operating parameters were as follows; 1550 W of RF power, Ar gas flow rate 15 L/min, carrier gas flow rate 1.07 L/min. He and H_2 were employed as octopolar collision and reaction gases, respectively. The percentage of dissolved Si was calculated by determining the dissolved Si from the original silica mass. The results were corrected by subtracting the analytical signal of the blanks from each sample.

2.7. Statistical analyses

The effect of treatment, particle type, concentration and functionalisation on zeta potential, particle size distribution and Si content were determined by a multifactor analysis of variance (ANOVA). A statistical analysis was carried out using Statgraphics Centurion XVI (Statpoint Technologies, Inc., Warrenton, VA, USA). The LSD (least significant difference) procedure was used to test the differences between averages at the 5% significance level.

3. Results and Discussion

3.1. Content of EOCs on the particles' surface

The TGA and elemental analyses of the functionalised particles showed that the yield of the immobilisation process was higher for the MCM-41 micro (values within the 1.5%-15% range), followed by MCM-41 nano (from 0.7%

to 11%) and SAS (0.06% and 3%) for all the tested EOCs. The compound with the biggest anchorage yield was vanillin, followed by eugenol and carvacrol. The quantity of immobilised compound for each particle type was considered while calculating the fraction of Si dissolved in the degradation tests. For the SAS functionalised with carvacrol, the amount of immobilised compound was very small (0.06%). Therefore, this material type was not used for the subsequent analysis.

3.2. Characterisation of the bare and functionalised silica particles

The physico-chemical characteristics of the materials (e.g. morphology, particle size, surface charge) are major factors that affect their behaviour in biological systems and toxicity and should, therefore, be considered in their risk assessment.

Figure 3 shows the TEM images of the different bare and vanillin functionalised silica particles before SID and ALF exposure. The vanillin-functionalised particles were selected as an example because no differences were found between the different EOCs functionalised materials. The TEM images allowed us to observe the particle size, shape, porosity and internal structure of the materials. Information about the size and shape of the different silica particles is summarised in Table S1. Regarding the microstructure of the materials before both treatment types, SAS exhibited a globular sponge-like microstructure with smooth edges, MCM-41 micro were irregularly elongated and MCM-41 nano were uniformly spherical particles with a marked tendency to agglomerate. The TEM images of the MCM-41 particles also allowed us to observe the characteristic hexagonal structure of mesoporous materials as alternate black and white lines (Fig. 3). Moreover, when comparing particles before and after functionalisation, we observed that this process neither altered the morphology or size of all three types of silica particles, nor affected the pore channel structure or porosity of the MCM-41 mesoporous materials,

which confirms that their structure was preserved after the functionalisation process.

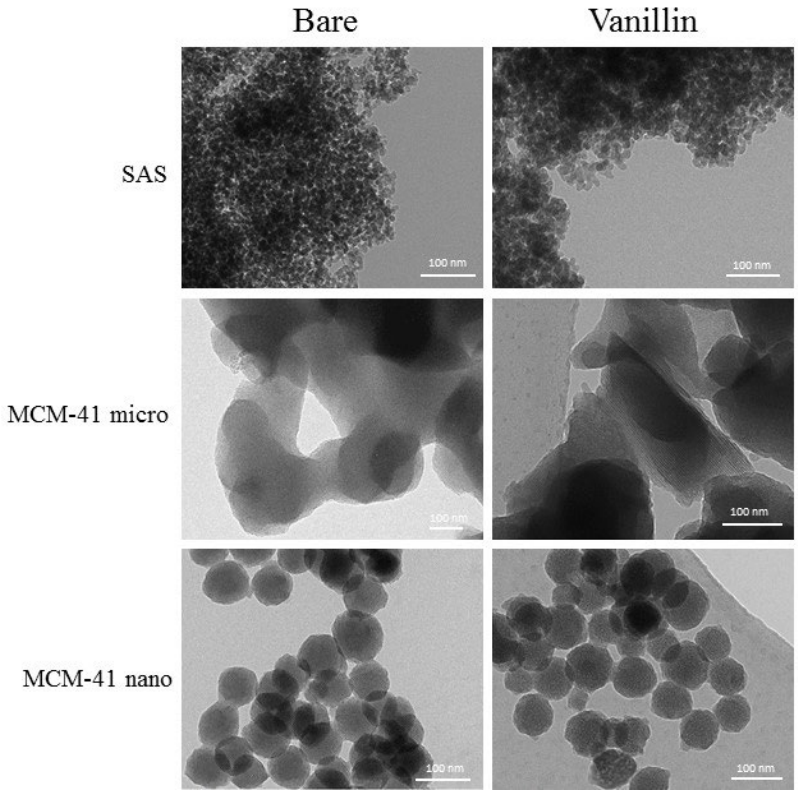

Fig. 3. Representative TEM images of the bare and vanillin functionalised SAS, MCM-41 micro and MCM-41 nano before SID and ALF exposures.

After SID or the 72-hour treatment with ALF, no changes in morphology, size or state of aggregation were observed for the bare or functionalised SAS and MCM-41 micro (Fig. 4). The TEM images revealed that the mesoporous structure of MCM-41 micro was preserved and no differences were found in the hexagonal network of the untreated and treated samples with both treatment types. However, for the bare MCM-41 nano, contact with the digestion fluids led to loss of textural properties. As seen in Figure 4, after the

SID procedure, the MCM-41 nano surface was partially degraded and became irregular shaped, although their ordered mesoporous conformation remained. Unlike the bare nanoparticles, the functionalised MCM-41 nano presented the same morphology, particle size and porous structure both before and after treating this material with digestion fluids. Thus, the immobilisation of the different EOCs on the surface of particles allowed their structure to be preserved during the SID process. Pérez-Esteve et al. (2016a) found that bare MCM-41 nanoparticles exhibited an evident degradation of their ordered structure, characterised by loss of specific surface area and pore volume as a result of the low pH of the gastric phase in the digestion process, while their microparticulated counterparts remained stable against degradation. These authors also found that the functionalisation of the silica MCM-41 nanoparticles with amines improved particle stability in the *in vitro* digestion procedure. The preservation of the mesoporous silica particles structure after organic functionalisation has also been observed by Izquierdo-Barba et al. (2010), who studied the long-term stability of bare and functionalised SBA-15 silica particles in different artificial physiological solutions. These authors reported the partial loss of the mesoporous structure of the unmodified particles, but the preserved structural properties of the SBA-15 particles functionalised with alkyl chains or aminopropyl groups.

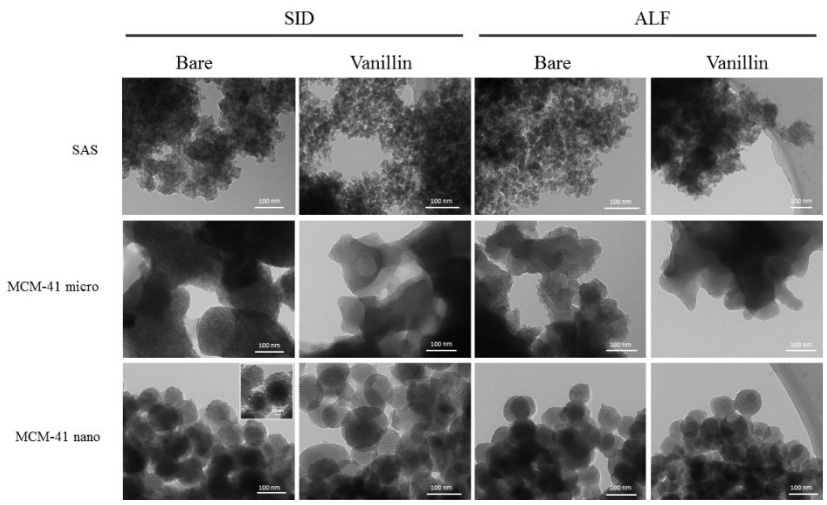

Fig. 4. Representative TEM images of the bare and vanillin functionalised SAS, MCM-41 micro and MCM-41 nano after SID and ALF exposure for 72 h.

The zeta potential values and particle size distribution of the bare and EOCs-functionalised particles before and after exposure to SID and 72 h of ALF are shown in Table 1. The effect of the different experimental factors (treatment, particle type, concentration and functionalisation) on both parameters was evaluated. The concentration of particles was not taken as a factor for the statistical analysis as it was previously verified that there are no significant differences ($p > 0.5$) between concentration levels.

The zeta potential results were significantly affected by all the studied factors and their interactions, and functionalisation was the most important factor (F-ratio = 12595.95). The most marked differences were found between the bare and functionalised particles, independently of the compound anchored to the surface of particles. The bared particles exhibited negative zeta potential values because silanol groups were present on their surface, while the functionalised materials obtained positive values because of the

grafting of the EOC-alkoxysilane derivatives. This change in the zeta potential values confirmed the efficiency of the functionalisation process. Moreover, the zeta potential values did not change after the treatment with biological fluids, which confirmed that anchored compounds were preserved. When the zeta potential value fell outside the instability range (± 30 mV), particles remained dispersed and suspended. When the zeta potential fell within this range, particles tended to agglomerate. So, all the analysed particles fell within or around this range, and tended to form agglomerates.

Table 1. The zeta potential and particle size distribution ($d_{0.5}$) values of the different bare and EOCs-immobilised silica particles before treatment (n.t.) and after dissolution in SID and ALF. Values are expressed as mean (SD).

		Zeta potential (mV)					$d_{0.5}$ (µm)				
			SID		ALF			SID		ALF	
Material	Functionalisation	n.t.	C1	C2	C1	C2	n.t.	C1	C2	C1	C2
SAS	Bare	-26.27 (2.31)	-28.08 (0.71)	-26.26 (0.68)	-18.31 (1.82)	-17.57 (1.22)	3.34 (0.03)	3.59 (0.19)	3.84 (0.18)	3.20 (0.12)	3.07 (0.03)
	Eugenol	8.95 (0.28)	2.70 (0.27)	2.23 (0.74)	5.38 (1.52)	5.03 (1.29)	4.05 (0.05)	3.68 (0.00)	3.95 (0.15)	4.06 (0.08)	4.10 (0.01)
	Vanillin	18.68 (1.44)	21.21 (0.79)	19.09 (1.63)	8.03 (0.99)	7.34 (0.64)	3.23 (0.03)	3.49 (0.03)	3.26 (0.31)	3.43 (0.04)	3.52 (0.07)
MCM-41 micro	Bare	-47.52 (1.79)	-33.63 (2.18)	-33.89 (2.18)	-22.96 (4.64)	-23.72 (1.55)	0.66 (0.01)	0.62 (0.02)	0.64 (0.00)	0.62 (0.01)	0.65 (0.03)
	Carvacrol	36.88 (1.08)	39.39 (4.73)	36.39 (2.55)	10.85 (0.62)	14.22 (0.75)	0.59 (0.00)	0.59 (0.01)	0.59 (0.00)	0.58 (0.00)	0.56 (0.01)
	Eugenol	5.34 (0.36)	4.61 (0.35)	-3.86 (1.93)	2.15 (1.06)	2.22 (0.19)	0.67 (0.01)	0.64 (0.01)	0.65 (0.01)	0.68 (0.06)	0.66 (0.00)
	Vanillin	39.83 (1.15)	41.27 (1.31)	38.37 (1.30)	17.34 (0.63)	17.14 (0.30)	0.59 (0.00)	0.61 (0.00)	0.61 (0.02)	0.62 (0.01)	0.63 (0.00)
MCM-41 nano	Bare	-37.60 (1.35)	-30.83 (1.91)	-33.08 (1.01)	-29.82 (4.94)	-28.71 (7.31)	4.92 (0.06)	4.82 (0.02)	4.80 (0.21)	4.95 (0.22)	4.89 (0.03)
	Carvacrol	22.82 (1.53)	29.44 (0.80)	30.73 (4.74)	12.79 (0.43)	12.80 (1.59)	3.37 (0.01)	3.03 (0.10)	3.04 (0.04)	3.25 (0.18)	3.33 (0.18)
	Eugenol	6.90 (0.78)	4.83 (1.14)	12.93 (3.32)	7.29 (2.25)	8.09 (3.23)	3.25 (0.07)	3.18 (0.01)	3.19 (0.10)	3.26 (0.11)	3.08 (0.06)
	Vanillin	29.19 (0.67)	27.02 (0.53)	31.32 (3.10)	13.02 (0.71)	10.05 (0.44)	0.70 (0.00)	0.68 (0.02)	0.69 (0.01)	0.70 (0.00)	0.70 (0.00)

Treating samples with ALF lowered the zeta potential values of particles, while the behaviour of the materials subjected to the SID process was similar to that of the untreated samples. Different properties of suspension media, such as pH, hardly influence the zeta potential values (Berg et al., 2009). In our study, the acidic nature of ALF facilitated the adsorption of ions of a complementary charge to the surface of particles by reducing the overall charge of materials, while the neutral pH of the intestinal phase of SID gave no significant differences to the untreated samples.

For particle size distribution, the most important factors were particle type, functionalisation, and the interaction between both. The particle size distribution analysis showed that the mean size of the bare SAS and MCM-41 micro was 3.34 (0.03) and 0.66 (0.01) μm, respectively. With MCM-41 nano, even though the individual mean diameter value found by TEM (64 (12) nm), the particle size distribution determined by DLS confirmed the strong tendency of this type of particles to agglomerate, and the secondary size diameter of the bulk material was 4.92 (0.06) μm. This trend to form large agglomerates found in MCM-41 nano could be explained by the stronger van der Waals forces and more marked Brownian movement found for smaller materials, which enhance interactions among particles (Oliveira and Andrada, 2019).

Regarding the effect of functionalisation on particle size distribution, the bare particles generally showed higher $d_{0.5}$ values than the functionalised materials. This effect was especially stronger for MCM-41 nano, for which particle size distribution lowered from 4.92 (0.06) to 0.70 (0.00) μm for the vanillin functionalised nanoparticles. This reduction in mean diameter size could be related to the steps included in the manufacturing of functionalised particles, such as milling or stirring, which could reduce the formation of agglomerates between adjacent particles.

Acidic conditions, the ionic strength of the solution or the presence of biopolymers have been demonstrated to promote particle agglomeration (McClements et al., 2017). However, in this study, exposure to SID and ALF did not modify the particle size distribution of the bare or functionalised materials. The results obtained for both treatment types were similar to those of the untreated samples, and revealed that the conditions used in these artificial media did not alter the primary size or state of aggregation of the analysed silica particles. Fashina et al. (2013) studied the dissolution of silica nanoparticles grafted with phthalocyanines on ALF. They observed that the aggregation level did not significantly change over a 96-hour period. Similarly, Sakai-Kato et al. (2014) found that silica hydrodynamic size was not affected by dispersion in fasted- and fed-state simulated gastric and fed-state simulated intestinal fluids. Consequently, other factors related to the properties of silica materials could also be responsible for the agglomeration state of particles under physiological conditions.

3.3. In vitro degradation of the bare and functionalised silica particles

The degradation of the silica particles under the SID and ALF conditions was measured by quantifying the free dissolved Si in biological fluids. Figure 5 illustrates the percentage of dissolved Si (g dissolved Si per 100 g of initial silica) after SID, and also after 24, 48 and 72 h of ALF treatment.

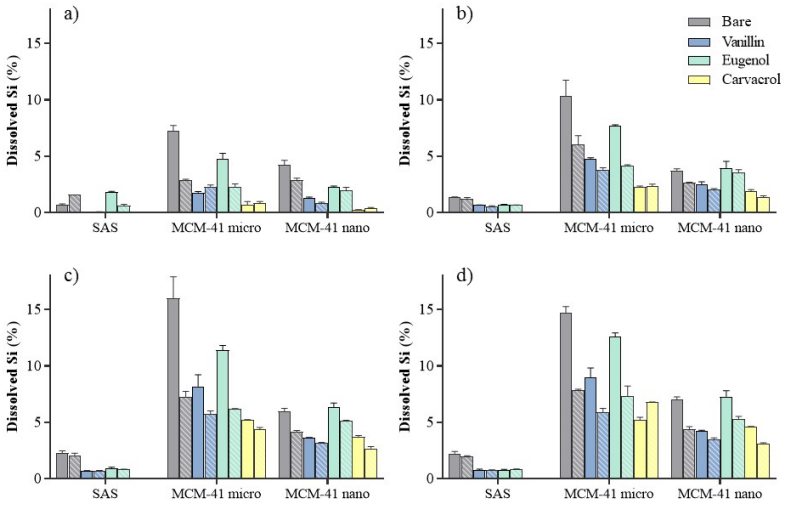

Fig 5. Percentage of dissolved Si after SID (a) and 24 (b), 48 (c) and 72 h (d) of ALF exposure. The plotted data represent the experimental results of three different particle types (SAS, MCM-41 micro, MCM-41 nano) at the C1 (straight bars) and C2 (dashed bars) particle concentrations.

The results obtained for both types of biological conditions were similar. Particle type was the most important factor to affect Si dissolution in SID (F-ratio = 267.75) and ALF (F-ratio = 1083, 85). Of the three types of silica particles herein analysed, MCM-41 micro showed the highest solubility, and reached a maximum percentage of 7.22 (0.5) under the SID conditions and 16.02 (1.89) after 48 h of the ALF treatment. In contrast, the lowest solubility levels went to SAS, with the Si content in dissolution falling within the 0.06-1.86% range for SID and within the 0.56-2.29% range for ALF. The lower solubility found for the SAS particles agrees with He et al. (2010), who observed lower degradation percentages and a milder degradation process for amorphous sol-gel derived silica than for MCM-41 particles in simulated biological fluids (pH 7.4, 37 ºC). The mild degradation behaviour found for

SAS particles was attributed to their non-mesoporous structure and smaller specific surface area. Different authors have pointed out that the most important variable to determine Si dissolution under experimental conditions is a larger surface area, which is usually related to a smaller particle size (Larson, 2010; Roelofs and Vogelsberger, 2004; Utembe et al., 2015). In this study, MCM-41 micro presented the narrowest hydrodynamic particle size distribution from all the studied materials and the highest solubility levels. Unlike what could be expected, loss of textural properties observed by TEM for the bare MCM-41 nano after SID (Fig. 4) did not correlate with a higher Si dissolved content. As previously mentioned, MCM-41 nano showed a high agglomeration tendency by reducing the surface of the mineral available to interact with the surrounding media, and explained the lesser degradation behaviour of these MCM-41 particles. Therefore, the surface erosion of this material type could be related not only to an increase in Si dissolution, but also to a reduction in the mechanical stability of particles and transformation into a new disorder phase (Pérez-Esteve et al., 2016a).

Functionalisation significantly reduced the amount of dissolved Si after exposure to both treatments, independently of the EOC anchored to the surface of particles. The carvacrol immobilised particles showed a lower Si dissolution level, while the eugenol functionalised particles were the least stable of all the functionalised materials. This increase in the stability of silica particles has also been observed after functionalisation with other organic groups. Lin et al. (2011) compared the stability of bare and pegylated mesoporous silica nanoparticles in two different biological media (PBS and DMEM). Their results showed that the amount of free Si was significantly lower for the modified nanoparticles. Interestingly, the pegylation of particles improved their biocompatibility and decreased macrophage uptake, which renders them more suitable for human applications. Izquierdo-Barba et al. (2010) studied the long-term stability of SBA-15 silica particles in three

different solutions that mimicked physiological fluids (a saline solution, an acellular aqueous solution similar to human plasma and DMEM) at 37 ºC. These authors found that the largest amount of lixiviated Si went to bare SBA-15, regardless of the tested media. In contrast, the functionalisation of SBA-15 particles with alkyl chains (methyl and octyl) and aminopropyl groups lowered the degradation rate compared to the unmodified SBA-15 and helped to preserve their structural properties. This reduction in the amount of Si dissolved in the media of the modified samples was attributed to the formation of an organic coverage, which would act as a protection barrier. Other authors have suggested that some molecules, such as amine groups, attached to the surface of particles would also be able to locally neutralise the acidic environment created by SGF (Pérez-Esteve et al., 2016a).

A lower initial concentration of particles led to a higher bulk degradation percentage. Other studies have also observed that an increased silica concentration reduces the overall amount of dissolved Si. Larson et al. (2010) found that a dissolved fraction of the 100 mg silica condition was 1.6-fold bigger that the dissolved fraction of 200 mg silica. He et al. (2010) also observed this phenomenon while studying the degradation behaviour of different MCM-41 types of mesoporous silica in simulated body fluid (SBF). In this media, a slow diffusion stage, caused by the deposition of a monolayer of calcium and magnesium species, was responsible for inhibiting silica dissolution. An increase in the initial silica concentration prolonged this degradation stage given the much bigger total surface area. Therefore, a much longer time was needed to cover the entire surface with calcium/magnesium silicates.

The solubility of silica particles depends on the pH of the dispersion medium and significantly increases under alkaline conditions. Larson et al. (2010) measured the dissolution rates of crystalline silica microparticles in a simulated lung fluid solution at different pHs over a 28-day period. These

authors found that the samples in solution at pH 7.5 exhibited dissolution rates that were 2.0-3.5-fold higher than those achieved at pH 6.5 and pH 6.0, respectively. Braun et al. (2016) studied the dissolution kinetics of mesoporous silica particles in different physiological media to find that the dissolution rate of materials was lower in SGF (pH 1.6) than in other simulated biological buffers (pH 7.25-7.40). These differences were explained by the increasing deprotonation of silanol groups and the hydrolysis of the Si–O–Si-bonds catalysed by OH-nucleophiles, which occurred under alkaline conditions. Accordingly, an increased dissolution of the different silica particles in the intestinal phase of the *in vitro* digestion procedure could be expected. However, in this study, all the materials presented higher levels of dissolved Si after the ALF exposure than under SID conditions, except for the eugenol immobilised SAS. In addition to pH, another important factor for determining the solubility of silica particles is the dispersion medium's composition. Together with alkali ions, the presence of Mg^{2+}, Ca^{2+} and Na^{+} ions, along with the presence of organic acid salts, enhance the dissolution rate of silica materials (Larson, 2010). So, ALF contains a higher concentration of Na^{+} and Mg^{2+} ions than SID fluids, and includes citric acid and different salts of organic acids like sodium citrate, lactate or pyruvate, among others. At the same time, significant differences in the degradation kinetics of silica materials have been found depending on whether proteins are present or absent in the dissolution medium (Izquierdo-Barba et al., 2010). Protein adsorption on the surface of particles may prevent Si leaching from the particles by reducing the dissolution of particles under SID conditions.

If we consider the exposure time of the particles in ALF, the analysis of the Si concentration in solution at the different time points revealed no significant differences between 48 and 72 h of exposure for the different materials. These results contrast with those reported by Fashina et al. (2013), who found that the solubility of silica nanoparticles in ALF still increased after

96 h exposure. However, lack of resemblance in the nature, size and agglomeration state of the bulk materials could be responsible for these differences. The increased Si dissolution observed between 24 and 48 h of ALF exposure, and the short duration of SID compared to ALF, could indicate that not only the chemical composition of dissolution media, but also exposure time, could be important factors for determining differences in particle dissolution between both treatment types.

4. Conclusions

Due to the potential applications in the food industry of the silica particles that are our study object, it is necessary to provide information about the fate of these materials under conditions that represent oral exposure in order to predict possible toxicological responses. Agglomeration state and dissolution behaviour are key properties for determining the toxic responses of particles. A poor agglomeration state of particles induces their bioaccumulation, while high dissolution behaviour induces the enhanced release of ions to medium. Both conditions are related to increased inflammatory responses. The results found in this study show that the agglomeration state of the different particle types did not change under physiological conditions, and that no nanosized particles formed. Nanoparticles may more easily cross the intestinal barrier after oral ingestion and reach cellular compartments and, therefore, more toxic effects can be expected. In contrast, microparticles are more likely to be eliminated while reducing the risk of these materials accumulating after oral ingestion. All the studied materials displayed low dissolution behaviour under both simulated conditions. However, SAS was the most stable material, followed by MCM-41 nano and finally by MCM-41 micro. These findings suggest that agglomeration state and surface area are the two main factors that determine the degradation behaviour of silica particles. Moreover, functionalisation of silica particles with EOCs gave lower dissolution levels

and, therefore, increased stability under both biological conditions. This effect could be attributed to the fact that EOCs derivatives immobilised on the surface of particles could act as a protection barrier by forming an organic coverage. Our results are relevant to understand the behaviour of these innovative silica particles under biological conditions and could help design new hybrid materials for oral applications. However, further research is necessary to study the stability behaviour of particles by considering the interactions of materials with components present in the food matrix or of the tissues that form the gastrointestinal tract. Safe applications of emerging materials should be guaranteed to minimise their impact on human health and the environment.

Acknowledgements

The authors gratefully acknowledge the financial support from the Spanish government (Project RTI2018-101599-B-C21 (MCUI/AEI/FEDER, EU)). Cristina Fuentes also thanks the *Generalitat Valenciana* for being funded by the predoctoral programme Vali+d (ACIF/2016/139). María Ruiz-Rico acknowledges the Generalitat Valenciana for her Postdoctoral Fellowship (APOSTD/2019/118).

References

Alothman, Z., 2012. A Review: Fundamental Aspects of Silicate Mesoporous Materials. Materials. 5, 2874–2902. https://doi.org/10.3390/ma5122874

Berg, J.M., Romoser, A., Banerjee, N., Zebda, R., Sayes, C.M., 2009. The relationship between pH and zeta potential of ~ 30 nm metal oxide nanoparticle suspensions relevant to in vitro toxicological evaluations. Nanotoxicology 3, 276–283. https://doi.org/10.3109/17435390903276941

Braun, K., Pochert, Alexander, Beck, M., Fiedler, Richard, Gruber, J., Lindén, M., 2016. Dissolution kinetics of mesoporous silica nanoparticles in different simulated body fluids. J. Sol-Gel Sci. Technol. 79, 319–327. https://doi.org/10.1007/s10971-016-4053-9

Brodkorb, A., Egger, L., Alminger, M., Alvito, P., Assunção, R., Ballance, S., Bohn, T., Bourlieu-Lacanal, C., Boutrou, R., Carrière, F., Clemente, A., Corredig, M., Dupont, D., Dufour, C., Edwards, C., Golding, M., Karakaya, S., Kirkhus, B., Le Feunteun, S., Lesmes, U., Macierzanka, A., Mackie, A.R., Martins, C., Marze, S., McClements, D.J., Ménard, O., Minekus, M., Portmann, R., Santos, C.N., Souchon, I., Singh, R.P., Vegarud, G.E., Wickham, M.S.J., Weitschies, W., Recio, I., 2019. INFOGEST static in vitro simulation of gastrointestinal food digestion. Nat. Protoc. 14, 991–1014. https://doi.org/10.1038/s41596-018-0119-1

Cho, W.-S., Duffin, R., Thielbeer, F., Bradley, M., Megson, I.L., MacNee, W., Poland, C.A., Tran, C.L., Donaldson, K., 2012. Zeta Potential and Solubility to Toxic Ions as Mechanisms of Lung Inflammation Caused by Metal/Metal Oxide Nanoparticles. Toxicol. Sci. 126, 469–477. https://doi.org/10.1093/toxsci/kfs006

Colas, A., Rafidison, P., 2005. Silicones in new pharmaceutical developments from formulations to manufacturing processes. Pharma. Chem. 4, 46–49.

Croissant, J.G., Fatieiev, Y., Almalik, A., Khashab, N.M., 2018. Mesoporous Silica and Organosilica Nanoparticles: Physical Chemistry, Biosafety, Delivery Strategies, and Biomedical Applications. Adv. Healthc. Mater. https://doi.org/10.1002/adhm.201700831

Diab, R., Canilho, N., Pavel, I.A., Haffner, F.B., Girardon, M., Pasc, A., 2017. Silica-based systems for oral delivery of drugs, macromolecules and cells. Adv. Colloid Interface Sci. 249, 346–362. https://doi.org/10.1016/j.cis.2017.04.005

Fashina, A., Antunes, E., Nyokong, T., 2013. Silica nanoparticles grafted with phthalocyanines: Photophysical properties and studies in artificial lysosomal fluid. New J. Chem. 37, 2800–2809. https://doi.org/10.1039/c3nj00439b

Flynn, J., Mallen, S., Durack, E., O'Connor, P.M., Hudson, S.P., 2019. Mesoporous matrices for the delivery of the broad spectrum bacteriocin, nisin A. J. Colloid Interface Sci. 537, 396–406. https://doi.org/10.1016/j.jcis.2018.11.037

García-Ríos, E., Ruiz-Rico, M., Guillamón, J.M., Pérez-Esteve, É., Barat, J.M., 2018. Improved antimicrobial activity of immobilised essential oil components against representative spoilage wine microorganisms. Food Control 94, 177–186. https://doi.org/10.1016/j.foodcont.2018.07.005

Hardy, A., Benford, D., Halldorsson, T., Jeger, M.J., Knutsen, H.K., More, S., Naegeli, H., Noteborn, H., Ockleford, C., Ricci, A., Rychen, G., Schlatter, J.R., Silano, V., Solecki, R., Turck, D., Younes, M., Chaudhry, Q., Cubadda, F., Gott, D., Oomen, A., Weigel, S., Karamitrou, M., Schoonjans, R., Mortensen, A., 2018. Guidance on risk assessment of the application of nanoscience and nanotechnologies in the food and feed chain: Part 1, human and animal health. EFSA J. 16. https://doi.org/10.2903/j.efsa.2018.5327

He, Q., Shi, J., Zhu, M., Chen, Y., Chen, F., 2010. The three-stage in vitro degradation behavior of mesoporous silica in simulated body fluid. Microporous Mesoporous Mater. 131, 314–320. https://doi.org/10.1016/J.MICROMESO.2010.01.009

He, Q., Zhang, Z., Gao, F., Li, Y., Shi, J., 2011. In vivo Biodistribution and Urinary Excretion of Mesoporous Silica Nanoparticles: Effects of Particle Size and PEGylation. Small 7, 271–280. https://doi.org/10.1002/smll.201001459

Henderson, R.G., Verougstraete, V., Anderson, K., Arbildua, J.J., Brock, T.O., Brouwers, T., Cappellini, D., Delbeke, K., Herting, G., Hixon, G., Odnevall Wallinder, I., Rodriguez, P.H., Van Assche, F., Wilrich, P., Oller, A.R., 2014. Inter-laboratory validation of bioaccessibility testing for metals. Regul. Toxicol. Pharmacol. 70, 170–181. https://doi.org/10.1016/j.yrtph.2014.06.021

Izquierdo-Barba, I., Colilla, M., Manzano, M., Vallet-Regí, M., 2010. In vitro stability of SBA-15 under physiological conditions. Microporous Mesoporous Mater. 132, 442–452. https://doi.org/10.1016/J.MICROMESO.2010.03.025

Larson, R., 2010. Assessing the Solubility of Silicon Dioxide Particles Using Simulated Lung Fluid. Open Toxicol. J. 4, 51–55. https://doi.org/10.2174/1874340401004010051

Lin, Y.-S., Abadeer, N., Haynes, C.L., 2011. Stability of small mesoporous silicananoparticles in biological media. Chem. Commun. 47, 532–534. https://doi.org/10.1039/C0CC02923H

Lührs, A.-K., Geurtsen, W., 2009. The Application of Silicon and Silicates in Dentistry: A Review, in: Biosilica in Evolution, Morphogenesis, and Nanobiotechnology (pp. 359–380). Springer, Berlin, Heidelberg. https://doi.org/10.1007/978-3-540-88552-8_16

Manzano, M., Aina, V., Areán, C.O., Balas, F., Cauda, V., Colilla, M., Delgado, M.R., Vallet-Regí, M., 2008. Studies on MCM-41 mesoporous silica for drug delivery: Effect of particle morphology and amine functionalization. Chem. Eng. J. 137, 30–37. https://doi.org/10.1016/J.CEJ.2007.07.078

McClements, D.J., Xiao, H., Demokritou, P., 2017. Physicochemical and colloidal aspects of food matrix effects on gastrointestinal fate of ingested inorganic nanoparticles. Adv. Colloid Interface Sci. 246, 165–180. https://doi.org/10.1016/J.CIS.2017.05.010

Minekus, M., Alminger, M., Alvito, P., Ballance, S., Bohn, T., Bourlieu, C., Carrière, F., Boutrou, R., Corredig, M., Dupont, D., Dufour, C., Egger, L., Golding, M., Karakaya, S., Kirkhus, B., Le Feunteun, S., Lesmes, U., Macierzanka, A., Mackie, A., Marze, S., McClements, D.J., Ménard, O., Recio, I., Santos, C.N., Singh, R.P., Vegarud, G.E., Wickham, M.S.J., Weitschies, W., Brodkorb, A., 2014. A standardised static *in vitro* digestion method suitable for food – an international consensus. Food Funct. 5, 1113–1124. https://doi.org/10.1039/C3FO60702J

Oliveira, D.M., Andrada, A.S., 2019. Synthesis of ordered mesoporous silica MCM-41 with controlled morphology for potential application in controlled drug delivery systems. Ceramica 65, 170–179. https://doi.org/10.1590/0366-69132019653742509

Pennington, J.A.T., 1991. Silicon in foods and diets. Food Addit. Contam. 8, 97–118. https://doi.org/10.1080/02652039109373959

Pérez-Esteve, É., Ruiz-Rico, M., de la Torre, C., Llorca, E., Sancenón, F., Marcos, M.D., Amorós, P., Guillem, C., Martínez-Máñez, R., Barat, J.M., 2016a. Stability of different mesoporous silica particles during an in vitro digestion. Microporous Mesoporous Mater. 230, 196–207. https://doi.org/10.1016/J.MICROMESO.2016.05.004

Pérez-Esteve, É., Ruiz-Rico, M., de la Torre, C., Villaescusa, L.A., Sancenón, F., Marcos, M.D., Amorós, P., Martínez-Máñez, R., Barat, J.M., 2016b. Encapsulation of folic acid in different silica porous supports: A comparative study. Food Chem. 196, 66–75. https://doi.org/10.1016/J.FOODCHEM.2015.09.017

Ribes, S., Ruiz-Rico, M., Pérez-Esteve, É., Fuentes, A., Barat, J.M., 2019. Enhancing the antimicrobial activity of eugenol, carvacrol and vanillin immobilised on silica supports against Escherichia coli or Zygosaccharomyces rouxii in fruit juices by their binary combinations. LWT 113, 108326. https://doi.org/10.1016/j.lwt.2019.108326

Ribes, S., Ruiz-Rico, M., Pérez-Esteve, É., Fuentes, A., Talens, P., Martínez-Máñez, R., Barat, J.M., 2017. Eugenol and thymol immobilised on mesoporous silica-based material as an innovative antifungal system: Application in strawberry jam. Food Control 81, 181–188. https://doi.org/10.1016/J.FOODCONT.2017.06.006

Roelofs, F., Vogelsberger, W., 2004. Dissolution Kinetics of Synthetic Amorphous Silica in Biological-Like Media and Its Theoretical Description. J. Phys. Chem. B 108, 11308–11316. https://doi.org/10.1021/jp048767r

Ruiz-Rico, M., Pérez-Esteve, É., Bernardos, A., Sancenón, F., Martínez-Máñez, R., Marcos, M.D., Barat, J.M., 2017. Enhanced antimicrobial activity of essential oil components immobilized on silica particles. Food Chem. 233, 228–236. https://doi.org/10.1016/J.FOODCHEM.2017.04.118

Sakai-Kato, K., Hidaka, M., Un, K., Kawanishi, T., Okuda, H., 2014. Physicochemical properties and in vitro intestinal permeability properties and intestinal cell toxicity of silica particles, performed in simulated gastrointestinal fluids. Biochim. Biophys. Acta - Gen. Subj. 1840, 1171–1180. https://doi.org/10.1016/J.BBAGEN.2013.12.014

Stebounova, L. V., Guio, E., Grassian, V.H., 2011. Silver nanoparticles in simulated biological media: a study of aggregation, sedimentation, and dissolution. J. Nanoparticle Res. 13, 233–244. https://doi.org/10.1007/s11051-010-0022-3

Stopford, W., Turner, J., Cappellini, D., Brock, T., 2003. Bioaccessibility testing of cobalt compounds. J. Environ. Monit. 5, 675–680. https://doi.org/10.1039/b302257a

Utembe, W., Potgieter, K., Stefaniak, A.B., Gulumian, M., 2015. Dissolution and biodurability: Important parameters needed for risk assessment of nanomaterials. Part. Fibre Toxicol. 12, 11. https://doi.org/10.1186/s12989-015-0088-2

Villota, R., Hawkes, J.G., 1986. Food applications and the toxicological and nutritional implications of amorphous silicon dioxide. C R C Crit. Rev. Food Sci. Nutr. 23, 289–321. https://doi.org/10.1080/10408398609527428

Wang, G., Otuonye, A.N., Blair, E.A., Denton, K., Tao, Z., Asefa, T., 2009. Functionalized mesoporous materials for adsorption and release of different drug molecules: A comparative study. J. Solid State Chem. 182, 1649–1660. https://doi.org/10.1016/j.jssc.2009.03.034

Supplementary material

EOCs and particles descriptors

Table S1. Descriptors of EOCs and silica particles used as indicators for bioaccumulation

Compound	Size[a] (Å)	MW (g/mol)	LogP[b]	PSA[b] (Å^2)	V[b] (Å^3)	Material	Size[c] (μm)
Carvacrol	8.121	150.22	3.81	20.23	158.57	***SAS***	2.63 (1.88)
Eugenol	8.293	164.20	2.10	29.46	162.14	***MCM-41 micro***	0.87 (0.31)
Vanillin	8.273	152.15	1.07	46.53	136.59	***MCM-41 nano***	0.06 (0.01)

[a]Chemdraw Software (PerkinElmer Inc.); [b]https://www.molinspiration.com/cgi-bin/properties; [c]Data measured by TEM.
MW (Molecular Weight); LogP (Octanol-water partition coefficient); PSA (Molecular Polar Surface Area); V (Molecular Volume).

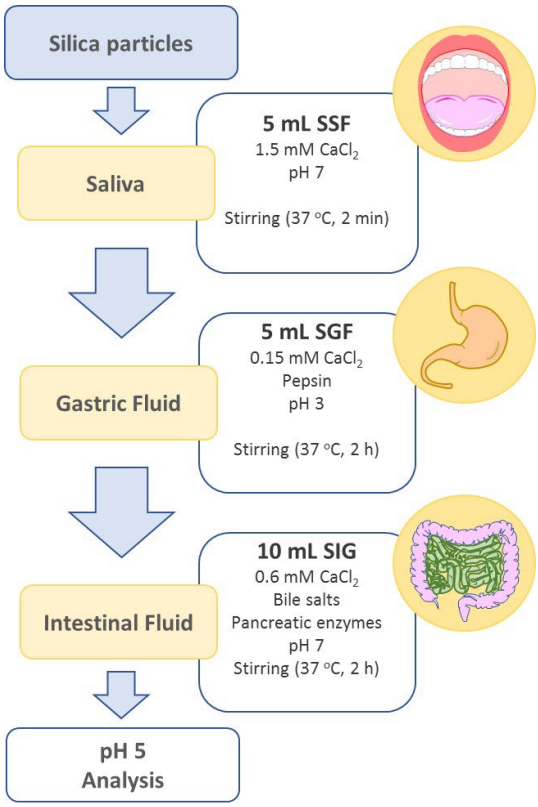

Fig. S1. Flow diagram of the three steps of the simulated *in vitro* digestion procedure. SSF: simulated salivary fluid; SGF: simulated gastric fluid; SIG: simulated intestinal fluid.

Characterisation of silica materials

Bare and EOCs-graphed silica materials were characterised by powder X-ray diffraction (PXRD) and Fourier transform infrared spectroscopy (FT-IR).

PXRD analysis

The synthesis process and the structure of the mesoporous materials were evaluated by PXRD. PXRD patterns were measured by a Bruker AXS D8 Advance diffractometer (Germany) with radiation CuKα (λ = 1.5406 Å).

Figures S2, S3 and S4 show the PXRD patterns of MCM-41 micro and MCM-41 nano as synthesised, calcined and after functionalisation with carvacrol, eugenol or vanillin, respectively. The PXRD patterns of the synthesised particles (a) showed the four low-angle reflections typical of the mesoporous hexagonal structure of MCM-41 materials, indexed as (1 0 0), (1 1 0), (2 0 0) and (2 1 0) Bragg reflections. After calcination (b), a shift in the d_{100} peak was observed, which corresponded to a cell contraction due to silanol coupling to MCM-41. After functionalisation, the preservation of peak d_{100} in the pattern of functionalised materials suggests that this process did not damage the mesoporous structure of particles. However, the reduction found in the diffraction of this peak demonstrated that a partial loss of the space in the pore structure occurred because EOCs-alkoxysilane derivatives were introduced.

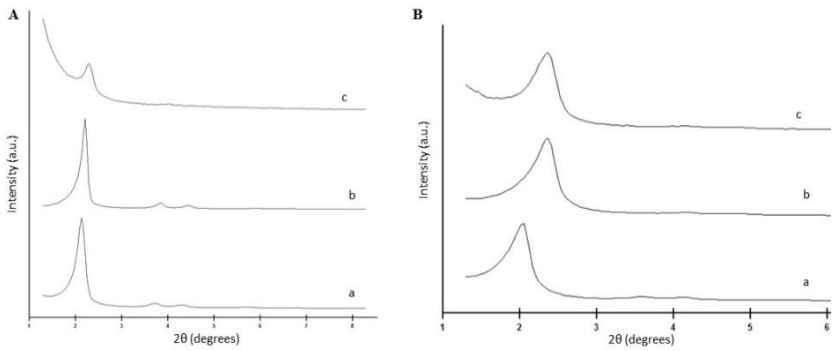

Fig. S2. PXRD patterns of synthesised (a), calcined (b) and carvacrol functionalised (c) MCM-41 micro (A) and MCM-41 nano (B).

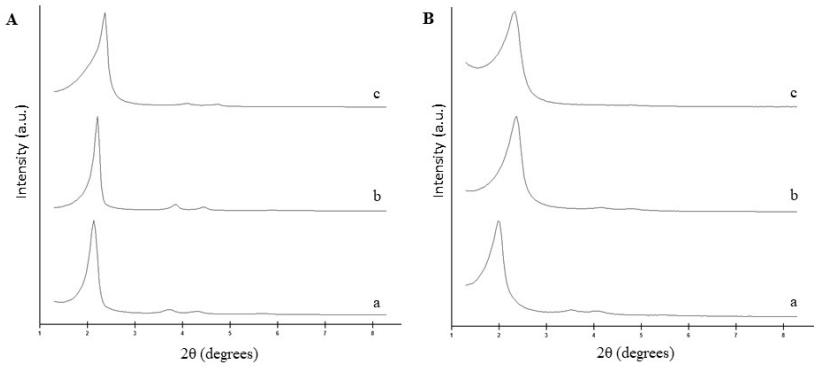

Fig. S3. PXRD patterns of synthesised (a), calcined (b) and eugenol functionalised (c) MCM-41 micro (A) and MCM-41 nano (B).

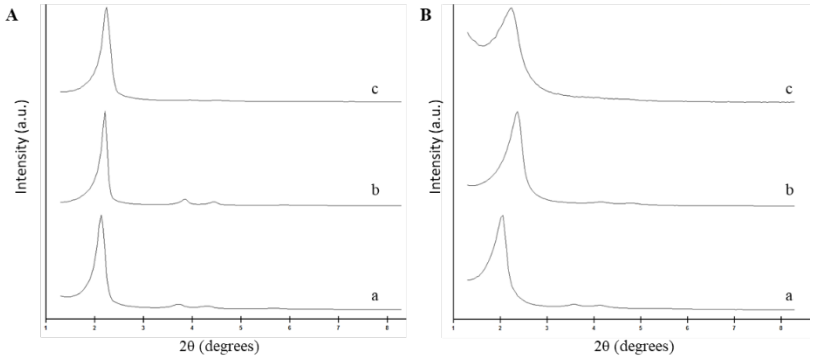

Fig. S4. PXRD patterns of synthesised (a), calcined (b) and vanillin functionalised (c) MCM-41 micro (A) and MCM-41 nano (B).

FT-IR spectroscopy

FT-IR was used to study the surface chemistry of silica particles. The FTIR spectra of the powder samples were recorded using the transmittance mode by a Bruker Infrared Spectroscopy Tensor 27 instrument (Massachusetts, US) within the wavelength range of 4000–400 cm^{-1}.

Figures S5, S6 and S7 report the IR spectra of the bare and EOC-functionalised silica particles. All the samples showed the characteristic absorption bands of silicon dioxide at 1080, 800, and 450 cm^{-1}, which respectively correspond to the modes of stretching, bending, and rocking of Si-O bonds. The presence of these bands in the functionalised particles confirmed the preserved structure in the modified silica materials. However, functionalisation led to an intensity change in the 1080 cm^{-1} band, which indicated a reduction in the free silanol groups due to the immobilisation of the EOCs-alkoxysilane derivatives. An observed deformation in this band may be attributed to an overlap with the bending vibrations of the phenolic hydroxyl group of the EOCs in the region 1410–1260 cm^{-1}. Moreover, the increase in the 800 cm^{-1} band may be associated with stretching vibrations of the benzene ring. In functionalised SAS and MCM-41 nano, the presence of a broad band from 3600 to 3000 cm^{-1} was associated with the stretching vibration of O-H and N-H bonds, and a band at 1637 cm^{-1} was associated with the C=C stretching of the aromatic ring, confirming the presence of the EOCs-alkoxysilane derivatives on the surface of silica particles.

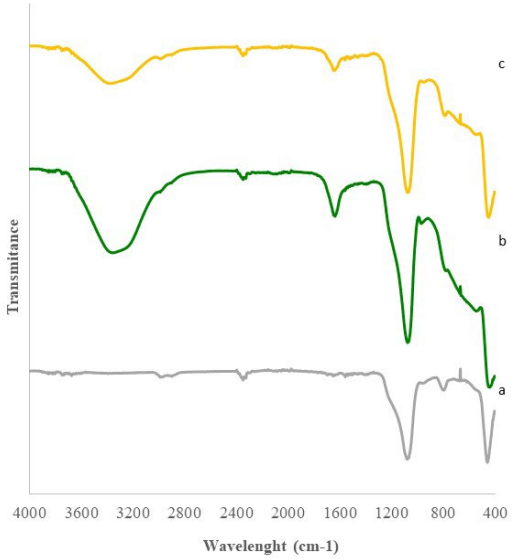

Fig. S5. FT-IR spectra of bare (a), eugenol (b) and vanillin (c) functionalised SAS.

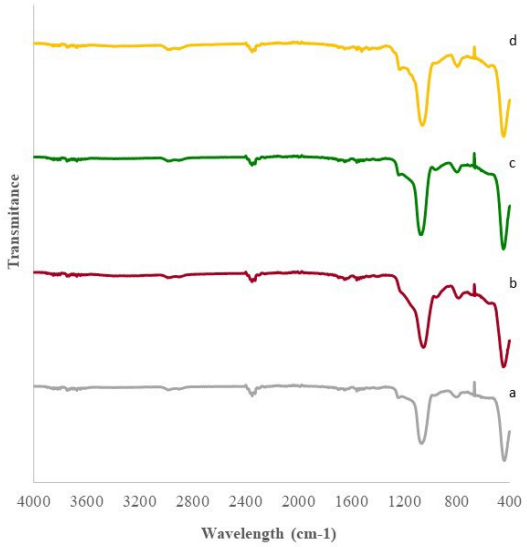

Fig. S6. FT-IR spectra of bare (a), carvacrol (b), eugenol (c) and vanillin (d) functionalised MCM-41 micro.

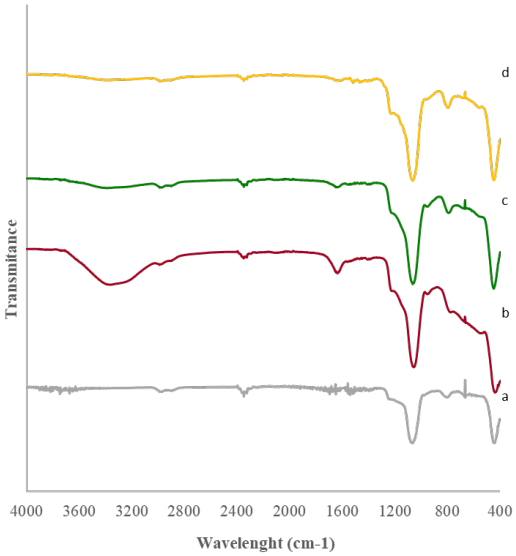

Fig. S7. FT-IR spectra of bare (a), carvacrol (b), eugenol (c) and vanillin (d) functionalised MCM-41 nano.

Chapter 2

In vitro toxicity study

Article 2

Fuentes, C., Ruiz-Rico, M., Fuentes, A., Barat, J. M., & Ruiz, M. J. (2021). Comparative cytotoxic study of silica materials functionalised with essential oil components in HepG2 cells. *Food and Chemical Toxicology*, 147, 111858.

Article 3

Fuentes, C., Fuentes, A., Byrne, H.J., Barat, J. M., & Ruiz, M. J. (2021). *In vitro* toxicological evaluation of mesoporous silica microparticles functionalised with carvacrol and thymol. Submitted to *Food and Chemical Toxicology,* 160, 112778.

The use of *in vitro* assays as an alternative method in toxicity testing is a relevant tool for enhancing our understanding of hazardous chemicals and predicting their effects on human beings during hazard and risk assessments (Eisenbrand et al., 2002). Cell culture assays allow the rapid identification of toxic compounds and can be employed to investigate toxicological mechanisms at cellular and subcellular levels. *In vitro* experiments exhibit a number of advantages as they are performed under controlled testing conditions in a particular environment, which results in simpler and more sensitive and reproducible tests than *in vivo* assays. They are less expensive and time-consuming than traditional animal experiments and allow a large number of compounds to be evaluated with only small amounts of test material. Most importantly, they allow shorter animal testing time, which meets the 3Rs principle. However, *in vitro* experiments also present limitations as chronic effects cannot be tested and they fail to completely replicate the conditions of cells in the organism, which limits the value of *in vitro* data to predict *in vivo* behaviour (Kandárová and Letaáiová, 2011).

In vitro toxicological assays can be used to determine basal cytotoxicity by measuring cell viability or cell death as a consequence of damage to basic cellular functions after acute exposure to cytotoxic compounds. *In vitro* cytotoxicity data are used to screen and rank chemicals (Eisenbrand et al., 2002), define the concentration range for mechanistic toxicity studies (Ciappellano et al., 2016), calculate starting doses for rodent acute oral toxicity tests (ICCVAM, 2006) and as a predictor of acute systemic toxicity *in vivo* (Severin et al., 2017). Moreover, these assays provide insight into the pathways and mechanisms of action involved in chemically induced toxicity at both molecular and cellular levels. Cytotoxicity tests are based on different cell functions, such as cell membrane permeability, enzyme activity, cell adherence, ATP production, co-enzyme production or nucleotide uptake activity, oxidative stress originated by nitric oxide (NO) and ROS

overproduction, DNA damage and mitochondrial dysfunction (Aslantürk, 2018; Zhang, 2018). Disturbances in cell homeostasis due to alterations to either of these processes can lead to cell death by necrosis or apoptosis (Miret et al., 2006). Depending on the investigated cellular process, *in vitro* assays can also suggest toxic compounds' mode of action.

Different compounds can cause cell toxicity by distinct mechanisms, and tested materials can interfere with the chemistry of some *in vitro* toxicity assays (Rampersad, 2012). Consequently, using a battery of toxicity endpoints that focuses on different cell metabolism aspects is necessary to provide a wide range of information to evaluate the potential cytotoxicity of compounds and to increase the robustness and reliability of the results (Miret et al., 2006).

Some of the most widely employed toxicity endpoints to determine basal toxicity and to study the underlying mechanisms of toxicity of chemicals are presented below.

MTT assay

The tetrazolium salts (MTT) assay is one of the most widely used methods to evaluate cell viability. In this method, yellow positively charged MTT (3-(4,5-dimethylthiazole-2-yl)-2,5-diphenyltetrazolium bromide) enters viable cells where it is metabolically reduced to the insoluble blue-violet form of formazan. As formazan crystals are not soluble in aqueous solutions, they have to be dissolved in organic solvents, such as DMSO, before absorbance is spectrophotometrically quantified (Mosmann, 1983). MTT are reduced by respiratory chain components, mainly by respiration (dehydrogenases mitochondria) and its electron flow, such as NADPH, FADH, FMNH and NADH, but not by cytochromes. Consequently, this method has been used as an indicator of mitochondrial function (Rampersad, 2012).

Alamar Blue assay

Similarly to the MTT method, the Alamar blue (AB) assay is a redox indicator of metabolic function. In viable cells, non-fluorescent blue molecule resazurin is chemically reduced to highly fluorescent pink resorufin. Resorufin quantification by either absorbance or fluorescent measurement allows modifications to be detected in the number of metabolic active cells after treatment with cytotoxic substances. Resazurin is reduced by both mitochondrial and cytoplasmic reducing agents by accepting electrons from NADPH, FADH, FMNH and NADH, as well as from cytochromes. Therefore, AB reduction is the result of multiple metabolic reactions in the cell, which broadly indicated cellular viability and does not specifically indicate a mitochondrial dysfunction (Rampersad, 2012). Unlike MMT assays, the soluble formazan products formed using AB do not require solubilisation with organic solvents that kill cells. This allows the continuous monitoring of cultures over time and multiplexed with other *in vitro* assays on the same plate (Aslantürk, 2018).

LDH assay

The lactate dehydrogenase (LDH) assay quantifies the cell death caused by cell membrane damage. LDH is a stable cytosolic enzyme present in all mammalian cells. When cell membrane integrity is altered or disrupted by exposure to cytotoxic substances, the enzyme is released from the cytosol of damaged cells to culture medium. LDH present in the supernatant can be quantified by a coupled enzymatic reaction. First of all, the released LDH catalyses the conversion of lactate into pyruvate by reducing NAD+ to NADH. Then oxidation of NADH by diaphorase leads to a reduction in yellow tetrazolium salt (INT) to a red formazan product that can be spectrophotometrically measured (Thermo Fisher Scientific, 2019).

Therefore, formazan production is proportional to released LDH that acts as an indicator of the cytotoxic effect of tested substances.

Mitochondrial membrane potential assay

The mitochondrial membrane potential (ΔΨm) is a key parameter for evaluating mitochondrial function and cell health. It is generated by proton pumps and is essential for the oxidative phosphorylation process (Zorova et al., 2018). Toxic substances can reduce ΔΨm by interacting with different macromolecules present in mitochondria, and lead to mitochondrial dysfunction and apoptotic processes (Sakamuru et al., 2016). In order to quantify changes in the ΔΨm of individual live cells or cells populations, permeant cationic fluorescent probes, together with fluorescence microscopy or spectroscopy, are widely employed (Solaini et al., 2007). These cell membrane permeable dyes, such as Rhodamine 123, accumulate in active mitochondria of healthy cells given their relative negative charge. However, ΔΨm decreases in inactive or depolarised mitochondria, which then fail to retain the probe and the fluorescence signal decreases (G-Biosciences, 2021). Reduced fluorescence is, therefore, used as an indicator of mitochondrial dysfunction and apoptosis.

Apoptosis and necrosis assay

Upon exposure to cytotoxic agents, cell death can occur mainly by two major mechanisms: necrosis and apoptosis. Necrosis consists in a rapid form of cell death induced by external injuries, such as hypothermia, radiation, hypoxia or chemicals that damage the cell membrane (D'Arcy, 2019). Destruction of the plasma membrane or the biochemical supports of its integrity leads to the release of intracellular material, local inflammatory responses, and cell swell and lysis. Necrosis is usually measured by the presence of the cytoplasmatic content in extracellular fluid, i.e. by measuring the activity of enzymes like LDH or adenylate kinase (Miret et al., 2006).

In contrast, apoptosis, or programmed cell death, is a slower form of cell death that can occur either under normal physiological conditions or be induced by apoptotic compounds. There are two pathways that lead to apoptosis: the extrinsic or death-receptor pathway that is activated from outside the cell by the ligation of transmembrane death receptors; the intrinsic or mitochondrial pathway that begins with the permeabilsation of the mitochondrial outer membrane triggered by different signals, such as DNA damage, ischaemia or oxidative stress (Wang and Youle, 2009). Apoptosis can be evaluated using different biomarkers like caspase activation, DNA fragmentation, changes in cell morphology, membrane rearrangements, cytochrome c release from mitochondria, among others (Eisenbrand et al., 2002).

A commonly followed method to differentiate necrotic and apoptotic cells consists in the Annexin V-FITC/PI apoptosis assay. An early event in apoptotic cells consists in the externalisation of membrane phospholipid phosphatidylserine from the inner to the outer leaflet of the plasma membrane. Phospholipid phosphatidylserine displays a strong binding affinity for Annexin V in the presence of calcium. The conjugation of this protein to fluorochromes like FTIC, together with the combination with a vital dye like propidium iodide (PI) that enters membrane-damaged cells, allows to differentiate among early apoptotic, late apoptotic, necrotic and viable cells by a flow cytometry analysis (Gel, 2012).

Oxidative stress: reactive oxygen species and lipid peroxidation

Oxidative stress consists in an imbalance between the production of oxidising molecular species and the antioxidants produced by cells for their removal. Under normal conditions, ROS species, such as superoxide anion (O_2•-), hydroxyl radical (OH•), or hydrogen peroxide (H_2O_2), are produced by cells as a result of aerobic metabolism (Ray et al., 2012). However, ROS production can drastically increase if toxic agents enter mitochondria and

block the electron flow by interacting with the electron-transport chain complexes in the inner mitochondrial membrane (Boelsterli, 2007). Moreover, given different particle properties, including their electronic and redox potential, or hydrophobic or hydrophilic interactions, ROS can also be produced on particles' surface (Santos et al., 2010). The overproduction of ROS and their accumulation in cells may lead to dysfunction of the antioxidant system, oxidative stress and oxidative damage to cellular macromolecules, such as proteins, fat, nucleic acids and carbohydrates, to cause severe cell toxicity. The quantification of these components is relevant in elucidating xenobiotics' mechanism of cytotoxicity. Accordingly, ROS generation and membrane lipid peroxidation (LPO) are two widely employed biomarkers to study the oxidative stress induced by toxic chemicals.

Dichlorofluorescein diacetate (DCFH-DA) is a ROS probe that undergoes intracellular deacetylation, followed by ROS-mediated oxidation to fluorescent species (λex. 485 nm and λem. 530 nm). DCFH-DA can be used to measure ROS generation in the cytoplasm and cellular organelles, such as mitochondria, by fluorescence intensity quantification.

If high ROS levels persist for a long period, oxidative stress may result in LPO. As a result of LPO, a number of oxidised products that can modify DNA, protein and other macromolecules are produced, including aldehydes like malondialdehyde (MDA) (Deavall et al., 2012). One of the most widely used assays to determine LPO and oxidative stress is the thiobarbituric acid reactive substances (TBARS) assay. This assay involves the reaction of MDA with thiobarbituric acid (TBA) in cell culture media and the cell lysate in a 1:2 ratio under acidic conditions and at high temperature to form MDA-TBA complexes called TBARS. TBARS yield a red-pink colour that can be spectrophotometrically measured and be expressed as MDA equivalents (Aguilar Diaz De Leon and Borges, 2020).

Comparative cytotoxic study of silica materials functionalised with essential oil components in HepG2 cells

Cristina Fuentes[a1], María Ruiz-Rico[a], Ana Fuentes[a], José Manuel Barat[a], María José Ruiz[b]

[a]Department of Food Technology, Universitat Politècnica de València. Camino de Vera s/n, 46022, Valencia, Spain

[b]Laboratory of Toxicology, Faculty of Pharmacy, Universitat de València, Av. Vicent Andrés Estellés s/n, 46100 Burjassot, Valencia, Spain

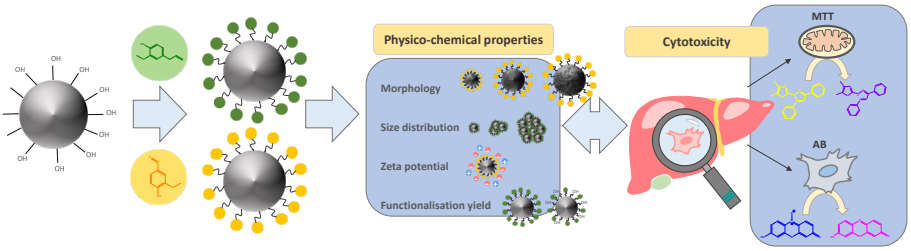

Abstract

This work evaluated the cytotoxic effect of different EOCs-functionalised silica particle types. The *in vitro* toxicity of eugenol and vanillin-immobilised SAS, MCM-41 microparticles and MCM-41 nanoparticles was evaluated on HepG2 cells, and compared to free EOCs and pristine materials. The results revealed that free essential oil components and bare silica had a mild cytotoxic effect on HepG2 cells. However, the comparative study showed that free eugenol and vanillin had a milder cytotoxic effect than the equivalent concentrations of immobilised components on the different silica particles, while differences in cell viability between the bare and functionalised particles relied on the type of analysed material. The most cytotoxic materials were eugenol and vanillin-functionalised MCM-41 micro with IC_{50} values of 0.19 and 0.17 mg/mL, respectively, at 48 h exposure. Differences in cytotoxicity between functionalised particles may be attributed to the density of the functional components on their surface as a result of the functionalisation reaction performance for different materials. The study of the physico-chemical properties of particles demonstrated that cationic nature and increased hydrophobicity could be responsible for promoting cell-particle interactions for the eugenol and vanillin functionalised silica particles, enhancing their cytotoxic behaviour.

Keywords: MCM-41; silica; eugenol; vanillin; cytotoxicity; HepG2

1. Introduction

Synthetic amorphous silica (SAS), in its fumed and hydrated forms, is a food additive (E551) authorised to be directly used in dry-powered food formulations and tablets as anticaking and antifoaming agents, or as a carrier in the preparation of food additives and nutrients (EU Commission, 2011a). For decades, SAS has been used with no clear evidence for adverse health effects. In fact, a recent re-evaluation of the safety of SAS by the EFSA Panel on Food Additives concluded that, based on available evidence, there was no indication of adverse effects for the reported uses and usage levels (Younes et al., 2018). However, the EFSA Panel emphasised the importance of considering the physico-chemical characteristics of the tested materials in their risk assessment as they may affect their biological behaviour. For this reason, any new SAS product that does not comply with specifications for bulk forms, or is designed for new technological functions in food, will require specific safety and risk assessments (Fruijtier-pölloth, 2016). Several authors have demonstrated that different types of surface chemical modifications induce distinct toxicological responses *in vitro*. Santos et al. (2010) studied the cytotoxicity of SAS microparticles on Caco-2 cells and found that the two main factors to affect cell viability were particle size and surface chemistry treatment. Thermally oxidised, thermally carbonised and thermally hydrocarbonised mesoporous silicon microparticles induce different toxic responses, and these effects are attributed to cell-particle surface interactions, which cause mitochondrial disruption as a result of ATP depletion and reactive oxygen species (ROS) production. Other processes, such as cellular uptake and localisation, are also regulated by different surface modifications (Slowing et al., 2006). Puerari et al. (2019) have demonstrated that primary and tri-amine functionalised SAS nanoparticles are more cytotoxic than pristine material to Vero cells due to increased ROS production and lipid peroxidation. These authors have hypothesised that functionalisation

promotes a *Trojan horse effect,* by means of which cells recognise molecules on the material's surface as nutrients, which facilitates entry in the cytosol. Conversely to this study, Yoshida et al. (2012) have found that functionalisation of nanosilica with amine or carboxyl groups results in lower cytotoxicity, ROS production and DNA damage in different cell lines, suggesting the surface functionalisation of silica nanoparticles to be a useful tool for developing safer materials.

The development of antimicrobial agents based on the immobilisation of essential oil components (EOCs) on the surface of different silica particles has emerged as a new tool to improve EOCs' antimicrobial activity and to reduce their sensorial impact on foods. These materials have proven effective against different bacteria, moulds and yeast *in vitro* (Ruiz-Rico et al., 2017), as part of different food matrices (Ribes et al., 2017), or as filtering aids for beverages (Peña-Gómez et al., 2020). At this point, the potential application of these emerging materials in the food industry requires toxicological studies to identify any possible hazards for human health associated with their use. In this context, the present work aimed to compare the cytotoxic effect of three different types of functionalised silica particles, designed as antimicrobial systems, to be applied in the food industry. In particular, the *in vitro* toxicity of eugenol and vanillin-immobilised SAS microparticles, MCM-41 microparticles and MCM-41 nanoparticles was evaluated on HepG2 cells and compared to the effect of free EOCs and pristine materials.

2. Materials and methods

2.1. Reagents

All the reagents and cell culture components were of standard laboratory grade. Synthetic amorphous silica (SAS) microparticles (SYLYSIA® SY350/FCP) were provided by Silysiamont (Italy). Acetonitrile, KOH, $MgSO_4$, HCl, $CHCl_3$, n-butanone, H_2SO_4 and dimethyl sulfoxide (DMSO)

were obtained from Scharlab (Spain). Vanillin (MW: 152.2 g/mol, purity ≥ 99%) was supplied by Ventós (Spain). Thiazolyl blue tetrazolium bromide (MTT), glycine, eugenol (MW: 164.2 g/mol, purity ≥ 98%), (3-aminopropyl)triethoxysilane (APTES), triethanolamine ($TEAH_3$), tetraethylorthosilicate (TEOS), hexadecyltrimethylammonium bromide (CTAB), NaOH, and all other reagents used in the synthesis and functionalisation of silica particles, were purchased from Sigma-Aldrich (Spain). Alamar Blue® (AB) reagent was acquired from Invitrogen (USA). Trypsin-EDTA 0.5%, antibiotics, newborn calf serum (NBCS), phosphate buffered saline (PBS) and Dulbecco's Modified Eagle Medium (DMEM-Glutamax™) with high glucose (4.5 g/L) and sodium pyruvate were supplied by Gibco (LifeTechnologies, USA).

Stock solutions of eugenol and vanillin (2.5 M) were prepared in DMSO and were left frozen until used. The final tested eugenol and vanillin concentrations were achieved by adding them to the culture medium at a final DMSO concentration ≤ 0.5% (*v/v*).

2.2. Cell culture

Human hepatocarcinoma (HepG2) cells (ATCC: HB-8065) were cultured in DMEM-Glutamax medium supplemented with 10% NBCS, 100 U/mL penicillin and 100 µg/mL streptomycin. The incubation conditions were pH 7.4, 5% CO_2 at 37 ºC and 95% air atmosphere at constant humidity. Cells were subcultured routinely twice weekly with only a few subpassages (< 40 subcultures) to maintain genetic homogeneity. HepG2 cells were subcultured after trypsinisation at the 1:3 split ratio. The medium was changed every 2-3 days. Absence of mycoplasma was checked routinely with the MycoAlert™ PLUS Mycoplasma kit (Lonza Rockland, USA).

2.3. Silica particles

2.3.1. Synthesis of MCM-41 particles

The synthesis of both types of MCM-41 mesoporous silica particles was performed using TEOS as the hydrolytic inorganic precursor and CTAB as the cationic surfactant agent. MCM-41 microparticles (MCM-41 micro) were synthesised by the "atrane route" using a molar ratio solution of 7 $TEAH_3$: 2 TEOS: 0.52 CTAB: 0.5 NaOH: 180 H_2O. Briefly, $TEAH_3$ and NaOH were heated to 120 ºC with stirring, the temperature was lowered to 70 ºC and TEOS was slowly added. After heating the mixture to 118 ºC, the temperature was lowered to 70 ºC, water was added and the white suspension that formed was stirred for 1 h without heating before being aged at 100 ºC for 24 h. For the synthesis of MCM-41 nanoparticles (MCM-41 nano), 1 g of CTAB was dissolved in 480 mL of deionised water with stirring. Then a solution of 7 mM of NaOH was added and the mixture was heated to 80 ºC. Stirring was increased and 22.4 mM of TEOS solution was added dropwise. The reaction was left stirring for 30 min and neutralised with 4 mL of HCl 1 M. For both materials, particles were recovered by centrifugation, washed repeatedly with deionised water and ethanol, and oven-dried at 70 ºC. Then dried solids were calcined at 550 ºC for 5 h to remove the template.

2.3.2. Silica particles functionalised with EOCs

The functionalisation of SAS, MCM-41 micro and MCM-41 nano with eugenol and vanillin was carried out by the method developed by García-Ríos et al. (2018). This method consists in a three- and two-stage protocol for eugenol and vanillin, respectively, as the presence of an aldehyde group in the vanillin structure avoids the first stage. Firstly, eugenol was transformed into its aldehyde derivative by a Reimer-Tiemann reaction. For this purpose, 22 mM of eugenol were dissolved in 150 mL of water at 80 ºC. The mixture was cooled at 60 ºC, and 400 mM of KOH and 88 mM of $CHCl_3$ were slowly

added, the latter at a rate of 1 mL/h. The solution was stirred at 60 ºC overnight. Next it was cooled and acidified with 50 mL of 10% H_2SO_4. The purification of the eugenol aldehyde was carried out by extraction with n-butanone and rotary evaporation. In a second stage, the alkoxysilane derivatives of eugenol and vanillin were formed via the reaction of the eugenol aldehyde or pure vanillin dissolved in dichloromethane, with 20 mM of APTES for 1 h at 38 ºC under reflux. Then solutions were rotary evaporated at 30 ºC. In a third stage, the alkoxysilane derivatives were immobilised on the surface of the different silica particles. For this purpose, 5 g of SAS, 5 g of MCM-41 micro or 1.5 g of MCM-41 nano were added to 120 mL of acetonitrile and the reaction was stirred for 5.5 h at room temperature. After centrifugation, the reduction of the imine bond of the vanillin functionalised materials was performed by adding an excess of sodium borohydride in 150 mL of methanol and stirring overnight. Finally, particles were washed with acetonitrile and distilled water (eugenol-functionalised materials), or with pH 4 distilled water (vanillin-functionalised materials), and dried in a vacuum for 12 h at room temperature.

2.3.3. Physico-chemical characterisation of silica particles

The bare and EOCs-functionalised silica materials were characterised by standard instrumental techniques. The morphological analysis of the silica materials was performed by transmission electron microscopy (TEM) with a Philips CM 10 microscope (Koninklijke Philips Electronics N.V, The Netherlands) operating at 80 kV. A Zetasizer Nano ZS (Malvern Instruments, UK) was used to determine the zeta potential of particles. This parameter was calculated from the particle mobility values using the Smoluchowski model. Particle size distribution was determined by a Malvern Mastersizer 2000 (Malvern Instruments, UK) and by applying the Mie theory (refractive index of 1.45, absorption index of 0.01 for SAS and 0.1 for the MCM-41 materials).

For the zeta potential and particle size distribution measurements, samples were dispersed in distilled water and sonicated for 2 min.

Thermogravimetric analysis (TGA) and elemental analyses were performed to quantify the concentration of the EOCs immobilised on the surface of the functionalised particles. The TGA was carried out on a TGA/SDTA 851e Mettler Toledo scale (Mettler Toledo Inc., Switzerland) in an oxidising atmosphere (air, 80 mL/min) with a heating programme (heating ramp of 10 ºC/min from 25 ºC to 1,000 °C) and a heating stage. The elemental analysis for C, H and N was carried out by a combustion analysis in a CHNOS Vario EL III model (Elemental Analyses System GMHB, Germany).

2.4. *In vitro* cytotoxicity

Cytotoxic effects were determined in HepG2 cells by the MTT and AB assays. They have been extensively used in *in vitro* toxicological studies to measure cell proliferation and survival. In the MTT assay, the soluble yellow tetrazolium salt is reduced to insoluble purple formazan by the mitochondrial NADH dehydrogenases present in viable cells (Holst & Oredsson, 2005). The AB assay determines cells' viability by reducing non-fluorescent blue resazurin, but only in the metabolically active cells, to a fluorescent pink resorufin. Due to the oxidation-reduction potential of resazurin, it can be reduced by all the components of the cellular respiration metabolic reactions (NADPH, FADH, FMNH, NADH as well as cytochromes), but also by the other enzymes located in the cytoplasm and mitochondria, such as reductases and diaphorases (Rampersad, 2012). Both redox assays determine cell viability by quantifying the metabolic activity of cells. However, while AB reduction is the result of multiple metabolic reactions within the cell, the MTT assay indicates a mitochondrial dysfunction (Davoren et al., 2007).

The MTT assay was performed according to Ruiz et al. (2006). Briefly, the HepG2 cells were grown in 96-well culture plates at a density of 1 x 10^5 and

3 x 10^4 cells/mL for 24-hour and 48-hour experiments, respectively. After cells reached 80% confluence, the culture medium was replaced with fresh medium containing serial dilutions of the tested compounds: from 0.3 to 5 mM (eugenol), from 0.9 to 15 mM (vanillin), from 0.11 to 28.5 mg/mL (bare SAS) and from 0.14 to 18.3 mg/mL (bare MCM-41 micro and MCM-41 nano). After 24 h or 48 h of exposure, the medium was removed and 200 µL of fresh medium were added to each well. Then 50 µL of MTT were added per well, and plates were returned to the incubator in the dark at 37 ºC, 5% CO_2 for 3 h. Next the MTT solution was discarded and 200 µL of DMSO were added, followed by 25 µL of Sorensen´s glycine buffer (glycine 0.1M, NaCl 0.1M, pH: 10.5 with 0.1 M NaOH). Plates were gently shaken for 10 min to achieve complete dissolution. Absorbance was measured at 570 nm by an automatic ELISA plate reader (Victor 3TM 1420, PerkinElmer, USA).

The cytotoxic effect of the functionalised materials was simultaneously determined by the AB and the MTT assays. When both methods were used, they were performed consecutively in the same plate, as described by Efeoglu et al. (2017). After growing cells on 96-well culture plates for 24 h, wells were washed with 100 µL of PBS and 100 µL of the test solution were added. Different ranges of the concentrations of the eugenol and vanillin functionalised SAS (0.02-10 mg/mL), eugenol functionalised MCM-41 micro and nano (0.005-2.5 mg/mL) and vanillin functionalised MCM-41 micro and nano (0.004-2 mg/mL) were assayed. Plates were incubated for 24 h or 48 h. During this time, neither the medium was, nor the tested compounds were, replenished. After incubation, the medium was removed and wells were washed with 100 µL of PBS. Then 100 µL of non-supplemented DMEM medium with 10% MTT stock solution (5 mg/mL in PBS) and 5% AB solution (v/v) were added. Plates were incubated (37 ºC, 5% CO_2, 3 h) and AB fluorescence was measured ($\lambda_{excitation}$=540, $\lambda_{emission}$=595 nm) by a microplate reader fluorometer (Fluoroskan Ascent, Fisher Scientific, Spain). Subsequently for the MTT assay, wells were washed with PBS and 100 µL of

DMSO were added. Then plates were shaken at 240 rpm for 10 min and absorbance was quantified at 570 nm.

For all the experiments, the control samples of each particle type were prepared by incubating the medium with particles in a non-cellular environment at all the tested concentrations (cell-free controls). All the solutions were prepared immediately prior to use and particles' suspensions were sonicated for 5 min before the experiments.

The final absorbance of the treated and unexposed cell wells was corrected for particle interference by subtracting the absorbance of the cell-free controls from the absorbance of the test wells.

For both the MTT and AB assays, cell viability was expressed as a percentage in relation to the control solvent (0.5% DMSO). Data were presented as the mean (SEM) of three independent experiments. The mean inhibition concentration (IC_{50}) values were calculated whenever possible by a non-linear regression test using version 8.0.1 of the GraphPad Prism software (GraphPad Software, USA).

2.5. Comparative evaluation of the toxic effects of EOCs, bare and functionalised silica particles

The MTT assay was used to determine and compare the toxic effects of eugenol, vanillin and the bare and EOCs-functionalised SAS, MCM-41 micro and MCM-41 nano. In the comparative studies, concentration ranges were selected by considering the IC_{50} values of eugenol and vanillin previously determined. The equivalent concentrations of particles were established based on the EOCs content in the functionalised materials determined by the TGA and elemental analyses. The grams of EOCs per gram of particle were calculated according to Ruiz-Rico et al. (2017). The assayed concentrations of the different components are shown in Table 1.

Table 1. Concentrations assayed in the comparative study of the eugenol (Eu), vanillin (Va), and bare and functionalised SAS, MCM-41 micro and MCM-41 nano.

	Concentrations			
	A	B	C	D
Eugenol (mM)	**0.5**	**1**	**2**	**4**
Bare SAS (mg/mL)	14.07	28.16	56.3	112.6
Bare MCM-41 micro (mg/mL)	1.86	3.73	7.45	14.94
Bare MCM-41 nano (mg/mL)	1.45	2.90	5.18	11.62
Eu SAS (mg/mL)	14.16	28.3	56.6	113.3
Eu MCM-41 micro (mg/mL)	1.95	3.90	7.80	15.60
Eu MCM-41 nano (mg/mL)	1.53	3.07	6.14	12.28
Vanillin (mM)	**1.25**	**2.5**	**5**	**10**
Bare SAS (mg/mL)	6.65	13.3	26.6	53.18
Bare MCM-41 micro (mg/mL)	1.52	3.04	6.08	12.16
Bare MCM-41 nano (mg/mL)	1.88	3.76	7.54	15.07
Va SAS (mg/mL)	6.84	13.7	27.4	54.70
Va MCM-41 micro (mg/mL)	1.71	3.42	6.84	13.68
Va MCM-41 nano (mg/mL)	2.09	4.14	8.29	16.57

2.6. Statistical analysis

The statistical data analysis was carried out using Statgraphics Centurion XVI (Statpoint Technologies, Inc., Warrenton, VA, USA). The differences observed between the cells exposed to test solutions and the control were analysed by the Student's *t*-test for paired samples. The differences between

functionalised silica particles' components were analysed by a one-way analysis of variance (ANOVA), followed by the LSD (least significant difference) *post hoc* test for multiple comparisons. Statistical significance was considered at $p \leq 0.05$.

3. Results

3.1. Physico-chemical characterisation of silica particles

Figure 1 shows the morphological characterisation of the bare and EOCs-functionalised silica materials. An irregular globular shape for SAS, but irregular and elongated for the MCM-41 micro, and homogeneous and round-shape for the MCM-41 nano, was evidenced. The individual particle size measured by TEM was 2.24 (0.80) μm, 1.22 (0.93) μm and 73.70 (12.80) nm for the bare SAS, MCM-41 micro and MCM-41 nano, respectively. No differences in either morphology or size were observed between the bare and functionalised silica particles. Additionally, the TEM images showed the well-defined hexagonal pore structure of the mesoporous MCM-41 materials in the form of parallel lines, which created channels in the bare and modified particles and confirmed that the mesoporous structure was preserved after functionalisation.

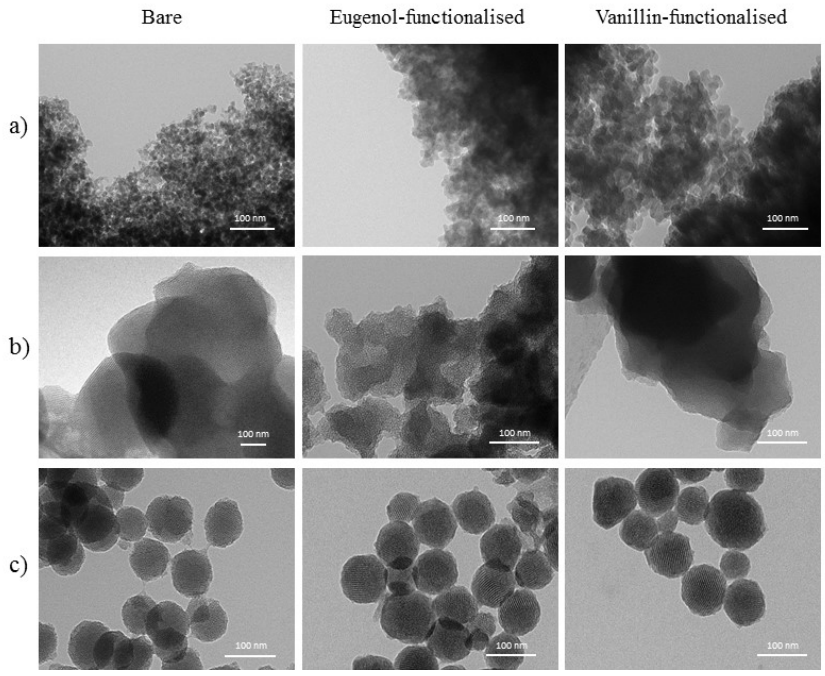

Figure 1. TEM images of the bare and EOCs-functionalised silica particles: a) SAS, b) MCM-41 micro and c) MCM-41 nano.

All the bare particles had negative zeta potential values due to the presence of silanol groups, while the functionalised materials presented positive values given the eugenol and vanillin alkoxysilane derivatives anchored to their surface (Table 2). This change in the zeta potential values confirmed the efficiency of the functionalisation method. Moreover, as all the particles analysed in this study were within or close to the instability range (+30 to -30 mV), formation of agglomerates and sedimentation of particles were expected.

The analysis of particle size distribution ($d_{0.5}$) showed that all the materials used in this study fell within the microscale size range (Table 2). The bare particles with the largest hydrodynamic particle size were the MCM-41 nano, followed by SAS and the MCM-41 micro. As the TEM analysis of the MCM-41 nano found a primary particle size within the range from 60 to 87 nm, these

results denote the marked tendency of this type of material to form large agglomerates.

Table 2. Zeta potential (ZP) values and particle size distribution ($d_{0.5}$) of the different bare and EOCs-functionalised particles. Values are expressed as mean (SD) (n=3).

Particle type	**Functionalisation**	**ZP (mV)**	**$d_{0.5}$ (µm)**
SAS	Bare	-19.36 (2.15)	3.02 (0.05)
	Eugenol	9.39 (0.40)	3.13 (0.00)
	Vanillin	28.96 (1.15)	2.33 (0.00)
MCM-41 micro	Bare	-42.07 (0.56)	0.67 (0.00)
	Eugenol	8.07 (2.21)	0.64 (0.00)
	Vanillin	43.22 (3.45)	0.61 (0.00)
MCM-41 nano	Bare	-43.10 (0.25)	4.79 (0.00)
	Eugenol	19.10 (0.32)	2.99 (0.01)
	Vanillin	23.00 (0.35)	0.70 (0.00)

The amount of functionalised particles needed to obtain the equivalent concentrations of free EOCs during the cell viability assays was determined by the TGA and the elemental analysis. As shown in Table 3, SAS presented the least functionalisation performance from the three studied types of silica particles. In addition, vanillin anchoring achieved higher functionalisation yields than eugenol, with differences of up to 5-fold bigger for SAS.

Table 3. Eugenol or vanillin content (α) in the functionalised SAS, MCM-41 micro and MCM-41 nano.

Particle type	$\alpha_{eugenol}$ (g/g SiO_2)	$\alpha_{vanillin}$ (g/g SiO_2)
SAS	0.0062	0.0318
MCM-41 micro	0.0479	0.1550
MCM-41 nano	0.0642	0.1130

3.2. Cell viability assays

3.2.1. IC_{50} determination of EOCs, bare and functionalised materials

The cytotoxic effect of the eugenol, vanillin and bare silica particles on HepG2 cells was evaluated by the MTT assay for 24 h and 48 h to determine the molar concentration that reached 50% inhibition of cellular proliferation (IC_{50}). The concentration-response curves for the different components after 24 h and 48 h of exposure are shown in Figures 2 and 3.

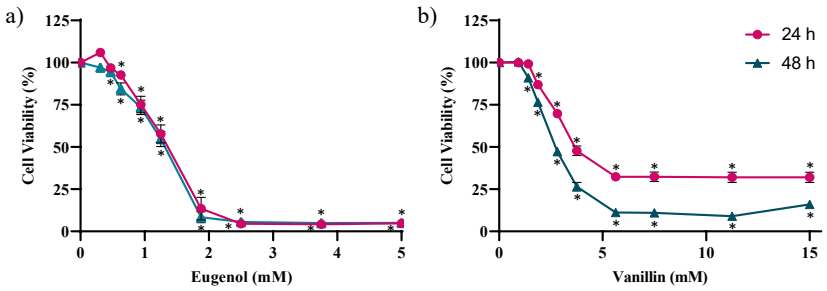

Figure 2. Concentration-effect curves of eugenol (a) and vanillin (b) in HepG2 cells after 24 h and 48 h of exposure by the MTT assay. The results are expressed as a percentage of cell viability in relation to the untreated controls and are represented as the mean (SEM) of three independent experiments, each carried out 6-fold. (*) $p \leq 0.05$ indicates significant differences compared to the control.

Cells exposed to eugenol and vanillin revealed diminished cell viability in a concentration-dependent manner (Fig. 2), with eugenol being the most cytotoxic essential oil in HepG2 cells. The IC_{50} values for eugenol were 1.29 (0.10) mM and 1.27 (0.10) mM at 24 h and 48 h, respectively, while the IC_{50} values obtained by vanillin for both exposure times were 2.87 (0.13) mM and 2.53 (0.10) mM.

The cells exposed to bare silica particles presented reduced cell viability in a concentration-dependent manner by the MTT assay (Fig. 3). The bare SAS were the most cytotoxic in HepG2 cells, followed by the bare MCM-41 micro, and finally by the bare MCM-41 nano. The IC_{50} values for the bare SAS were 11.03 (3.52) mg/mL and 6.91 (1.78) mg/mL at 24 h and 48 h, respectively. Exposing HepG2 cells to the bare MCM-41 micro for 24 h and 48 h gave IC_{50} values of 18.90 (2.89) mg/mL and 15.82 (0.90) mg/mL, respectively. No IC_{50} value was obtained for the bare MCM-41 nano at any tested time within the range of evaluated concentrations. Moreover, the concentration-effect curves of the bare silica particles showed that low SAS and MCM-41 micro concentrations brought about a stimulatory response of the mitochondrial function in HepG2 cells (Fig. 3a and 3b).

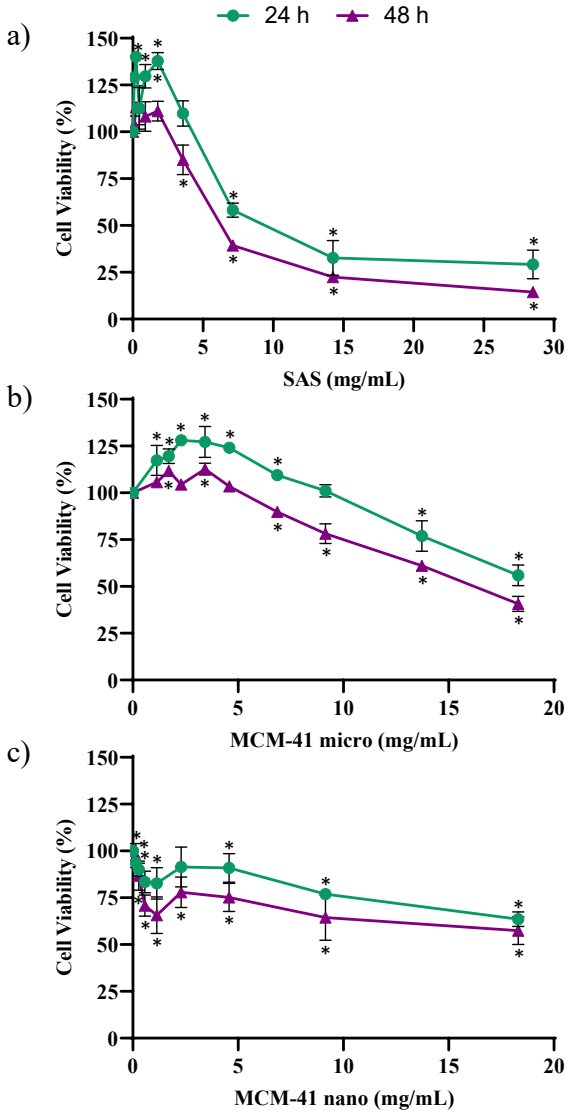

Figure 3. Concentration-effect curves of the bare SAS (a), bare MCM-41 micro (b) and bare MCM-41 nano (c) in HepG2 cells after 24 h and 48 h of exposure by the MTT assay. The results are expressed as a percentage of cell viability in relation to the untreated controls, and are represented as the mean (SEM) of three independent experiments, each carried out 6-fold. (*) $p \leq 0.05$ indicates significant differences compared to the control.

The comparative effect related to cell viability between functionalised silica particles was evaluated in HepG2 cells by the MTT and AB assays at 24 h and 48 h of exposure. The concentration-response curves are shown in Figure 4.

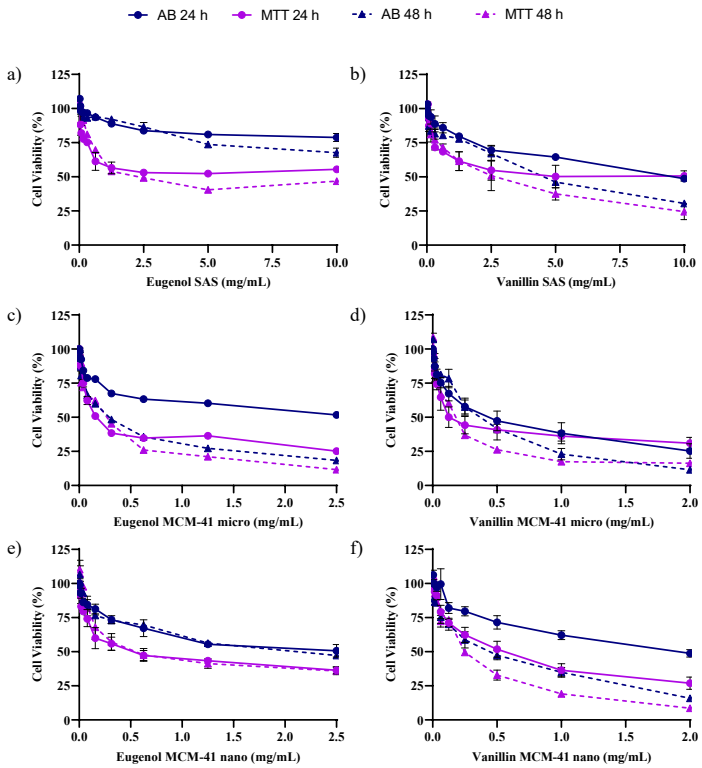

Figure 4. Concentration-effect curves of eugenol and vanillin funtionalised SAS (a and b), MCM-41 micro (c and d) and MCM-41 nano (e and f) in HepG2 cells after 24 h and 48 h of exposure by the MTT and AB assays. The results are expressed as a percentage of cell viability in relation to the untreated controls, represented as the mean (SEM) of three independent experiments, each carried out 6-fold. (*) $p \leq 0.05$ indicates significant differences compared to the control.

The IC_{50} values for the functionalised silica particles are shown in Table 4. The functionalised SAS particles displayed the least cytotoxic effect from the three types of silica materials, while functionalised MCM-41 micro were the most cytotoxic against HepG2 cells. In the case of MCM-41 nano the strongest cytotoxic effect was for the vanillin-functionalised particles after 48 h exposure. For the different functionalised materials, the strongest cytotoxic effect was observed by the MTT than by the AB assay according to the obtained IC_{50} values.

Table 4. IC_{50} (SEM, n=3) values of the eugenol and vanillin-functionalised silica in HepG2 cells by the MTT and AB assays at 24 h and 48 h of exposure.

EOCs-functionalised silica	**Assay**	**IC_{50} (mg/mL)**	
		Exposure time (h)	
		24	**48**
Eugenol SAS	MTT	5.45 (3.70)	3.18 (1.01)
	AB	> 10	> 10
Eugenol MCM-41 micro	MTT	0.24 (0.05)	0.19 (0.03)
	AB	2.47 (0.69)	0.27 (0.03)
Eugenol MCM-41 nano	MTT	0.58 (0.19)	0.68 (0.27)
	AB	2.32 (0.79)	1.93 (0.56)
Vanillin SAS	MTT	5.00 (3.00)	2.29 (0.69)
	AB	10.18 (2.91)	4.57 (1.36)
Vanillin MCM-41 micro	MTT	0.23 (0.09)	0.17 (0.03)
	AB	0.41 (0.10)	0.33 (0.06)
Vanillin MCM-41 nano	MTT	0.50 (0.10)	0.25 (0.03)
	AB	1.79 (0.74)	0.37 (0.07)

3.2.2. Comparative evaluation of the toxic effects of the EOCs, bare and functionalised silica particles

The concentration-response plots for the equivalent concentrations of the eugenol, eugenol-functionalised silica particles and bare silica particles in HepG2 cells after 24 h and 48 h of exposure are shown in Figure 5 (assayed concentrations are offered in detail in Table 1). Free eugenol exhibited a milder cytotoxic effect than eugenol-immobilised on silica particles' surface at concentrations below the IC_{50} value (concentrations A and B). When considering both exposure times, differences in cell viability between free eugenol and eugenol-functionalised materials ranged from 47% to 26% for SAS, and from 55% to 17% for the MCM-41 micro. Significant differences were also observed after 24 h of exposure to the lowest concentration of the eugenol functionalised MCM-41 nano (A). At the highest tested concentration (D), less than 94% of HepG2 cells survived after treatment with free eugenol or eugenol immobilised on SAS and MCM-41 nano at both exposure times.

Differences in cell viability between the bare and eugenol-functionalised particles depended on the analysed type of material. These differences ranged from 50% to 80% for the MCM-41 micro and from 43% to 57% for concentrations exceeding 6.14 mg/mL of the MCM-41 nano (C), whereas no significant differences in cell viability were observed for the lowest concentration (D) of the MCM-41 nano or SAS particles at any tested time. The eugenol-functionalised MCM-41 micro was significantly more cytotoxic than the bare MCM-41 micro at all the tested concentrations.

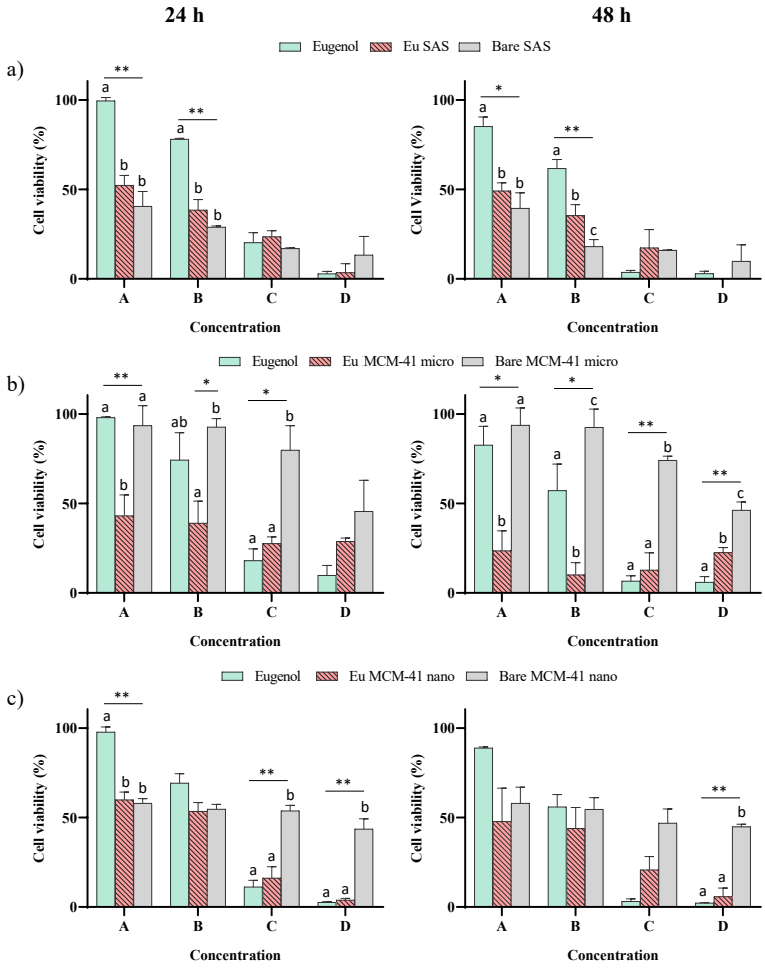

Figure 5. Concentration-cell viability plots of eugenol, bare and eugenol-functionalised SAS (a), MCM-41 micro (b) and MCM-41 nano (c) in HepG2 cells after 24 h and 48 h of exposure by the MTT assay. The results are expressed as a percentage of cell viability in relation to the untreated controls, represented as the mean (SEM) of three independent experiments, each carried out 6-fold. The bars with different letters (a-c) indicate significant differences (** $p \leq 0.01$, * $p \leq 0.05$). The bars with no letters correspond to non-significant differences ($p > 0.05$).

The comparative study of the vanillin-functionalised particles and their components gave similar results to those obtained for eugenol (Fig. 6). Free vanillin was less cytotoxic than the equivalent vanillin concentrations anchored to the different silica particles at the two highest studied concentrations (concentrations A and B in Table 1). Differences between free vanillin and vanillin-functionalised materials ranged from 40% to 37% for SAS, from 78% to 4% for MCM-41 micro and from 76% to 3% for MCM-41 nano after 24 h of exposure.

Both the bare and vanillin-functionalised silica particles presented a concentration-dependent effect on cell viability, but differences appeared depending on the type of material. No significant differences in cell viability were observed between the bare and vanillin functionalised SAS, but the vanillin-functionalised MCM-41 particles were significantly more cytotoxic than the bare MCM-41 at all the tested concentrations. The cell viability percentages ranged from 17% to 26% for 24 h exposure for the vanillin functionalised MCM-41 micro, while the bare MCM-41 micro only reduced cell viability to 57% at the maximum tested concentration. After exposure to the vanillin functionalised MCM-41 nano for 24 h and 48 h, cell viability ranged from 11% to 25% and from 8% to 22%, respectively. In contrast, bare MCM-41 nano did not present a concentration-dependent cytotoxic effect, and displayed a cell viability range from 45% to 59% after 24 h of exposure, and from 40% to 56% after 48 h.

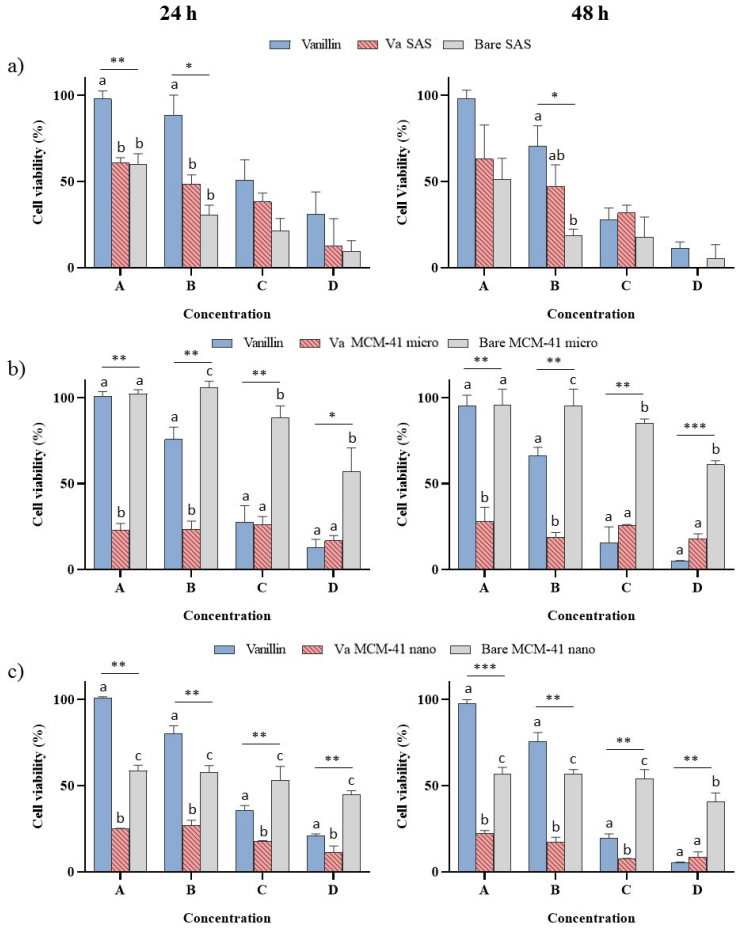

Figure 6. Concentration-cell viability plots of the vanillin functionalised SAS (a), MCM-41 micro (b) and MCM-41 nano (c) in HepG2 cells after 24 h and 48h of exposure by the MTT assay. The results are expressed as a percentage of cell viability in relation to the untreated controls, represented as the mean (SEM) of three independent experiments, each carried out 6-fold. The bars with different letters (a-c) indicate significant differences (***) $p \leq 0.001$, (**) $p \leq 0.01$, (*) $p \leq 0.05$, while the bars with no letters correspond to non-significant differences ($p > 0.05$).

4. Discussion

The presence of silanol groups on the surface of silica particles enables a wide variety of surface modifications by the covalent attachment of specific functional groups and organic molecules (Diab et al., 2017). This fact, along with their biocompatibility and low toxicity, make silica particles very interesting for designing hybrid materials in a number of oral applications (Bagheri et al., 2018; Ros-Lis et al., 2018). As surface properties are key factors for determining toxicological responses to particles (Vicentini et al., 2017), the study of the cytotoxicity aspects of modified silica structures will be crucial for successful applications.

Previously, the functionalisation of silica particles with EOCs has been demonstrated to prevent the degradation of materials under physiological conditions (Fuentes et al., 2020). However, lack of information about the toxicological behaviour of these materials indicates the need for specific toxicological evaluations. This paper describes the *in vitro* cytotoxicity assessment of different types of eugenol and vanillin-functionalised silica particles designed as antimicrobial systems to be applied in the food industry. This effect was compared with the cytotoxic behaviour of free EOCs and bare silica particles using HepG2 cells as an *in vitro* model system.

Eugenol and vanillin are both listed as "Generally Recognized as Safe" (GRAS) by the US Food and Drug Administration (FDA, 2020) and are included on the EU list of flavouring substances approved for use in foods without any specific restriction (EU Commission, 2011a). In this study, both EOCs reduced cell viability in a concentration-dependent manner. The cytotoxic effect on HepG2 cells was stronger with eugenol as vanillin presented an IC_{50} value, which increased by roughly 2-fold. A wide range of eugenol IC_{50} values can be found in the literature depending on the employed cell type. The IC_{50} values for eugenol ranged from approximately 0.75 mM in

osteoblastic cells (U2OS) (Ho et al., 2006) to 400 μg/mL (2.4 mM) in mesenchymal stem cells (MSCs) (Sisakhtnezhad et al., 2018) after 24 h of exposure, while an IC_{50} value as high as 285 mM has been found for human submandibular gland carcinoma (HSG) after 48 h of exposure (Fujisawa et al., 2002). With vanillin, the IC_{50} values after 72 h of exposure ranged from 200 μg/mL (1.31 mM) in HepG2 cells (Al-Naqeb et al., 2010) to 574.33 μg/mL (3.77 mM) in colorectal human cancer cells (HT-29) (Shakeel et al., 2016).

Bare silica materials also had a mild effect on HepG2 cell viability, as measured by the MTT assay. Some studies have suggested that the MTT method could fail to accurately predict the toxicity of mesoporous silica due to spontaneous redox reactions between particles and MTT (Braun et al., 2018). So cell-free controls were included in each experiment to avoid the potential influence of materials on cytotoxicity assays. The results evidenced no reaction between the MTT reagent and the bare MCM-41 particles, which could be explained by the completely oxidised SiO_2 surface of particles (Laaksonen et al., 2007).

Of the three different studied pristine particles, SAS was the most cytotoxic material, followed by MCM-41 micro and MCM-41 nano in that order. A mild cytotoxic effect was expected for the commercial SAS herein used as this hydrated silica form has been declared to meet the requirements for use in plastic, inks and other articles that are intended to come into contact with food according to EU regulations (EU Commission, 2011b). Despite the low SAS toxicity observed, our results were higher than those reported by Sakai-Kato et al. (2014), who studied the cytotoxicity of different sized SAS in Caco-2 cells by the WST-8 assay. These authors did not observe any cytotoxic effect for particles larger than 100 nm, not even at the 10 mg/mL concentration. In contrast, Reus et al. (2020) evaluated cytotoxic effects at high concentrations (0.192-7.750 mg/mL) of 100 nm of silica nanoparticles on a skin fibroblast cell line (BALB/c 3T3) by the neutral red uptake assay, which gave an IC_{50}

value of 1.99(0.24) mg/mL after 48 h of exposure. However, the results obtained in both studies are not completely comparable because of the physico-chemical differences in silica particles that may consequently affect their behaviour (Younes et al., 2018).

One of the most versatile classes of amorphous silica particles is mesostructured silica materials, such as MCM-41. Due to their biocompatibility, ordered pore structure, large surface area and high-density surface silanol groups, these materials show a high ability to be chemically modified, and are particularly useful tools for designing hybrid materials (Jaganathan & Godin, 2012). Several studies have evaluated cell viability after exposure to low concentrations of MCM-41 materials on different cell lines, and observed no cytotoxic effects (Giménez et al., 2015; Pérez-Esteve et al., 2016). However, very few studies have investigated the effect of high concentrations on cell viability. This is the case of Heikkilä et al. (2010), who studied the cytotoxicity of MCM-41 microparticles on Caco-2 cells as a model for oral drug delivery to be administered at frequent intervals. The MCM-41 particles induced cell membrane integrity damage, diminished cell metabolism and increased apoptotic signalling after a 24-hour treatment at concentrations of 1 mg/mL. The cytotoxic mechanisms of MCM-41 included an increase in ROS, especially superoxide radical ($O^{\cdot-}_2$) formation, a drop in cell antioxidant defences, and increases in both mitochondrial dysfunction and apoptotic signalling.

MCM-41 nano had the least effect on cell viability of the three bare silica particles studied. Literature data report higher cytotoxicity associated with silica nanomaterials compared to their microsized counterparts for non-phagocytic cells (Li et al., 2011). However, this effect has been described only for particles with a diameter below 100 nm (Sakai-Kato et al., 2014). The high surface area to volume ratio provides silica nanoparticles with high surface energy, which is minimised by the formation of aggregates and agglomerates

(Bantz et al., 2014; Seipenbusch et al., 2010). As previously mentioned, the bare MCM-41 nano presented an individual particle size range from 60 to 87 nm, but the largest hydrodynamic size of the three silica particles. Therefore, the lesser cytotoxic effect evidenced in MCM-41 nano could be related to their trend to form large agglomerates, which has been explained by reduced absorption by cells (Li et al., 2011).

Interestingly, the bare SAS and bare MCM-41 micro had a hormetic effect at the low tested concentrations. The biphasic concentration-response or hormetic effect, characterised by low concentration stimulation and a high concentration toxic effect, has been attributed to defensive and adaptive responses of cells to stress (Calabrese, 2008), and this effect has been previously reported for silica nanoparticles (Mytych et al., 2016; Reus et al., 2020).

The comparative analysis of EOCs, bare silica and EOCs-functionalised particles allowed us to observe the effect of equivalent concentrations of each compound on HepG2 cells' viability. Eugenol and vanillin presented a lesser cytotoxic effect in their free form than when immobilised on silica particles' surfaces. Chen et al. (2009) studied the cytotoxic effect of chitosan nanoparticles functionalised with eugenol and carvacrol. Unlike the results reported herein, cytotoxicity assays using 3T3 mouse fibroblast showed that both the eugenol and carvacrol functionalised particles were significantly less cytotoxic than free EOCs. Other than the characteristics of the starting material could be responsible for these differences. As previously mentioned, major differences have been found in the IC_{50} values of eugenol in different works depending on the employed cell type. These authors reported that eugenol caused cell death only at a concentration above 0.31 μg/mL (1.89 μM), while the cytotoxic effects in our study fell within the milimolar range. Moreover, the degree of grafting achieved for eugenol on chitosan nanoparticles was higher (26.7%) than on MCM-41 nano (6.4%), which was

the most efficient eugenol functionalisation reaction in our study. So, the substantially lower concentrations of functionalised particles analysed by these authors might also be responsible for the differences that lie in both studies.

The immobilisation of eugenol and vanillin on silica particles has been demonstrated to increase their antimicrobial activity against different microorganisms compared to free components (García-Ríos et al., 2018; Ribes et al., 2019; Ruiz-Rico et al., 2017). Indeed, using immobilised compounds lowers the concentration of EOCs required to inhibit microorganism growth and, therefore, the expected differences in the cytotoxic effect between the free EOCs and EOCs-functionalised silica at effective antimicrobial concentrations should also reduce.

The improved antimicrobial effectiveness of immobilised molecules has been attributed to an increased interaction of EOCs with cell membranes, either for the high density of molecules on silica particles' surfaces or the reduced volatility of immobilised compounds (Ribes et al., 2017). These phenomena might also be responsible for the increased cytotoxic response to immobilised compounds because, as with bacteria, the cytotoxicity of EOCs in eukaryotic cells appears to include damage to cell membranes (Bakkali et al., 2008).

By comparing the bare and EOCs-functionalised materials, the obtained results differed depending on particle type. SAS functionalisation did not increase cytotoxicity in HepG2 cells, but cells were more sensitive to the functionalised than the bare MCM-41 particles. Moreover, the SAS functionalised particles had the mildest cytotoxic effect, while the eugenol and vanillin-functionalised MCM-41 micro were the most cytotoxic materials. Similarly to this work, Chen et al. (2009) found increased cytotoxicity in association with the eugenol and carvacrol functionalised chitosan compared

to bare chitosan. The IC_{50} value found for functionalised chitosan was around 1 mg/mL after 72 h of exposure, while cell viability was over 80% for the higher tested concentration (2 mg/mL) of bare chitosan nanoparticles. Other researchers have also observed increased cytotoxic behaviour of silica materials after different surface chemical treatments (Santos et al., 2010) or by anchoring functional groups, such as amine molecules (Bhattacharjee et al., 2010; Puerari et al., 2019; Ruizendaal et al., 2009; Vicentini et al., 2017) or carboxylic acid groups (Petushkov et al., 2009).

The physico-chemical characteristics of particles are main factors that determine their interaction with biological systems and are, therefore, crucial when assessing toxicity (Bouwmeester et al., 2011). In this study, shape, particle size, zeta potential and degree of functionalisation were analysed to correlate the specific physico-chemical properties of materials with their cytotoxic profiles. As expected, no differences were found in the shape and individual mean diameter size of materials before and after the functionalisation process. However, changes in the surface properties and particle size distribution of materials were observed by introducing new functional groups. In particular, the functionalisation of silica particles with both EOCs led to a shift in the zeta potential values from negative to positive. The change in the charge observed after functionalisation could be interesting because, as cell membranes are negatively charged, a more marked interaction is expected for cationic compared to negatively charged particles (Cho et al., 2012). Indeed, different studies have demonstrated that positively charged particles are more cytotoxic than negative or neutral variants of similar sizes in non-phagocytic cells (Bhattacharjee et al., 2010; Ruizendaal et al., 2009). It has been described that while anionic particles may cause intracellular damage, positively charged materials are more prone to produce membrane damage either directly or by detachment of adsorbed polymers (Fröhlich, 2012). Kurtz-Chalot et al. (2014) compared cellular uptake and toxicity

against RAW 264.7 murine macrophages of different degrees of positive, neutral and negatively charged silica nanoparticles coated with amino groups, polyethylene glycol and carboxylic acid groups, respectively. These authors found that the highly positively charged nanoparticles were the most adsorbed on cell surfaces and were the most cytotoxic of different nanoparticle types, while no cellular uptake took place. Moreover, these particles caused the most severe membrane integrity loss and the highest pro-inflammatory signal. These results suggest that adsorption on the cell membrane plays a more important role than nanoparticle uptake in the cytotoxicity of cationic particles. In our study, as all the functionalised materials presented a positive surface charge, but SAS functionalisation did not increase their cytotoxicity behaviour, not only the cationic nature of particles, but also other factors of particles' surface chemistry, may also have an effect. Together with surface charge, the hydrophobicity levels and nature of surface modifications are considered essential for determining different biological effects (Sun et al., 2019). As described for cationic particles, hydrophobic surfaces promote cell-particle interactions and react more cytotoxically than hydrophilic surfaces (Fröhlich, 2012). The hydrophilicity of silica materials is related to the number of silanol groups available to form hydrogen bonds with water molecules (Napierska et al., 2010). The hydrophobicity of EOCs-functionalised materials is no doubt expected to be due to both a decrease in silanol groups on their surface and the hydrophobicity provided by the presence of the alkoxysilane derivatives of eugenol and vanillin anchored to particles. The differences in cytotoxic behaviour observed between the functionalised SAS and MCM-41 materials could, therefore, be explained by the functionalisation yield. This parameter was lower for SAS than mesoporous particles, but no significant differences appeared in the performance of the functionalisation reaction for both MCM-41 material types. Both the porosity and ordered structure of mesoporous materials provide a suitable platform for the covalent anchoring of organic groups (Moritz & Geszke-Moritz, 2015). Indeed, the

larger amount of EOCs found in the immobilisation reaction on MCM-41 particles could be attributed to the higher density of silanol groups on their inner and outer surfaces compared to SAS.

The analysis of the particle size distribution of the silica materials showed smaller hydrodynamic size values for the functionalised particles. Certain conditions, such as pH, temperature or ion strength, applied to prepare functionalised materials can change the surface properties of the particles and modify their agglomeration state (Halamoda-Kenzaoui et al., 2017; Schneider & Jensen, 2009), which are responsible for the differences between the bare and functionalised particles. Internalisation of individual silica microparticles has been found in the cytoplasm of different cell lines (Yu et al., 2009), but the cellular uptake of silica has been found in an inverse proportion to their size for non-phagocytic cells, and to depend on the degree of particle aggregation and agglomeration (Rancan et al., 2012; Sakai-Kato et al., 2014). Indeed, the highest cellular uptake rate in non-phagocytic cells has been found for nanoparticles between 20 and 50 nm (Fröhlich, 2012). The big hydrodynamic particle size found for the different bare and functionalised materials suggests that the adsorption of particles by HepG2 cells would be negligible, even for MCM-41 nano, given their high agglomeration state in solution.

All this information suggests that the cytotoxicity of modified materials for HepG2 cell is probably due to the physical interaction of particles with cell membranes. The good adhesion of cationic particles has been related to occur by either direct electrostatic interactions with cell membranes (Su et al., 2012) or indirectly through the protein corona formed on the surfaces of charged particles (Kurtz-Chalot et al., 2014). After adhesion, particles may have different biological effects on cell surfaces, including physical damage of the membrane by focal dissolution or hole formation, interaction with membrane-bound proteins (Fröhlich, 2012) and extracellular ROS generation (Santos et

al., 2010). Therefore, these biological effects may be related to the strong cytotoxic effect found for the EOCs-functionalised MCM-41 compared to pristine materials.

In order to quantify and compare the cytotoxic effect of the different functionalised silica particles, the MTT and AB methods were assayed. Concentration- and time-dependent effects on HepG2 viability were observed after exposure to all the tested functionalised materials using both metabolic endpoints. Both methods provided useful information for identifying the *in vitro* cytotoxity of these materials and it is noteworthy that no interference took place between particles and the AB assay, although subtracting the absorbance of the functionalised particles was necessary in the MTT test. However, MTT was a more sensitive endpoint than AB. This effect was more pronounced for the functionalised SAS, eugenol-functionalised MCM-41 nano and for 24 h exposure to the eugenol-functionalised MCM-41 micro and vanillin-functionalised MCM-41 nano, when no accurate estimation of the IC_{50} values was possible by the AB method. As observed in the comparative study, and independently of the EOCs, the functionalised SAS exerted the least cytotoxic effect against HepG2 cells, while the functionalised MCM-41 micro was the most cytotoxic material. Indeed, when comparing the bare and functionalised IC_{50} values, the modified MCM-41 micro had a cytotoxic effect that was around 40-fold stronger than for pristine materials.

By comparing the IC_{50} values of the different silica particles obtained by the MTT assay, no significant differences were found between the cytotoxic behaviour of the eugenol and vanillin-functionalised materials. As previously explained, the cytotoxic effect of free eugenol was 2-fold higher than the effect found for free vanillin. However, in the modified silica particles, these differences may be offset by the functionalisation yield for both EOCs. Vanillin anchoring achieved better results than eugenol anchoring, with differences of up to 5-fold bigger for SAS or 3-fold for MCM-41 micro.

Different degrees of steric hindrance have been responsible for differences in the functionalisation yield between EOCs (Chen et al., 2009). In this study, these differences could be due to the lesser efficiency of the formylation process to obtain the aldehyde derivative eugenol as the presence of an aldehyde group in the vanillin structure avoids this first synthesis stage. These results suggest that the number of molecules from the EOCs anchored to silica surfaces is an important factor for determining their cytotoxic behaviour.

This study provides information that clarifies the possible risk which derives from using these new materials in food applications. The obtained results indicate that the eugenol and vanillin-functionalised silica particles exhibited a stronger cytotoxic effect on HepG2 cells than the free EOCs and pristine silica materials. The milder cytotoxic effect found for the functionalised SAS than the functionalised MCM-41 materials seemed to be related to the functionalisation yield. The relation between the physico-chemical properties and cytotoxicity found for the different particle types herein analysed suggest that the mechanism responsible for enhanced cytotoxicity could depend on increased cell-particle interactions to some extent. In fact, the properties of the functionalised particles' surface, such as cationic nature and hydrophobicity, seemed the most important factors to determine their interactions with cells and, hence, their cytotoxic behaviour. Basal cytotoxicity data may help to predict the acute toxicological effects of materials for food applications, but further studies are necessary to elucidate the mechanism of toxicity induced by exposure to these new particles. All this information will help to develop new effective and safer materials for food applications.

Acknowledgements

The authors gratefully acknowledge the financial support from the Spanish government (Project RTI2018-101599-B-C21 (MCUI/AEI/FEDER, EU)).

C.F. thanks the Generalitat Valenciana for being funded by the predoctoral programme Vali+d (ACIF/2016/139). M.R.R. also acknowledges the Generalitat Valenciana for her postdoctoral fellowship (APOSTD/2019/118).

References

Al-Naqeb, G., Ismail, M., Bagalkotkar, G., & Adamu, H. A. (2010). Vanillin rich fraction regulates LDLR and HMGCR gene expression in HepG2 cells. *Food Research International*, *43*(10), 2437–2443. https://doi.org/10.1016/j.foodres.2010.09.015

Bagheri, E., Ansari, L., Abnous, K., Taghdisi, S. M., Charbgoo, F., Ramezani, M., & Alibolandi, M. (2018). Silica based hybrid materials for drug delivery and bioimaging. In *Journal of Controlled Release* (Vol. 277, pp. 57–76). Elsevier B.V. https://doi.org/10.1016/j.jconrel.2018.03.014

Bakkali, F., Averbeck, S., Averbeck, D., & Idaomar, M. (2008). Biological effects of essential oils – A review. *Food and Chemical Toxicology*, *46*(2), 446–475. https://doi.org/10.1016/j.fct.2007.09.106

Bantz, C., Koshkina, O., Lang, T., Galla, H.-J., Kirkpatrick, J., Stauber, R. H., & Maskos, M. (2014). The surface properties of nanoparticles determine the agglomeration state and the size of the particles under physiological conditions. *Beilstein J. Nanotechnol*, *5*, 1774–1786. https://doi.org/10.3762/bjnano.5.188

Bhattacharjee, S., de Haan, L. H. J., Evers, N. M., Jiang, X., Marcelis, A. T. M., Zuilhof, H., Rietjens, I. M. C. M., & Alink, G. M. (2010). Role of surface charge and oxidative stress in cytotoxicity of organic monolayer-coated silicon nanoparticles towards macrophage NR8383 cells. *Particle and Fibre Toxicology*, *7*(1), 25. https://doi.org/10.1186/1743-8977-7-25

Bouwmeester, H., Byrne, H., Casey, A., Chambers, G., Lynch, I., Marvin, H. J. P., Dawson, K. A., Berges, M., Braguer, D., Byrne, H. J., Clift, M. J. D., Elia, G., Fernandes, T. F., Fjellsbo, L. B., Hatto, P., Juillerat, L., Klein, C., Kreyling, W. G., Nickel, C., … Stone, V. (2011). Minimal Analytical Characterisation of Engineered Nanomaterials Needed for Hazard Assessment in Biological

Matrices Recommended Citation Minimal analytical characterization of engineered nanomaterials needed for hazard assessment in biological matrices. *Nanotoxicology*, *5*, 1–11. https://doi.org/10.3109/17435391003775266

Braun, K., Stürzel, C. M., Biskupek, J., Kaiser, U., Kirchhoff, F., & Lindén, M. (2018). Comparison of different cytotoxicity assays for in vitro evaluation of mesoporous silica nanoparticles. *Toxicology in Vitro*, *52*, 214–221. https://doi.org/10.1016/j.tiv.2018.06.019

Calabrese, E. J. (2008). Hormesis: Why it is important to toxicology and toxicologists. In *Environmental Toxicology and Chemistry* (Vol. 27, Issue 7, pp. 1451–1474). John Wiley & Sons, Ltd. https://doi.org/10.1897/07-541.1

Chen, F., Shi, Z., Neoh, K. G., & Kang, E. T. (2009). Antioxidant and antibacterial activities of eugenol and carvacrol-grafted chitosan nanoparticles. *Biotechnology and Bioengineering*, *104*(1), 30–39. https://doi.org/10.1002/bit.22363

Cho, W.-S., Duffin, R., Thielbeer, F., Bradley, M., Megson, I. L., MacNee, W., Poland, C. A., Tran, C. L., & Donaldson, K. (2012). Zeta Potential and Solubility to Toxic Ions as Mechanisms of Lung Inflammation Caused by Metal/Metal Oxide Nanoparticles. *Toxicological Sciences*, *126*(2), 469–477. https://doi.org/10.1093/toxsci/kfs006

Davoren, M., Herzog, E., Casey, A., Cottineau, B., Chambers, G., Byrne, H. J., & Lyng, F. M. (2007). In vitro toxicity evaluation of single walled carbon nanotubes on human A549 lung cells. *Toxicology in Vitro*, *21*(3), 438–448. https://doi.org/10.1016/j.tiv.2006.10.007

Diab, R., Canilho, N., Pavel, I. A., Haffner, F. B., Girardon, M., & Pasc, A. (2017). Silica-based systems for oral delivery of drugs, macromolecules and cells. *Advances in Colloid and Interface Science*, *249*, 346–362. https://doi.org/10.1016/j.cis.2017.04.005

Efeoglu, E., Maher, M. A., Casey, A., & Byrne, H. J. (2017). Label-free, high content screening using Raman microspectroscopy: The toxicological response

of different cell lines to amine-modified polystyrene nanoparticles (PS-NH2). *Analyst*, *142*(18), 3500–3513. https://doi.org/10.1039/c7an00461c

EU Commission. (2011a). Commission Regulation (EU) No 1129/2011 of 11 November 2011 amending Annex II to Regulation (EC) No 1333/2008 of the European Parliament and of the Council by establishing a Union list of food additives. *Official Journal of the European Union,* L, 295(4),. https://eur-lex.europa.eu/legal-content/EN/TXT/PDF/?uri=CELEX:32011R1129&from=ES

EU Commission. (2011b). Commission Regulation (EU) No 10/2011 of 14 January 2011 on plastic materials and articles intended to come into contact with food. *Official Journal of the European Union*, L,12. https://eur-lex.europa.eu/legal-content/EN/TXT/PDF/?uri=CELEX:32011R0010&from=EN

FDA. (2020). *Electronic Code of Federal Regulations (eCFR)*. Part 182-Substances Generally Recognized as Safe. https://www.ecfr.gov/cgi-bin/text-idx?SID=e956d645a8b4e6b3e34e4e5d1b690209&mc=true&node=pt21.3.182&rgn=div5

Fröhlich, E. (2012). The role of surface charge in cellular uptake and cytotoxicity of medical nanoparticles. In *International Journal of Nanomedicine* (Vol. 7, pp. 5577–5591). Dove Press. https://doi.org/10.2147/IJN.S36111

Fruijtier-pölloth, C. (2016). The safety of nanostructured synthetic amorphous silica (SAS) as a food additive (E 551). *Archives of Toxicology*, *90*, 2885–2916. https://doi.org/10.1007/s00204-016-1850-4

Fuentes, C., Ruiz-Rico, M., Fuentes, A., Ruiz, M. J., & Barat, J. M. (2020). Degradation of silica particles functionalised with essential oil components under simulated physiological conditions. *Journal of Hazardous Materials*, *399*, 123120. https://doi.org/10.1016/j.jhazmat.2020.123120

Fujisawa, S., Atsumi, T., Kadoma, Y., & Sakagami, H. (2002). Antioxidant and prooxidant action of eugenol-related compounds and their cytotoxicity. *Toxicology*, *177*(1), 39–54. https://doi.org/10.1016/S0300-483X(02)00194-4

García-Ríos, E., Ruiz-Rico, M., Guillamón, J. M., Pérez-Esteve, É., & Barat, J. M. (2018). Improved antimicrobial activity of immobilised essential oil components against representative spoilage wine microorganisms. *Food Control*, *94*, 177–186. https://doi.org/10.1016/j.foodcont.2018.07.005

Giménez, C., de la Torre, C., Gorbe, M., Aznar, E., Sancenón, F., Murguía, J. R., Martínez-Máñez, R., Marcos, M. D., & Amorós, P. (2015). Gated Mesoporous Silica Nanoparticles for the Controlled Delivery of Drugs in Cancer Cells. *Langmuir*, *31*(12), 3753–3762. https://doi.org/10.1021/acs.langmuir.5b00139

Halamoda-Kenzaoui, B., Ceridono, M., Urbán, P., Bogni, A., Ponti, J., Gioria, S., & Kinsner-Ovaskainen, A. (2017). The agglomeration state of nanoparticles can influence the mechanism of their cellular internalisation. *Journal of Nanobiotechnology*, *15*, 48. https://doi.org/10.1186/s12951-017-0281-6

Heikkilä, T., Santos, H. A., Kumar, N., Murzin, D. Y., Salonen, J., Laaksonen, T., Peltonen, L., Hirvonen, J., & Lehto, V.-P. (2010). Cytotoxicity study of ordered mesoporous silica MCM-41 and SBA-15 microparticles on Caco-2 cells. *European Journal of Pharmaceutics and Biopharmaceutics*, *74*(3), 483–494. https://doi.org/10.1016/J.EJPB.2009.12.006

Ho, Y.-C., Huang, F.-M., & Chang, Y.-C. (2006). Mechanisms of cytotoxicity of eugenol in human osteoblastic cells in vitro. *International Endodontic Journal*, *39*(5), 389–393. https://doi.org/10.1111/j.1365-2591.2006.01091.x

Holst, C. M., & Oredsson, S. M. (2005). Comparison of three cytotoxicity tests in the evaluation of the cytotoxicity of a spermine analogue on human breast cancer cell lines. *Toxicology in Vitro*, *19*(3), 379–387. https://doi.org/10.1016/j.tiv.2004.10.005

Jaganathan, H., & Godin, B. (2012). Biocompatibility assessment of Si-based nano- and micro-particles. *Advanced Drug Delivery Reviews*, *64*(15), 1800–1819. https://doi.org/10.1016/J.ADDR.2012.05.008

Kurtz-Chalot, A., Klein, J. P., Pourchez, J., Boudard, D., Bin, V., Alcantara, G. B., Martini, M., Cottier, M., & Forest, V. (2014). Adsorption at cell surface and

cellular uptake of silica nanoparticles with different surface chemical functionalizations: impact on cytotoxicity. *Journal of Nanoparticle Research*, *16*(11), 1–15. https://doi.org/10.1007/s11051-014-2738-y

Laaksonen, T., Santos, H., Vihola, H., Salonen, J., Riikonen, J., Heikkilä, T., Peltonen, L., Kumar, N., Murzin, D. Y., Lehto, V. P., & Hirvonen, J. (2007). Failure of MTT as a toxicity testing agent for mesoporous silicon microparticles. *Chemical Research in Toxicology*, *20*(12), 1913–1918. https://doi.org/10.1021/tx700326b

Li, Y., Sun, L., Jin, M., Du, Z., Liu, X., Guo, C., Li, Y., Huang, P., & Sun, Z. (2011). Size-dependent cytotoxicity of amorphous silica nanoparticles in human hepatoma HepG2 cells. *Toxicology in Vitro*, *25*(7), 1343–1352. https://doi.org/10.1016/J.TIV.2011.05.003

Moritz, M., & Geszke-Moritz, M. (2015). Mesoporous materials as multifunctional tools in biosciences: Principles and applications. *Materials Science and Engineering: C*, *49*, 114–151. https://doi.org/10.1016/J.MSEC.2014.12.079

Mytych, J., Wnuk, M., & Rattan, S. I. S. (2016). Low doses of nanodiamonds and silica nanoparticles have beneficial hormetic effects in normal human skin fibroblasts in culture. *Chemosphere*, *148*, 307–315. https://doi.org/10.1016/j.chemosphere.2016.01.045

Napierska, D., Thomassen, L. C., Lison, D., Martens, J. A., & Hoet, P. H. (2010). The nanosilica hazard: Another variable entity. *Particle and Fibre Toxicology*, *7*(1), 39. https://doi.org/10.1186/1743-8977-7-39

Peña-Gómez, N., Ruiz-Rico, M., Pérez-Esteve, É., Fernández-Segovia, I., & Barat, J. M. (2020). Microbial stabilization of craft beer by filtration through silica supports functionalized with essential oil components. *LWT*, *117*, 108626. https://doi.org/10.1016/j.lwt.2019.108626

Pérez-Esteve, É., Ruiz-Rico, M., de la Torre, C., Villaescusa, L. A., Sancenón, F., Marcos, M. D., Amorós, P., Martínez-Máñez, R., & Barat, J. M. (2016). Encapsulation of folic acid in different silica porous supports: A comparative

study. *Food Chemistry*, *196*, 66–75. https://doi.org/10.1016/J.FOODCHEM.2015.09.017

Petushkov, A., Intra, J., Graham, J. B., Larsen, S. C., & Salem, A. K. (2009). Effect of crystal size and surface functionalization on the cytotoxicity of silicalite-1 nanoparticles. *Chemical Research in Toxicology*, *22*(7), 1359–1368. https://doi.org/10.1021/tx900153k

Puerari, R. C., Ferrari, E., de Cezar, M. G., Gonçalves, R. A., Simioni, C., Ouriques, L. C., Vicentini, D. S., & Matias, W. G. (2019). Investigation of toxicological effects of amorphous silica nanostructures with amine-functionalized surfaces on Vero cells. *Chemosphere*, *214*, 679–687. https://doi.org/10.1016/j.chemosphere.2018.09.165

Rampersad, S. N. (2012). Multiple Applications of Alamar Blue as an Indicator of Metabolic Function and Cellular Health in Cell Viability Bioassays. *Sensors*, *12*, 12347–12360. https://doi.org/10.3390/s120912347

Rancan, F., Gao, Q., Graf, C., Troppens, S., Hadam, S., Hackbarth, S., Kembuan, C., Blume-Peytavi, U., Rühl, E., Lademann, J., & Vogt, A. (2012). Skin penetration and cellular uptake of amorphous silica nanoparticles with variable size, surface functionalization, and colloidal stability. *ACS Nano*, *6*(8), 6829–6842. https://doi.org/10.1021/nn301622h

Reus, T. L., Marcon, B. H., Paschoal, A. C. C., Ribeiro, I. R. S., Cardoso, M. B., Dallagiovanna, B., & Aguiar, A. M. de. (2020). Dose-dependent cell necrosis induced by silica nanoparticles. *Toxicology in Vitro*, *63*, 104723. https://doi.org/10.1016/j.tiv.2019.104723

Ribes, S., Ruiz-Rico, M., Pérez-Esteve, É., Fuentes, A., Talens, P., Martínez-Máñez, R., & Barat, J. M. (2017). Eugenol and thymol immobilised on mesoporous silica-based material as an innovative antifungal system: Application in strawberry jam. *Food Control*, *81*, 181–188. https://doi.org/10.1016/J.FOODCONT.2017.06.006

Ribes, S., Ruiz-Rico, M., Pérez-Esteve, É., Fuentes, A., & Barat, J. M. (2019).

Enhancing the antimicrobial activity of eugenol, carvacrol and vanillin immobilised on silica supports against Escherichia coli or Zygosaccharomyces rouxii in fruit juices by their binary combinations. *LWT*, *113*, 108326. https://doi.org/10.1016/j.lwt.2019.108326

Ros-Lis, J. V., Bernardos, A., Pérez, É., Barat, J. M., & Martínez-Máñez, R. (2018). Functionalized Silica Nanomaterials as a New Tool for New Industrial Applications. In *Impact of Nanoscience in the Food Industry* (pp. 165–196). Elsevier Inc. https://doi.org/10.1016/B978-0-12-811441-4.00007-8

Ruiz-Rico, M., Pérez-Esteve, É., Bernardos, A., Sancenón, F., Martínez-Máñez, R., Marcos, M. D., & Barat, J. M. (2017). Enhanced antimicrobial activity of essential oil components immobilized on silica particles. *Food Chemistry*, *233*, 228–236. https://doi.org/10.1016/J.FOODCHEM.2017.04.118

Ruiz, M. J., Festila, L. E., & Fernández, M. (2006). Comparison of basal cytotoxicity of seven carbamates in CHO-K1 cells. *Toxicological and Environmental Chemistry*, *88*(2), 345–354. https://doi.org/10.1080/02772240600630622

Ruizendaal, L., Bhattacharjee, S., Pournazari, K., Rosso-Vasic, M., De Haan, L. H. J., Alink, G. M., Marcelis, A. T. M., & Zuilhof, H. (2009). Synthesis and cytotoxicity of silicon nanoparticles with covalently attached organic monolayers. *Nanotoxicology*, *3*(4), 339–347. https://doi.org/10.3109/17435390903288896

Sakai-Kato, K., Hidaka, M., Un, K., Kawanishi, T., & Okuda, H. (2014). Physicochemical properties and in vitro intestinal permeability properties and intestinal cell toxicity of silica particles, performed in simulated gastrointestinal fluids. *Biochimica et Biophysica Acta (BBA) - General Subjects*, *1840*(3), 1171–1180. https://doi.org/10.1016/J.BBAGEN.2013.12.014

Santos, H. A., Riikonen, J., Salonen, J., Mäkilä, E., Heikkilä, T., Laaksonen, T., Peltonen, L., Lehto, V.-P., & Hirvonen, J. (2010). In vitro cytotoxicity of porous silicon microparticles: Effect of the particle concentration, surface chemistry and size. *Acta Biomaterialia*, *6*(7), 2721–2731.

https://doi.org/10.1016/J.ACTBIO.2009.12.043

Schneider, T., & Jensen, K. A. (2009). Relevance of aerosol dynamics and dustiness for personal exposure to manufactured nanoparticles. *Journal of Nanoparticle Research*, *11*(7), 1637–1650. https://doi.org/10.1007/s11051-009-9706-y

Seipenbusch, M., Rothenbacher, S., Kirchhoff, M., Schmid, H. J., Kasper, G., & Weber, A. P. (2010). Interparticle forces in silica nanoparticle agglomerates. *Journal of Nanoparticle Research*, *12*(6), 2037–2044. https://doi.org/10.1007/s11051-009-9760-5

Shakeel, F., Haq, N., Raish, M., Siddiqui, N. A., Alanazi, F. K., & Alsarra, I. A. (2016). Antioxidant and cytotoxic effects of vanillin via eucalyptus oil containing self-nanoemulsifying drug delivery system. *Journal of Molecular Liquids*, *218*, 233–239. https://doi.org/10.1016/j.molliq.2016.02.077

Sisakhtnezhad, S., Heidari, M., & Bidmeshkipour, A. (2018). Eugenol enhances proliferation and migration of mouse bone marrow-derived mesenchymal stem cells in vitro. *Environmental Toxicology and Pharmacology*, *57*, 166–174. https://doi.org/10.1016/j.etap.2017.12.012

Slowing, I., Trewyn, B. G., & Lin, V. S. Y. (2006). Effect of surface functionalization of MCM-41-type mesoporous silica nanoparticles on the endocytosis by human cancer cells. *Journal of the American Chemical Society*, *128*(46), 14792–14793. https://doi.org/10.1021/ja0645943

Su, G., Zhou, H., Mu, Q., Zhang, Y., Li, L., Jiao, P., Jiang, G., & Yan, B. (2012). Effective surface charge density determines the electrostatic attraction between nanoparticles and cells. *Journal of Physical Chemistry C*, *116*(8), 4993–4998. https://doi.org/10.1021/jp211041m

Sun, H., Jiang, C., Wu, L., Bai, X., & Zhai, S. (2019). Cytotoxicity-Related Bioeffects Induced by Nanoparticles: The Role of Surface Chemistry. In *Frontiers in Bioengineering and Biotechnology* (Vol. 7, p. 414). Frontiers Media S.A. https://doi.org/10.3389/fbioe.2019.00414

Vicentini, D. S., Puerari, R. C., Oliveira, K. G., Arl, M., Melegari, S. P., & Matias,

W. G. (2017). Toxicological impact of morphology and surface functionalization of amorphous SiO2 nanomaterials. *NanoImpact*, *5*, 6–12. https://doi.org/10.1016/J.IMPACT.2016.11.003

Yoshida, T., Yoshioka, Y., Matsuyama, K., Nakazato, Y., Tochigi, S., Hirai, T., Kondoh, S., Nagano, K., Abe, Y., Kamada, H., Tsunoda, S., Nabeshi, H., Yoshikawa, T., & Tsutsumi, Y. (2012). Surface modification of amorphous nanosilica particles suppresses nanosilica-induced cytotoxicity, ROS generation, and DNA damage in various mammalian cells. *Biochemical and Biophysical Research Communications*, *427*(4), 748–752. https://doi.org/10.1016/J.BBRC.2012.09.132

Younes, M., Aggett, P., Aguilar, F., Crebelli, R., Dusemund, B., Filipič, M., Frutos, M. J., Galtier, P., Gott, D., Gundert-Remy, U., Kuhnle, G. G., Leblanc, J., Lillegaard, I. T., Moldeus, P., Mortensen, A., Oskarsson, A., Stankovic, I., Waalkens-Berendsen, I., Woutersen, R. A., … Lambré, C. (2018). Re-evaluation of silicon dioxide (E 551) as a food additive. *EFSA Journal*, *16*(1). https://doi.org/10.2903/j.efsa.2018.5088

Yu, K. O., Grabinski, C. M., Schrand, A. M., Murdock, R. C., Wang, W., Gu, B., Schlager, J. J., & Hussain, S. M. (2009). Toxicity of amorphous silica nanoparticles in mouse keratinocytes. *Journal of Nanoparticle Research*, *11*(1), 15–24. https://doi.org/10.1007/s11051-008-9417-9.

In vitro toxicological evaluation of mesoporous silica microparticles functionalised with carvacrol and thymol

Cristina Fuentes[a1], Ana Fuentes[a], Hugh J. Byrne[b], José Manuel Barat[a], María José Ruiz[c]

[a]Department of Food Technology, Universitat Politècnica de València. Camino de Vera s/n, 46022, Valencia, Spain

[b]FOCAS Research Institute, City Campus, Technological University Dublin, Dublin 8, Ireland

[c]Laboratory of Toxicology, Faculty of Pharmacy, Universitat de València, Av. Vicent Andrés Estellés s/n, 46100 Burjassot, Valencia, Spain

Abstract

The cytotoxicity of carvacrol- and thymol-functionalised mesoporous silica microparticles (MCM-41) was assessed in the human hepatocarcinoma cell line (HepG2). Cell viability, lactate dehydrogenase (LDH) activity, reactive oxygen species (ROS) production, mitochondrial membrane potential (ΔΨm), lipid peroxidation (LPO) and apoptosis/necrosis analyses were used as endpoints. The results showed that both materials induced cytotoxicity in a time- and concentration-dependent manner, and were more cytotoxic than free essential oil components and bare MCM-41. This effect was caused by cell-particle interactions and not by degradation products released to the culture media, as demonstrated in the extract dilution assays. LDH release was a less sensitive endpoint than the MTT (thiazolyl blue tetrazolium bromide) assay, which suggests the impairment of the mitochondrial function as the primary cytotoxic mechanism. *In vitro* tests on specialised cell functions showed that exposure to sublethal concentrations of these materials did not induce ROS formation during 2 h of exposure, but produced LPO and ΔΨm alterations in a concentration-dependent manner when cells were exposed for 24 h. The obtained results generally support the hypothesis that the carvacrol- and thymol-functionalised MCM-41 microparticles induced toxicity in HepG2 cells by an oxidative stress-related mechanism that resulted in apoptosis through the mitochondrial pathway.

Keywords: mesoporous microparticles; silica; essential oil components; cytotoxicity; HepG2

1. Introduction

Consumer awareness of additives and chemicals in their diets has forced the food industry to search for alternatives to synthetic preservatives to prolong their products' shelf life (Faleiro and Miguel, 2020; Ribes et al., 2018). In line with this, essential oils and their constituent components have attracted considerable attention for their natural origin and well-known antimicrobial and antioxidant activity (Burt, 2004; Hyldgaard et al., 2012). The monoterpenoids carvacrol and thymol, major components in essential oils from different plant species like origanum or thyme, are two of the most investigated essential oil components (EOCs) because of their marked action against a wide spectrum of foodborne and food spoilage microorganisms (Abbaszadeh et al., 2014; Abdelhamid and Yousef, 2021; Čabarkapa et al., 2019; Karam et al., 2019; Tippayatum and Chonhenchob, 2007; Walczak et al., 2021). These components' antimicrobial action has been attributed mainly to the presence of a hydroxyl group and a system of delocalised electrons in their chemical structure capable of disrupting the cytoplasmic membrane and leading to the leakage of intracellular content and, ultimately, lysis (Xu et al., 2008). However, their application to food products poses some challenges, such as high volatility, low solubility or strong sensory properties (Hyldgaard et al., 2012). Grafting EOCs onto the surface of silica particles has been proposed as a strategy to increase these components' antimicrobial activity and to overcome drawbacks. These hybrid organic-inorganic particles have efficiently performed as preservatives in different food matrices (Ribes et al., 2017, 2019) and as filtering materials for cold beverage pasteurisation (García-Ríos et al., 2018; Peña-Gómez et al., 2019a, 2019b, 2020).

Mobile composition of matter (MCM)-41 is one of the most widely employed scaffolds for the synthesis of organic-inorganic hybrid systems thanks to easy surface functionalisation, large surface area, uniform pore size and high stability (Diab et al., 2017). Moreover, as a result of reported high

biocompatibility and low toxicity (Aburawi et al., 2012; Al-Salam et al., 2011; Garrido-Cano et al., 2021), MCM-41 materials have been studied for the covalent attachment of functional groups and organic molecules in a number of oral applications (Bagheri et al., 2018; Ros-Lis et al., 2018). However, as the surface properties of particles are key factors for determining their interactions with biological systems (Kyriakidou et al., 2020; Puerari et al., 2019; Vicentini et al., 2017), the analysis of the *in vitro* and *in vivo* behaviours of surface-modified silica structures is crucial to guarantee the safety and innocuousness of their use for human health purposes.

Previous *in vitro* studies have evaluated the stability of different types of synthetic amorphous silica particles functionalised with carvacrol, eugenol and vanillin under conditions that represent the human gastrointestinal tract, lysosomal fluid and the cytotoxicity of these materials (Fuentes et al., 2020, 2021). The results showed that functionalisation with EOCs resulted in lower dissolution levels than bare MCM-41 microparticles and, therefore, increased stability under both biological conditions (Fuentes et al., 2020). Conversely, the comparative analysis of the cytotoxic effect of eugenol- and vanillin-functionalised silica particles revealed that free EOCs and bare particles had a milder cytotoxic effect on HepG2 cells than the functionalised MCM-41 materials. A relation between cytotoxicity and the density of EOC molecules on the surface of the functionalised particles was found. According to the physico-chemical analysis of the materials, properties like cationic nature and hydrophobicity were suggested to enhance the cytotoxic behaviour of the functionalised silica particles (Fuentes et al., 2021). All together, these results demonstrate that the functionalisation of MCM-41 particles with EOC derivatives enhances the stability of these materials under biological conditions, but may increase their cytotoxic behaviour that implies potential toxicological hazards. Besides, the molecular mechanism underlying these materials' cytotoxic behaviour remains to be elucidated. Accordingly, with

this work we aimed to investigate the cytotoxic effect of the carvacrol- and thymol-functionalised MCM-41 microparticles and to further elucidate the related toxicity mechanism. HepG2 cells were selected for the *in vitro* toxicology studies because this cell type is a standard model for xenobiotic metabolism and toxicity studies, and displays a high degree of reproducibility. Thus, HepG2 human liver cells were exposed to the modified silica materials, and then cell viability, lactate dehydrogenase (LDH) activity, reactive oxygen species (ROS) production, mitochondrial membrane potential ($\Delta\Psi m$), lipid peroxidation (LPO), and apoptotic and necrotic responses, were evaluated.

2. Materials and Methods

2.1. Reagents

Triethanolamine ($TEAH_3$), hexadecyltrimethylammonium bromide (CTAB), carvacrol (≥ 98% w/w), thymol (≥ 99% w/w), (3-aminopropyl) triethoxysilane (APTES), thiazolyl blue tetrazolium bromide (MTT), 2′,7′-dichlorodihydrofluorescein diacetate (H_2-DCFDA), Rhodamine 123, thiobarbituric acid (TBA), deferoxamine mesylate salt (DFA) and di-ter-butyl- methylphenol (BHT) were obtained from Sigma-Aldrich (Spain). Dimethyl sulfoxide (DMSO) was purchased from Scharlab (Spain).

The HepG2 human hepatocarcinoma cell line was obtained from the American Type Culture collection (ATCC HB-8065). Dulbecco's Modified Eagle Medium (DMEM-Glutamax™) with high glucose (4.5 g/L), phosphate buffered saline (PBS), newborn calf serum (NBCS), penicillin, streptomycin, trypsin-EDTA 0.5% and sodium pyruvate were supplied by Gibco (Life-Technologies, USA).

2.2. Preparation of the EOCs-functionalised MCM-41 microparticles

The mesoporous silica microparticles MCM-41 were prepared via the 'atrane route'. Under basic conditions, this is based on the use of $TEAH_3$, which generates atrane complexes as inorganic hydrolytic precursors and CTAB as a structural directing agent (Cabrera et al., 2000). The procedure of the synthetic process is fully described in Fuentes et al. (2020).

Once synthesised, the functionalisation of the MCM-41 silica particles with carvacrol and thymol was performed by a three-stage protocol that includes the: (1) synthesis of the carvacrol and thymol aldehyde derivatives by direct formylation with paraformaldehyde; (2) synthesis of the alkoxysilane derivatives by a reaction of carvacrol and thymol aldehydes with APTES; (3) immobilisation of the alkoxysilane derivatives on the surface of silica particles (García-Ríos et al., 2018).

2.3. Physico-chemical characterisation of MCM-41 microparticles

The bare and functionalised MCM-41 microparticles were analysed by transmission electron microscopy (TEM), particle size distribution, zeta potential and the elemental analysis. For the morphological analysis of the materials by TEM, particles were dispersed in dichloromethane and sonicated for 2 min to avoid aggregation. The suspension was placed on copper grids coated with a carbon film (Aname SL, Spain). The imaging of the particle samples was done using a JEOL JEM-1010 (JEOL Europe SAS, France) that operated at an acceleration voltage of 80 kV. The zeta potential of particles was studied by laser Doppler microelectrophoresis using a Zetasizer Nano ZS (Malvern Instruments, UK) and the Smoluchowski mathematical model. Particle size distribution was determined by a laser diffractometer Mastersizer 2000 (Malvern Instruments, UK) and applying the Mie theory (refractive index of 1.45, absorption index of 0.1). For the zeta potential and the particle size distribution analysis, samples were measured in triplicate on previously

sonicated diluted dispersions in deionised water. Finally, the elemental composition of the EOCs-functionalised particles was determined by a combustion analysis for C, H and N using a CHNS1100 Elemental Analyser (CE Instruments, UK).

2.4. Toxicological evaluation of the EOCs-functionalised MCM-41 microparticles

2.4.1. Cell culture

Human hepatocarcinoma (HepG2) cells were cultured in DMEM-Glutamax medium supplemented with 10% NBCS, 100 U/mL of penicillin and 100 μg/mL of streptomycin. Cells were maintained in a 5% CO_2 humidified incubator at 37 ºC. Growth medium was changed every 2–3 days or as required. Cells were subcultured by trypsinisation when about 80% confluence was reached and were used for experiments at passages between 9 and 24. Lack of mycoplasma contamination was examined regularly in cell cultures with the MycoAlert™ PLUS Myco-plasma kit (Lonza Rockland, USA).

2.4.2. Test solutions

Stock solutions of EOCs were prepared in DMSO (2.5 M) and were maintained at -20 ºC until used. Particle suspensions were prepared in the DMEM-supplemented medium and were sonicated for 10 min immediately before use. While studying the cytotoxic effect of carvacrol and thymol exposure, the final DMSO concentration in the test solutions was below 0.1%. Appropriate negative controls containing the same amount of solvents were included in each experiment. To analyse the MCM-41 materials, the cell-free particle control samples were included for each particle type and concentration, and were used to correct particle interference from test wells whenever necessary.

2.4.3. MTT assays

Direct exposure cytotoxicity assays

The MTT assay is one of the most widely used colorimetric assays to evaluate cell viability. In this method, the yellow positively charged tetrazolium salt enters viable cells, whereupon it is metabolically reduced to the insoluble blue-violet form of formazan by respiratory chain components (Rampersad, 2012). This assay was used to determine the mean inhibition concentration (IC_{50}) values of EOCs and the EOCs-functionalised silica, and to compare the cytotoxic effect of the functionalised particle constituents. Briefly, cells were seeded in 96-well plates at a density of 1 x 10^5 and 3 x 10^4 cells/mL for 24-hour and 48-hour experiments, respectively. After the 24-hour attachment, cells were exposed to serial dilutions of carvacrol (0.01-2.5 mM), thymol (0.06-1 mM), carvacrol- and thymol-functionalised MCM-41 microparticles (0.01-2.5 mg/mL) and to the equivalent concentrations of the EOCs, bare and functionalised particles for their comparative analysis (Table 1). The concentration ranges of EOCs and the functionalised particles were selected according to previous works (Fuentes et al., 2021). In the comparative studies, concentration ranges were established from the IC_{50} values found for carvacrol and thymol. Then the equivalent particle concentrations were calculated from the EOCs content determined by the elemental analysis. After a 24-hour or 48-hour incubation period, wells were washed with 100 µL of PBS. Next 100 µL of 10% MTT stock solution (5 mg/mL in PBS) in supplemented DMEM medium were added per well. Then plates were incubated in the dark at 37 ºC, 5% CO_2 for 3 h. Afterwards, the MTT solution was discarded, wells were washed with PBS and 100 µL of DMSO were added to dissolve formazan crystals. Finally, plates were shaken at 300 rpm for 10 min and absorbance was measured at 570 nm using a MultiSkan EX ELISA plate reader (Thermo Scientific, USA). Cell viability was expressed as a percentage in relation to the negative control (unexposed cells).

Exposure to sublethal concentrations of toxicants triggers the adaptative cellular responses linked with their cytotoxicity mechanism (Severin et al., 2017). For this reason, sublethal concentrations ($<IC_{50}$) were used to further investigate the toxicity mechanism underlying the exposure of the EOCs-functionalised particles. To this end, the IC_{50} values of the particles found in the MTT assay were used to calculate the sublethal concentrations ($IC_{50/2}$, $IC_{50/4}$, $IC_{50/8}$) for the different *in vitro* endpoints: ROS formation, ΔΨm, LPO, and apoptotic and necrotic responses.

Table 1. Concentrations assayed in the comparative study of carvacrol, thymol, and bare and EOCs-functionalised MCM-41 microparticles.

	Concentrations			
	A	**B**	**C**	**D**
Carvacrol (mM)	0.25	0.5	1	2
Bare MCM-41 (mg/mL)	4.5	8.9	17.9	35.7
Carvacrol MCM-41 (mg/mL)	4.4	8.8	17.7	35.4
Thymol (mM)	0.25	0.5	1	2
Bare MCM-41 (mg/mL)	3.8	7.7	15.3	30.6
Thymol MCM-41 (mg/mL)	3.7	7.6	15.1	30.3

Extract exposure cytotoxicity assays

An extract dilution exposure method was applied to evaluate a possible cytotoxic effect due to the components leached from the surface of the functionalised particles to the culture medium. For this purpose, a stock solution of the carvacrol- or thymol-functionalised particles in the DMEM-supplemented medium (2.5 mg/mL) was vigorously stirred, sonicated in an ultrasonic bath for 10 min and maintained at 37 ºC for 24 h. After this time,

the stock solution was serially diluted (0.01-2.5 mg/mL) and dilutions were filtered with 0.2 μm cellulose acetate filters to remove particles. Then cells were exposed to the filtered solutions and samples' cytotoxicity was determined by the MTT assay as described previously.

2.4.4. Lactate dehydrogenase (LDH) activity

LDH activity was determined by the CyQUANT LDH Cytotoxicity Assay kit (Thermo Scientific, USA) according to the manufacturer's protocol. Briefly, cells were seeded in 96-well plates at 10^5 cells/mL (100 μL/well) and allowed to attach for 24 h. Then cells were treated with 10 μL of the functionalised particle concentrations (0.01-2.5 mg/mL) for a 24-hour period. Next 10 μL of sterile ultrapure water (Spontaneous LDH Activity) or 10 μL of lysis buffer (Maximum LDH Release) were added to the control wells. Plates were incubated in the dark at 37 °C and 5% CO_2 for 45 min. This was followed by transferring 50 μL of each sample medium to a new plate and 50 μL of the reaction mixture were incorporated. After incubation at room temperature for 30 min, reactions were ended by adding 50 μL of the stop solution. Absorbance measurements were taken in a microtiter plate reader at 490 nm. The results were expressed as LDH release (%) in the exposed cells in relation to the spontaneous and maximum LDH controls.

2.4.5. ROS formation

ROS formation was determined as described by Ruiz-Leal and George (2004). Cells were seeded in black 96-well microplates at 2×10^5 cells/mL density. After 24 h of cell attachment, cells were washed with PBS and 20 μM of H_2-DCFDA dye in culture medium were added. Following a 20-minute incubation time in the dark at room temperature, the dye solution was removed and cells were exposed to different concentrations of the functionalised particles (18.75, 37.5 and 75 μg/mL). Then fluorescence was measured every 15 min for 2 h at 490 nm excitation and a 545 nm emission wavelength on a

Wallace Victor2 model 1420 multilabel counter (PerkinElmer, Finland). The ROS generation percentage was expressed as the percentage of the fluorescence values obtained compared to the negative control (unexposed cells).

2.4.6. Determination of the mitochondrial membrane potential

Mitochondrial membrane potential was determined by the uptake of green-fluorescent dye Rhodamine 123 upon the exposure of the functionalised microparticles. Cells were seeded at a density of 2×10^5 cells/mL in black 96-well microplates. After 24 h of cell attachment, cells were washed with 100 µl/well PBS and were exposed to three different concentrations of the functionalised particles (18.75, 37.5 and 75 µg/mL) in the 10% NCBS-supplemented medium for 24 h. Following the exposure time, cells were washed with 100 µl/well of PBS and Rhodamine-123 (5 µM) was added in the non-supplemented medium. After 15 min of incubation at 37 ºC and 5% of CO_2 in the dark, the dye solution was removed, and cells were washed twice and finally resuspended in 200 µl/well PBS. Fluorescence (λexcitation=485 nm, λemission=535 nm) was measured using a microplate reader Wallace Victor2, model 1420 multilabel counter (PerkinElmer, Finland). The results were expressed as the fluorescence percentage of Rhodamine 123 dye in the exposed cells compared to the negative control (unexposed cells).

2.4.7. Lipid peroxidation assays

The effect of sublethal concentrations' exposure to the functionalised particles upon LPO was performed by determining the formation of thiobarbituric acid reactive substances (TBARS) according to the method described by Ferrer et al. (2009). Briefly, 3×10^4 cells/well were seeded in 6-well plates, allowed to attach for 24 h and then exposed to the functionalised particles (18.75, 37.5 and 75 µg/mL). After 24 h of exposure, cells were washed with PBS, homogenised in 150 mM of sodium phosphate buffer pH

7.4, and lysate in the Ultra-Turrax T8 IKA®-WERKE for 30 s. Cell samples were mixed with 0.5% TBA, 1.5 mM of DFA and 3.75% BHT and heated at 100 ºC in a boiling water bath for 20 min. After cooling for 5 min, samples were centrifuged at 4,000 rpm for 15 min to remove the precipitate. The absorbance of the supernatant was then determined at 535 nm. Simultaneously, samples' protein content was measured following the Lowry method by the DC Protein Assay (BIO-RAD Laboratories, USA) at the 690 nm wavelength. The results were expressed as ng of malondialdehyde (MDA) per mg of protein.

2.4.8. Apoptosis/necrosis assays

The apoptosis/necrosis assays were performed by flow cytometry using the FITC Annexin V apoptosis detection kit (BD Biosciences, USA). Briefly, cells were seeded in 6-well plates at a density of 3 x 10^4 cells/well. After attachment, cells were exposed to the functionalised particles (18.75, 37.5 and 75 µg/mL) for 24 h. Then they were trypsinised, washed twice with ice-cold PBS and resuspended in binding buffer. A volume of cells of 100 µL (1 x 10^5 cells/mL) was stained by adding 5 µl of FITC Annexin V and 5 µl of propidium iodide (PI), which was incubated at room temperature in the dark for 15 min. After this time, 400 µL of binding buffer were added to each tube and samples were analysed in a BD LSRFortessa flow cytometer (BD Biosciensces, USA). Quadrant statistics were carried out to differentiate necrotic, early apoptotic and late apoptotic cells. The percentage of cells in each category was calculated by subtracting the number of cells in the control group from the number of cells in the treated population.

2.5. Statistical analysis

The statistical data analysis was performed using the Statgraphics Centurion XVI software package (Statpoint Technologies, Inc., USA). Data were expressed as the mean (SEM) of three independent experiments for each

endpoint. The data from the cytotoxicity assays were transferred to GraphPad Prism, version 8.0.1 (GraphPad Software, USA), to adjust the IC_{50} curve by using a four-parameter sigmoidal fit. The statistical analysis of the results was carried out by a Student's t-test for paired samples. In the MTT comparative study, differences between groups were analysed statistically by a one-way ANOVA, followed by the Tukey HDS *post-hoc* test for multiple comparisons. The difference level of $p \leq 0.05$ was considered statistically significant.

3. Results

3.1. Physico-chemical characterisation of the MCM-41 microparticles

To study the morphology and structure of the bare and carvacrol- or thymol-functionalised MCM-41 particles, a TEM analysis was performed. As shown in Figure 1, the three particle types exhibited an irregular external shape and a hexagonal periodic structure of internal channels in the form of alternate black and white parallel lines, typical of the ordered mesoporous structure of MCM-41 materials (Alothman, 2012; Meynen et al., 2009). These results confirmed that the synthesis process of the MCM-41 materials was correct and the functionalisation process did not significantly modify these materials' characteristic structure.

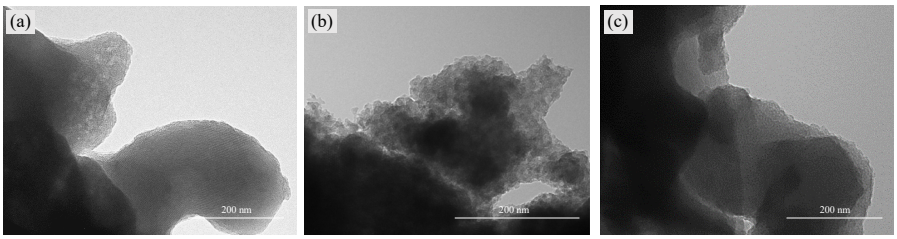

Figure 1. TEM images of the bare MCM-41 (a), carvacrol-functionalised MCM-41 (b) and thymol-functionalisedMCM-41 microparticles (c). Scale bar indicates 200 nm.

The zeta potential values and the particle size distribution of the bare and functionalised MCM-41 particles and the carvacrol or thymol contents of the MCM-41-functionalised materials are shown in Table 2. The negative zeta potential value observed for the bare MCM-41 was related to the negatively charged hydroxyl groups on the silica surface. In contrast, the functionalised particles displayed positive zeta potential values, which evidenced the presence of the carvacrol and thymol alkoxysilane derivatives grafted on their surface. Particle size distribution and TEM analysis showed that the three MCM-41 microparticles types were under 700 nm. This value was slightly higher for the bare than the functionalised particles as the larger number of steps included during the functionalisation process has been suggested to reduce the formation of agglomerates (Fuentes et al., 2020). Finally, the quantification of the carvacrol and thymol grafted onto particles' surface was determined by the elemental analysis. Small differences were found in the reaction yield for both types of EOCs, and the content of the thymol immobilised on the surface of the MCM-41 functionalised microparticles was slightly higher than carvacrol (Table 2). These results were used to establish the equal concentrations of the free EOCs and functionalised particles for the comparative cell viability assays (Table 1).

Table 2. Zeta potential (ZP) values, particle size distribution ($d_{0.5}$), particle size measured by TEM and EOC content (α) of the different MCM-41 microparticles.

Type of particle	ZP (mV)	$d_{0.5}$ (µm)	Size (µm)	α (g/gSiO_2)
Bare MCM-41	-33.43 (0.84)	0.68 (0.00)	0.63 (0.4)	
Carvacrol-MCM-41	27.37 (2.06)	0.62 (0.00)	0.57 (0.3)	0.0084
Thymol-MCM-41	21.07 (1.74)	0.65 (0.00)	0.50 (0.6)	0.0098

ZP and $d_{0.5}$ values are expressed as mean (SD) (n=3).

3.2. Toxicological evaluation of the EOCs-functionalised MCM-41 microparticles

3.2.1. MTT assays

Firstly, the cytotoxic effect of carvacrol and thymol was determined after the 24 h and 48 h exposures of HepG2 cells, as determined by the MTT assay. Both components reduced cell viability in a time- and concentration-dependent manner (Figs. S1 and S2). Carvacrol was slightly less cytotoxic than thymol when cells were exposed to EOCs for 24 h. However, no differences were found after the 48-hour incubation period. The IC_{50} values obtained after 24 h exposure were 0.45 (0.01) mM and 0.40 (0.03) mM for carvacrol and thymol, respectively. At 48 h, the IC_{50} value for both components was similar: 0.32 (0.02) mM for carvacrol and 0.32 (0.03) mM for thymol.

Figure 2 displays the cytotoxicity-response curves for the carvacrol- and thymol-functionalised MCM-41, added either directly to the culture medium or in an extract dilution form. Both materials reduced cell viability in a concentration-dependent manner (Fig. S3) when HepG2 cells were directly exposed to the functionalised particles for 24 h and 48 h, as measured by the MTT assay. The IC_{50} values obtained for the carvacrol-functionalised MCM-41 were 0.15 (0.01) mg/mL and 0.09 (0.04) mg/mL for 24 h and 48 h, respectively. The thymol-functionalised microparticles gave an IC_{50} value of 0.15 (0.08) mg/mL after a 24-hour cell exposure and 0.11 (0.08) mg/mL after 48 h. However, when cells were treated with the filtered medium which previously contained each particle type, cell viability was significantly higher. A cell viability of 75% and 78% for the carvacrol- and thymol-functionalised silica was, respectively, observed after 24 h of exposure to the highest tested concentrations (2.5 mg/mL). After 48 h of treatment, these percentages were 92% for the carvacrol-functionalised particles and 85% for the thymol-

functionalised silica. When cells were exposed to the filtered solutions equivalent to the IC_{50} values obtained for both functionalised particle types, cell viability remained around 100%.

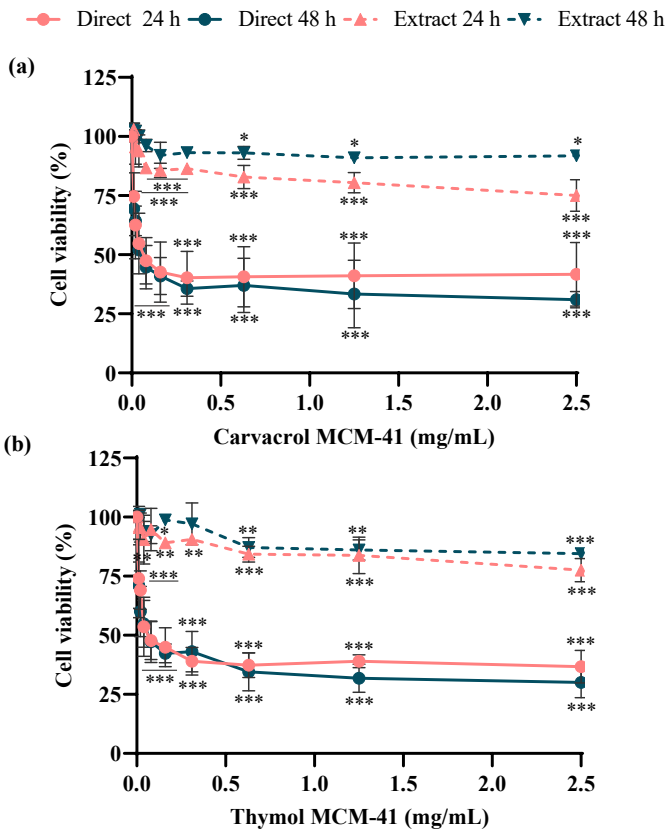

Figure 2. Concentration-cell viability plots of the HepG2 cells exposed either directly or in an extract dilution form to the carvacrol-functionalised MCM-41 (a); and the thymol-functionalised MCM-41 (b) for 24 h and 48 h by the MTT assay. Each bar represents the mean (SEM) of three independent assays, each performed 6-fold. (*) $p \leq 0.05$; (**) $p \leq 0.01$; (***) $p \leq 0.001$ indicates significant differences compared to the control according to the Student's t-test.

The IC_{50} values previously found for carvacrol and thymol were used to define the concentration range for the comparative analysis of the cytotoxic effects of the free EOCs, EOC-functionalised MCM-41 and bare MCM-41 microparticles. The results of the comparative analysis are shown in Figure 3. Free carvacrol was significantly less cytotoxic than the equivalent concentrations of carvacrol anchored to the surface of silica microparticles at the two lowest assayed concentrations (0.25 and 0.5 mM). Differences in cell viability between the free carvacrol and carvacrol-functionalised MCM-41 ranged from 75% to 32% and from 61% to 24% after 24 h and 48 h exposure, respectively. The bare MCM-41 microparticles also showed a lower cytotoxic response than the equivalent concentrations of the functionalised materials at the three highest concentrations tested for both exposure times. Differences in cell viability between the bare MCM-41 and carvacrol-functionalised MCM-41 ranged from 75% to 47% and from 89% to 47% after treating cells for 24 h and 48 h, respectively.

For thymol, the free compound was significantly less cytotoxic than the equivalent concentration of the immobilised compound on the MCM-41 microparticles at the highest tested concentration (0.25 mM). At this concentration, the differences in cell viability between the free thymol and thymol-functionalised MCM-41 were 59% and 61% after 24 h and 48 h exposure, respectively. The bare MCM-41 was less cytotoxic than the thymol-functionalised MCM-41 at the 0.25 mM and 0.5 mM concentrations. At these concentrations, the differences in cell viability between both particle types ranged from 65% to 44% and from 61% to 55% after 24 h and 48 h exposure, respectively.

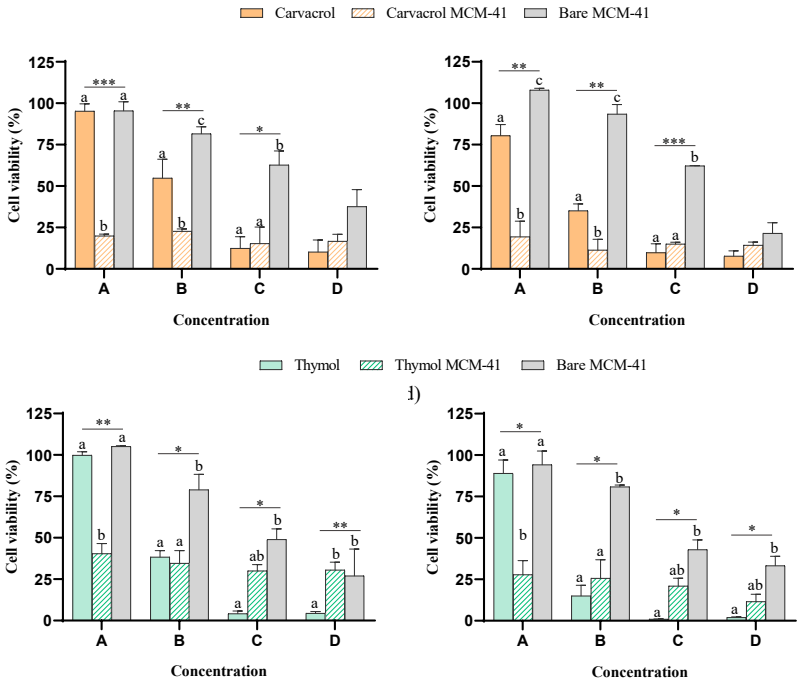

Figure 3. Concentration-cell viability plots of the HepG2 cells exposed to the equivalent concentrations of carvacrol, the carvacrol-functionalised MCM-41 and the bare MCM-41 for 24 h (a) and 48 h (b) or to the equivalent concentrations of thymol, the thymol-functionalised MCM-41 and the bare MCM-41 for 24 h (c) and 48 h (d). Each bar represents the mean (SEM) of three independent assays, each performed 6-fold. Significant differences (***$p \leq 0.01$, **$p \leq 0.01$, *$p \leq 0.05$) are indicated by different letters (a–c).

3.2.2. LDH assay

The LDH assay measures the activity of LDH released in cell culture medium after exposure to cytotoxic substances. It is an indicator of irreversible cell death due to cell membrane damage (Aslantürk, 2018). Therefore, higher LDH values in the medium indicate higher toxicity levels.

Figure 4 depicts the effect of the EOCs-functionalised particles on LDH release to the medium after 24 h of exposure. As this figure illustrates, the carvacrol- and thymol-functionalised silica exposures resulted in a significant increase in LDH release compared to the controls at the highest tested concentrations. Exposure to 2.5 mg/mL of the carvacrol-functionalised silica increased the LDH release by more than 10% compared to the control. For the thymol-functionalised silica at the two highest tested concentrations (1.25 and 2.5 mg/mL), LDH leakage into the culture medium increased by 14% and 16%, respectively. No differences were observed at all the other tested concentrations compared to the control.

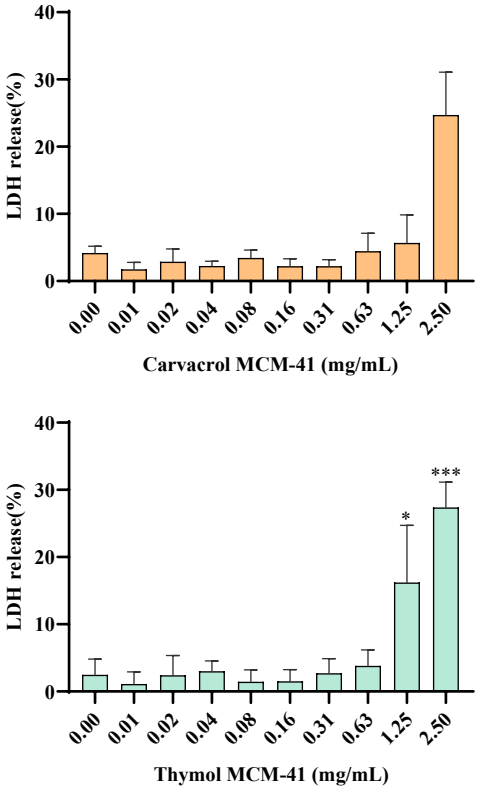

Figure 4. LDH activity in the HepG2 cells exposed to the carvacrol-functionalised MCM-41 microparticles (a) and the thymol-functionalised MCM-41 microparticles (b) for 24 h. The results are expressed as the mean (SEM, n=3). (*) $p \leq 0.05$; (**) $p \leq 0.01$; (***) $p \leq 0.001$ indicates significant differences compared to the control according to the Student's t-test.

3.2.3. ROS formation

ROS formation was studied as an indicator of oxidative stress using fluorescein derivative H_2DCF-DA. Figure 5 shows ROS production on the HepG2 cells exposed to 18.75, 37.5 and 75 µg/mL of the carvacrol- and

thymol-functionalised MCM-41 microparticles 120 min postexposure. As shown, exposure to the three concentrations of both the functionalised particle types did not induce ROS formation over this time period as no significant differences in DCFDA dye fluorescence intensity were observed compared to the control cells.

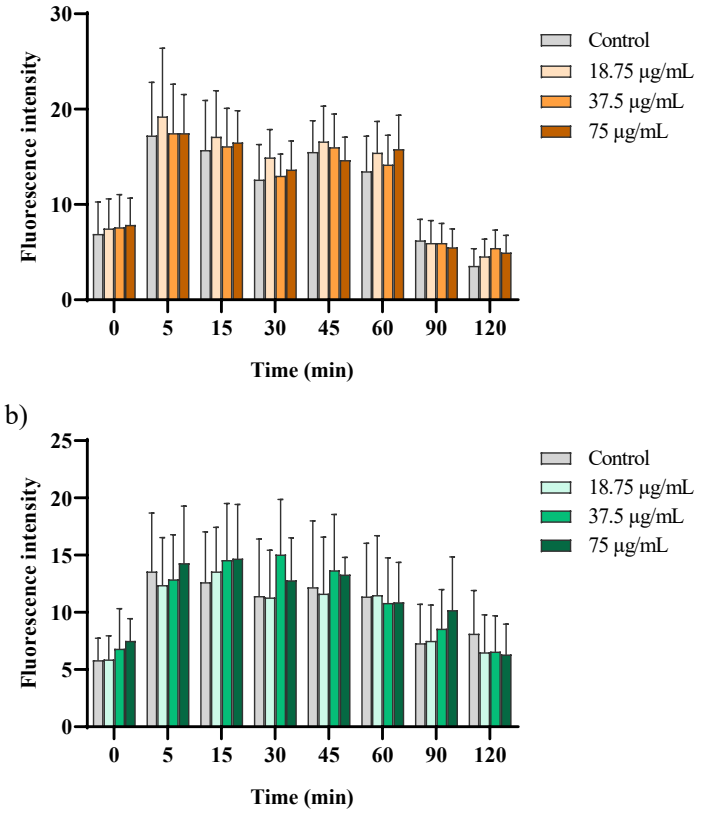

Figure 5. ROS induction according to time (0-120 min) in the HepG2 cells exposed to the sublethal concentrations of the carvacrol-functionalised MCM-41 microparticles (a) and thymol-functionalised MCM-41 microparticles (b). The results are expressed as the mean (SEM, n=3). No significant differences were found between the different test solutions and the control.

3.2.4. Lipid peroxidation assays

The MDA levels were measured as an indicator of LPO and oxidative stress by the TBARS assay. LPO production on HepG2 cells in the presence of the carvacrol- and thymol-functionalised silica at 18.75, 37.5 and 75 μg/mL is observed in Figure 6. The obtained results demonstrated that 24 h of exposure to the carvacrol-functionalised particles significantly increased MDA production by 44% (18.75 μg/mL), 15% (37.5 μg/mL) and 54% (75 μg/mL) in relation to the control cells. Similarly, 24 h of exposure to the thymol-functionalised particles significantly increased MDA levels in a concentration-dependent manner (Fig. 6). Exposure to 18.75, 37.5 and 75 μg/mL of the thymol-functionalised MCM-41 for 24 h resulted in an increase of 17%, 24% and 55%, respectively, compared to the control.

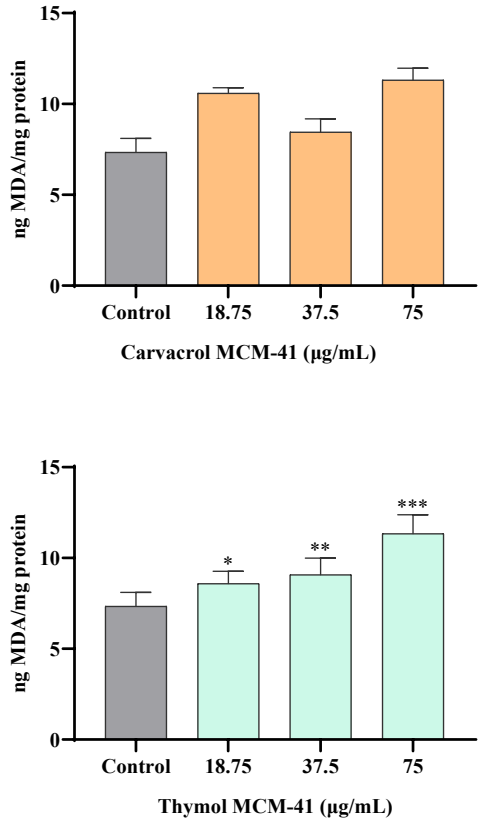

Figure 6. Effect on LPO as measured by MDA production after HepG2 cells exposure to sublethal concentrations of the carvacrol-functionalised MCM-41 microparticles (a) and thymol-functionalised MCM-41 microparticles (b) for 24 h. The results are expressed as the mean (SEM, n=3). (*) $p \leq 0.05$; (**) $p \leq 0.01$; (***) $p \leq 0.001$ indicates significant differences compared to the control according to the Student's t-test.

3.2.5. ΔΨm determination

To assess whether the exposure of the functionalised particles affected mitochondrial function, potential changes in ΔΨm were analysed by employing mitochondria fluorescent dye Rhodamine 123. As shown in Figure

7, 24 h of exposure to both materials induced a significant drop in ΔΨm in a concentration-dependent manner. This effect was stronger for the carvacrol-functionalised particles that decreased ΔΨm at the two highest tested concentrations (37.5 µg/mL and 75 µg/mL) by 19% and 28% in relation to the control, respectively. The thymol-functionalised particles at the 75 µg/mL concentration resulted in a significant 24% decrease in ΔΨm compared to the untreated control cells.

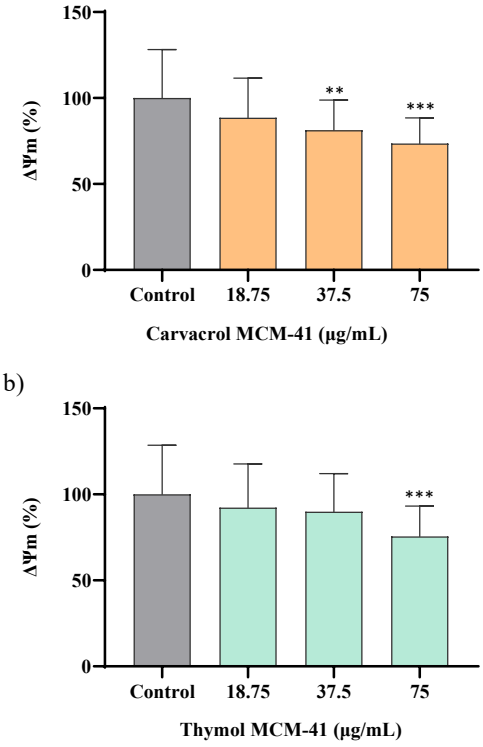

Figure 7. Effect on mitochondrial membrane potential (ΔΨm) after HepG2 cells' exposure to sublethal concentrations of the carvacrol-functionalised MCM-41 microparticles (a) and thymol-functionalised MCM-41 microparticles (b) for 24 h. The results are expressed as the mean (SEM, n=3). (**) $p \leq 0.01$; (***) $p \leq 0.001$ indicates significant differences compared to the control according to the Student's t-test.

3.2.6. Apoptosis and necrosis assays

The flow cytometry analysis was applied to determine the related death mechanism underlying the cytotoxic effect observed for the functionalised materials. Fluorescein Annexin V-FITC/PI double staining was used to distinguish and quantify the percentage of the necrotic, early apoptotic and late apoptotic cells after exposure to sublethal concentrations of the carvacrol- and thymol-functionalised MCM-41 (Fig. 8 and Fig. 9, respectively). The results revealed an increase in the percentage of the necrotic, early apoptotic and late apoptotic cells following treatment with rising concentrations of both the functionalised particles. However, significant differences were found only between the control cells and the cells exposed to the highest tested concentrations of both materials (75 µg/mL). The basal necrotic population in the control was 2.76 (0.40) %. After the treatment with 75 µg/mL of the carvacrol- and thymol-functionalised particles for 24 h, the necrotic rate rose to 10.20 (3.82) % and 8.63 (3.54) %, respectively. The percentage of the early apoptotic HepG2 cells increased from 6.65 (1.73) % in the unexposed control cells to 15.90 (3.46) % and 13.31 (1.83) % for the carvacrol- and thymol-functionalised MCM-41, and in this order. Similarly, the percentage of the late apoptotic cells went from 8.16 (0.26) % in the untreated culture to 16.27 (0.20) % and 13.98 (2.18) % for the carvacrol- and thymol-functionalised particles' exposed cells, respectively.

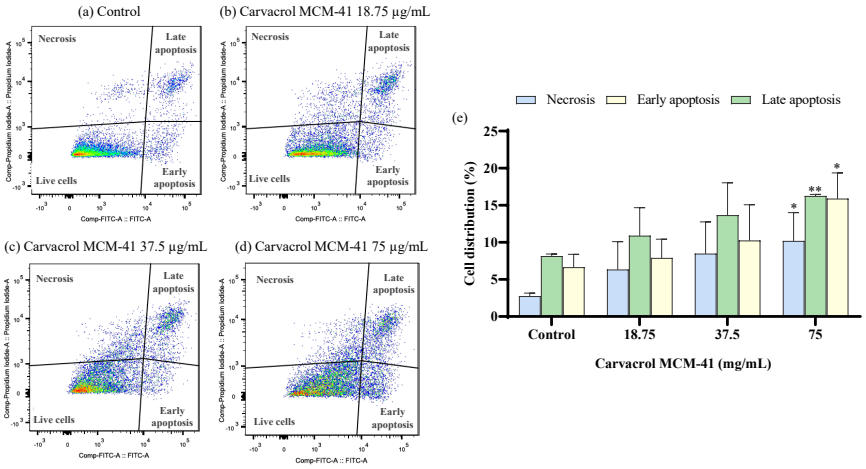

Figure 8. Flow cytometry analysis of the apoptotic and necrotic HepG2 cells exposed to sublethal concentrations of the carvacrol-functionalised MCM-41 microparticles using Annexin V-FITC/PI double staining. Representative two-dimensional dot plot diagrams of three independent experiments for: (a) the untreated cells; (b) the cells treated with 18.75 µg/mL; (c) 37.5 µg/mL; (d) 75 µg/mL of the carvacrol-functionalised MCM-41 microparticles. The upper left quadrant (PI+/Annexin V-FITC-) represents the necrotic cells, the left lower quadrant (PI-/Annexin V-FITC-) depicts the live cells, the upper right quadrant (PI+ /Annexin V-FITC+) refers to the late apoptotic cells and the lower right quadrant (PI-/Annexin V-FITC+) represents the early apoptotic cells. (e) The percentage of the early apoptotic, late apoptotic and necrotic cells. The results are expressed as the mean (SEM, n=3). (*) $p \leq 0.05$; (**) $p \leq 0.01$ indicates a significant difference compared to the control according to the Student's t-test.

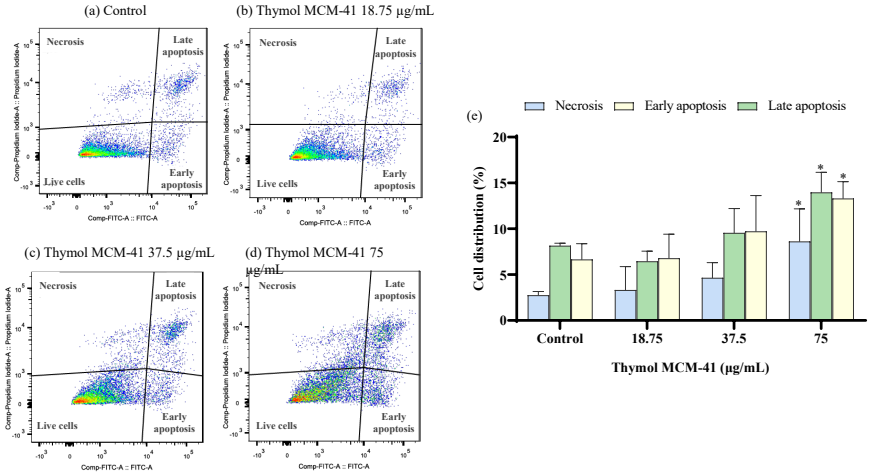

Figure 9. Flow cytometry analysis of the apoptotic and necrotic HepG2 cells exposed to sublethal concentrations of the thymol-functionalised MCM-41 microparticles using Annexin V-FITC/PI double staining. Representative two-dimensional dot plot diagrams of three independent experiments for: (a) the untreated cells; (b) the cells treated with 18.75 µg/mL; (c) 37.5 µg/mL; (d) 75 µg/mL of the thymol-functionalised MCM-41 microparticles. The upper left quadrant (PI+/Annexin V-FITC-) represents the necrotic cells, the left lower quadrant (PI-/Annexin V-FITC-) denotes the live cells, the upper right quadrant (PI+ /Annexin V-FITC+) refers to the late apoptotic cells and the lower right quadrant (PI-/Annexin V-FITC+) represents the early apoptotic cells. (e) The percentage of the early apoptotic, late apoptotic and necrotic cells. The results are expressed as the mean (SEM, n=3). (*) $p \leq 0.05$ indicates a significant difference compared to the control according to the Student's t-test.

4. Discussion

The immobilisation of natural EOCs on the surface of silica particles has emerged as an innovative technology to enhance their antimicrobial and antioxidant properties. However, their safety needs to be addressed given their possible application to food or food contact materials. For this purpose, the potential health hazards that derive from exposure to these new materials for consumer health should be thoroughly investigated at the cellular level. The use of cell cultures is a relevant tool in toxicity testing to improve our understanding of hazardous materials and to predict their effects on human health (Eisenbrand et al., 2002). Assays that determine basal cytotoxicity measure cell viability or cell death as a consequence of damage to basic cellular functions, and allow the rapid identification of toxic compounds. Moreover, *in vitro* tests of specialised cell functions and metabolic endpoints provide insight into the pathways and mechanisms of action involved in chemically induced toxicity at both the molecular and cellular levels. This study examines the *in vitro* toxic effect of the carvacrol- and thymol-functionalised MCM-41 silica particles on HepG2 cells as a model cell line. The aim was to evaluate their potential toxicity and to fully understand the associated involved mechanism.

Firstly, a comparative analysis of the functionalised-particles and their constituents was carried out. It revealed that the free EOCs and bare MCM-41 microparticles exhibited significantly milder cytotoxic effects than the equivalent EOC-functionalised silica concentrations. Similar results have been found for eugenol- and vanillin-functionalised MCM-41 microparticles (Fuentes et al., 2021). In that study, the stronger cytotoxic effect observed for the EOCs-functionalised silica was attributed to physico-chemical properties, such as surface charge and hydrophobicity, which could be responsible for promoting interactions of EOCs with cell membranes. Previous studies have demonstrated that surface functionalisation may enhance the toxicity of silica

particles (Dumitrescu et al., 2017; Paatero et al., 2017; Puerari et al., 2021; Yu et al., 2011). Chen et al. (2009) indicated that functionalisation with carvacrol increased the cytotoxicity of chitosan nanoparticles in a 3T3 mouse fibroblast cell line. The IC_{50} value observed for carvacrol-grafted chitosan nanoparticles was around 1 mg/mL, whereas cell viability was still higher than 80% at the 2 mg/mL concentration of the unmodified chitosan nanoparticles as measured by the MTT assay. However, carvacrol-modified chitosan nanoparticles were significantly less cytotoxic to mammalian cells than free carvacrol. As previously reported, this discrepancy may be the result of differences in the starting material, the cell type employed for the cytotoxicity assays or the lower degree of grafting achieved for silica particles (Fuentes et al., 2021).

Cytotoxicity data may serve to predict acute systemic toxicity *in vivo* and to also define the concentration range for mechanistic toxicity studies (Ciappellano et al., 2016; Severin et al., 2017). With this 2-fold objective, the cytotoxicity of the carvacrol- and thymol-functionalised microparticles was analysed by two methods based on different physiological endpoints; the MTT and the LDH release assays. As measured by the MTT method, 24 h of exposure gave an IC_{50} value of 0.15 mg/mL for both the functionalised materials, and this value lowered to 0.09 mg/mL and 0.11 mg/mL after the 48-hour treatment, for carvacrol- and thymol-silica, respectively. In a previous work, Fuentes et al., 2021 determined the cytotoxic effect of bare MCM-41 silica microparticles on HepG2 cells by the MTT assay and confirmed the biocompatibility reported for calcined mesoporous silica (Aburawi et al., 2012; Al-Salam et al., 2011; Samri et al., 2012; Shamsi et al., 2010). Exposing cells to bare MCM-41 silica for 24 h and 48 h led to IC_{50} values of 18.90 mg/mL and 15.82 mg/mL, respectively (Fuentes et al., 2021). In comparison to these results, we found herein that the functionalisation of MCM-41 microparticles with carvacrol or thymol increased the cytotoxicity of the starting material by approximately 100-fold. However, when cells were

exposed to the filtered medium which previously contained the particles during the extract dilution assays, cell viability remained at around 100% at the IC_{50} values calculated for both materials. These results can be interpreted as a confirmation of a direct interaction of cells with particles that is responsible for the cytotoxic behaviour found for both the carvacrol- and thymol-functionalised particles; while an indirect cytotoxicity effect due to components leached from the functionalised particles' surface or by the depletion of nutrients from the culture medium (Casey et al., 2008) is not expected.

The cytotoxic effects assessed by the LDH assay were observed at higher particle concentrations than with the MTT assay and, thus, demonstrates that the MTT assay was more sensitive than the LDH assay for determining cell viability after the exposure of the EOCs-functionalised microparticles. The sensitivity of the different cytotoxicity assays differs depending on the mechanisms leading to cell death (Weyermann et al., 2005). The MTT method determines mitochondrial metabolic activity of viable cells, while the LDH assay measures cell death due to cell membrane damage. Hence concerning their sensitivity, the differences observed between both assays may suggest that impairment of the mitochondrial function may precede the disruption of membrane integrity and cell lysis in cells exposed to the carvacrol- and thymol-functionalised microparticles. Moreover, these results support the widespread consensus than more than one cell viability assay should be used to increase the reliability of the results during *in vitro* studies (Aslantürk, 2018; Eisenbrand et al., 2002; Fotakis and Timbrell, 2006).

It is worth mentioning that different studies have described particle interference when testing cytotoxicity with both methods (Holder et al., 2012; Kroll et al., 2012). Distinct factors have been proven to limit the sensitivity of the MTT method, including pH, optical activity or surface reactivity of particles (Abbasi et al., 2021; Laaksonen et al., 2007). In the LDH assay,

different inorganic particles have been demonstrated to interfere with this assay by either adsorbing or inactivating the LDH protein, and both mechanisms involve decreased absorbance in the LDH assay that results in a false indication of a non-toxic response (Holder et al., 2012). Korhonen et al. (2016) used the LDH assay to evaluate the cytotoxic effect of mesoporous silica microparticles on human corneal epithelial (HCE) and retinal pigment epithelial (ARPE-19) cells. These authors found increased or decreased reactivity in the LDH assay depending on the employed cell culture medium. Herein the MTT and LDH viability assays were also performed under cell-free conditions to evaluate any interference of the functionalised particles with both assays. At low concentrations, the EOCs-functionalised materials did not induce any non-specific response in the MTT and LDH viability assays. At concentrations higher than 0.31 mg/mL of particles, significantly increased absorbance was observed for both the cell-free assays. Consequently, data were corrected to avoid any particle interferences by subtracting the absorbance of the cell-free controls from that of the test wells.

In order to gain insight into the cytotoxicity mechanism induced by these materials, different endpoints related to oxidative stress, mitochondrial dysfunction and the cell death pathway were investigated. In this aspect of the work, the IC_{50} values for both materials obtained by the MTT assay were used to define the concentration range for further assays.

Oxidative stress is a major mechanism involved in the toxicity induced by many xenobiotics (Zhang, 2018). It results from an imbalance between the production of oxidising molecular species and the protective mechanisms produced by cells for their removal. Under normal conditions, ROS are oxygen-containing chemically-reactive molecules are produced by cells as a consequence of aerobic metabolism (Ray et al., 2012). However, the overproduction and accumulation of ROS due to interactions of cells with toxic agents may lead to an antioxidant system dysfunction, and also to

oxidative damage to cellular macromolecules like lipids, proteins or nucleic acids, which causes severe cell toxicity (Eisenbrand et al., 2002). To evaluate whether oxidative stress was involved in carvacrol- and thymol-functionalised MCM-41 cytotoxicity, two different biomarkers were used: ROS production and LPO generation. The results showed that exposure to the sublethal concentrations of both materials did not induce early ROS formation as measured by the DCFDA assay. However, the MDA levels significantly increased when cells were exposed to particles for 24 h, which indicates that oxidative stress occurred through LPO.

High ROS levels that persist for a long period are thought to be the major factor responsible for reacting with polyunsaturated fatty acids of lipid membranes and for inducing LPO (Barrera, 2012). Lack of ROS in this study may be explained by the differences in the exposure times employed between both assays. ROS formation was measured within 2 hours after exposure to the sublethal functionalised silica concentrations, while LPO was determined when cells were treated with these materials for 24 h. Accordingly, Santos et al. (2010) evaluated ROS production following exposure to different mesoporous silicon microparticles in human colon carcinoma Caco-2 cell line by the DCFDA assay. These authors found no significant increases in hydrogen peroxide concentrations or mitochondrial superoxide after a 3-hour incubation time, but observed a significant increase in hydrogen peroxide formation after 24 h exposure. Longer exposure times than those usually employed by this method have also been necessary to detect oxidative stress caused by other toxic insults (Aranda et al., 2013). Some authors also suggest that, although the DCFDA probe has been extensively employed as a biomarker of oxidative stress and is assumed to reflect the overall oxidative status of cells, it can only detect hydrogen peroxides, peroxyl radicals and peroxynitrite anions, and not all the different ROS types (Herzog et al., 2009).

Toxic agents can generate ROS by directly interacting with the electron-transport chain complexes in the inner mitochondrial membrane (Boelsterli, 2007). Moreover, cell-particle interactions can induce ROS formation by a surface-catalysed reaction (Lehman et al., 2016). Indeed silica particles have been demonstrated to induce ROS formation by both mechanisms; direct contact of the cell membrane with particles' surface and by triggering cell-signalling pathways that initiate cytokine release and apoptosis within cells (Hamilton et al., 2008). Different phenomena, including hydrophobic or hydrophilic interactions, active electron configurations, redox potential or semiconductor and electronic properties, may be responsible for ROS generation upon the interactions of particles with biological systems (Santos et al., 2010). In line with this, Lehman et al. (2016) studied the free radical species generated from the surface of non-porous and mesoporous nanoparticles by electron paramagnetic resonance spectroscopy. These authors found a correlation between the ROS released from the nanoparticle surface, intracellular ROS and cellular toxicity in murine macrophage cell line RAW 264.7. Moreover, amine-functionalisation reduced the amount of the free radical generated at the solid–liquid interface by non-porous nanosilica and, as suggested by the authors, this would mitigate their toxic behaviour. Similarly, Santos et al. (2010) found surface chemistry to be a determinant factor that establishes ROS production and cell-particle interactions. According to their work, thermally carbonised particles induced toxicity as a result of stimulating ROS production on Caco-2 cells, while thermally oxidised particles did not induce significant ROS formation and resulted in less cell damage as a result of weak cell-particle interactions. In our work, the increased cytotoxicity found for the EOCs-functionalised compared to the native microparticles may be attributed to differences in the surface properties between the bare and EOCs-functionalised particles. Cationic nature and hydrophobic surfaces have been demonstrated to increase *in vitro* toxicity and the number of apoptotic cells as a result of strong cell-particle interactions

(Saei et al., 2017; Santos et al., 2010). These properties may, therefore, be related to the increased cytotoxicity found for the functionalised materials in our study.

A close relation exists between ROS formation and mitochondria as these organelles are considered the main source of ROS in the cell. At the same time, mitochondrial damage by ROS formation is a main mechanism of toxicant-induced cytotoxicity (Zhang, 2018). Accordingly, mitochondrial dysfunction is one of the most sensitive indicators of adverse cell effects that can be evaluated by monitoring changes in ΔΨm of exposed cells (Xu et al., 2004). In this study, ΔΨm depletion was observed after treating HepG2 cells with the carvacrol- and thymol-functionalised silica. The generated ΔΨm is an essential component within a range of processes, including energy storage during oxidative phosphorylation, calcium homeostasis or cellular differentiation. Moreover, mitochondrial integrity disruption has been described as one of the early events that lead to apoptosis and may serve as a biomarker for apoptotic cell death (Jeong and Seol, 2008).

Exposure to cytotoxic agents can lead to cell death mainly by two major mechanisms: apoptosis and necrosis. In this work, the death mechanism related to the cytotoxic effects induced by modified-MCM-41 exposure was evaluated using the Annexin V-FITC/PI double staining and flow cytometry analysis. This method allows healthy, early apoptotic, late apoptotic and necrotic cells to be discriminated. We found that all three early apoptotic, late apoptotic and necrotic rates significantly rose after treating HepG2 cells at the highest sublethal concentration of both the carvacrol- and thymol-functionalised silica for 24 h. According to these results, both mechanisms of cell death are involved in the cytotoxicity induced by the EOCs-functionalised MCM-41.

Apoptosis, or programmed cell death, is a slow form of cell death that can occur under normal physiological conditions or may be induced by apoptotic compounds. There are two main pathways that lead to apoptosis: the extrinsic or death-receptor pathway, which is activated from outside the cell by the ligation of transmembrane death receptors; the intrinsic or mitochondrial pathway, which begins with the permeabilisation of the mitochondrial outer membrane triggered by different signals, such as DNA damage, ischaemia or oxidative stress (Wang and Youle, 2009). ΔΨm depletion brings about the release of mitochondrial intermembrane space proteins to the cytoplasm, including cytochrome c, which consequently triggers other apoptotic factors, such as caspases activation or chromosome fragmentation, to lead to apoptosis through the mitochondrial or intrinsic pathway apoptotic death pathway (Tait and Green, 2013). Therefore, loss of ΔΨm serves as a biomarker of apoptotic cell death.

Unlike apoptosis, necrosis consists in a rapid cell death form that is induced by external injuries, such as hypothermia, radiation, hypoxia or chemicals that damage the cell membrane (D'Arcy, 2019). Destruction of the plasma membrane or the biochemical supports of its integrity leads to the release of intracellular material, local inflammatory responses, cell swell and lysis (Miret et al., 2006). Consequently, necrosis can be measured by the presence of the cytoplasmic content in extracellular fluid i.e. by measuring the activity of enzymes like LDH. As previously explained, the LDH assay was far less sensitive that the MTT assay for evaluating the basal cytotoxicity on HepG2 cells as a result of microparticles' exposure, and suggests impairment of mitochondrial activity rather than cell membrane disruption. As a result, we hypothesise that apoptosis is the most likely mechanism of cell death after the exposure of the EOCs-functionalised particles.

According to our results, the mechanism underlying the cytotoxic effect of the carvacrol- and thymol-functionalised silica microparticles on HepG2 cells

involves oxidative stress induction, which will cause mitochondrial dysfunction and lead to apoptotic death pathway activation. This mechanism of toxic action bears similarities with the mechanism described for their constituents. Essential oils and their components have been demonstrated to induce toxicity in eukaryotic cells due to a phenolic-like prooxidant mechanism (Bakkali et al., 2008). These components penetrate cells and permeabilise cytoplasmic, and especially, mitochondrial membranes. Then damaged mitochondria produce ROS by generating reactive phenoxyl radicals with a pro-oxidant potential that may oxidise EOCs. Ultimately, this sequence of events leads to cell death by apoptosis (Bakkali et al., 2008). Different sized MCM-41 and SBA-15 microparticles induce ROS formation, especially O_2^-, at concentrations over 1 mg/mL after 3 h of incubation on Caco-2 cells, which overwhelms antioxidant defences, causes mitochondrial dysfunction and increases apoptotic signalling (Heikkilä et al., 2010). As found herein for the EOCs-functionalised silica, metabolic activity is a more sensitive endpoint, as measured by ATP depletion, than cell membrane integrity (Heikkilä et al., 2010). However, both the bare MCM-41 microparticles and EOCs exhibited cytotoxic effects and ROS generation at much higher concentrations that those found for the functionalised particles, which are the object of this study. Our results suggest that either a synergistic effect given the presence of both silanol groups from the bulk material and EOCs derivatives from the functionalisation process on the functionalised particles surface or a boosting effect of EOCs as a consequence of their higher density or reduced volatility increased EOCs-cell membrane interactions (Fuentes et al., 2021). Another possible explanation is that EOCs in their free form can be partly metabolised by cells and this phenomenon is not possible for immobilised compounds. Nonetheless, the cellular uptake of microparticles by HepG2 cells would still need to be dismissed by confocal microscopy analyses in the future.

Alternatives to synthetic preservatives for food applications are not free of potential toxicological hazards. As observed in this work, toxicity studies are necessary to understand the interactions of new materials with biological systems and to guarantee their safety for human health. In summary, our results show that the functionalisation of silica MCM-41 microparticles with natural EOCs carvacrol and thymol increased these materials' cytotoxic potential compared to their free constituents. Both particle types behaved similarly as regards their cytotoxic effects, which emerged from microparticles themselves, and not from the degradation products released to culture media. The results found in this study generally support the hypothesis that the carvacrol- and thymol-functionalised MCM-41 induce toxicity on HepG2 cells by an oxidative stress-related mechanism. A direct physical interaction between the particles surface and cell membranes could be responsible for inducing ROS overproduction. Oxidative stress would lead to the oxidation of different cellular components like lipids, and also to the impairement of the $\Delta\Psi m$ function that would, in turn, trigger apoptosis signalling through the mitochondrial pathway, and would ultimately lead to cell death by both the proteolytic cascade of pro-apoptotic enzymes and the damage caused to the mitochondrial function. These results should be considered when designing new hybrid materials for food-industry applications.

Acknowledgements

The authors gratefully acknowledge the financial support from the Spanish government (Project RTI2018-101599-B-C21 (MCUI/AEI/FEDER, EU)).

References

Abbasi, F., Hashemi, H., Samaei, M.R., SavarDashtaki, A., Azhdarpoor, A., Fallahi, M.J., 2021. The synergistic interference effect of silica nanoparticles concentration and the wavelength of ELISA on the colorimetric assay of cell toxicity. Sci. Rep. 11, 15133. https://doi.org/10.1038/s41598-021-92419-1

Abbaszadeh, S., Sharifzadeh, A., Shokri, H., Khosravi, A.R., Abbaszadeh, A., 2014. Antifungal efficacy of thymol, carvacrol, eugenol and menthol as alternative agents to control the growth of food-relevant fungi. J. Mycol. Med. 24, 51–56. https://doi.org/10.1016/J.MYCMED.2014.01.063

Abdelhamid, A.G., Yousef, A.E., 2021. Natural Antimicrobials Suitable for Combating Desiccation-Resistant Salmonella enterica in Milk Powder. Microorg. 2021, Vol. 9, Page 421 9, 421. https://doi.org/10.3390/MICROORGANISMS9020421

Aburawi, E.H., Qureshi, M.A., Oz, D., Jayaprakash, P., Tariq, S., Hameed, R.S., Das, S., Goswami, A., Biradar, A. V., Asefa, T., Souid, A.-K., Adeghate, E., Howarth, F.C., 2012. Biocompatibility of Calcined Mesoporous Silica Particles with Ventricular Myocyte Structure and Function. Chem. Res. Toxicol. 26, 26–36. https://doi.org/10.1021/TX300255U

Al-Salam, S., Balhaj, G., Al-Hammadi, S., Sudhadevi, M., Tariq, S., Biradar, A. V., Asefa, T., Souid, A.-K., 2011. In Vitro Study and Biocompatibility of Calcined Mesoporous Silica Microparticles in Mouse Lung. Toxicol. Sci. 122, 86–99. https://doi.org/10.1093/TOXSCI/KFR078

Alothman, Z., 2012. A Review: Fundamental Aspects of Silicate Mesoporous Materials. Materials (Basel). 5, 2874–2902. https://doi.org/10.3390/ma5122874

Aranda, A., Sequedo, L., Tolosa, L., Quintas, G., Burello, E., Castell, J. V., Gombau, L., 2013. Dichloro-dihydro-fluorescein diacetate (DCFH-DA) assay: A quantitative method for oxidative stress assessment of nanoparticle-treated cells. Toxicol. Vitr. 27, 954–963. https://doi.org/10.1016/j.tiv.2013.01.016

Aslantürk, Ö.S., 2018. In Vitro Cytotoxicity and Cell Viability Assays: Principles,

Advantages, and Disadvantages, in: Genotoxicity - A Predictable Risk to Our Actual World. InTech. https://doi.org/10.5772/intechopen.71923

Bagheri, E., Ansari, L., Abnous, K., Taghdisi, S.M., Charbgoo, F., Ramezani, M., Alibolandi, M., 2018. Silica based hybrid materials for drug delivery and bioimaging. J. Control. Release. https://doi.org/10.1016/j.jconrel.2018.03.014

Bakkali, F., Averbeck, S., Averbeck, D., Idaomar, M., 2008. Biological effects of essential oils – A review. Food Chem. Toxicol. 46, 446–475. https://doi.org/10.1016/j.fct.2007.09.106

Barrera, G., 2012. Oxidative Stress and Lipid Peroxidation Products in Cancer Progression and Therapy. ISRN Oncol. 2012, 1–21. https://doi.org/10.5402/2012/137289

Boelsterli, U.A., 2007. Mechanistic toxicology : the molecular basis of how chemicals disrupt biological targets. CRC Press.

Burt, S., 2004. Essential oils: their antibacterial properties and potential applications in foods—a review. Int. J. Food Microbiol. 94, 223–253. https://doi.org/10.1016/J.IJFOODMICRO.2004.03.022

Čabarkapa, I., Čolović, R., Đuragić, O., Popović, S., Kokić, B., Milanov, D., Pezo, L., 2019. Anti-biofilm activities of essential oils rich in carvacrol and thymol against Salmonella Enteritidis. https://doi.org/10.1080/08927014.2019.1610169 35, 361–375.

Cabrera, S., El Haskouri, J., Guillem, C., Latorre, J., Beltrán-Porter, A., Beltrán-Porter, D., Marcos, M.D., Amorós, P., 2000. Generalised syntheses of ordered mesoporous oxides: The atrane route. Solid State Sci. 2, 405–420. https://doi.org/10.1016/S1293-2558(00)00152-7

Casey, A., Herzog, E., Lyng, F.M., Byrne, H.J., Chambers, G., Davoren, M., 2008. Single walled carbon nanotubes induce indirect cytotoxicity by medium depletion in A549 lung cells. Toxicol. Lett. 179, 78–84. https://doi.org/10.1016/J.TOXLET.2008.04.006

Chen, F., Shi, Z., Neoh, K.G., Kang, E.T., 2009. Antioxidant and antibacterial activities of eugenol and carvacrol-grafted chitosan nanoparticles. Biotechnol. Bioeng. 104, 30–39. https://doi.org/10.1002/bit.22363

Ciappellano, S.G., Tedesco, E., Venturini, M., Benetti, F., 2016. In vitro toxicity assessment of oral nanocarriers. Adv. Drug Deliv. Rev. https://doi.org/10.1016/j.addr.2016.08.007

D'Arcy, M.S., 2019. Cell death: a review of the major forms of apoptosis, necrosis and autophagy. Cell Biol. Int. 43, 582–592. https://doi.org/10.1002/CBIN.11137

Diab, R., Canilho, N., Pavel, I.A., Haffner, F.B., Girardon, M., Pasc, A., 2017. Silica-based systems for oral delivery of drugs, macromolecules and cells. Adv. Colloid Interface Sci. 249, 346–362. https://doi.org/10.1016/j.cis.2017.04.005

Dumitrescu, E., Karunaratne, D.P., Prochaska, M.K., Liu, X., Wallace, K.N., Andreescu, S., 2017. Developmental toxicity of glycine-coated silica nanoparticles in embryonic zebrafish. Environ. Pollut. 229, 439–447. https://doi.org/10.1016/J.ENVPOL.2017.06.016

Eisenbrand, G., Pool-Zobel, B., Baker, V., Balls, M., Blaauboer, B.J., Boobis, A., Carere, A., Kevekordes, S., Lhuguenot, J.C., Pieters, R., Kleiner, J., 2002. Methods of in vitro toxicology. Food Chem. Toxicol. https://doi.org/10.1016/S0278-6915(01)00118-1

Faleiro, M.L., Miguel, G., 2020. Antimicrobial and Antioxidant Activities of Natural Compounds: Enhance the Safety and Quality of Food. Foods 2020, Vol. 9, Page 1145 9, 1145. https://doi.org/10.3390/FOODS9091145

Ferrer, E., Juan-García, A., Font, G., Ruiz, M.J., 2009. Reactive oxygen species induced by beauvericin, patulin and zearalenone in CHO-K1 cells. Toxicol. Vitr. 23, 1504–1509. https://doi.org/10.1016/j.tiv.2009.07.009

Fotakis, G., Timbrell, J.A., 2006. In vitro cytotoxicity assays: Comparison of LDH, neutral red, MTT and protein assay in hepatoma cell lines following exposure to cadmium chloride. Toxicol. Lett. 160, 171–177.

https://doi.org/10.1016/J.TOXLET.2005.07.001

Fuentes, C., Ruiz-Rico, M., Fuentes, A., Barat, J.M., Ruiz, M.J., 2021. Comparative cytotoxic study of silica materials functionalised with essential oil components in HepG2 cells. Food Chem. Toxicol. 147, 111858. https://doi.org/10.1016/j.fct.2020.111858

Fuentes, C., Ruiz-Rico, M., Fuentes, A., Ruiz, M.J., Barat, J.M., 2020. Degradation of silica particles functionalised with essential oil components under simulated physiological conditions. J. Hazard. Mater. 399, 123120. https://doi.org/10.1016/j.jhazmat.2020.123120

García-Ríos, E., Ruiz-Rico, M., Guillamón, J.M., Pérez-Esteve, É., Barat, J.M., 2018. Improved antimicrobial activity of immobilised essential oil components against representative spoilage wine microorganisms. Food Control 94, 177–186. https://doi.org/10.1016/j.foodcont.2018.07.005

Garrido-Cano, I., Candela-Noguera, V., Herrera, G., Cejalvo, J.M., Lluch, A., Marcos, M.D., Sancenon, F., Eroles, P., Martínez-Máñez, R., 2021. Biocompatibility and internalization assessment of bare and functionalised mesoporous silica nanoparticles. Microporous Mesoporous Mater. 310, 110593. https://doi.org/10.1016/J.MICROMESO.2020.110593

Hamilton, R.F., Thakur, S.A., Holian, A., 2008. Silica binding and toxicity in alveolar macrophages. Free Radic. Biol. Med. 44, 1246–1258. https://doi.org/10.1016/j.freeradbiomed.2007.12.027

Heikkilä, T., Santos, H.A., Kumar, N., Murzin, D.Y., Salonen, J., Laaksonen, T., Peltonen, L., Hirvonen, J., Lehto, V.-P., 2010. Cytotoxicity study of ordered mesoporous silica MCM-41 and SBA-15 microparticles on Caco-2 cells. Eur. J. Pharm. Biopharm. 74, 483–494. https://doi.org/10.1016/J.EJPB.2009.12.006

Herzog, E., Byrne, H.J., Davoren, M., Casey, A., Duschl, A., Oostingh, G.J., 2009. Dispersion medium modulates oxidative stress response of human lung epithelial cells upon exposure to carbon nanomaterial samples. Toxicol. Appl. Pharmacol. 236, 276–281. https://doi.org/10.1016/J.TAAP.2009.02.007

Holder, A.L., Goth-Goldstein, R., Lucas, D., Koshland, C.P., 2012. Particle-Induced Artifacts in the MTT and LDH Viability Assays. https://doi.org/10.1021/tx3001708

Hyldgaard, M., Mygind, T., Meyer, R.L., 2012. Essential oils in food preservation: Mode of action, synergies, and interactions with food matrix components. Front. Microbiol. 3, 1–12. https://doi.org/10.3389/fmicb.2012.00012

Jeong, S.Y., Seol, D.W., 2008. The role of mitochondria in apoptosis. J. Biochem. Mol. Biol. https://doi.org/10.5483/bmbrep.2008.41.1.011

Karam, L., Roustom, R., Abiad, M.G., El-Obeid, T., Savvaidis, I.N., 2019. Combined effects of thymol, carvacrol and packaging on the shelf-life of marinated chicken. Int. J. Food Microbiol. 291, 42–47. https://doi.org/10.1016/J.IJFOODMICRO.2018.11.008

Korhonen, E., Rönkkö, S., Hillebrand, S., Riikonen, J., Xu, W., Järvinen, K., Lehto, V.P., Kauppinen, A., 2016. Cytotoxicity assessment of porous silicon microparticles for ocular drug delivery. Eur. J. Pharm. Biopharm. 100, 1–8. https://doi.org/10.1016/J.EJPB.2015.11.020

Kroll, A., Pillukat, M.H., Hahn, D., Schnekenburger, J., 2012. Interference of engineered nanoparticles with in vitro toxicity assays. Arch. Toxicol. 86, 1123–1136. https://doi.org/10.1007/s00204-012-0837-z

Kyriakidou, K., Brasinika, D., Trompeta, A.F.A., Bergamaschi, E., Karoussis, I.K., Charitidis, C.A., 2020. In vitro cytotoxicity assessment of pristine and carboxyl-functionalized MWCNTs. Food Chem. Toxicol. 141, 111374. https://doi.org/10.1016/j.fct.2020.111374

Laaksonen, T., Santos, H., Vihola, H., Salonen, J., Riikonen, J., Heikkilä, T., Peltonen, L., Kumar, N., Murzin, D.Y., Lehto, V.P., Hirvonen, J., 2007. Failure of MTT as a toxicity testing agent for mesoporous silicon microparticles. Chem. Res. Toxicol. 20, 1913–1918. https://doi.org/10.1021/tx700326b

Lehman, S.E., Morris, A.S., Mueller, P.S., Salem, A.K., Grassian, V.H., Larsen, S.C., 2016. Silica nanoparticle-generated ROS as a predictor of cellular toxicity:

Mechanistic insights and safety by design. Environ. Sci. Nano 3, 56–66. https://doi.org/10.1039/c5en00179j

Meynen, V., Cool, P., Vansant, E.F., 2009. Verified syntheses of mesoporous materials. Microporous Mesoporous Mater. 125, 170–223. https://doi.org/10.1016/J.MICROMESO.2009.03.046

Miret, S., De Groene, E.M., Klaffke, W., 2006. Comparison of in vitro assays of cellular toxicity in the human hepatic cell line HepG2. J. Biomol. Screen. 11, 184–193. https://doi.org/10.1177/1087057105283787

Paatero, I., Casals, E., Niemi, R., Özliseli, E., Rosenholm, J.M., Sahlgren, C., 2017. Analyses in zebrafish embryos reveal that nanotoxicity profiles are dependent on surface-functionalization controlled penetrance of biological membranes. Sci. Rep. 7. https://doi.org/10.1038/S41598-017-09312-Z

Peña-Gómez, N., Ruiz-Rico, M., Fernández-Segovia, I., Barat, J.M., 2019a. Study of apple juice preservation by filtration through silica microparticles functionalised with essential oil components. Food Control 106, 106749. https://doi.org/10.1016/j.foodcont.2019.106749

Peña-Gómez, N., Ruiz-Rico, M., Pérez-Esteve, É., Fernández-Segovia, I., Barat, J.M., 2020. Microbial stabilization of craft beer by filtration through silica supports functionalized with essential oil components. LWT 117, 108626. https://doi.org/10.1016/j.lwt.2019.108626

Peña-Gómez, N., Ruiz-Rico, M., Pérez-Esteve, É., Fernández-Segovia, I., Barat, J.M., 2019b. Novel antimicrobial filtering materials based on carvacrol, eugenol, thymol and vanillin immobilized on silica microparticles for water treatment. Innov. Food Sci. Emerg. Technol. 58, 102228. https://doi.org/10.1016/j.ifset.2019.102228

Puerari, R.C., Ferrari, E., de Cezar, M.G., Gonçalves, R.A., Simioni, C., Ouriques, L.C., Vicentini, D.S., Matias, W.G., 2019. Investigation of toxicological effects of amorphous silica nanostructures with amine-functionalized surfaces on Vero cells. Chemosphere 214, 679–687.

https://doi.org/10.1016/j.chemosphere.2018.09.165

Puerari, R.C., Ferrari, E., Oscar, B.V., Simioni, C., Ouriques, L.C., Vicentini, D.S., Matias, W.G., 2021. Acute and chronic toxicity of amine-functionalized SiO2 nanostructures toward Daphnia magna. Ecotoxicol. Environ. Saf. 212, 111979. https://doi.org/10.1016/J.ECOENV.2021.111979

Ray, P.D., Huang, B.-W., Tsuji, Y., 2012. Reactive oxygen species (ROS) homeostasis and redox regulation in cellular signaling. Cell. Signal. 24, 981. https://doi.org/10.1016/J.CELLSIG.2012.01.008

Ribes, S., Fuentes, A., Talens, P., Barat, J.M., 2018. Prevention of fungal spoilage in food products using natural compounds: A review. Crit. Rev. Food Sci. Nutr. 58, 2002–2016. https://doi.org/10.1080/10408398.2017.1295017

Ribes, S., Ruiz-Rico, M., Pérez-Esteve, É., Fuentes, A., Barat, J.M., 2019. Enhancing the antimicrobial activity of eugenol, carvacrol and vanillin immobilised on silica supports against Escherichia coli or Zygosaccharomyces rouxii in fruit juices by their binary combinations. LWT 113, 108326. https://doi.org/10.1016/j.lwt.2019.108326

Ribes, S., Ruiz-Rico, M., Pérez-Esteve, É., Fuentes, A., Talens, P., Martínez-Máñez, R., Barat, J.M., 2017. Eugenol and thymol immobilised on mesoporous silica-based material as an innovative antifungal system: Application in strawberry jam. Food Control 81, 181–188. https://doi.org/10.1016/J.FOODCONT.2017.06.006

Ros-Lis, J. V., Bernardos, A., Pérez, É., Barat, J.M., Martínez-Máñez, R., 2018. Functionalized Silica Nanomaterials as a New Tool for New Industrial Applications, in: Impact of Nanoscience in the Food Industry. Elsevier Inc., pp. 165–196. https://doi.org/10.1016/B978-0-12-811441-4.00007-8

Ruiz-Leal, M., George, S., 2004. An in vitro procedure for evaluation of early stage oxidative stress in an established fish cell line applied to investigation of PHAH and pesticide toxicity. Mar. Environ. Res. 58, 631–635. https://doi.org/10.1016/J.MARENVRES.2004.03.054

Saei, A.A., Yazdani, M., Lohse, S.E., Bakhtiary, Z., Serpooshan, V., Ghavami, M., Asadian, M., Mashaghi, S., Dreaden, E.C., Mashaghi, A., Mahmoudi, M., 2017. Nanoparticle Surface Functionality Dictates Cellular and Systemic Toxicity. Chem. Mater. 29, 6578–6595. https://doi.org/10.1021/ACS.CHEMMATER.7B01979

Samri, M.T. Al, Biradar, A. V, Alsuwaidi, A.R., Balhaj, G., Al-Hammadi, S., Shehab, S., Al-Salam, S., Tariq, S., Pramathan, T., Benedict, S., Asefa, T., Souid, A.-K., 2012. In vitro biocompatibility of calcined mesoporous silica particles and fetal blood cells. Int. J. Nanomedicine 7, 3111. https://doi.org/10.2147/IJN.S32711

Santos, H.A., Riikonen, J., Salonen, J., Mäkilä, E., Heikkilä, T., Laaksonen, T., Peltonen, L., Lehto, V.-P., Hirvonen, J., 2010. In vitro cytotoxicity of porous silicon microparticles: Effect of the particle concentration, surface chemistry and size. Acta Biomater. 6, 2721–2731. https://doi.org/10.1016/J.ACTBIO.2009.12.043

Severin, I., Souton, E., Dahbi, L., Chagnon, M.C., 2017. Use of bioassays to assess hazard of food contact material extracts: State of the art. Food Chem. Toxicol. 105, 429–447. https://doi.org/10.1016/J.FCT.2017.04.046

Shamsi, M. Al, Samri, M.T. Al, Al-Salam, S., Conca, W., Shaban, S., Benedict, S., Tariq, S., Biradar, A. V., Penefsky, H.S., Asefa, T., Souid, A.-K., 2010. Biocompatibility of Calcined Mesoporous Silica Particles with Cellular Bioenergetics in Murine Tissues. Chem. Res. Toxicol. 23, 1796–1805. https://doi.org/10.1021/TX100245J

Tait, S.W.G., Green, D.R., 2013. Mitochondrial regulation of cell death. Cold Spring Harb. Perspect. Biol. 5, a008706. https://doi.org/10.1101/cshperspect.a008706

Tippayatum, P., Chonhenchob, V., 2007. Antibacterial activities of thymol, eugenol and nisin against some food spoilage bacteria. Nat. Sci. 41, 319–23.

Vicentini, D.S., Puerari, R.C., Oliveira, K.G., Arl, M., Melegari, S.P., Matias,

W.G., 2017. Toxicological impact of morphology and surface functionalization of amorphous SiO2 nanomaterials. NanoImpact 5, 6–12. https://doi.org/10.1016/J.IMPACT.2016.11.003

Walczak, M., Michalska-Sionkowska, M., Olkiewicz, D., Tarnawska, P., Warżyńska, O., 2021. Potential of Carvacrol and Thymol in Reducing Biofilm Formation on Technical Surfaces. Mol. 2021, Vol. 26, Page 2723 26, 2723. https://doi.org/10.3390/MOLECULES26092723

Wang, C., Youle, R.J., 2009. The Role of Mitochondria in Apoptosis. Annu. Rev. Genet. 43, 95. https://doi.org/10.1146/ANNUREV-GENET-102108-134850

Weyermann, J., Lochmann, D., Zimmer, A., 2005. A practical note on the use of cytotoxicity assays. Int. J. Pharm. 288, 369–376. https://doi.org/10.1016/J.IJPHARM.2004.09.018

Xu, J., Zhou, F., Ji, B.P., Pei, R.S., Xu, N., 2008. The antibacterial mechanism of carvacrol and thymol against Escherichia coli. Lett. Appl. Microbiol. 47, 174–179. https://doi.org/10.1111/j.1472-765X.2008.02407.x

Xu, J.J., Diaz, D., O'Brien, P.J., 2004. Applications of cytotoxicity assays and pre-lethal mechanistic assays for assessment of human hepatotoxicity potential. Chem. Biol. Interact. 150, 115–128. https://doi.org/10.1016/J.CBI.2004.09.011

Yu, T., Malugin, A., Ghandehari, H., 2011. Impact of silica nanoparticle design on cellular toxicity and hemolytic activity. ACS Nano 5, 5717–5728. https://doi.org/10.1021/NN2013904/SUPPL_FILE/NN2013904_SI_001.PDF

Zhang, Y., 2018. Cell toxicity mechanism and biomarker. Clin. Transl. Med. 7, 34. https://doi.org/10.1186/s40169-018-0212-7

Supplementary material

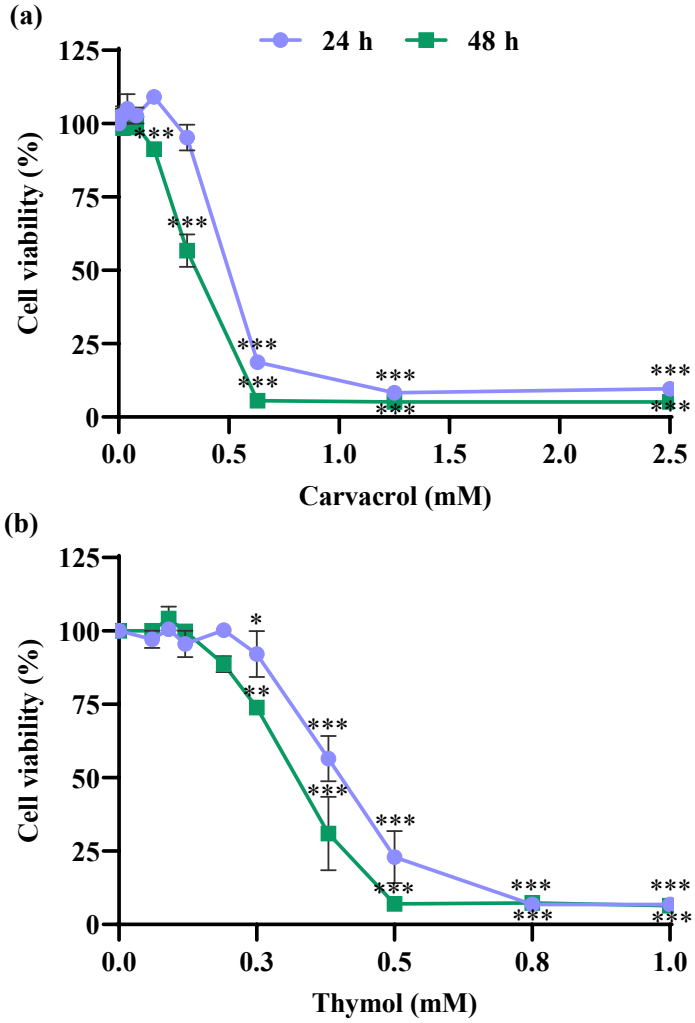

Figure S1. Cell viability (%) in HepG2 cells by the MTT assay after exposure to carvacrol (a) and thymol (b) for 24 h and 48 h in relation to untreated controls. Results are expressed as mean (SEM, n=3). (*) $p \leq 0.05$; (**) $p \leq 0.01$; (***) $p \leq 0.001$ indicates significant differences compared to the control according to the Student's t-test.

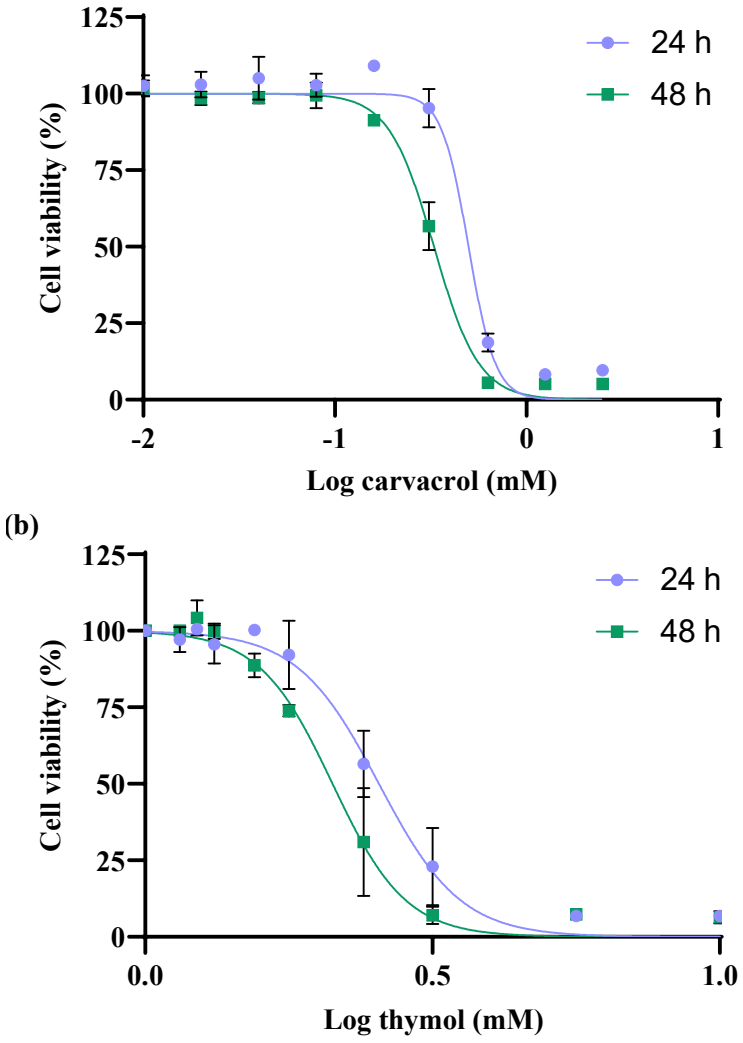

Figure S2. Concentration–response curves (using GraphPad Prism®) of carvacrol (a) and thymol (b). Data represent the mean of three experiments (SEM).

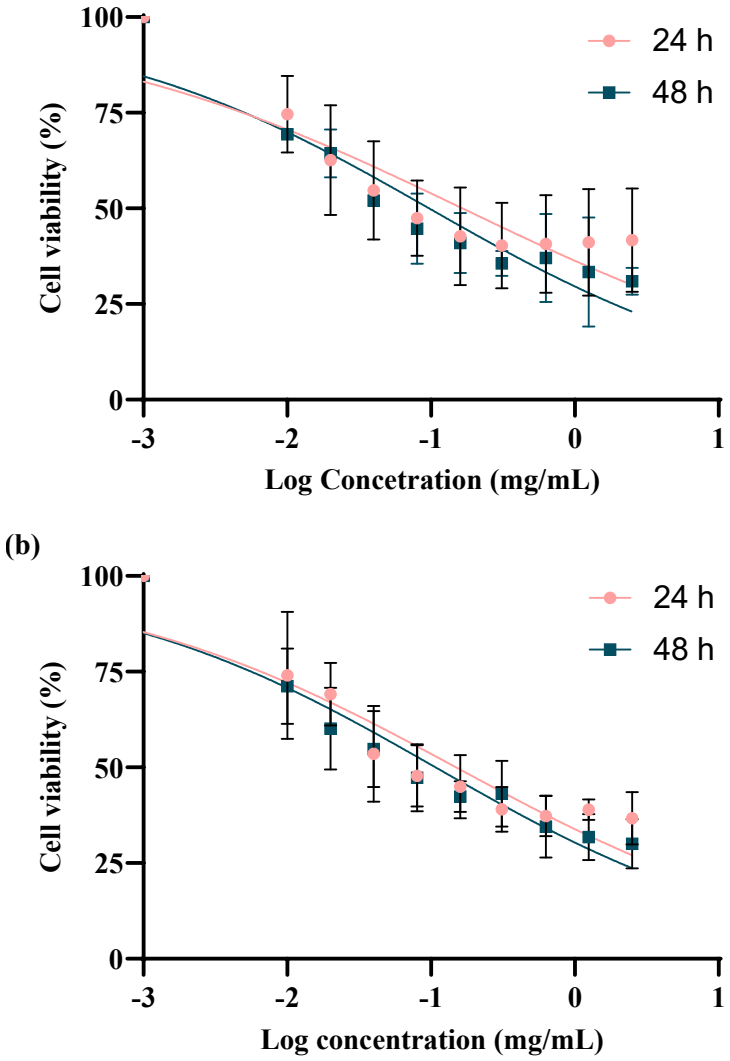

Figure S3. Concentration–response curves (using GraphPad Prism®) of carvacrol-functionalised MCM-41 (a) and thymol-functionalised MCM-41 (b). Data represent the mean of three experiments (SEM).

Table S1. IC_{50} (SEM, n=3) values of carvacrol, thymol, and EOCs-functionalised MCM-41 in HepG2 cells by the MTT assay at 24 h and 48 h of exposure.

	IC_{50}	
	24 h	**48 h**
EOCs (mM)		
Carvacrol	0.45 (0.01)	0.32 (0.02)
Thymol	0.40 (0.03)	0.32 (0.03)
EOCs-functionalised MCM-41 (mg/mL)		
Carvacrol MCM-41 micro	0.15 (0.01)	0.09 (0.04)
Thymol MCM-41 micro	0.15 (0.08)	0.11 (0.08)

Chapter 3

In vivo toxicity study

Article 4

Fuentes, C., Verdú, S., Fuentes, A., Ruiz, M. J., & Barat, J. M. (2022). Effects of essential oil components exposure on biological parameters of *Caenorhabditis elegans*. *Food and Chemical Toxicology,* 159, 112763.

Article 5

Fuentes, C., Verdú, S., Fuentes, A., Ruiz, M. J., & Barat, J. M. *In vivo* toxicity assessment of eugenol and vanillin-functionalised silica particles using *Caenorhabditis elegans*. Under review in *Ecotoxicology and Environmental Safety.*

C. elegans is a free-living nematode found in soil samples and aquatic sediments. It is present mainly in decomposing plant matter in both cultivated and wild areas as it is rich in bacteria, its primary food source. *C. elegans* can be found worldwide, but has been collected mostly from areas with temperate and humid climates (Frézal and Félix, 2015).

This nematode was used as an experimental model system for the first time by Sydney Brenner in the 1960s to study embryonic development (Brenner, 1974). The discovery of this organism as a research model allowed this author to receive the Nobel Prize in Physiology or Medicine in 2002. Major molecular and cell biology discoveries have been made using *C. elegans* as a model organism, including apoptosis (Ellis and Horvitz, 1986; Hedgecock et al., 1983), RNA interference (Fire et al., 1998) or the introduction of fluorescent protein GFP as a biological marker (Chalfie et al., 1994). It was also the first multicellular organism whose genome was completely sequenced (the *C. elegans* Sequencing Consortium, 1998). In fact, *C. elegans* has become one of the most widely employed model systems and its use has expanded to several research fields like molecular biology, pharmacology, medicine and toxicology (Tejeda-Benitez and Olivero-Verbel, 2016).

The success of *C. elegans* lies in its several advantages as a biological model system for research:

- It is easy and inexpensive to handle and maintain in the laboratory as it possesses minimal nutritional and growth requirements. *C. elegans* is usually maintained in the laboratory on nematode growth medium (NGM) agar Petri plates using *E. coli* OP50 as a food source (Brenner, 1974), a uracil auxototroph *E. coli* strain that allows limited bacterial lawn formation. Large quantities of nematodes can also be grown in liquid medium (Stiernagle, 2006). The optimal temperature for worm growth is 20 ºC, although stocks can be maintained within the 16-25 ºC

range. However, growth is temperature-dependant as *C. elegans* grows 2.1- and 1.3-fold faster at 25 ºC and 20 ºC than at 16 ºC, respectively (Stiernagle, 2006). *C. elegans* can be frozen and stored indefinitely in liquid nitrogen (−196 ºC) (Brenner, 1974), and is one of the few multicellular organisms that can be frozen and thawed, but remains viable.

- Adult worms are approximately 1 mm long and 50 µm in diameter (Andrews, 2019). Its small size allows large populations of animals to be maintained in small spaces in the laboratory, unlike other larger model organisms like *Mus musculus*. Its size also allows the use of different *in vitro* techniques at the same time to provide information from the whole organism level (Hunt, 2017). A toxicological assessment with *C. elegans* determines multiple endpoints from both biological functions and molecular markers (Wu et al., 2019).
- Its body is transparent allowing for the *in vivo* visualisation of individual cells, subcellular structures and biological processes under a microscope.
- *C. elegans* presents a short life cycle of about 3 days under optimal conditions. The *C. elegans* life cycle goes through an embryonic phase and four larval stages (Fig. 8), from L1 to L4, and each ended with moult. Under stress conditions, such as overcrowding or lack of food, L1 to L2 larvae can arrest development and go through an alternative larvae stage called *dauer*. In this stage, larvae can survive without food for months. When returning to favourable conditions, *dauer* larvae feed again and recover their reproductive development in larval stage L4 (Félix and Braendle, 2010).

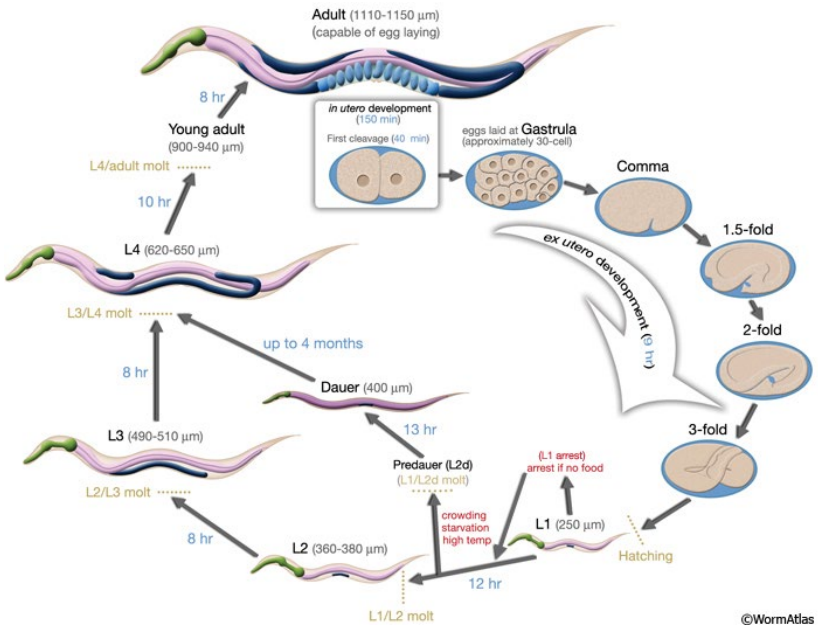

Figure 8. *C. elegans* life cycle at 22 ºC (artwork by Altun and Hall, © Wormatlas).

- Moreover, *C. elegans* life span is short, approximately 2-3 weeks under standard laboratory conditions, which enable whole-life survival experiments and chronic exposure assays during short periods of time.
- Wild-type adult *C. elegans* exist in two sexual forms: hermaphrodites (XX) and males (XO). This means that they can reproduce by both self- and cross-fertilizations. Populations are formed by hermaphrodites in more than 99%, while males are spontaneously generated at a frequency under 0.2% due to the spontaneous non-disjunction of X chromosomes during meiosis (Corsi et al., 2015). Hermaphrodites have oviducts, ovaries and a spermatheca where sperm is stored, while males have a copulatory fan-shaped tail for mating. A single hermaphrodite can produce up to 300 genetically identical embryos by self-fertilisation, with more than 1,000 offspring when mating. Self-fertilisation simplifies the

maintenance of stocks in the laboratory as a single animal can give rise to a whole population (Félix and Braendle, 2010). Reproduction between males and hermaphrodites contributes to maintain the populations' genetic variability. Together, short generation time and a large number of offspring allow experiments to be performed with many individuals during short periods of time (Leung et al., 2008), which increases the statistical value of the results. So, *C. elegans* provides an appropriate *in vivo* platform for high-throughput experiments.

- Another relevant aspect of this organism is its well annotated genome and the wide availability of mutants or transgenic strains for a large number of genes (Hunt, 2017). Moreover, worms express homologues to approximately 80% of human genes (Ruszkiewicz et al., 2018). Consequently, a wide variety of physiological processes, including different signalling pathways, stress responses, metabolic processes and pathologies, is conserved between nematodes and mammals (Kaletta and Hengartner, 2006; Leung et al., 2008; Ruszkiewicz et al., 2018). This means that the findings obtained from *C. elegans* studies can be extrapolated to higher eukaryotes and mammals, and are further confirmed in vertebrate systems.
- *C. elegans* has a simple anatomy with a defined number of cells, which simplifies its study. An adult hermaphrodite has a complete lineage of 959 somatic cells, which are maintained from animal to animal. Despite its simplicity, these cells are organised into simple tissues and organs to result in a complex organism. Its body is cylindrical, surrounded by a layer of epithelial cells and protected by a secreted cuticle made mainly of collagen, lipids and other glycoproteins (Gonzalez-Moragas et al., 2015). Inside the epidermis, the muscle bands and the ventral and dorsal nerve cords that innervate muscles are found (Fig. 9). The neuromuscular region encloses the pseudocoelom, a fluid-filled body cavity that contains the alimentary and reproductive systems. (Corsi et al., 2015). The *C.*

elegans nervous system is the organ with the most cells. An adult hermaphrodite contains 302 neurons and an adult male has 383 (Hobert, 2013). The alimentary system is formed by the digestive and excretory systems. Food (bacteria) suspended in liquid enters the worms' pharynx by pumping, where a neuromuscular pump called a grinder mechanically breaks up food particles before being passed on to the intestine for digestion, while liquid is ejected (Dimov and Maduro, 2019). *C. elegans* and human alimentary systems bear many similarities. As with mammals, *C. elegans* feeding involves food ingestion, digestion, nutrient absorption and defecation (Gonzalez-Moragas et al., 2017). Important features like acidified lumen, microvilli, digestive enzyme secretion, uptake of digested components or peristalsis are also found (Hunt, 2017). All these properties make *C. elegans* an excellent animal model for assessing chemicals' toxicity after oral exposure.

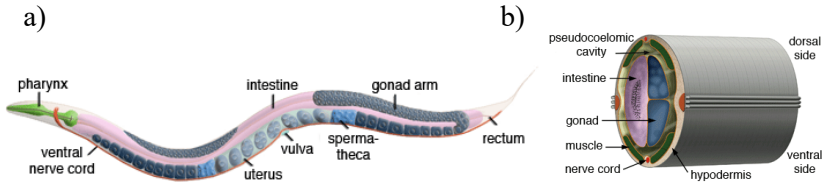

Figure 9. *C. elegans* anatomy. Major anatomical features of a hermaphrodite (a) and cross-section through the anterior region of the *C. elegans* hermaphrodite (b) (artwork by Altun and Hall, © Wormatlas).

- Additionally, despite their simple anatomy, worms show a wide variety of biological functions like foraging, feeding, defecation, egg laying, locomotion or sensory responses to light, touch, smell, taste and temperature; and more complex behaviours, such as mating, social behaviour, learning and memory (Wormatlas database, 2020)

- Another important aspect is the vast amount of free online resources available about different worm biology aspects, including anatomy, physiology, genome sequence, gene function, expression patterns, published papers or protocols and methods for *C. elegans* maintenance and testing (Lee, 2005). The reason for all this is the collaborative and altruistic character of the *C. elegans* community from its origins. Some examples of these online databases and repositories are *WormBase*, *Textpresso, Caenorhabditis Genetics Center (CGC), WormBook* or *WormAtlas.*
- Finally, and importantly, the use of *C. elegans* complies with the ethical principles for animal experiments for the 3Rs by avoiding the ethical constraints normally encountered when working with phylogenetically higher species like mammals (Erkekoglu et al., 2011).

Albeit not comparable to its large number of advantages, *C. elegans* also presents some limitations for toxicological research. The *C. elegans* body is surrounded by a thick cuticle that protects it from environmental hazards, which means that higher exposure concentrations are required to induce toxicological effects (Xiong et al., 2017). Nematodes lack some specific mammalian organs and structures like eyes, heart, kidney, liver, lungs, bones and circulatory and adaptive immunity systems, and also present less conserved biological pathways with humans than other vertebrate model organisms like *Mus musculus* (Gonzalez-Moragas et al., 2015). Moreover, incorrect handling and variations in the experimental conditions can result in altered gene expression patterns and invalid results (Hunt, 2017).

In recent years, *C. elegans* has been successfully used as an alternative *in vivo* animal model to assess the toxicological impact of heavy metals, pesticides, drugs, nanoparticles, and many other chemicals, on human health and the environment (Clavijo et al., 2016; Gao et al., 2018; Lei et al., 2018; Nagar et al., 2020; Tang et al., 2019; Wittkowski et al., 2019; Yun et al., 2015).

As a free-living nematode that can be found in soil and water samples, *C. elegans* has become an essential tool in ecotoxicological assays for environmental assessing risks (Yang et al., 2016). For human toxicity assessments, toxicity ranking screens in *C. elegans* successfully predict rat and mouse LD_{50} rankings (Hunt, 2017), although the homology between nematodes and humans is not comparable to that of vertebrate model systems. So, despite being successfully implemented, *C. elegans* is not expected to completely replace mammalian models, but to supplement them for the toxicity testing of human risks. According to some authors, *C. elegans* can supplement the information obtained with cell culture assays and *in vivo* vertebrate models (Gao et al., 2018; Kaletta and Hengartner, 2006; Leung et al., 2008). It could form part of a battery of assays together with many types of *in silico*, *in vitro* and other non-mammalian organism models to improve human toxicity predictions (Hunt, 2017) and be a useful tool for the rapid screening of toxic compounds in early stages of new products development (Leung et al., 2008; Xiong et al., 2017). Moreover, due to the high conservation of signalling pathways and genes between *C. elegans* and mammals, this worm can help to elucidate the molecular mechanisms underlying toxicological responses to different chemicals (Ruszkiewicz et al., 2018). Therefore, the application of *C. elegans* in toxicological research is expected to continue to grow and help to reduce the number of vertebrate animals used in toxicity studies.

Effects of essential oil components exposure on biological parameters of *Caenorhabditis elegans*

Cristina Fuentes[a], Samuel Verdú[a], Ana Fuentes[a], María José Ruiz[b], José Manuel Barat[a]

[a]Department of Food Technology, Universitat Politècnica de València. Camino de Vera s/n, 46022, Valencia, Spain: crifuelp@upvnet.upv.es

[b]Laboratory of Toxicology, Faculty of Pharmacy, Universitat de València. Av. Vicent Andrés Estellés s/n, 46100, Burjassot, Valencia, Spain

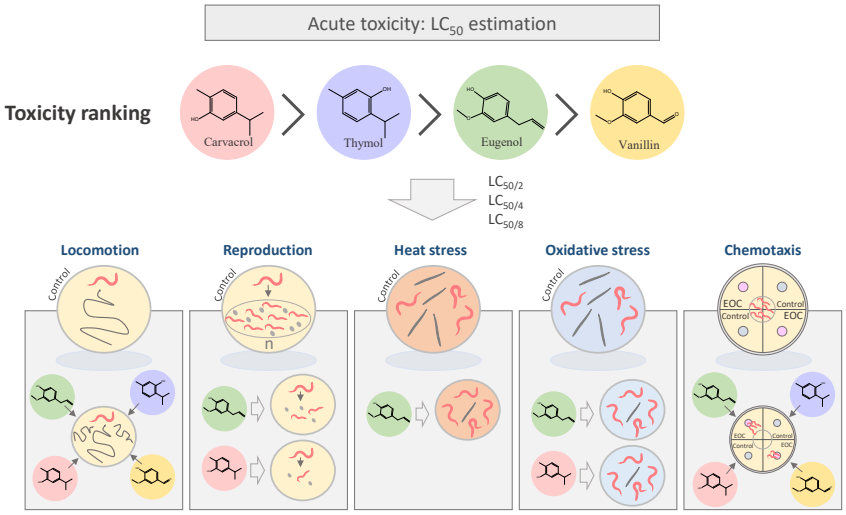

Abstract

The extensive use of essential oil components in an increasing number of applications can substantially enhance exposure to these compounds, which leads to potential health and environmental hazards. This work aimed to evaluate the toxicity of four widely used essential oil components (carvacrol, eugenol, thymol, vanillin) using the *in vivo* model *Caenorhabditis elegans*. For this purpose, the LC_{50} value of acute exposure to these components was first established; then the effect of sublethal concentrations on nematodes' locomotion behaviour, reproduction, heat and oxidative stress resistance and chemotaxis was evaluated. The results showed that all the components had a concentration-dependent effect on nematode survival at moderate to high concentrations. Carvacrol and thymol were the two most toxic compounds, while vanillin had the mildest toxicological effect. Reproduction resulted in a more sensitive endpoint than lethality to evaluate toxicity. Only pre-exposure to carvacrol and eugenol at the highest tested sublethal concentrations conferred worms oxidative stress resistance. However, at these and lower concentrations, both components induced reproductive toxicity. Our results evidence that these compounds can be toxic at lower doses than those required for their biological action. These findings highlight the need for a specific toxicological assessment of every EOC application.

Keywords: nematode, toxicity, carvacrol, thymol, eugenol, vanillin

1. Introduction

Essential oils are oily aromatic liquids obtained from different plant material structures (Hyldgaard et al., 2012) that consist in a complex mixture of compounds, including terpenoids, esters, aldehydes, ketones, acids and alcohols (Ramos et al., 2013). The biological functions of essential oils have been related to their content in phenolic components. The two isomeric monoterpenoids carvacrol and thymol, and the phenylpropenes eugenol and vanillin, are widely studied essential oil components (EOCs) (Hyldgaard et al., 2012). All four are widely distributed in several aromatic plants and its products. Carvacrol and thymol are primary components of thyme and oregano oils; eugenol is the main active compound of the oil extracted from clove and is also found in other plant sources such as basil, cinnamon or pepper; and vanillin is the main constituent of vanilla beans (Jadhav et al., 2009; Kachur and Suntres, 2020; Khalil et al., 2017). They are common flavouring agents in fragrances, cosmetics and food products, and are also used for other purposes in various industries like pharmaceutical, dentistry or agriculture (Kachur and Suntres, 2020; Memar et al., 2017; Nejad et al., 2017; Priefert et al., 2001).

Carvacrol, thymol, eugenol and vanillin display antimicrobial activity against foodborne and food spoilage bacteria, moulds and yeasts (Hyldgaard et al., 2012; Kachur and Suntres, 2020; Tippayatum and Chonhenchob, 2007). They also have a demonstrated high antioxidant potential at low concentrations (Fujisawa et al., 2002; Oliveira et al., 2014), which minimises the oxidation of lipid components in foods (Yanishlieva et al., 1999). Because of their antimicrobial and antioxidant activity, these components have been proposed as natural preservatives for a wide variety of food products (Kachur and Suntres, 2020). Other beneficial properties reported for pharmaceutical and medical applications include analgesic, anti-inflammatory, antimutagenic and anticarcinogenic potentials (Bezerra et al., 2016; Khalil et al., 2017; Lee

et al., 2014; Salehi et al., 2018; Sharifi-Rad et al., 2018; Sisakhtnezhad et al., 2018), as well as a protective effect against different metabolic disorders, such as diabetes mellitus, obesity, renal or gastrointestinal diseases, among others (Al-Naqeb et al., 2010; Nagoor Meeran et al., 2017).

As flavourings, EOCs are employed at low concentrations because of their strong flavour, while higher concentrations may be required to accomplish sufficient activity to be used in other applications (Maisanaba et al., 2015). However, evidence reveals that moderate to high concentrations of EOCs may cause toxicological effects. *In vitro* studies show that carvacrol, thymol and eugenol present cytotoxic effects in a dose-, frequency- and duration-dependent manner on different cell lines, including the human osteoblastic cell line U2OS, the colon carcinoma cell line Caco-2, the human hepatoma cells HepG2, different human skin cells, and the mouse lymphoma cells V79 (Ho et al., 2006; Llana-Ruiz-Cabello et al., 2014a; Prashar et al., 2006; Slamenová et al., 2007). Several authors have suggested that the cytotoxic effect of these components on eukaryotic cells consists in inducing apoptosis by direct mitochondrial pathway activation (Bakkali et al., 2008; Yin et al., 2012). Some studies have investigated the mutagenic and genotoxic potentials of these components. Although the *in vitro* genotoxic potential of carvacrol and eugenol has been reported using V79, Caco-2, and mouse lymphoma cells (Llana-Ruiz-Cabello et al., 2014b; Maisanaba et al., 2015; Maralhas et al., 2006), these results are still limited. *In vivo* toxicity studies are scarce, and potential adverse effects after acute and prolonged exposure to carvacrol, thymol and eugenol have appeared in different species (Andersen, 2006; Nejad et al., 2017). In humans, it is known that exposure to carvacrol, thymol and eugenol is able to cause allergic reactions because skin irritation, ulcer formation, dermatitis or reduced healing have been reported (Kamatou et al., 2012; Salehi et al., 2018). The toxicological effects of vanillin have been less described, but this compound is considered to have a low cytotoxic potential

because only high concentrations (mM range) reduce cell viability in a dose- and time-dependent manner (Fuentes et al., 2021; Oliveira et al., 2014).

In recent years, toxicological research has focused on searching for alternatives to mammalian animal models for the *in vivo* screening of chemicals because these assays are expensive and time-consuming, and they involve ethical concerns (Gao et al., 2018; Xiong et al., 2017). The free-living nematode *Caenorhabditis elegans* is one of the most intensively studied animals ever since it was proposed as an experimental model organism (Brenner, 1974). Its use has extended to many research areas, including toxicology, where it has been utilised as an alternative *in vivo* animal model to evaluate the potential toxic effects of chemicals for human health and the environment (Nagar et al., 2020; Wang et al., 2009; Yang et al., 2015). The popularity of *C. elegans* is because of the many advantages it offers as a model organism, including small body size, short life cycle, efficient reproduction, and easy and inexpensive maintenance (Hunt, 2017; Kumar and Suchiang, 2020). It also presents a simple anatomy with a defined number of cells. At the same time, these cells are organised into simple tissues and organs that bear similarities with human structures (Gonzalez-Moragas et al., 2015). Many cellular and molecular processes are also conserved between worms and humans given the presence of homologous genes and proteins in both species (Kumar and Suchiang, 2020; Leung et al., 2008). Another major feature of *C. elegans* for toxicity testing consists in the wide range of biological parameters and molecular markers that can be studied after toxicant exposure to obtain molecular- and whole organism-related information (Wu et al., 2019). However, this model also presents some limitations since *C. elegans* lack of particular mammalian organs, molecular pathways or a circulatory and an adaptive immune system (Hunt, 2017). Moreover, variations in the experimental conditions can significantly alter toxicological responses for multiple generations, making good *C. elegans* culture practice mandatory for

obtaining reliable results (Hunt, 2017). Still *C. elegans* may develop a relevant role for predictive toxicology.

Previously, Lanzerstorfer et al. (2020) evaluated the impact of rosemary, citrus and eucalyptus essential oils on acute, developmental and reproductive toxicity in *C. elegans* and found severe toxic properties at already low concentrations. Also, some EOCs have been studied using *C. elegans* as a model to evaluate their anthelmintic activity against plant and animal parasitic nematode species (Abdel-Rahman et al., 2013; Marjanović et al., 2018). However, to the best of our knowledge, the effect of EOCs' exposure on different biological *C. elegans* parameters to predict their potential toxicity has not yet been reported. This work aimed to evaluate the acute toxicity of carvacrol, eugenol, thymol and vanillin, and to investigate the effect of sublethal concentrations on different biological parameters, using the *in vivo* model *C. elegans*.

2. Materials and Methods

2.1. Chemicals

Carvacrol (≥ 98% w/w), eugenol (≥ 98% w/w), thymol (≥ 98.5% w/w), vanillin (≥ 98% w/w), sodium azide (NaN_3) and 30% hydrogen peroxide (H_2O_2) solution (w/w) were obtained from Sigma-Aldrich (Spain). Dimethyl sulfoxide (DMSO), NaOH, sodium hypochlorite (NaClO), and all the other reagents used to prepare Nematode growth medium (NGM) agar (3 g/L NaCl, 2.5 g/L peptone, 17 g/L agar, 1 M potassium phosphate buffer [25 mL], 1 M $CaCl_2 \cdot 2H_2O$ [1 mL], 1 M $MgSO_4 \cdot 7H_2O$ [1 mL], and [1 mL] 5% cholesterol in ethanol), K-medium (32 mM KCl, 51 mM NaCl) and M9 buffer (3 g/L KH_2PO_4, 6 g/L Na_2HPO_4, 5 g/L NaCl, 1 ml 1 M $MgSO_4$) were purchased from Scharlab (Spain), except for cholesterol (95% w/w), which was supplied by Acros Organics (Spain). All the chemicals used in this study were of standard reagent grade.

Stock solutions of carvacrol, eugenol, thymol and vanillin (2.5 M) were completely dissolved in DMSO and remained frozen until used. The final tested EOCs concentrations were prepared in K-medium (final DMSO concentration ≤ 0.6% (v/v)).

2.2. *C. elegans strain and maintenance*

Wild-type Bristol (N2) *C. elegans* worms were grown on NGM agar plates seeded with a lawn of *Escherichia coli* strain OP50 as feed and were left under standard conditions (Brenner, 1974). Regular subculturing was performed to avoid crowding and to maintain the *C. elegans* population. For all the experiments, adult hermaphrodites were synchronised to the same larval stage using an alkaline hypochlorite solution (1 M NaOH, 5% NaClO) and cultured at 20 ºC in the dark for 3 days after the late L4 stage was reached.

2.3. Lethality test and LC_{50} estimation

The lethality assays for the different EOCs were performed in 24-well plates in a final volume of 1 mL of liquid media in the presence of food (10 µL *E. coli* suspension at 1,000 FAU). About 30 age-synchronised L4 worms were transferred to each well, which contained serial dilutions of carvacrol (0.47-2.5 mM), eugenol (0.94-5 mM), thymol (0.47-2.5 mM), or vanillin (2.25-12 mM) in K-medium. The concentration range used during the toxicity tests were selected according to previous *in vitro* studies (Fuentes et al., 2021) and preliminary tests. The negative controls (0.6% DMSO in K-medium) were included in triplicate on each plate. Plates were incubated at 20 ºC in the dark for 24 h. After exposure, the number of live and dead worms was recorded by visual inspection under a dissection microscope. Nematodes were considered dead if they did not respond to stimulus when touched with a metal wire. Results were expressed as the percentage of live worms of the total number of nematodes in each well (survival rate). Data were presented as the mean (SEM) of three independent experiments. The lethal concentration (LC_{50})

value for each EOC was calculated by a non-linear regression test using version 8.0.1 of the GraphPad Prism software (GraphPad Software, USA).

2.4. Effect of sublethal concentrations on biological parameters

Based on the LC_{50} values obtained from the lethality test experiments, three sublethal concentrations ($LC_{50/2}$, $LC_{50/4}$, $LC_{50/8}$) were set to further study the effect of EOCs on different nematode biological parameters. For this purpose, the L4 synchronised worms were exposed to sublethal concentrations of EOCs in K-medium in the presence of food (10 µL *E. coli* suspension at 1,000 FAU), and incubated in the dark at 20 ºC for 24 h. After exposure, nematodes were washed with M9 buffer and transferred to new plates to evaluate the different endpoints. In addition, the chemotactic response to EOCs was determined to evaluate the attractive or repellent potential of these components for *C. elegans*. All the conditions were tested in at least three independent experiments with three replicates per condition.

2.4.1. Locomotion behaviour

Locomotion behaviour was assessed on the same plates employed for the reproduction assays by examining the tracks produced while worms moved on the agar surface by an image analysis. Images of agar surfaces were taken after the reproduction assays with a CMOS camera Moticam 3+ (Motic, Hong Kong) connected to a BA310E microscope (Motic, Hong Kong) at the10X magnification. These were taken in RGB (red, green and blue) at the 2048x1536 resolution, and stored in the JPEG format. Then images were transformed to a grey-scale and the tracks formed while nematodes moved on agar wells were quantified by imaging segmentation. By this method, pixels' areas were attributed to tracks or background according to a 145-255 grey-level threshold (Buckingham and Sattelle, 2008). The results were expressed as a percentage of tracks area from the total well (%). The image analysis was

carried out with the Fiji image processing package (Schindelin et al., 2012) using the *threshold* and *measure* functions.

2.4.2. *Reproduction*

Reproduction was evaluated by the brood size endpoint. The pre-exposed worms were individually transferred to NGM agar 24-well plates (1 nematode/well), seeded with *E. coli* OP50, and incubated at 20 ºC for 72 h. Parent worms were daily transferred to new wells in identical plates until the end of the assay. Brood size was determined by counting under a BA310E microscope (Motic, Hong Kong) the number of larvae in all the stages and the number of eggs laid per adult worm at the end of the experiment (72 h).

2.4.3. Stress resistance

The effect of EOCs exposure on *C. elegans* resistance against thermal and oxidative stress was evaluated by two different survival assays. Thermal stress resistance was evaluated by exposing pre-treated young adult worms to 38 ºC for 90 min (approx. 30 worms/well). The oxidative stress resistance assays were performed according to Acosta et al. (2018) with modifications. The pre-exposed worms to the sublethal concentrations of EOCs were transferred to K-medium 24-well plates (approx. 30 worms/well) containing 2 mM of H_2O_2 and were incubated at 20 ºC for 5.5 h. After exposure to both stress factors, plates were incubated at 20 ºC for 2 h. Next the number of live and dead nematodes was determined by the touch-provoked method, and the survival rates were calculated as the percentage of live worms of the total number of animals per well. Data were presented as the mean (SEM) of three independent experiments.

2.4.4. Chemotaxis

The chemotaxis assays were conducted in 60 mm-diameter Petri plates containing 6 mL of NGM agar. One EOC was analysed separately in each

plate. For this purpose, plates were divided into four equal quadrants and a circular mark was made in the centre of each quadrant, which was equidistant between them and the centre of the plate. Five μL of the tested compound or K-medium were placed on the agar surface over the centre of two perpendicular circular marks. Sodium azide (0.25 M) was used in all the quadrants to paralyse nematodes for counting purposes. In the centre of the plate, 5 μL of M9 buffer containing about 30 synchronised worms were placed. Then plates were sealed with Parafilm® and incubated in the dark at 20 ºC for 90 min. After this time, the number of nematodes present in each quadrant was counted and the chemotaxis index was calculated as CI = A−B/A+B, where A is the number of worms at both test quadrants and B is the number of worms at both controls (K-medium). Evaluations were made for each concentration at least in triplicate.

2.4.5. Prediction of LD_{50} values

LD_{50} values were calculated from the experimental LC_{50} obtained for each EOC during the lethality assays using the regression function described at ICCVAM (2006):

$$Log(LD50) = 0.439 * \log(LC50) + 0.621$$

2.5. Statistical analyses

Minimum sample size for each endpoint was selected to ensure normal distribution of data. Only L4 adults' hermaphrodites were used in the experiments. The statistical analysis was performed using Statgraphics Centurion XVI (Statpoint Technologies, Inc., Warrenton, VA, USA). The differences observed in the nematodes exposed to test solutions and the control were analysed by the Student's t-test for paired samples. Differences were considered significant at $p \leq 0.05$.

3. Results

3.1. Lethality test and LC_{50} estimation

The results of the lethality assays for the different EOCs are shown in Figure 1. All the compounds exhibited a dose-dependent effect on the mortality of adult nematodes after 24 h of exposure. The data from the concentration-response curves were used to calculate the LC_{50} values. Carvacrol had the highest toxicological effect on *C. elegans,* and its LC_{50} value was 1.10 (0.07) mM after 24 h exposure. This value slightly increased for thymol, which obtained an LC_{50} value of 1.32 (0.03) mM. With eugenol, *C. elegans* was found to be approximately 2-fold less sensitive to this compound than to carvacrol and thymol, and the LC_{50} value was 2.08 (0.21) mM. Moreover, while carvacrol and thymol induced significant lethal effects at concentrations above 0.47 mM (Fig. 1a and 1c), mortality only increased significantly for eugenol at concentrations above 1.37 mM (Fig. 1b). Vanillin showed the lowest acute toxic effect on young adult nematodes of all the different analysed EOCs, with an LC_{50} of 5.84 mM (Fig. 1d), which was approximately 5-fold less toxic than carvacrol and thymol, and 3-fold less toxic than eugenol.

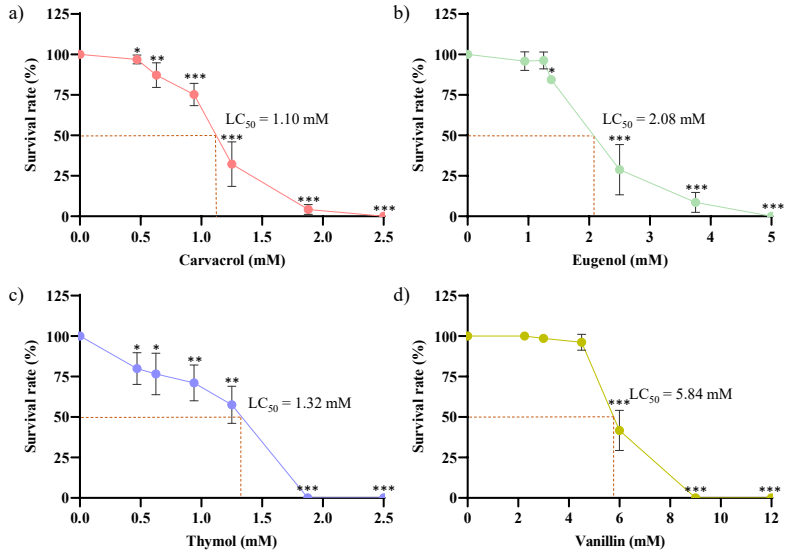

Figure 1. Concentration-response curves of the nematodes exposed to carvacrol (a), eugenol (b), thymol (c) and vanillin (d) for 24 h. Each point represents the mean mortality percentage (SEM) in at least three independent experiments, and each was performed in triplicate. (*) $p \leq 0.05$; (**) $p \leq 0.01$; (***) $p \leq 0.001$ indicates significant differences compared to the control according to the Student's t-test.

3.2. Effect of sublethal concentrations on biological parameters

Three different concentrations of each compound were calculated according to the acute toxicity tests (Table 1) and used to evaluate the effect on the behavioural endpoints of nematodes: locomotion, reproduction, stress resistance, and chemotaxis.

Table 1. Sublethal concentrations of carvacrol, eugenol, thymol and vanillin assayed for the assessment of different biological parameters.

	Concentration (mM)		
EOC	**$LC_{50/8}$**	**$LC_{50/4}$**	**$LC_{50/2}$**
Carvacrol	0.14	0.28	0.55
Eugenol	0.26	0.52	1.04
Thymol	0.17	0.33	0.66
Vanillin	0.73	1.46	2.92

3.2.1. Locomotion behaviour

Figure 2 shows that displacement of *C. elegans* on agar surfaces was greater for the worms treated with EOCs compared to the untreated controls. Moreover, worm motility was concentration-dependent and tended to be determined by the analysed compound. Monoterpenoids carvacrol and thymol enhanced motility with increasing compound concentrations, while lower concentrations of phenylpropenes eugenol and vanillin gave higher displacement percentages compared to the control. A 0.55 mM carvacrol concentration increased worm motility by 12% 24 h post-exposure, while all the thymol sublethal concentrations enhanced worm locomotive behaviour. The lowest tested thymol concentration (0.17 mM) increased the area covered by worms by 11%, and the 0.33 mM and 0.66 mM thymol concentrations enhanced motility by 23% and 26%, respectively. For eugenol, the 0.26 mM and 0.52 mM concentrations respectively increased motility by 17% and 13%, while no differences were observed for the control at the lowest analysed concentration. Finally, a maximum increase of 23% was recorded for vanillin compared to the control for the 0.73 mM concentration, but this rise remained at 13% at both the lower concentrations.

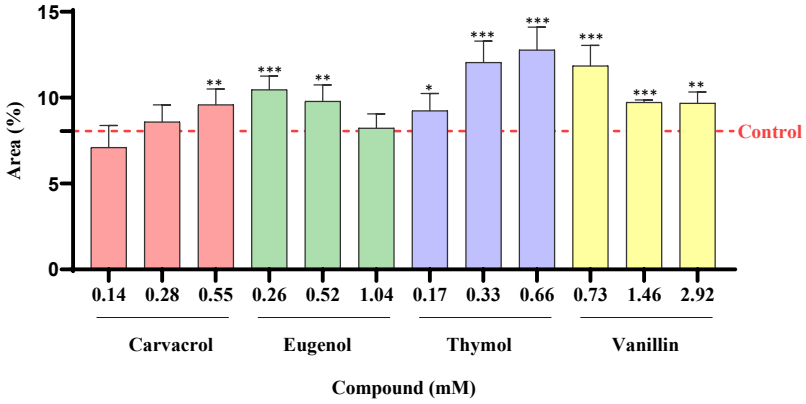

Figure 2. Area (%) of the tracks generated on the surface of agar wells by the pre-exposed worms to sublethal carvacrol, eugenol, thymol and vanillin concentrations for 24 h. Bars represent the mean (SEM) of at least three different experiments, each carried out in triplicate. (*) $p \leq 0.05$; (**) $p \leq 0.01$; (***) $p \leq 0.001$ indicates significant differences compared to the control by the Student's t-test.

Moreover, exposure to sublethal EOCs concentrations altered nematodes' rhythmic locomotory pattern. Figure 3 shows the representative micrographs of the locomotion tracks generated by the control nematodes or those worms acutely pre-exposed to different thymol concentrations on agar surfaces. The control worms produced shorter and less curved sinusoidal tracks, while the EOCs pre-exposed worms made more undulatory waves with increased curvatures, which suggests that undulating body shortens during crawling. This observation shows that exposure to the sublethal concentrations of these components not only enhances motility, but also modifies locomotor patterns in *C. elegans*.

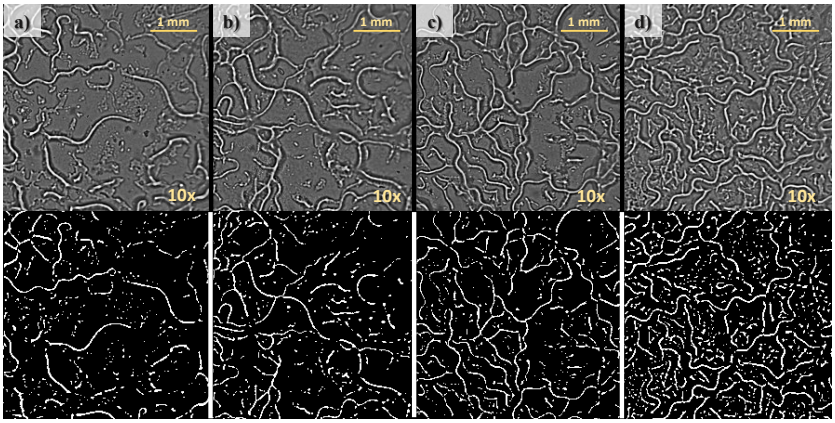

Figure 3. Tracks formed after worms crawled freely on a bacterial lawn on agar wells. The control (a) and pre-exposed nematodes to increasing thymol concentrations for 24 h: 0.17 mM (b), 0.33 mM (c) and 0.66 mM (d).

3.2.2. Reproduction

Depending on the tested concentration, carvacrol and eugenol exposure affected *C. elegans* reproduction (Figure 4). The strongest effect was for carvacrol, which significantly reduced the total brood size by 43% and 42% after exposure to the 0.28 mM and 0.55 mM concentrations, respectively. Moreover, the number of eggs laid per worm for the nematodes pre-exposed to the lowest carvacrol concentration (0.14 mM) decreased compared to the untreated controls. Eugenol also compromised nematodes' reproductive capability as pre-exposure for 24 h to a 1.04 mM concentration of this compound also resulted in fewer worms and eggs, and a smaller total brood size, and fewer eggs were also observed at 0.52 mM. Unlike carvacrol and eugenol, no reproductive toxicity was observed after exposure to sublethal thymol and vanillin concentrations (Figure 4c and Figure 4d, respectively).

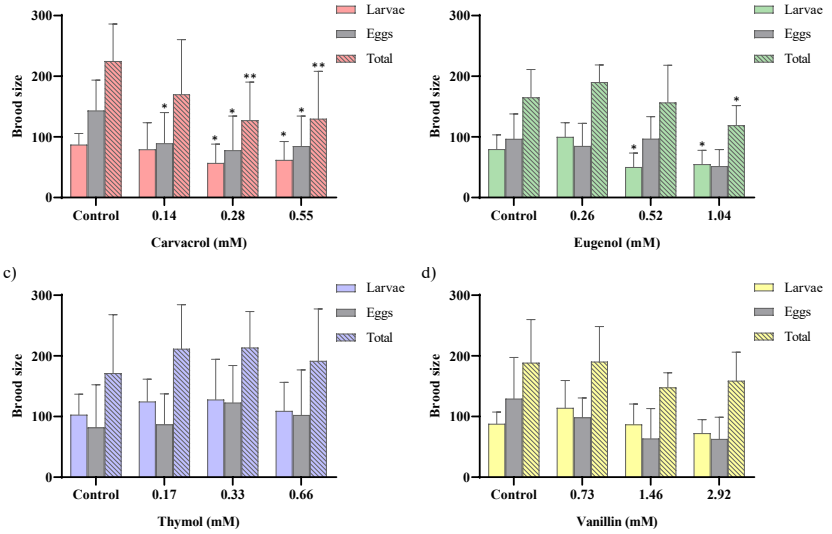

Figure 4. Effects on *C. elegans* brood size of exposure to carvacrol (a), eugenol (b), thymol (c) and vanillin (d) for 24 h. Bars represent the mean (SEM) from at least three different experiments, each carried out in triplicate. (*) $p \leq 0.05$; (**) $p \leq 0.01$ indicates significant differences compared to the control by the Student's t-test.

3.2.3. Stress resistance

The effect of EOCs exposure on *C. elegans* resistance against two abiotic factors was analysed. To evaluate thermotolerance, pre-treated worms were exposed to 38 ºC for 1.5 h and then the survival rate was determined. As shown in Figure 5a, no significant effect on heat stress resistance of worms was observed ($p > 0.05$), except for the lowest assayed eugenol concentration. At this concentration (0.26 mM), the mean life span increased by 42% compared to the untreated control worms, and higher doses did not further increase survival.

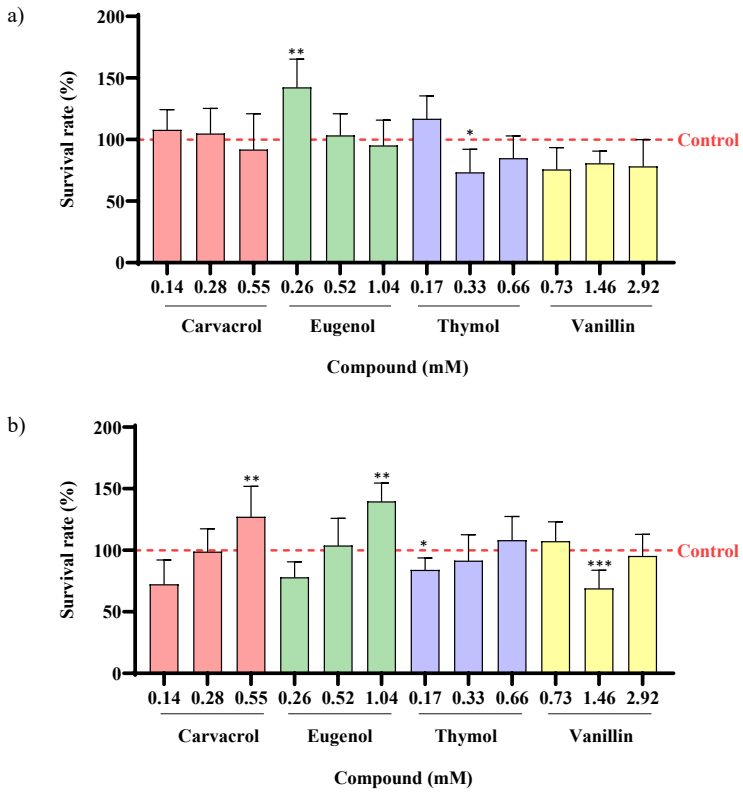

Figure 5. Survival rates after heat stress (a) and oxidative stress (b) of the nematodes pre-exposed to different concentrations of EOCs for 24 h. Each bar represents the mean survival rate (SEM) in at least three independent experiments, each carried out in triplicate. (*) $p \leq 0.05$; (**) $p \leq 0.01$; (***) $p \leq 0.001$ indicates significant differences compared to the control by the Student's t-test.

Oxidative stress was measured by the hydrogen peroxide resistance assay. As Figure 5b reflects, a general trend to higher survival rates values at rising concentrations appeared for the different EOCs. However, only carvacrol and eugenol at the highest tested concentrations conferred worms oxidative stress resistance. Pre-exposure to both compounds for 24 h significantly increased

the survival rates by 27% and 40% compared to the controls, respectively. Neither lower carvacrol and eugenol concentrations, nor any of tested thymol and vanillin concentration, enhanced the antioxidant resistance of nematodes.

3.2.4. Chemotaxis

The present work tested the chemotactic responses of *C. elegans* to carvacrol, eugenol, thymol and vanillin to evaluate the attractive or repellent effect of these components on worms. The compounds with a chemotaxis index of ≥ 0.2 are considered attractants, those with a chemotaxis index between 0 and 0.2 are described as weak attractants, while the molecules presenting a chemotaxis index ≤ -0.02 are considered to be repellent (O'Halloran and Burnell, 2003). All four EOCs were attractive for nematodes at all the tested concentrations (Figure 6).

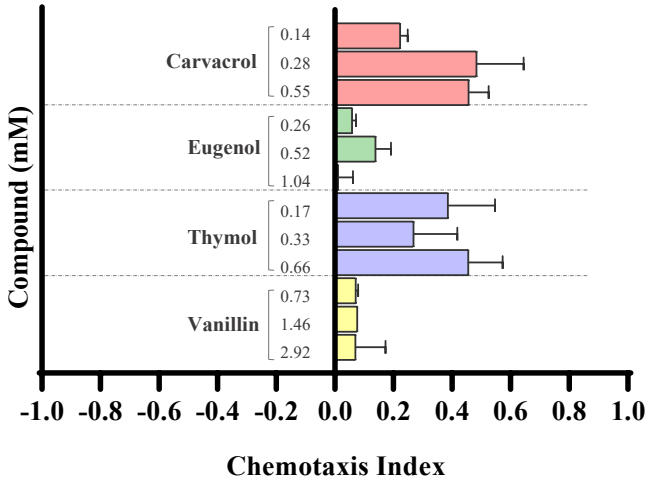

Figure 6. Chemotaxis indices of the wild-type *C. elegans* exposed to carvacrol, eugenol, thymol and vanillin. Bars represent the mean (SEM) of at least three different experiments, each carried out in triplicate (n > 200 worms) for each condition.

In wild-type *C. elegans*, we found that carvacrol and thymol had a potent chemoattractant effect, and both were the most attractive components with a maximum chemotaxis index of 0.48 (0.07) and 0.46 (0.11), respectively. A weaker response was detected to eugenol and vanillin as they reached a maximum chemotactic response of 0.13 (0.05) and 0.10 (0.00), respectively, and both were weak attractants.

3.2.5. Prediction of LD_{50} values

LD_{50} values were calculated from the experimental LC_{50} obtained for each EOC during the lethality assays using the regression function described at ICCVAM (2006). The predicted LD_{50} values were compared to the oral LD_{50} reported for rats by the European Chemicals Agency (ECHA, 2021). As depicted in Table 2, estimated LD_{50} values displayed a significant correlation with the values reported for rats since the toxicity ranking between *C. elegans* and rodents was maintained. As in nematodes, carvacrol is the most acutely toxic EOC for rats, followed by thymol, eugenol and lastly, vanillin.

Table 2. Comparison of predicted LD_{50} values and Rat LD_{50} values obtained from the ECHA toxicological information for the different EOCs.

Compound	Predicted LD_{50} (mg/kg)	LD_{50} Rat (mg/kg)
Carvacrol	655	810
Eugenol	946	> 2000
Thymol	709	980
Vanillin	1380	3978

4. Discussion

Carvacrol, eugenol, thymol and vanillin, are authorised as flavouring agents with no specific restricted use in Regulation (EC) 1334/2008 (EC, 2008), and are approved as Generally Recognized as Safe (GRAS) compounds by the US Food and Drug Administration (FDA, 2021). They are also considered safe by the Joint FAO/WHO Expert Committee on Food Additives as "No safety concern at current levels of intake when used as a flavouring agent" has been established for these components (JECFA, 2021). However, despite these EOCs being considered safe as a food additive when consumed in commonly employed quantities, their increasing and extensive use in a wide range of different applications means that consumers' exposure to these components can be substantially enhanced. Moreover, in addition to their pure form, these compounds are part of complex mixtures in multiple essential oils and spices where cumulative and countervailing effects can occur. Consequently, there is concern about adverse health effects related to exposure to high doses (Kamatou et al., 2012). Indeed, the need for comprehensive toxicological studies using animal models to support the safety of these components has been suggested (Nagoor Meeran et al., 2017). Accordingly, this study aimed to investigate the toxicological properties of these four EOCs *in vivo,* using the model system *C. elegans*. For this purpose, the LC_{50} value of acute exposure to these components was first established; then the effect of sublethal concentrations on different nematodes' biological parameters was evaluated.

Based on the lethality assays, carvacrol was the most toxic compound for *C. elegans*, followed by thymol, eugenol, and lastly by vanillin. These results about the descending toxicity ranking of the EOCs are consistent with those reported by different authors who evaluated the anthelmintic potential of phenolic terpenes against *C. elegans* as a model for parasitic nematodes (Abdel-Rahman et al., 2013; Marjanović et al., 2018; Tsao and Yu, 2000).

Similarly to our work, the acute toxic effect of carvacrol and, to a lesser extent, that of thymol, have been found to be more potent than the antinematodal effect of eugenol. This effect has been attributed to differences in their chemical structure, such as hydroxyl group position (D'addabbo and Avato, 2021; Park et al., 2007), since molecular structure determines important properties for insecticidal or nematicidal activity including the capability of these molecules to penetrate through the cuticle. Indeed Gaire et al. (2019) point out the higher lipophilicity of carvacrol and thymol than that of eugenol as a relevant factor determining their higher ability to penetrate insect's cuticle and their related toxicity. By contrast, the underlying toxicological mechanisms seem to be shared for these components. The anthelmintic action of these EOCs has been related to their inhibitory effect on the neuromuscular system of nematodes (Trailović et al., 2015). Despite the molecular mechanisms of the paralysing effects not being completely elucidated, they seem to involve different receptors as main targets. Hernando et al. (2019) studied the effect of carvacrol, eugenol and thymol on *C. elegans* mutant strains for different worm locomotion-related receptors. These authors found that terpenoid-induced paralysis by inhibiting receptors is involved in muscle contraction and locomotion, such as levamisole sensitive acetylcholine (L-AChR), γ-aminobutyric acid (GABA) type A (UNC-49) receptors and, to a lesser extent, nicotine-sensitive acetylcholine receptors (N-AChRs). They also demonstrated that the inhibitory effect of terpenoids on acetylcholine and GABA neurotransmitters occurs by acting as the negative allosteric modulators of these receptors. Other authors have demonstrated that carvacrol and eugenol reduce the acetylcholine response by the non-competitive inhibition of levamisole sensitive (L-type) nAChRs from *Oesophagostomum dentatum* and a nicotine-sensitive (N-type) nAChR (ACR-16) from *Ascaris suum* (Choudhary et al., 2019; Trailović et al., 2015), which are two relevant porcine parasitic nematodes. The SER-2 tyramine receptor has also been suggested as a target site for carvacrol and thymol in *C. elegans* because both

components are able to trigger the signalling cascade downstream from the receptor in those cells expressing wild-type, but not SER-2, mutants (Lei et al., 2010). The SER-2 receptor is also involved in the regulation of muscle contraction and locomotion and in other nematode behavioural processes, such as pharyngeal pumping, foraging behaviour and egg lying (Branicky and Schafer, 2009; Chase and Koelle, 2007; Kagawa-Nagamura et al., 2018; Rex et al., 2004).

For vanillin, no significant toxic effects were observed after exposing worms to a 4.5 mM concentration. This finding demonstrated the low acute toxicological potential of vanillin. Likewise, the effects of long-term vanillin exposure on *C. elegans* have been evaluated by Venkata et al. (2020), who did not find any toxic effects after treating worms with a 0.8 mM concentration for 4 days. Interestingly, Schmeisser et al. (2013) observed that 1 μM of vanillin extended *C. elegans* life span, while 1 mM had the opposite effect, which reflects a hormetic and non-linear dose-response for this compound. These authors found that exposure to low vanillin concentrations induced a transient increase in ROS formation, followed by a persistent reduction in the steady state. Conversely, high vanillin concentrations did not decrease ROS production in the steady state, but increased ROS formation after a 4-day exposure to produce an excessive ROS load that was responsible for a shorter life span.

Exposure to sublethal concentrations of chemicals may cause behavioural changes that are indicative of developmental and neurological adverse effects. For this reason, sublethal concentrations were used to investigate the effect of each compound on the behavioural endpoints of nematodes: locomotion, reproduction, stress resistance, and chemotaxis.

C. elegans locomotes in a rhythmic and undulatory forward and backward fashion by alternating ventral and dorsal bends along its body (Izquierdo and

Beer, 2018). This undulatory movement results freely crawling nematodes carving sinusoidal tracks on the surface of agar plates. In our study, worm motility was measured by directly quantifying those tracks made on the agar surface by the nematodes pre-exposed to EOCs sublethal concentrations or to the control for 24 h. As previously mentioned, terpenoids' antinematodal action has been related to their paralysing effects, which occur because of their interfering activity on muscle contraction and locomotion receptors (André et al., 2017; Shu et al., 2016; Trailović et al., 2015). These receptors control not only *C. elegans*' locomotion, but also other key behavioural processes like pharyngeal pumping or egg laying (Driscoll and Kaplan, 1997; Rand, 2007). According to our results, exposure to sublethal concentrations of carvacrol, eugenol, thymol and vanillin resulted in stimulatory responses of wild-type adult *C. elegans* locomotive behaviour, which suggests that they act in a hormetic-like manner on the neuromuscular system.

Previous healthspan assays have demonstrated that hormesis may enhance locomotion-related behaviours of *C. elegans*, such as bending frequency and pumping rate, by 28.9% (Sun et al., 2020). This phenomenon has also been observed with different constituents of essential oils in other biological parameters like lifespan and fecundity rates in Mediterranean fruit fly (Papanastasiou et al., 2017) or the larvae production of *Sitophilus zeamais* (Haddi et al., 2015), which suggest disruptions to endocrine, antioxidant or detoxification systems as being the physiological mechanisms responsible for regulating such stimulatory responses (Farias et al., 2020).

C. elegans reproduction has been demonstrated as useful endpoint in toxicity testing since a broad spectrum of chemicals disrupt this behaviour (Eom and Choi, 2019; Li et al., 2020; Zhou et al., 2021). Herein, exposure to sublethal concentrations of carvacrol and eugenol affected *C. elegans* reproduction. Similarly, Hernando et al. (2019) found that carvacrol affected egg hatching to a greater extent than eugenol and thymol when *C. elegans*

eggs were incubated in the presence of these components for 12 h. In the present study, eugenol and carvacrol reduced brood size as a result of fewer larvae and eggs. Therefore, our results suggest that the effect of pre-exposure to these components on reproduction may be due to other reproductive dysfunctions other than egg-hatching inhibition like alteration of the egg-laying behaviour. Egg-laying results from contraction of specialised muscle cells that open the vulva and compress the uterus, allowing eggs to be deposited (Schafer, 2016). As described for the anthelmintic action and the effects on *C. elegans*' locomotion of the EOCs, a number of serotonin and acetylcholine receptors have been demonstrated to modulate vulval muscle activity (Bradford et al., 2020; Collins et al., 2016; Rand, 2007; Schafer, 2016). Moreover, egg-lying behaviour may also be indirectly inhibited as a consequence of motility defects deriving from neurotoxicity, since an inverse correlation has been described between egg-laying and locomotion (Schafer, 2016). Other factors related to toxicant-induced reproductive deficits, such as oxidative damage events in gonad and vulva (Wu et al., 2011) during germline development (Rodrigues et al., 2018) or structural changes in the external reproductive organs of nematodes (Andre et al., 2016) may also play a role.

The no reproductive toxicity herein observed after exposure to sublethal thymol concentrations was also found by Shu et al. (2016) when evaluating thymol's safety as an antifungal agent. Exposure to the 0.21 mM and 0.42 mM concentrations for 6 h did not influence the exposed worms' brood size. However, these authors found that a 0.85 mM thymol concentration significantly reduced brood size in *C. elegans* compared to the untreated controls.

Several plant essential oils rich in different monoterpenes have a protective effect against thermal and oxidative stress in the *in vivo* model *C. elegans* (Kamireddy et al., 2018; Link et al., 2016; Pandey et al., 2018; Rathor et al., 2017; Rodrigues et al., 2018; Yu et al., 2014; Zhang et al., 2021). The

molecular mechanism responsible for their enhanced stress resistance activity has been related to different biological markers, such as decreased ROS production, altered expression patterns of important stress-response genes like sod-3 and gst-4, or the nuclear translocation of FOXO transcription factor DAF-16 from the cytoplasm. Unlike these studies, Piao et al. (2020) found that the essential oil of flesh fingered citron and its main components (d-limonene, γ-terpinene, α-pinene, β-pinene) shorted nematodes' lifespan as a result of increased oxidative stress. The differences in the biological effects between essential oils would depend on the nature and the relative content of their constituents, which could vary not only between plant species, but also due to environmental and growth factors (Yu et al., 2014), which means that studying their individual components is necessary. Our results show that only the highest sublethal carvacrol and eugenol concentrations resulted in increased survival rates as a consequence of their antioxidant effect. Thus, a narrow range of concentrations exists between antioxidant and antinematodal effects, and attention should be paid when using bioactive concentrations of these components because of their potential toxicological implications.

C. elegans has a highly developed chemosensory system that consists of neurons in the amphid, phasmid and inner labial organs that are able to sense chemicals from the environment (Bargmann, 2006). Indeed, this nematode responds to a wide spectrum of both water-soluble and volatile chemicals (O'Halloran and Burnell, 2003). Chemosensory signals are associated with food searches, the rapid avoidance of noxious conditions or mating, and can stimulate different behaviours, including chemotaxis (Margie et al., 2013). The present work tested the chemotactic responses of *C. elegans* to carvacrol, eugenol, thymol and vanillin to evaluate the attractive or repellent effect of these components on worms. Volatile molecules can be detected within the nanomolar range, with nematodes being more sensitive to volatile compounds than to water-soluble chemicals (Bargmann, 2006). In our work, the smallest

amounts of compounds were effective attractants to *C. elegans* and no significant differences were observed in worms' response to higher concentrations. The attractant effect of these components has been previously reported in different *Meloidogyne* nematode species (Oka, 2021). Surprisingly, worms were attracted to these aromatic compounds despite their nematicidal activity. Indeed, the two components displaying the greatest nematicidal action in the lethality assays were carvacrol and thymol, which also exhibited the most potent chemoattractant effect. Plant roots are often the storage site for the organic molecules that soil-dwelling organisms may use as nutrients and metabolites. These organisms have evolved to detect and respond to chemical signals for successful foraging purposes (Rasmann et al., 2012). According to Oka (2021), although this "suicidal behaviour" by which nematodes are attracted to nematicidal compounds remains unknown, it may be due to the fact that these chemoattractants act as signals for root finding under natural conditions in the soil matrix, but they never encounter them at nematicidal concentrations during their evolution.

The acute oral toxicity potential of chemicals is usually determined by the calculation of the median lethal dose (LD_{50}) that is the dose that is expected to kill 50% of the test population. This parameter is crucial for hazard and risk assessment purposes, since it helps the industry, regulatory agencies and the international community for the hazard classification and labelling of chemicals and test materials (NIH, 2001). In this work, a regression model was applied for prediction of acute mammalian oral LD_{50} values from the acute toxicity *C. elegans* experimental data. This mathematical model was developed to determine the starting doses for rodent acute oral toxicity tests from basal *in vitro* cytotoxicity data (ICCVAM, 2006) but it has also been successfully used to predict LD_{50} values for different essential oils based on calculated LC_{50} in *C. elegans* (Lanzerstorfer et al., 2020). The predicted LD_{50} values obtained for the four EOCs were compared to the oral LD_{50} reported

for rats by the European Chemicals Agency (ECHA, 2021). The results showed that estimated LD_{50} values displayed a significant correlation with the values reported for rats since the toxicity ranking was maintained. Various studies have proposed the use of mutant strains with increased absorption properties during toxicity assessment, since the tough nematode cuticle may prevent from chemical uptake and lead to an underestimation of effects (Lanzerstorfer et al., 2020; Xiong et al., 2017). However, the predicted LD_{50} values found in our study are lower than those reported by the ECHA. Particularly, small differences were found between predicted and experimental LD_{50} for the two more toxic compounds, carvacrol and thymol, while the two EOCs that showed the mildest toxicity effect, eugenol and vanillin, both exhibited a toxic effect up to 2- fold stronger for *C. elegans* than rats. Li et al. (2013) described that the pH of chemicals could affect the *C. elegans* LC_{50} value, leading to an overestimation of the toxicity effects of acidic chemicals and low correlations with acute toxicity in rodents. In this study, at the higher concentrations tested of EOCs, the pH of K-medium (pH 7.2) was slightly acidified in the case of carvacrol (pH 6.8) and thymol (pH 6.9), but a further decrease was observed for eugenol (pH 6.5) and vanillin (pH 5). However, at these ranges of pH no effects on C. elegans survival have been described. Indeed, Khanna et al. (1997) demonstrated that worms survived in K-medium a pH range of 3.1 to 11.9 for 24 h. Therefore, other factors should be responsible for these differences.

5. Conclusions

The extensive use of carvacrol, eugenol, thymol and vanillin, either pure or in the form of essential oils and spices, in an increasing number of applications, could pose potential human health and environmental hazards. This study describes the effect of acute exposure to these four EOCs on

different biological *C. elegans* parameters. All the components exhibited a concentration-dependent effect on nematode survival at moderate to high concentrations. Carvacrol and thymol were the two more toxic EOCs, while vanillin had the mildest toxicological effect. The study of acute exposure to sublethal concentrations of these components revealed that they significantly influenced nematode parameters, such as locomotion behaviour and reproduction, at low concentrations. As observed in the stress resistance assays, only the pre-exposure to carvacrol and eugenol at the highest sublethal tested concentrations conferred worms oxidative stress resistance. However, at these low concentrations, both components induced reproductive toxicity, as shown by brood size reduction. Moreover, the correlation found in the acute toxicity ranking of EOCs between nematodes and rodents.

The model organism *C. elegans* was demonstrated as a useful *in vivo* model to evaluate the toxicological properties of EOCs. By comparing different assays, reproduction resulted in a more sensitive endpoint than lethality for evaluating toxicity. However, further studies should be conducted to elucidate the underlying toxic mechanisms involved in the exposure to these compounds. In addition, chronic exposure to these components still needs to be investigated. In summary, our results evidence that these compounds can be toxic at lower doses than those required for their biological action. These findings highlight the need for a specific toxicological assessment of every EOC application.

Acknowledgments

This research has been supported by the Spanish Government (Project RTI2018-101599-B-C21 (MCUI/AEI/FEDER, EU)). The *C. elegans* strain was provided by the CGC, which is funded by the NIH Office of Research Infrastructure Programmes (P40 OD010440).

References

Abdel-Rahman, F.H., Alaniz, N.M., Saleh, M.A., 2013. Nematicidal activity of terpenoids. J. Environ. Sci. Heal. Part B 48, 16–22. https://doi.org/10.1080/03601234.2012.716686

Acosta, C., Barat, J.M., Martínez-Máñez, R., Sancenón, F., Llopis, S., González, N., Genovés, S., Ramón, D., Martorell, P., 2018. Toxicological assessment of mesoporous silica particles in the nematode Caenorhabditis elegans. Environ. Res. 166, 61–70. https://doi.org/10.1016/J.ENVRES.2018.05.018

Al-Naqeb, G., Ismail, M., Bagalkotkar, G., Adamu, H.A., 2010. Vanillin rich fraction regulates LDLR and HMGCR gene expression in HepG2 cells. Food Res. Int. 43, 2437–2443. https://doi.org/10.1016/j.foodres.2010.09.015

Andersen, A., 2006. Final report on the safety assessment of sodium p-Chloro-m-Cresol, p-Chloro-m-Cresol, Chlorothymol, Mixed Cresols, m-Cresol, o-Cresol, p-Cresol, Isopropyl Cresols, Thymol, o-Cymen-5-ol, and Carvacrol. Int. J. Toxicol. 25, 29–127. https://doi.org/10.1080/10915810600716653

André, W.P.P., Cavalcante, G.S., Ribeiro, W.L.C., Dos Santos, J.M.L., Macedo, I.T.F., De Paula, H.C.B., De Morais, S.M., De Melo, J.V., Bevilaqua, C.M.L., 2017. Anthelmintic effect of thymol and thymol acetate on sheep gastrointestinal nematodes and their toxicity in mice. Rev. Bras. Parasitol. Vet. 26, 323–330. https://doi.org/10.1590/S1984-29612017056

Andre, W.P.P., Ribeiro, W.L.C., Cavalcante, G.S., Santos, J.M.L. do., Macedo, I.T.F., Paula, H.C.B. d., de Freitas, R.M., de Morais, S.M., Melo, J.V. d., Bevilaqua, C.M.L., 2016. Comparative efficacy and toxic effects of carvacryl acetate and carvacrol on sheep gastrointestinal nematodes and mice. Vet. Parasitol. 218, 52–58. https://doi.org/10.1016/j.vetpar.2016.01.001

Bakkali, F., Averbeck, S., Averbeck, D., Idaomar, M., 2008. Biological effects of essential oils – A review. Food Chem. Toxicol. 46, 446–475. https://doi.org/10.1016/j.fct.2007.09.106

Bargmann, C.I., 2006. Chemosensation in C. elegans., WormBook: The Online

Review of C. elegans Biology. https://doi.org/10.1895/wormbook.1.123.1

Bezerra, D.P., Soares, A.K.N., De Sousa, D.P., 2016. Overview of the role of vanillin on redox status and cancer development. Oxid. Med. Cell. Longev. 2016, 1–9. https://doi.org/10.1155/2016/9734816

Bradford, B.R., Whidden, E., Gervasio, E.D., Checchi, P.M., Raley-Susman, K.M., 2020. Neonicotinoid-containing insecticide disruption of growth, locomotion, and fertility in Caenorhabditis elegans. PLoS One 15, e0238637. https://doi.org/10.1371/JOURNAL.PONE.0238637

Branicky, R., Schafer, W.R., 2009. Tyramine: A New Receptor and a New Role at the Synapse. Neuron 62, 458–460. https://doi.org/10.1016/j.neuron.2009.05.005

Brenner, S., 1974. The Genetics of Caenorhabditis elegans. Genetics 77, 71–94.

Buckingham, S.D., Sattelle, D.B., 2008. Strategies for automated analysis of C. elegans locomotion. Invertebr. Neurosci. 8, 121–131. https://doi.org/10.1007/s10158-008-0077-3

Chase, D.L., Koelle, M.R., 2007. Biogenic amine neurotransmitters in C. elegans., WormBook : the online review of C. elegans biology. https://doi.org/10.1895/wormbook.1.132.1

Choudhary, S., Marjianović, D.S., Wong, C.R., Zhang, X., Abongwa, M., Coats, J.R., Trailović, S.M., Martin, R.J., Robertson, A.P., 2019. Menthol acts as a positive allosteric modulator on nematode levamisole sensitive nicotinic acetylcholine receptors. Int. J. Parasitol. Drugs Drug Resist. 9, 44–53. https://doi.org/10.1016/j.ijpddr.2018.12.005

Collins, K.M., Bode, A., Fernandez, R.W., Tanis, J.E., Brewer, J.C., Creamer, M.S., Koelle, M.R., 2016. Activity of the C. elegans egg-laying behavior circuit is controlled by competing activation and feedback inhibition. Elife 5. https://doi.org/10.7554/ELIFE.21126

D'Addabbo, T., Avato, P., 2021. Chemical Composition and Nematicidal

Properties of Sixteen Essential Oils

—A Review. Plants 10 (7), 1368. doi:https://doi.org/10.3390/plants10071368.

Driscoll, M., Kaplan, J., 1997. Introduction: the Neural Circuit For Locomotion, in: C. Elegans II. Cold Spring Harbor Laboratory Press.

EC, 2008. Regulation (EC) no 1334/2008 of the European Parliament and of the council of 16 December 2008 on flavourings and certain food ingredients with flavouring properties for use in and on foods and amending council regulation (EEC) no 1601/91, regulations (EC. Off. J. Eur. Communities L354, 34–50.

ECHA, 2021. European Chemicals agency [WWW Document]. URL https://echa.europa.eu/es/ (accessed 1.7.21).

Eom, H.J., Choi, J., 2019. Clathrin-mediated endocytosis is involved in uptake and toxicity of silica nanoparticles in Caenohabditis elegans. Chem. Biol. Interact. 311, 108774. https://doi.org/10.1016/j.cbi.2019.108774

Farias, A.P., dos Santos, M.C., Viteri Jumbo, L.O., Oliveira, E.E., de Lima Nogueira, P.C., de Sena Filho, J.G., Teodoro, A.V., 2020. Citrus essential oils control the cassava green mite, Mononychellus tanajoa, and induce higher predatory responses by the lacewing Ceraeochrysa caligata. Ind. Crops Prod. 145, 112151. https://doi.org/10.1016/j.indcrop.2020.112151

FDA, 2021. FDA (U.S. Food and Drug Administration, U.S. Department of Health and Human Services). Database of Select Committee on Gras Substances (SCOGS) [WWW Document]. https://doi.org/10.1201/9781420037838.ch1

Fuentes, C., Ruiz-Rico, M., Fuentes, A., Barat, J.M., Ruiz, M.J., 2021. Comparative cytotoxic study of silica materials functionalised with essential oil components in HepG2 cells. Food Chem. Toxicol. 147, 111858. https://doi.org/10.1016/j.fct.2020.111858

Fujisawa, S., Atsumi, T., Kadoma, Y., Sakagami, H., 2002. Antioxidant and prooxidant action of eugenol-related compounds and their cytotoxicity. Toxicology 177, 39–54. https://doi.org/10.1016/S0300-483X(02)00194-4

Gaire, S., Scharf, M.E., Gondhalekar, A.D., 2019. Toxicity and neurophysiological impacts of plant essential oil components on bed bugs (Cimicidae: Hemiptera). Sci. Reports 2019 91 9, 1–12. https://doi.org/10.1038/s41598-019-40275-5

Gao, S., Chen, W., Zeng, Y., Jing, H., Zhang, N., Flavel, M., Jois, M., Han, J.D.J., Xian, B., Li, G., 2018. Classification and prediction of toxicity of chemicals using an automated phenotypic profiling of Caenorhabditis elegans. BMC Pharmacol. Toxicol. 19, 1–11. https://doi.org/10.1186/s40360-018-0208-3

Gonzalez-Moragas, L., Roig, A., Laromaine, A., 2015. C. elegans as a tool for in vivo nanoparticle assessment. Adv. Colloid Interface Sci. 219, 10–26. https://doi.org/10.1016/j.cis.2015.02.001

Haddi, K., Oliveira, E.E., Faroni, L.R.A., Guedes, D.C., Miranda, N.N.S., 2015. Sublethal Exposure to Clove and Cinnamon Essential Oils Induces Hormetic-Like Responses and Disturbs Behavioral and Respiratory Responses in *Sitophilus zeamais* (Coleoptera: Curculionidae). J. Econ. Entomol. 108, 2815–2822. https://doi.org/10.1093/jee/tov255

Hernando, G., Turani, O., Bouzat, C., 2019. Caenorhabditis elegans muscle Cys-loop receptors as novel targets of terpenoids with potential anthelmintic activity. PLoS Negl. Trop. Dis. 13, e0007895. https://doi.org/10.1371/journal.pntd.0007895

Ho, Y.C., Huang, F.M., Chang, Y.C., 2006. Mechanisms of cytotoxicity of eugenol in human osteoblastic cells in vitro. Int. Endod. J. 39, 389–393. https://doi.org/10.1111/j.1365-2591.2006.01091.x

Hunt, P.R., 2017. The C. elegans model in toxicity testing. J. Appl. Toxicol. https://doi.org/10.1002/jat.3357

Hyldgaard, M., Mygind, T., Meyer, R.L., 2012. Essential oils in food preservation: Mode of action, synergies, and interactions with food matrix components. Front. Microbiol. 3, 1–12. https://doi.org/10.3389/fmicb.2012.00012

ICCVAM, I.C.C. on the V. of A.M., 2006. ICCVAM Test Method Evaluation Report (TMER): In Vitro Cytotoxicity Test Methods for Estimating Starting

Doses For Acute Oral Systemic Toxicity Testing: NIH Publication No: 07-4519 1–334.

Izquierdo, E.J., Beer, R.D., 2018. From head to tail: A neuromechanical model of forward locomotion in Caenorhabditis elegans. Philos. Trans. R. Soc. B Biol. Sci. 373, 20170374. https://doi.org/10.1098/rstb.2017.0374

Jadhav, D., Rekha, B. N, Gogate, P. R., Rathod, V. K., 2009. Extraction of vanillin from vanilla pods: A comparison study of conventional soxhlet and ultrasound assisted extraction. J. Food Eng. 93 (4), 421–426. doi:https://doi.org/10.1016/j.jfoodeng.2009.02.007.

JECFA, 2021. WHO | JECFA [WWW Document]. Eval. Jt. FAO/WHO Expert Comm. Food Addit. URL https://apps.who.int/food-additives-contaminants-jecfa-database/search.aspx. (accessed 3.1.21).

Kachur, K., Suntres, Z., 2020. The antibacterial properties of phenolic isomers, carvacrol and thymol. Crit. Rev. Food Sci. Nutr. 60, 3042–3053. https://doi.org/10.1080/10408398.2019.1675585

Kagawa-Nagamura, Y., Gengyo-Ando, K., Ohkura, M., Nakai, J., 2018. Role of tyramine in calcium dynamics of GABAergic neurons and escape behavior in Caenorhabditis elegans. Zool. Lett. 4, 1–14. https://doi.org/10.1186/s40851-018-0103-1

Kamatou, G.P., Vermaak, I., Viljoen, A.M., 2012. Eugenol—From the Remote Maluku Islands to the International Market Place: A Review of a Remarkable and Versatile Molecule. Molecules 17, 6953–6981. https://doi.org/10.3390/molecules17066953

Kamireddy, K., Chinnu, S., Priyanka, P.S., Rajini, P.S., Giridhar, P., 2018. Neuroprotective effect of Decalepis hamiltonii aqueous root extract and purified 2-hydroxy-4-methoxy benzaldehyde on 6-OHDA induced neurotoxicity in Caenorhabditis elegans. Biomed. Pharmacother. 105, 997–1005. https://doi.org/10.1016/j.biopha.2018.06.002

Khalil, A.A., Rahman, U.U., Khan, M.R., Sahar, A., Mehmood, T., Khan, M., 2017.

Essential oil eugenol: Sources, extraction techniques and nutraceutical perspectives. RSC Adv. 7, 32669–32681. https://doi.org/10.1039/c7ra04803c

Khanna, N., Cressman, C.P., Tatara, C.P., Williams, P.L., 1997. Tolerance of the nematode Caenorhabditis elegans to pH, salinity, and hardness in aquatic media. Arch. Environ. Contam. Toxicol. 32, 110–114. https://doi.org/10.1007/s002449900162

Kumar, S., Suchiang, K., 2020. Caenorhabditis elegans: Evaluation of Nanoparticle Toxicity, in: Model Organisms to Study Biological Activities and Toxicity of Nanoparticles. Springer Singapore, pp. 333–369. https://doi.org/10.1007/978-981-15-1702-0_17

Lanzerstorfer, P., Sandner, G., Pitsch, J., Mascher, B., Aumiller, T., Weghuber, J., 2020. Acute, reproductive, and developmental toxicity of essential oils assessed with alternative in vitro and in vivo systems. Arch. Toxicol. 1, 3. https://doi.org/10.1007/s00204-020-02945-6

Lee, Jienny, Cho, J.Y., Lee, S.Y., Lee, K.W., Lee, Jongsung, Song, J.Y., 2014. Vanillin protects human keratinocyte stem cells against Ultraviolet B irradiation. Food Chem. Toxicol. 63, 30–37. https://doi.org/10.1016/j.fct.2013.10.031

Lei, J., Leser, M., Enan, E., 2010. Nematicidal activity of two monoterpenoids and SER-2 tyramine receptor of Caenorhabditis elegans. Biochem. Pharmacol. 79, 1062–1071. https://doi.org/10.1016/j.bcp.2009.11.002

Leung, M.C.K., Williams, P.L., Benedetto, A., Au, C., Helmcke, K.J., Aschner, M., Meyer, J.N., 2008. Caenorhabditis elegans: An Emerging Model in Biomedical and Environmental Toxicology. Toxicol. Sci. 106, 5–28. https://doi.org/10.1093/toxsci/kfn121

Li, D., Ji, J., Yuan, Y., Wang, D., 2020. Toxicity comparison of nanopolystyrene with three metal oxide nanoparticles in nematode Caenorhabditis elegans. Chemosphere 245, 125625. https://doi.org/10.1016/j.chemosphere.2019.125625

Li, Y., Gao, S., Jing, H., Qi, L., Ning, J., Tan, Z., Yang, K., Zhao, C., Ma, L., Li, G., 2013. Correlation of chemical acute toxicity between the nematode and the rodent. Toxicol. Res. (Camb). 2, 403–412. https://doi.org/10.1039/C3TX50039J

Link, P., Roth, K., Sporer, F., Wink, M., 2016. Carlina acaulis Exhibits Antioxidant Activity and Counteracts Aβ Toxicity in Caenorhabditis elegans. Molecules 21, 871. https://doi.org/10.3390/molecules21070871

Llana-Ruiz-Cabello, M., Gutiérrez-Praena, D., Pichardo, S., Moreno, F.J., Bermúdez, J.M., Aucejo, S., Cameán, A.M., 2014a. Cytotoxicity and morphological effects induced by carvacrol and thymol on the human cell line Caco-2. Food Chem. Toxicol. 64, 281–290. https://doi.org/10.1016/j.fct.2013.12.005

Llana-Ruiz-Cabello, M., Maisanaba, S., Puerto, M., Prieto, A.I., Pichardo, S., Jos, Á., Cameán, A.M., 2014b. Evaluation of the mutagenicity and genotoxic potential of carvacrol and thymol using the Ames Salmonella test and alkaline, Endo III- and FPG-modified comet assays with the human cell line Caco-2. Food Chem. Toxicol. 72, 122–128. https://doi.org/10.1016/j.fct.2014.07.013

Maisanaba, S., Prieto, A.I., Puerto, M., Gutiérrez-Praena, D., Demir, E., Marcos, R., Cameán, A.M., 2015. In vitro genotoxicity testing of carvacrol and thymol using the micronucleus and mouse lymphoma assays. Mutat. Res. - Genet. Toxicol. Environ. Mutagen. 784–785, 37–44. https://doi.org/10.1016/j.mrgentox.2015.05.005

Maralhas, A., Monteiro, A., Martins, C., Kranendonk, M., Laires, A., Rueff, J., Rodrigues, A.S., 2006. Genotoxicity and endoreduplication inducing activity of the food flavouring eugenol. Mutagenesis 21, 199–204. https://doi.org/10.1093/mutage/gel017

Margie, O., Palmer, C., Chin-Sang, I., 2013. C. elegans chemotaxis assay. J. Vis. Exp. 74, e50069. https://doi.org/10.3791/50069

Marjanović, S.Đ., Bogunović, D., Milovanović, M., Marinković, D., Zdravković,

N., Magaš, V., S., T., 2018. Antihelminic activity of carvacrol, thymol, cinnamaldehyde and p-cymen against the free-living nematode Caenorhabditis elegans and rat pinworm Syphacia muris. Acta Vet. Brno. 68, 445–456.

Memar, M.Y., Raei, P., Alizadeh, N., Akbari Aghdam, M., Kafil, H.S., 2017. Carvacrol and thymol. Rev. Med. Microbiol. 28, 63–68. https://doi.org/10.1097/MRM.0000000000000100

Nagar, Y., Thakur, R.S., Parveen, T., Patel, D.K., Ram, K.R., Satish, A., 2020. Toxicity assessment of parabens in Caenorhabditis elegans. Chemosphere 246, 125730. https://doi.org/10.1016/j.chemosphere.2019.125730

Nagoor Meeran, M.F., Javed, H., Taee, H. Al, Azimullah, S., Ojha, S.K., 2017. Pharmacological properties and molecular mechanisms of thymol: Prospects for its therapeutic potential and pharmaceutical development. Front. Pharmacol. 8, 380. https://doi.org/10.3389/fphar.2017.00380

Nejad, S.M., Özgüneş, H., Başaran, N., 2017. Pharmacological and Toxicological Properties of Eugenol. Turkish J. Pharm. Sci. 14, 201–206. https://doi.org/10.4274/tjps.62207

NIH, N.I. of E.H.S., 2001. The Revised Up-and-Down Procedure: A Test Method for Determining the Acute Oral Toxicity of Chemicals. Tech. Rep. 1, 2–4501.

O'Halloran, D.M., Burnell, A.M., 2003. An investigation of chemotaxis in the insect parasitic nematode Heterorhabditis bacteriophora. Parasitology 127, 375–385. https://doi.org/10.1017/S0031182003003688

Oka, Y., 2021. Screening of chemical attractants for second-stage juveniles of Meloidogyne species on agar plates. Plant Pathol. 70, 912–921. https://doi.org/10.1111/ppa.13336

Oliveira, C., Meurer, Y., Oliveira, M., Medeiros, W., Silva, F., Brito, A., Pontes, D., Andrade-Neto, V., 2014. Comparative Study on the Antioxidant and Anti-Toxoplasma Activities of Vanillin and Its Resorcinarene Derivative. Molecules 19, 5898–5912. https://doi.org/10.3390/molecules19055898

Pandey, S., Tiwari, S., Kumar, A., Niranjan, A., Chand, J., Lehri, A., Chauhan, P.S., 2018. Antioxidant and anti-aging potential of Juniper berry (Juniperus communis L.) essential oil in Caenorhabditis elegans model system. Ind. Crops Prod. 120, 113–122. https://doi.org/10.1016/j.indcrop.2018.04.066

Papanastasiou, S.A., Bali, E.M.D., Ioannou, C.S., Papachristos, D.P., Zarpas, K.D., Papadopoulos, N.T., 2017. Toxic and hormetic-like effects of three components of citrus essential oils on adult Mediterranean fruit flies (Ceratitis capitata). PLoS One 12, e0177837. https://doi.org/10.1371/journal.pone.0177837

Park, I. K., Kim, J., Lee, S. G., Shin, S. C, 2007. Nematicidal activity of plant essential oils and components from ajowan (Trachyspermum ammi), allspice (Pimenta dioica) and litsea (Litsea cubeba) essential oils against pine wood nematode (Bursaphelenchus xylophilus). J. Nematol. 39 (3), 275–279.

Piao, X., Sun, M., Yi, F., 2020. Evaluation of Nematocidal Action against Caenorhabditis elegans of Essential Oil of Flesh Fingered Citron and Its Mechanism. J. Chem. 2020, 1–9. https://doi.org/10.1155/2020/1740938

Prashar, A., Locke, I.C., Evans, C.S., 2006. Cytotoxicity of clove (Syzygium aromaticum) oil and its major components to human skin cells. Cell Prolif. 39, 241–248. https://doi.org/10.1111/j.1365-2184.2006.00384.x

Priefert, H., Rabenhorst, J., Steinbüchel, A., 2001. Biotechnological production of vanillin. Appl. Microbiol. Biotechnol. 56, 296–314. https://doi.org/10.1007/s002530100687

Ramos, M., Beltran, A., Valdes, A., Peltzer, M.A., Jimenez, A., Garrigos, M.C., Zaikov, G.E., 2013. Carvacrol and thymol for fresh food packaging. J. Bioequivalence Bioavailab. 5, 154–160. https://doi.org/10.4172/jbb.1000151

Rand, J.B., 2007. Acetylcholine, WormBook : the online review of C. elegans biology. https://doi.org/10.1895/wormbook

Rasmann, S., Ali, J.G., Helder, J., van der Putten, W.H., 2012. Ecology and Evolution of Soil Nematode Chemotaxis. J. Chem. Ecol. 38, 615–628. https://doi.org/10.1007/s10886-012-0118-6

Rathor, L., Pant, A., Nagar, A., Tandon, S., Trivedi, S., Pandey, R., 2017. Trachyspermum ammi L. (Carom) Oil Induces Alterations in SOD-3, GST-4 Expression and Prolongs Lifespan in Caenorhabditis elegans. Proc. Natl. Acad. Sci. India Sect. B - Biol. Sci. 87, 1355–1362. https://doi.org/10.1007/s40011-016-0710-6

Rex, E., Molitor, S.C., Hapiak, V., Xiao, H., Henderson, M., Komuniecki, R., 2004. Tyramine receptor (SER-2) isoforms are involved in the regulation of pharyngeal pumping and foraging behavior in Caenorhabditis elegans. J. Neurochem. 91, 1104–1115. https://doi.org/10.1111/j.1471-4159.2004.02787.x

Rodrigues, C.F., Salgueiro, W., Bianchini, M., Veit, J.C., Puntel, R.L., Emanuelli, T., Dernadin, C.C., Ávila, D.S., 2018. Salvia hispanica L. (chia) seeds oil extracts reduce lipid accumulation and produce stress resistance in Caenorhabditis elegans. Nutr. Metab. 15, 1–9. https://doi.org/10.1186/s12986-018-0317-4

Salehi, B., Mishra, A.P., Shukla, I., Sharifi-Rad, M., Contreras, M. del M., Segura-Carretero, A., Fathi, H., Nasrabadi, N.N., Kobarfard, F., Sharifi-Rad, J., 2018. Thymol, thyme, and other plant sources: Health and potential uses. Phyther. Res. 32, 1688–1706. https://doi.org/10.1002/ptr.6109

Schafer, W., 2016. Nematode nervous systems. Curr. Biol. https://doi.org/10.1016/j.cub.2016.07.044

Schindelin, J., Arganda-Carreras, I., Frise, E., Kaynig, V., Longair, M., Pietzsch, T., Preibisch, S., Rueden, C., Saalfeld, S., Schmid, B., Tinevez, J.Y., White, D.J., Hartenstein, V., Eliceiri, K., Tomancak, P., Cardona, A., 2012. Fiji: An open-source platform for biological-image analysis. Nat. Methods 9, 676–682. https://doi.org/10.1038/nmeth.2019

Schmeisser, K., Mansfeld, J., Kuhlow, D., Weimer, S., Priebe, S., Heiland, I., Birringer, M., Groth, M., Segref, A., Kanfi, Y., Price, N.L., Schmeisser, S., Schuster, S., Pfeiffer, A.F.H., Guthke, R., Platzer, M., Hoppe, T., Cohen, H.Y., Zarse, K., Sinclair, D.A., Ristow, M., 2013. Role of sirtuins in lifespan regulation is linked to methylation of nicotinamide. Nat. Chem. Biol. 9, 693–

700. https://doi.org/10.1038/nchembio.1352

Sharifi-Rad, M., Varoni, E.M., Iriti, M., Martorell, M., Setzer, W.N., del Mar Contreras, M., Salehi, B., Soltani-Nejad, A., Rajabi, S., Tajbakhsh, M., Sharifi-Rad, J., 2018. Carvacrol and human health: A comprehensive review. Phyther. Res. https://doi.org/10.1002/ptr.6103

Shu, C., Sun, L., Zhang, W., 2016. Thymol has antifungal activity against Candida albicans during infection and maintains the innate immune response required for function of the p38 MAPK signaling pathway in Caenorhabditis elegans. Immunol. Res. 64, 1013–1024. https://doi.org/10.1007/s12026-016-8785-y

Sisakhtnezhad, S., Heidari, M., Bidmeshkipour, A., 2018. Eugenol enhances proliferation and migration of mouse bone marrow-derived mesenchymal stem cells in vitro. Environ. Toxicol. Pharmacol. 57, 166–174. https://doi.org/10.1016/j.etap.2017.12.012

Slamenová, D., Horváthová, E., Sramková, M., Marsálková, L., 2007. DNA-protective effects of two components of essential plant oils carvacrol and thymol on mammalian cells cultured in vitro. Neoplasma 54, 108–12.

Sun, T., Wu, H., Cong, M., Zhan, J., Li, F., 2020. Meta-analytic evidence for the anti-aging effect of hormesis on Caenorhabditis elegans. Aging (Albany. NY). 12, 2723–2746. https://doi.org/10.18632/aging.102773

Tippayatum, P., Chonhenchob, V., 2007. Antibacterial activities of thymol, eugenol and nisin against some food spoilage bacteria. Nat. Sci. 41, 319–23.

Trailović, S.M., Marjanović, D.S., Nedeljković Trailović, J., Robertson, A.P., Martin, R.J., 2015. Interaction of carvacrol with the Ascaris suum nicotinic acetylcholine receptors and gamma-aminobutyric acid receptors, potential mechanism of antinematodal action. Parasitol. Res. 114, 3059–3068. https://doi.org/10.1007/s00436-015-4508-x

Tsao, R., Yu, Q., 2000. Nematicidal Activity of Monoterpenoid Compounds against Economically Important Nematodes in Agriculture. J. Essent. Oil Res. 12, 350–354. https://doi.org/10.1080/10412905.2000.9699533

Venkata, S., Zeeshan, F., Kamal, A., Luqman, A.K., Saif, H., 2020. Efficiency of vanillin in impeding metabolic adaptability and virulence of Candida albicans by inhibiting glyoxylate cycle, morphogenesis, and biofilm formation. Curr. Med. Mycol. 6, 1–8. https://doi.org/10.18502/CMM.6.1.2501

Wang, H., Wick, R.L., Xing, B., 2009. Toxicity of nanoparticulate and bulk ZnO, Al2O3 and TiO2 to the nematode Caenorhabditis elegans. Environ. Pollut. 157, 1171–1177. https://doi.org/10.1016/j.envpol.2008.11.004

Wu, Q., He, K., Liu, P., Li, Y., Wang, D., 2011. Association of oxidative stress with the formation of reproductive toxicity from mercury exposure on hermaphrodite nematode Caenorhabditis elegans. Environ. Toxicol. Pharmacol. 32, 175–184. https://doi.org/10.1016/j.etap.2011.04.009

Wu, T., Xu, H., Liang, X., Tang, M., 2019. Caenorhabditis elegans as a complete model organism for biosafety assessments of nanoparticles. Chemosphere 221, 708–726. https://doi.org/10.1016/j.chemosphere.2019.01.021

Xiong, H., Pears, C., Woollard, A., 2017. An enhanced C. elegans based platform for toxicity assessment. Sci. Rep. 7, 1–11. https://doi.org/10.1038/s41598-017-10454-3

Yang, Z., Xue, K., Sun, X., Tang, L., Wang, J.-S., 2015. Multi-Toxic Endpoints of the Foodborne Mycotoxins in Nematode Caenorhabditis elegans. Toxins (Basel). 7, 5224–5235. https://doi.org/10.3390/toxins7124876

Yanishlieva, N. V, Marinova, E.M., Gordon, M.H., Raneva, V.G., 1999. Antioxidant activity and mechanism of action of thymol and carvacrol in two lipid systems. Food Chem. 64, 59–66. https://doi.org/10.1016/S0308-8146(98)00086-7

Yin, Q.H., Yan, F.X., Zu, X.Y., Wu, Y.H., Wu, X.P., Liao, M.C., Deng, S.W., Yin, L.L., Zhuang, Y.Z., 2012. Anti-proliferative and pro-apoptotic effect of carvacrol on human hepatocellular carcinoma cell line HepG-2. Cytotechnology 64, 43–51. https://doi.org/10.1007/s10616-011-9389-y

Yu, C.W., Li, W.H., Hsu, F.L., Yen, P.L., Chang, S.T., Liao, V.H.C., 2014.

Essential oil alloaromadendrene from mixed-type cinnamomum osmophloeum leaves prolongs the lifespan in caenorhabditis elegans. J. Agric. Food Chem. 62, 6159–6165. https://doi.org/10.1021/jf500417y

Zhang, L., Gu, B., Wang, Y., 2021. Clove essential oil confers antioxidant activity and lifespan extension in C. elegans via the DAF-16/FOXO transcription factor. Comp. Biochem. Physiol. Part - C Toxicol. Pharmacol. 242, 108938. https://doi.org/10.1016/j.cbpc.2020.108938

Zhou, R., Liu, R., Li, W., Wang, Y., Wan, X., Song, N., Yu, Y., Xu, J., Bu, Y., Zhang, A., 2021. The use of different sublethal endpoints to monitor atrazine toxicity in nematode Caenorhabditis elegans. Chemosphere 274, 129845. https://doi.org/10.1016/j.chemosphere.2021.129845

In vivo* toxicity assessment of eugenol and vanillin-functionalised silica particles using *Caenorhabditis elegans

Cristina Fuentes[a], Samuel Verdú[a], Ana Fuentes[a], María José Ruiz[b], José Manuel Barat[a]

[a]Department of Food Technology, Universitat Politècnica de València. Camino de Vera s/n, 46022, Valencia, Spain: crifuelp@upvnet.upv.es

[b]Laboratory of Toxicology, Faculty of Pharmacy, Universitat de València. Av. Vicent Andrés Estellés s/n, 46100, Burjassot, Valencia, Spain

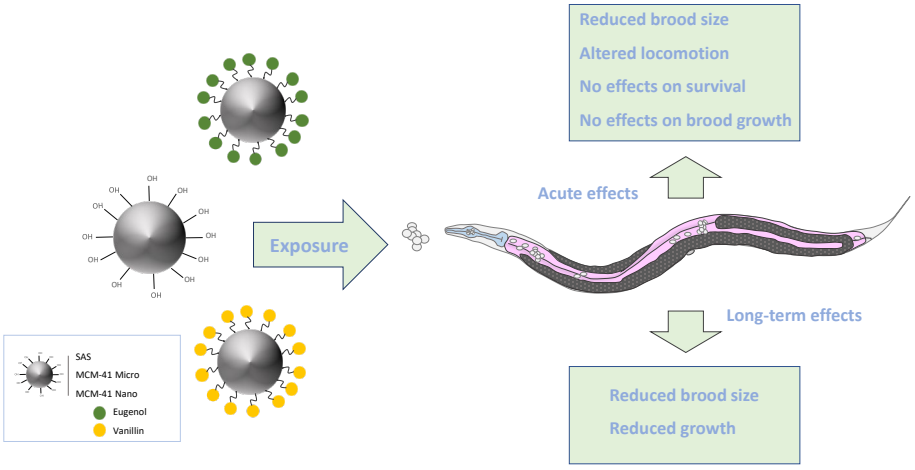

Abstract

The toxicological properties of different silica particles functionalised with essential oil components (EOCs) were herein assessed using the *in vivo* model *C. elegans*. In particular, the effects of the acute and long-term exposure to three silica particle types (SAS, MCM-41 micro, MCM-41 nano), either bare or functionalised with eugenol or vanillin, were evaluated on different biological parameters of nematodes. Acute exposure to the different particles did not reduce nematodes survival, brood growth or locomotion, but reproduction was impaired by all the materials, except for vanillin-functionalised MCM-41 nano. Moreover, long-term exposure to particles led to strongly inhibited nematodes growth and reproduction. The eugenol-functionalised particles exhibited higher functionalisation yields and had the strongest effects during acute and long-term exposures. Overall, the vanillin-functionalised particles displayed milder acute toxic effects on reproduction than pristine materials, but severer toxicological responses for the 96-hour exposure assays. Our findings suggest that the EOC type anchored to silica surfaces and functionalisation yield are crucial for determining the toxicological effects of particles on *C. elegans*. The results obtained with this alternative *in vivo* model can help to anticipate potential toxic responses to these new materials for human health and the environment.

Keywords: silicon dioxide, functionalisation, nematode, essential oil components, oral exposure

1. Introduction

Modification of materials' properties to provide them with novel functionalities gives rise to a wide range of hybrid systems for advanced applications every year (Bagheri et al., 2018; Hildebrand et al., 2006; Lu et al., 2019). Synthetic amorphous silica (SAS) is an ideal candidate for designing hybrid materials due to the high concentration of silanol groups on their surface, large surface area, and good stability and biocompatibility (Bagheri et al., 2018). Different compounds have been used to react with silica surface, which give rise to a wide variety of functional groups, including phenyl, amine, carboxyl or thiol groups, among others (Alothman, 2012). Quite often silica particles have been functionalised with PEG-silanes to enhance particles' biocompatibility and stability (Brown et al., 2007; Hao et al., 2012; He et al., 2011) and with chlorosilanes or alkoxysilanes as a linker for other functional molecules (Liberman et al., 2014). Not only small molecules, but also macromolecules like polymers and lipids, can be covalently attached to silica particles' surface (Maleki et al., 2017). One example of these silica-based hybrid structures consists in the functionalisation of silica particles' surface with essential oil components (EOCs) to improve the antimicrobial activity of these compounds and to reduce their sensory perception in food products (Ribes et al., 2017, 2019; Ruiz-Rico et al., 2018). Despite the efficacy of these antimicrobial devices having been demonstrated, the safety and innocuousness of their use in foods or food contact materials for human health and the environment is still being investigated. Previously, *in vitro* studies have demonstrated that the functionalisation of silica particles with essential oil derivatives prevents their degradation under physiological conditions (Fuentes et al., 2020) and increases the cytotoxic effect on HepG2 cells compared to their free constituents (Fuentes et al., 2021b).

In vitro methods are useful tools for predicting acute toxic effects of chemicals and enhancing our understanding of their mechanisms of action (Eisenbrand et al., 2002). Notwithstandingly, when evaluating particles' toxicity after oral exposure, different features like external barriers of the gastro-intestinal tract or their persistence and accumulation in the organism, are not easy to evaluate by *in vitro* assays, and *in vivo* studies are still needed (Gamboa and Leong, 2013; Riediker et al., 2019). Public concerns about using animal models in biological research have led scientists to search for alternatives during the toxicological evaluation of chemicals. One of these alternatives consists in replacing vertebrate animals by the non-mammalian model *Caenorhabditis elegans.* This 1 mm-long non-parasitic nematode has become one of the most widely used model organisms in several research fields thanks to its many advantages, such as small size, transparent body, simple anatomy, high reproduction rate, short life cycle and fully-annotated genome (Hunt, 2017; Wu et al., 2019). In addition, many physiological processes are conserved between nematodes and mammals given the presence of homologous genes and proteins (Kaletta and Hengartner, 2006; Leung et al., 2008). Indeed *C. elegans* and human alimentary systems bear many similarities. As in mammals, nematode feeding involves food ingestion, digestion, nutrient absorption and defecation (Gonzalez-Moragas et al., 2017). Moreover, important features like acidified lumen, microvilli, digestive enzymes secretion, uptake of digested components or peristalsis are also found (Hunt, 2017). All these properties make *C. elegans* an excellent *in vivo* model for assessing chemicals' toxicity after oral exposure.

This study aimed to investigate the toxicological properties of different silica particles functionalised with EOCs using the *in vivo* model system *C. elegans*. In particular, the acute and prolonged exposure to three silica particle types (commercial amorphous silica microparticles, mesoporous MCM-41 microparticles and MCM-41 nanoparticles), bare or functionalised with eugenol or vanillin, was evaluated in different biological nematode

parameters, such as survival, reproduction, locomotion behaviour or growth. The results obtained with this alternative *in vivo* model will anticipate potential toxicological effects of exposure to these new materials for human health and the environment.

2. Materials and Methods

2.1. Reagents and media composition

Nematode growth media (NGM) agar medium and M9 buffer were prepared in the laboratory as described by Stiernagle (2006). NGM agar medium composition was 3 g/L NaCl, 2.5 g/L peptone, 17 g/L agar, 1 M potassium phosphate buffer (108.3 g/L KH_2PO_4 and 35.6 g/L), 1 M $CaCl_2$, 1 M $MgSO_4$, and 1 mL of 5% cholesterol in ethanol. M9 buffer consisted of 3 g/L KH_2PO_4, 6 g/L Na_2HPO_4, 5 g/L NaCl, 1 ml 1 M $MgSO_4$.

Synthetic amorphous silica (SAS) microparticles (SYLYSIA® SY350/FCP; 4 (0.1) μm) were supplied by Silysiamont (Italy). N-cetyltrimethylammonium bromide (CTAB), tetraethylorthosilicate (TEOS), chloroform, n-butanone, (3-Aminopropyl) triethoxysilane (APTES), isopropyl alcohol (IPA), formic acid, agar-agar, NaCl, $MgSO_4$, and all the other inorganic salts used to prepare *C. elegans* media, were purchased from Scharlab (Spain). Eugenol (≥ 98% w/w), vanillin (≥ 98% w/w), KOH, H_2SO_4, trimethyl orthoformate, Rose Bengal dye (95%) and sodium azide (NaN_3) were provided by Sigma-Aldrich (Spain). Cholesterol (95%) was obtained from Acros Organics (Spain).

2.2. C. elegans maintenance and synchronisation

Wild-type *C. elegans* Bristol strain N2 and *Escherichia coli* strain OP50 used in this study were kindly provided by the Caenorhabditis Genetics Center (CGC) (University of Minnesota, MN, USA). Worms were maintained on NGM agar plates at 20 ºC in the dark with an *E. coli* lawn as the food source

(Brenner, 1974). Regular subculturing by the chunking method was carried out to maintain the *C. elegans* population.

Before the experiments, nematodes were synchronised to obtain uniformly aged populations and to reduce variation. Synchronisation was performed by bleaching gravid hermaphrodite nematodes with an alkaline hypochlorite solution (1 M NaOH, 3% NaClO), followed by washes with M9 buffer. For the acute toxicity tests, eggs were maintained in falcon tubes without food at 20 ºC until hatching. Then larvae were transferred to NGM plates with *E. coli* and maintained for 3 days until reaching L4 to the young adult stage. For the long-term toxicity assays, eggs were directly transferred to NMG plates without food and incubated at 20 ºC for a maximum of 16 h to obtain a L1 larvae population.

For all the experiments, *E. coli* suspensions were prepared in M9 buffer with 0.02% v/v cholesterol at a turbidity of 1000 FAU (Formazine Attenuation Units) in a spectrophotometer (Thermofisher Scientific, Helios Zeta UV-VIS) at 600 nm.

2.3. Preparing materials

Three different silica particle types were used in this study: commercial non-porous amorphous silica microparticles (SAS), MCM-41 microparticles and MCM-41 nanoparticles. Mesoporous silica particles (MCM-41 micro and MCM-41 nano) were synthesised under basic conditions using CTAB as the structure-directing agent and TEOS as the silica precursor. The synthesis process followed for both MCM-41 particle types is fully described by Fuentes et al. (2020).

Functionalisation of silica particles with eugenol. The functionalisation process with eugenol was done by a 3-stage reaction. In a first stage, eugenol aldehyde synthesis was carried out by a Reimer-Tiemann reaction. In this method, 22 mmol of eugenol were dissolved in 150 mL of distilled water at

80 ºC in a round-bottomed flask. After cooling to 60 ºC, 400 mmol KOH were slowly mixed and then 88 mmol of chloroform were gradually added (1 mL/h for 7 h). The reaction was left to shake at 60 ºC overnight, cooled again and acidified with 50 mL of 10% H_2SO_4 (v/v) to reach pH 3. Then purification of the eugenol derivative was performed by extraction with n-butanone and subsequent rotary evaporation. In a second stage, the synthesis of the eugenol alkoxysilane derivative was performed to allow its covalent anchoring to silica particles' surface. In this reaction, eugenol aldehyde was dissolved in 20 mL of IPA, mixed with APTES at a molar ratio of 1:1 (v/v) (4.64 mL) and stirred under reflux at 60 ºC for 1 h. In a last stage, the obtained eugenol alkoxysilane derivative was dissolved in 150 mL of IPA and the mixture was divided into three flasks, where 1 g of SAS, 1 g of MCM-41 micro or 0.5 g of MCM-41 nano was added to each one. After 3 h of stirring at room temperature, samples were centrifuged (9,000 rpm, 8 min) and submitted to consecutive washing and centrifugation cycles with IPA and distilled water. Finally, the functionalised particles were dried in a vacuum at room temperature for 12 h.

Functionalisation of silica particles with vanillin. The functionalisation process was as follows: 1 g of each silica particle type was mixed with 5 mL of IPA and 362.5 µL of APTES. After stirring for 1 h at room temperature, the mixture was centrifuged (9,000 rpm, 8 min) and the supernatant was discarded. Then 250 mg of vanillin previously dissolved in 2.5 mL IPA were added to the precipitate and the mixture was stirred for 1 h. After adding 352.5 µL of trimethyl orthoformate and 120 µL of formic acid, samples were still stirred at 60 ºC for 1 h. After cooling, the final particles were washed with IPA and distilled water several times and finally dried in a vacuum at room temperature overnight.

2.4. Materials characterisation

The characterisation of the bare and functionalised particles was performed by instrumental techniques. Transmission electron microscopy (TEM) images were acquired under a Philips CM10 microscope operating at 100 kV. Particle size distribution was measured with dynamic light scattering (DLS) in a Malvern Matersizer 2000 (Malvern Instruments, UK). The data analysis was based on the Mie theory using a refractive index of 1.45 and absorption indices of 0.01 and 0.1 for the SAS and MCM-41 particles, respectively. A Zeta potential analysis was performed with a Zetasizer Nano ZS (Malvern Instruments, UK). Zeta potential values were calculated from the particle mobility values by applying the Smoluchowski model. Both size distribution and zeta potential measurements were performed in triplicate. Before the analyses, samples were dispersed in deionised water and sonicated for 2 min to avoid aggregation. Finally, the elemental analysis of the functionalised silica was performed with a CHNS1100 elemental analyser (CE Instruments, UK) to estimate the content of eugenol and vanillin immobilised on particles.

2.5. Particles uptake

Silica particles uptake by *C. elegans* was examined by light microscopy. The bare and functionalised silica particles were stained with crystal violet dye. Then worms were exposed to 1 mg/mL of stained particles in the presence of *E. coli* for 24 h, immobilised with 0.25 M of sodium azide and sealed with coverslips. Nematodes were visualised under a microscope BA310E (Motic, Hong Kong) at 4X magnification and images were captured by a CMOS camera Moticam 3+ (Motic, Hong Kong).

2.6. Toxicity assessment using C. elegans

The effects of *C. elegans* exposure to bare and functionalised silica were evaluated using different biological parameters after acute and long-term exposures. A Nine particle types were evaluated: three silica types (SAS,

MCM-41 micro, MCM-41 nano), bare or functionalised with two EOCs (eugenol, vanillin). Stock solutions (10 mg/mL) were prepared on M9 buffer and dispersed by sonication in an ultrasound bath for 5 min before each experiment to reduce the formation of agglomerates. Three different concentrations of particles were assayed: 0.2, 1, 5 mg/mL. Negative (M9 buffer) and positive (15 mg/L BAC-C16) controls were included in each plate. All the experiments were carried out in at least three independent weeks. The data obtained from the toxicological assays were expressed as mean (SEM).

2.6.1. Acute exposure

Acute toxicity was evaluated on *C. elegans* lethality, reproduction and locomotion behaviour.

Lethality tests were carried out on 24-well culture plates in a final volume of 1 mL of test solution. At least 30 synchronised 3-day-old young adult worms (L4) were transferred to each well. Then plates were incubated at 20 ºC in the dark for 24 h. At the end of the exposure time, the numbers of live and dead nematodes were counted. The worms that did not respond to gentle prodding when touched with a platinum wire were scored as dead. The survival rate was calculated as the percentage of live nematodes from the total number of worms per well.

In order to investigate whether acute exposure to particles affected *C. elegans* reproduction, pre-exposed nematodes were individually transferred to 24-well NGM agar plates seeded with *E. coli*. Plates were incubated at 20 ºC for 72 h. Then brood size was calculated by counting the number of larvae and eggs laid per adult worm at each time point. Additionally, brood growth was determined by measuring the body length of flat larvae and the surface area of eggs using the Fiji image processing software (Schindelin et al., 2012). The number of pixels occupied by individual worms and eggs was transformed

into mm^2 of previous calibration. The average brood size was calculated for each treatment condition and compared to the control group.

Locomotion assays were carried out in the 24-well NGM agar plates used for the reproduction experiments. Locomotion behaviour was estimated by the tracks produced by worms' sinusoidal movement on solid surfaces. Agar surfaces were captured with a CMOS camera Moticam 3+ (Motic, Hong Kong) connected to a BA310E microscope (Motic, Hong Kong) at 10X magnification. Images were transformed and analysed as described by Fuentes et al. (2022). The results were expressed as the percentage of agar surface covered by the tracks area generated by worm movement (%).

2.6.2. Long-term exposure

The effect of long-term exposure to particles on *C. elegans* reproduction and growth was evaluated according to ISO 10872:2010 (ISO, 2010), with slight modifications. Briefly, a drop of M9 buffer containing 5-10 synchronised L1 larvae was transferred to each well of 12-well plates. Then 500 µL of *E. coli* suspension and 500 µL of particles' suspension or M9 buffer (negative control) or 15 mg/L of BAC-C16 (positive control) were added. Plates were incubated at 20 ºC in the dark for 96 h. After this time, nematodes were heated at 80 ºC for 10 min in an oven and stained with 250 µL of Rose Bengal (0.3 g/L) to kill and straighten nematodes. Reproduction and growth were used as toxicity endpoints. Reproduction, as assessed by the fertility rate, was calculated by counting the total number of larvae per well at the end of the test, divided by the total parents included per well. Growth was evaluated by body length by comparing the adult nematode length at the end of experiments to the initial body length of the L1 worms (n = 30) not used in tests. Nematode length was measured by an image analysis as described for the acute exposure assays. Growth inhibition (GI) and reproduction inhibition (RI) were calculated by comparing the exposed worms to the control ones.

2.7. Statistical analysis

The Student's t-test for paired samples was carried out with Statgraphics Centurion XVI (Statpoint Technologies, Inc., USA) to compare the nematodes exposed to test solutions with the control at the different biological endpoints. Statistical significance was considered for $p \leq 0.05$. The multivariate statistical methods of principal component analysis (PCA) and correlation matrix were performed to relate particles' physico-chemical parameters to their toxicological effects on worms using the MATLAB® PLS Tool-box, 6.3 (Eigenvector Research Inc., USA). Only the toxicity endpoints for which significant differences were found between the control and exposed worms according to the Student's t-test were included in the multivariate analysis.

3. Results

3.1. Materials characterisation

A morphological analysis of the bare and functionalised particles was carried out by TEM. Different silica materials types depicted distinct particles' shapes; globular for SAS, angular and elongated for MCM-41 micro and spherical for MCM-41 nano (Fig. 1). Moreover, the TEM images showed the surface pattern of the hexagonal channels characteristic of the inner structure of mesoporous materials in both the bare and functionalised particles. This observation revealed the ordered mesoporous structure of the synthesised MCM-41 materials and the preservation of the structure in the functionalised particles.

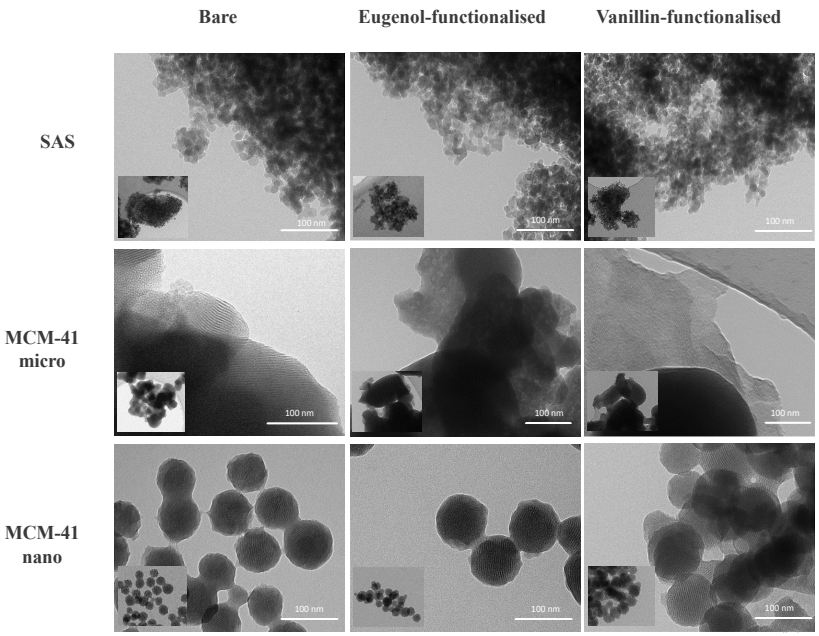

Figure 1. TEM images of the bare, eugenol- and vanillin-functionalised SAS, MCM-41 micro and MCM-41 nano.

Table 1 shows the particle size, the average hydrodynamic diameter and the zeta potential values of the different bare and functionalised materials. The TEM analysis revealed no significant differences in particle size for the different particles both before and after the functionalisation process with both EOCs. However, when particles were characterised by DLS to determine the particle size distribution in aqueous suspensions, SAS particles and MCM-41 nano had considerably higher hydrodynamic particle size values than those obtained by TEM. This effect was particularly relevant for the bare and vanillin-functionalised MCM-41 nano, which increased the mean particle size from 70 nm (as measured by TEM) to a hydrodynamic particle size of 4.34 (0.01) and 3.55 (0.02) μm, respectively. The bare silica particles exhibited negative zeta potential values due to the presence of silanol groups on their

surface. After functionalisation, a modification in the zeta potential to positive values was observed independently of the type of silica material and EOC as a result of the presence of alkoxysilane derivatives of the vanillin and eugenol anchored to particles' surfaces. Finally, the analysis of the elemental composition of the different functionalised materials showed that the highest functionalisation yield was for the MCM-41 micro and the MCM-41 nano functionalised with eugenol, while the worst immobilisation performance was achieved by the eugenol-functionalised SAS particles.

Table 1. Size, particle size distribution ($d_{0.5}$) zeta potential (ZP) and EOC content (α) of the different bare and functionalised silica particle types. Values are expressed as mean (SD, n=3).

Material	Immobilisation	Size (µm)	$d_{0.5}$ (µm)	ZP (mV)	α (g_{EOC}/g_{SiO2})
SAS	bare	2.49 (0.47)	3.34 (0.02)	-20.93 (0.99)	–
	eugenol	2.03 (0.32)	2.92 (0.01)	11.01 (1.55)	0.0010
	vanillin	2.35 (0.15)	3.37 (0.00)	13.74 (0.65)	0.0307
MCM-41 micro	bare	0.57 (0.09)	0.58 (0.00)	-27.63 (0.71)	–
	eugenol	0.56 (0.13)	0.54 (0.00)	0.19 (1.70)	0.0589
	vanillin	0.63 (0.23)	0.59 (0.00)	17.88 (0.58)	0.0255
MCM-41 nano	bare	0.07 (0.01)	4.34 (0.01)	-31.03 (0.85)	–
	eugenol	0.07 (0.01)	0.58 (0.00)	9.65 (0.73)	0.0860
	vanillin	0.07 (0.01)	3.55 (0.02)	13.47 (0.53)	0.0099

3.2. Particles' uptake

In order to confirm that silica particles were ingested by nematodes, and *C. elegans* could be employed to evaluate oral exposure to these materials, the uptake and accumulation of the stained bare and functionalised silica were evaluated by light microscopy before performing the toxicity tests. As shown in Figure 2, particles' staining with crystal violet confirmed their oral uptake

by worms. After 24 of exposure, the different silica particle types were observed along the whole nematode intestinal tract, from the buccal cavity and the pharynx to the posterior intestine region and the rectum (Fig.S1).

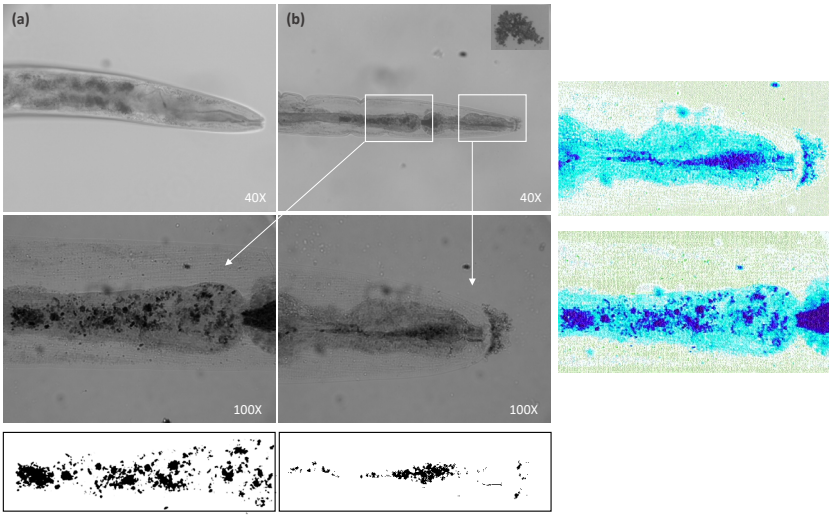

Figure 2. Representative microscope images (40X magnification) of a control worm (a) and a worm exposed to 1 mg/mL of eugenol MCM-41 micro for 24 h (b). Magnification images (100X) of the anterior intestine, the pharynx and the buccal cavity were transformed into black and white (down) and blue tones (right) to improve visualisation.

3.3. Acute toxicity assessment

Lethality. Exposure to the different bare and EOCs-functionalised silica particles for 24 h did not affect nematode survival. No significant differences (p <0.05) were observed between the survival rates of the control and treated worms at any of the tested concentrations. The average survival rates were around 100%, independently of the tested conditions (Fig.S2).

Reproduction. The effect of particles' exposure on nematode reproductive capacity was evaluated by brood size. No differences in the number of larvae laid per worm were observed between the treated and control nematodes, except for the eugenol-functionalised MCM-41 micro and MCM-41 nano at the two highest tested concentrations (Fig. 3). The eugenol-functionalised MCM-41 micro at the concentrations of 1 mg/mL and 5 mg/mL exposure decreased the number of larvae by 45% and 46%, respectively. The percentage of larvae reduction was 52% and 60% compared to the control worms for 1 mg/mL and 5 mg/mL of the eugenol-functionalised MCM-41 nano, and in that order. However, except for vanillin-functionalised MCM-41 nano, the different materials showed an adverse impact on brood size when the number of eggs was used as an endpoint (Fig. 3). The three bare silica particle types reduced egg production, although this effect was more pronounced for MCM-41 nano. Similar results were observed between the bare SAS and bare MCM-41 micro, which reduced brood size by 52% as a maximum in both cases. The bare MCM-41 nano exposure resulted in stronger effects on reproduction with an 82% decrease in the eggs laid for the 5 mg/mL concentration compared to the control worms (Fig. 3f). Brood size, as measured by egg number, significantly reduced at all the tested concentrations for the eugenol-functionalised materials. This effect was higher for the eugenol-functionalised MCM-41 micro and MCM-41 nano, which showed a maximum respective reduction of 78% and 75% in egg number at the 1 mg/mL concentration. In contrast, the vanillin-functionalised particles exhibited the mildest effect on nematode reproductive fitness. The vanillin-functionalised SAS reduced egg laying by 40% at the highest tested concentration, while no significant differences were found between 0.2 mg/mL and the control. Vanillin-functionalised MCM-41 micro brought about a 71% reduction for the 5 mg/mL concentration *versus* the control. This value lowered to 34% for both 0.2 and 1 mg/mL of particles. Finally, vanillin-functionalised MCM-41 nano did not significantly affect egg laying at any of the tested concentrations.

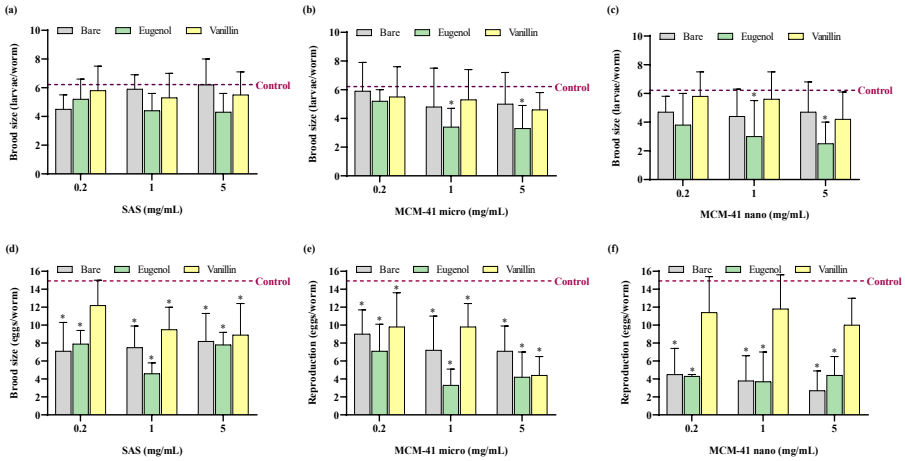

Figure 3. Effects on *C. elegans* brood size as measured by the larvae born per adult worm after 24 h exposure to the bare, eugenol-functionalised and vanillin-functionalised SAS (a), MCM-41 micro (b) and MCM-41 nano (c). Effects on *C. elegans* brood size as measured by the number of eggs laid per adult worm after 24 h exposure to the bare, eugenol-functionalised and vanillin-functionalised SAS (d), MCM-41 micro (e) and MCM-41 nano (f). Bars express the mean (SEM) of at least three independent assays. (*) $p \leq 0.05$ indicates significant differences compared to the control by the Student's t-test.

Figure 4 shows brood growth as determined by body larvae length and the surface area of the eggs laid by pre-exposed adults. We can see that none of the bare or functionalised materials affected progeny size at any of the tested concentrations compared to the control group.

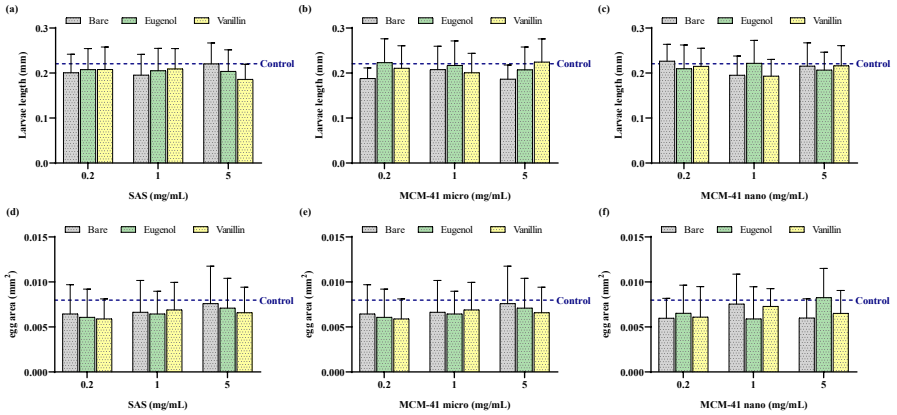

Figure 4. Effects on *C. elegans* brood growth as measured by the larvae body length from adults after 24 h exposure to the bare, eugenol-functionalised and vanillin-functionalised SAS (a), MCM-41 micro (b) and MCM-41 nano (c). Effects on *C. elegans* brood growth as measured by the eggs laid area per adult worms after 24 h exposure to the bare, eugenol-functionalised and vanillin-functionalised SAS (d), MCM-41 micro (e) and MCM-41 nano (f). Bars express the mean (SEM) of at least three independent assays.

Locomotion behaviour. The results showed that *C. elegans* did not reduce movement after treatment with any of the different bare and EOCs-functionalised silica particles. Instead exposure to the bare SAS (0.2 mg/mL), bare MCM-41 micro (5 mg/mL), bare MCM-41 nano (0.2 mg/mL and 1 mg/mL), and also to the vanillin-functionalised SAS (1 mg/mL) and vanillin-functionalised MCM-41 nano (5 mg/mL), resulted in a significant increase in the total area covered by worms (Fig.5).

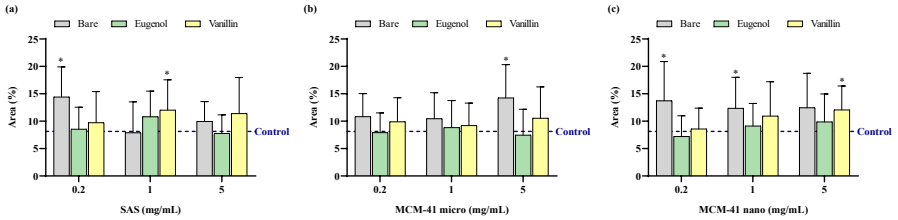

Figure 5. Area (%) of the tracks generated on the surface of agar wells by the nematodes pre-exposed for 24 h to different concentrations of the bare and EOCs-functionalised SAS (a), MCM-41 micro (b) and MCM-41 nano (c). Bars represent the mean (SEM) of at least three different experiments, and each was carried out in triplicate. (*) $p \leq 0.05$ indicates significant differences compared to the control by the Student's t-test.

3.4. Long-term toxicity assessment

Exposure to the different bare and EOCs-functionalised silica particles for 96 h had a significant deleterious effect on both brood size and nematode growth. Inhibition of *C. elegans* reproduction was observed after exposure to all the materials at all the tested concentrations (Fig. 6a-6c). A concentration-dependent effect was noted for the bare materials, vanillin functionalised SAS and the different types of studied eugenol-functionalised particles. Exposure to vanillin-functionalised MCM-41 micro and nano resulted in similar reproduction inhibition (RI) percentages. The reduction in brood size ranged from a minimum of 56% for 0.2 mg/mL for the eugenol-functionalised SAS to 100% for 1 mg/mL of the bare MCM-41 micro, bare MCM-41 nano and for all the different materials at a 5 mg/mL concentration for all three concentrations assayed for vanillin functionalsed MCM-41 nano.

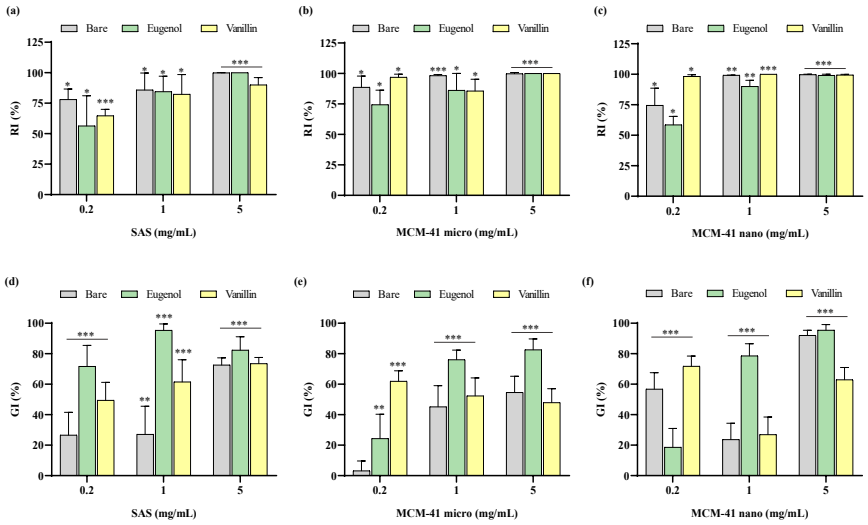

Figure 6. Inhibition of *C. elegans* reproduction (%) after 96 h exposure to different concentrations of the bare and EOCs-functionalised SAS (a), MCM-41 micro (b) and MCM-41 nano (c). Inhibition of *C. elegans* growth (%) after 96 h exposure to different concentrations of the bare and EOCs-functionalised SAS (d), MCM-41 micro (e) and MCM-41 nano (f). Bars represent the mean (SEM) of at least three different experiments, and each one was carried out in triplicate. (*) $p \leq 0.05$; (**) $p \leq 0.01$; (***) $p \leq 0.01$ indicates significant differences compared to the control by the Student's t-test.

Long-term exposure to the bare and EOC-functionalised silica particles markedly inhibited nematode growth (Fig. 6d-6f). Functionalisation with eugenol led to higher GI percentages for the three silica particle types at all the tested concentrations, except for 0.2 mg/mL of MCM-41 nano and micro, where vanillin functionalisation caused GI to a greater extent. The eugenol-functionalised particles caused 72–95% reductions in body length for SAS, 25–83% for MCM-41 micro and 19-95% for MCM-41 nano. These values

ranged from 49% to 74% for the vanillin-functionalised SAS, from 48% to 62% for vanillin-functionalised MCM-41 micro and from 27% to 72% for vanillin-functionalised MCM-41 nano. Finally, the bare silica particles inhibited growth of 27-73%, 3-55% and 24-92% for SAS, MCM-41 micro and MCM-41 nano, respectively.

3.5. Correlation between physico-chemical parameters and toxicity data/multivariate analysis

The Pearson analysis aimed to determine the correlation between the physico-chemical characteristics and the toxicity data. As shown in the Pearson correlation matrix (Table S1), a significant positive correlation was observed between concentration and both long-term exposure assays: RI (r=0.4655; p=0.0000) and GI (r=0.4642; p=0.0000). A significant negative correlation was observed between concentration and the number of eggs laid by worms after acute exposure (r=-0.2131; p=0.0268), and also between the functionalisation yield and number of larvae (r=-0.2941; p=0.0020) or number of eggs (r=-0.2078; p=0.0309) counted during acute tests. Moreover, the functionalisation yield positively correlated with growth inhibition (r=0.3347; p=0.0004). Finally, a positive correlation appeared in the acute endpoints, number of larvae and number of eggs (r=0.4816; p=0.0000), and also between long-term endpoints RI and GI (r=0.2539; p=0.0080).

Simultaneously, the PCA analysis was carried out to reduce dimensionality and to visualise samples distribution and the relation with the original variables. The results revealed that 83.2% of variability was explained by four principal components (Fig. 7). The first principal component (PC1) described 30.5% of total variance, while the second principal component (PC2) described 21.7% (Fig.7). Together both components explained the largest fraction of the total variance observed for the original variables (52.2%). The

most important variables for PC1 were physico-chemical parameters: size distribution and functionalisation yield, and toxicity data: number of larvae, number of eggs and growth inhibition. PC2 was mainly explained by two physico-chemical properties (zeta potential and yield) and three toxicity endpoints (number of larvae and eggs and RI). As shown in Figure 7, the functionalised-particles were distributed in the upper half of the plot, while the bare materials were clustered in the lower part based on physico-chemical parameters like zeta potential, yield and size distribution. Moreover, the eugenol-functionalised samples were clustered together on the left of the plot according to functionalisation yield, with low scores for number of larvae and eggs. The vanillin-functionalised and bare particles were clearly separated and located on the right with high progeny production scores.

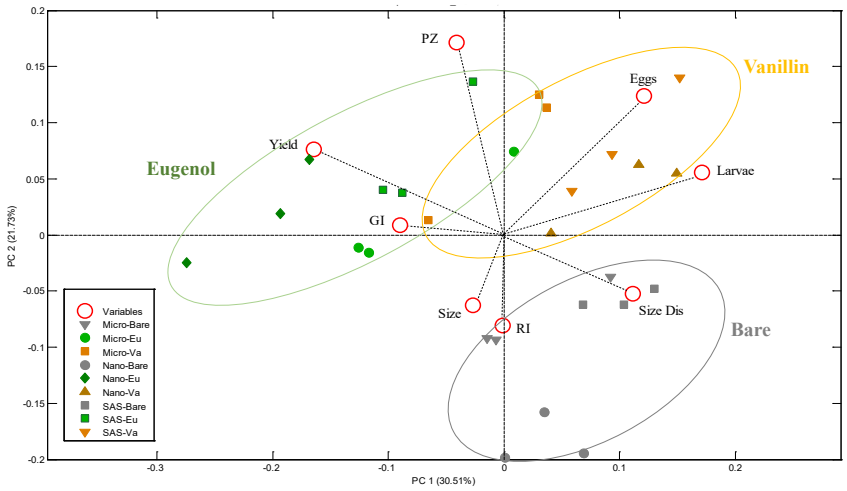

Figure 7. PCA biplot of the physico-chemical parameters of the silica particles and the toxicity data in *C. elegans*. The drawn ellipses highlight the natural samples clustering, but do not represent statistical significance.

4. Discussion

Amorphous silica particles have been proposed for a vast number of food, medical and environmental applications. The abundant presence of silanol groups on their surface makes these particles especially favourable for chemical functionalisation, which gives rise to many new materials (Diab et al., 2017). However, their growing production and application increase the risk of exposure for the public and the environment. In this study, the potential toxicity of three types of pristine or EOCs-functionalised amorphous silica particles was evaluated using the *in vivo* model *C. elegans*. This organism has been used to assess different types of particles' toxicity deriving from oral exposure (Ahn et al., 2014; Angelstorf et al., 2014; Dong et al., 2018; Kim et al., 2020) given the conserved structures and properties from the metabolically active digestive system between nematodes and mammals (Hunt, 2017; Kumar and Suchiang, 2020). Nematode ingestion of particles depends on different *C. elegans* biology factors, such as feeding strategy or buccal cavity size, and also on particle properties like concentration, shape or size (Fueser et al., 2020a, 2019). The light microscopy analysis revealed that all the bare and functionalised particles analysed in this study were ingested by worms during feeding. The different materials were observed in the pharynx and the intestine of nematodes after 24 h of exposure in liquid media, independently of their particle size, agglomeration state or surface functionalisation. In our study, the mean particle size ranged from 70 nm to 2.5 µm, while the average size distribution in aqueous solution ranged from approximately 0.6 µm for the different MCM-41 micro and eugenol-functionalised-MCM-41 nano types to 4.3 µm for the bare MCM-41 nano. According to Fueser et al. (2019), the buccal cavity of nematodes (4.4 ± 0.5 µm) must be at least 1.3-fold larger than the particles to be ingested. Fang-Yen et al. (2009) found that the *C. elegans* pharynx may efficiently transport particles within the size range of most bacterial strains isolated from soil (0.5-3 µm). It has been previously reported

that latex microbeads with a maximum diameter of 3.4 μm can be ingested by *C. elegans* (Boyd et al., 2003) or 5.0 μm polystyrene particles are present at low levels in the nematode intestine (Lei et al., 2018), while 6.0 μm polystyrene beads cannot be detected (Fueser et al., 2020b). Having demonstrated that *C. elegans* is an appropriate model system to assess the oral toxicity to these materials, nematodes were exposed to the different silica particles for 24 h and 96 h, and different biological parameters were evaluated, including survival, reproduction, locomotion behaviour or growth.

Acute exposure to the bare and EOCs-functionalised silica particles did not reduce nematode survival, brood growth or locomotion at any of the tested concentrations, but reproduction was impaired as observed by brood size reduction. Smaller brood size may be indicative of delayed egg lying as a consequence of gonad maturation deficiencies or reduced fertility as a result of a diminished germline in adult hermaphrodites (Williams et al., 2017). However, reproduction inhibition can also be a consequence of effects on other biological processes. Zhang et al. (2020) found fecundity as a more sensitive endpoint than survival, development or behavioural activity when studying exposure to 30 nm amorphous nanosilica for 24 h. According to these authors, the significant reduction in the total number of eggs was a result of a significant increase in apoptotic cell number. Pluskota et al. (2009) observed reduced progeny at increasing concentrations of 50 nm silica nanoparticles, while worms' life span remained unchanged. This effect came with a significant increase in the bag of worms' phenotype, an egg laying deficiency characterised by eggs hatching inside the parent's body, which normally occurs in old nematodes. According to these authors, the effect of silica nanoparticles on progeny production was not due to impaired vulva development, but to induced reproductive senescence in nematodes caused by degenerative changes in the reproductive system. Scharf et al. (2013) also found that the reduced egg lying phenotype observed after 24 h of exposure

to silica nanoparticles was due to prematurely induced ageing-related phenotypes caused by intracellular nanosilica accumulation in vulval cells. Notwithstanding, Scharf et al. (2016) demonstrated that silica nanoparticles did not modify the morphology or function of vulval muscles, but caused protein aggregation in axons of serotonergic HSN motor neurons to lead to neurotoxicity and ageing pathways. However, all these effects were specific of silica nanoparticles and were not observed when nematodes were exposed to bulk material (500 nm). Given their primary size and their agglomeration state in aqueous suspension, the particles herein studied were not likely to translocate to vulval cells, but to remain in the intestine and cover the vulva's surface of hermaphrodites. So for the herein analysed SAS, MCM-41 micro and MCM-41 nano particles, a more similar scenario to that reported for polystyrene beads exposure would be expected, which would indirectly inhibit reproduction as a result of the heavy body burdens and dietary restrictions caused by these materials (Fueser et al., 2021).

The chronic effects of the different materials' exposure were evaluated according to Standard ISO 10872:2010 (ISO, 2010). The ISO standard specifies a method for determining the toxicity of environmental samples on *C. elegans* growth, fertility and reproduction. Traditionally, this method has been applied to the toxicological evaluation of contaminated water, sediments, soils and waste, but has been more recently and satisfactorily employed for the toxicological assessment of different particle types (Bosch et al., 2018; Hanna et al., 2016). Nematode reproduction and growth were used as endpoints after a 96-hour exposure period to cover the whole nematode development from the four larval stages (L1 to L4) to the hermaphrodite adult stage. Our results showed that all nine particle types significantly reduced both growth and brood size. In general terms for the acute toxicity tests, the eugenol-functionalised particles exhibited the higher inhibition rates. No differences were observed in the reproduction inhibition parameter for the

different particle types, and reproductive fitness was a more sensitive parameter after long-term exposure. Furthermore, the correlation between RI and GI could support the notion that hermaphrodite worms did not reach the required body size to be fertile due to particles' exposure and, consequently, reproduction was indirectly inhibited (Schertzinger et al., 2017).

Different physico-chemical properties, such as particle size, shape, surface area and surface chemistry, have been reported to influence their interaction with biological systems and affect the toxic potential of materials *in vitro* and *in vivo* (Heikkilä et al., 2010; Santos et al., 2010; Wu et al., 2019). Therefore, a comprehensive physico-chemical characterisation of the particles under study is crucial during toxicity testing. In this study, the multivariate statistical analysis allowed relations to be established between the physico-chemical parameters of particles and toxicity on *C. elegans*. The results demonstrated that functionalisation, zeta potential and concentration were the most important factors to determine their toxicological effects.

The EOC content in the functionalised particles correlated to reproductive toxicity in the acute assays and to inhibited growth in the long-term exposure experiments. The different eugenol-functionalised silica particles presented high functionalisation yields, high growth inhibition and reduced progeny production after acute exposure, and were more toxic than the vanillin-functionalised or bare silica ones. Of the different silica types used, eugenol-functionalised MCM-41 nano exhibited the highest content of immobilised compound on surfaces and severer toxicological responses. The vanillin-functionalised particles exhibited milder acute toxicity effects, which were similar to or lower than those of the bare particles in some cases. However, greater growth inhibition and lower larvae and eggs production were observed for vanillin-functionalised MCM-41 micro, which also presented a larger amount of immobilised vanillin. Similarly, eugenol had been reported to induce more toxicological effects than vanillin *in vitro* and *in vivo* (Fuentes et

al., 2021a). All this information points out that the type and quantity of the EOC anchored to silica surfaces are the most relevant physico-chemical properties to determine their toxic behaviour. These results agree with Verdú et al. (2020), who evaluated the toxicological properties of MCM-41 microparticles that were bare or functionalised with gallic acid. These authors found that the functionalised particles exposure resulted in increased lethality, velocity of movements and a repellent chemotactic effect. These authors attributed the observed toxicological effects to the high local concentrations of immobilised gallic acid on nematode surfaces, which could have toxic effects.

Surface functionality of particles has been demonstrated to determine toxicity by controlling the dispersion state of materials and interactions with *C. elegans* (Jung et al., 2015). Herein the zeta potential values were more positive for the analysed EOCs-functionalised than the bare silica particles. A larger number of electrostatic interactions between positively charged particles and the negative charge *of C. elegans'* cuticle surface and, consequently a toxic effect, have been suggested (Wang et al., 2009). Notwithstanding, Que et al. (2020) conducted a comparative toxicological study between bare and amine-functionalised silica nanoparticles on *C. Elegans.* They found that exposure to both particle types lowered the survival rate and shortened the life span of nematodes, and reduced progeny production, head thrashing and body bending movements, and significantly shortened body size. However, bare particles were more toxic than amine-functionalised materials as lower doses had a stronger effect on almost all the parameters. The higher toxicity found for the bare silica was attributed by these authors to a disturbance in protein homeostasis caused by a higher interaction between the negatively charged OH groups of its surface and biomolecules, particularly proteins and lipids, compared to the positively charged surface of the amine groups functionalised silica. Similarly, Acosta et

al. (2018) reported that starch-functionalisation significantly reduced the toxicity of silica nanoparticles, even if the zeta potential changed from negative to positive upon functionalisation. By taking into account all this information, the nature of the molecules immobilised on particles' surface seems to play a decisive role in toxicity, independently of the electrostatic particle-nematode interactions.

An agreement has been reached about considering smaller particles being more toxic than larger particles because of a larger surface area and the better facility to accumulate (Angelstorf et al., 2014; Ma et al., 2019; Wang et al., 2009; Yang et al., 2018). However, some authors have reported that *C. elegans* is more sensitive to particles with a moderate size (Kim et al., 2020; Lei et al., 2018). Lei et al. (2018) found that the lethal effects of microplastic particles exposure on *C. elegans* were independent of chemical composition, but correlated with their size. Of the different analysed particle sizes, the 0.1 μm particles brought about a slight reduction in the survival rate, while the 5.0 μm-sized particles presented moderate lethality. In contrast, the 1 μm particles were the most lethal, caused the most extensive reproductive damage, the lowest level of intestinal calcium and the most accumulation. According to those authors, the toxic effects of microplastics on reproduction and survival are related to the ability to enter and accumulate in nematode intestines, where they induce tissue damage by mechanical injury or insufficient nutrition. In our work, a moderate significant positive correlation was observed between hydrodynamic particle size distribution and the number of larvae laid by worms after acute exposure, while no effect was observed on the other toxicity parameters. However, individual particle size did not affect any analysed toxicity endpoint. Our results support the notion that agglomeration state is more important than primary particle size on the toxicity of the studied materials.

Increasing particle concentrations significantly reduced the number of eggs laid by worms upon acute exposure, and more severely resulted in RI and GI after 96 h of exposure. Indeed, during the long-term exposure assay, concentration was the most relevant factor to determine toxicity in nematodes. The likelihood of ingestion of particles at higher concentrations increase as is, therefore, the ability of particles to enter and accumulate in nematodes intestines. As a result, particle accumulation may lead to toxic effects on reproduction and growth. Accordingly, Lei et al (2018) found a direct relation between intestinal microplastics accumulation and functional damage, as revealed by low calcium levels in exposed *C. elegans*. However, other authors suggest that the particles co-ingested with bacterial cells may reduce food consumption in a particle concentration-dependent manner and result in altered nematode energy-requiring processes, including reproduction (Fueser et al., 2021). Thus, the distribution and accumulation of particles should be quantified at the different concentrations used in this study to corroborate the accumulation or food deprivation hypothesis.

5. Conclusions

In short, *C. elegans* was employed as an *in vivo* model to determine the toxicological effects deriving from the acute and prolonged exposures to different bare and EOC-functionalised silica particles designed as antimicrobial materials. Particle accumulation was observed in the intestinal tract of the worms exposed to all the different particles under study, which demonstrates the oral ingestion of particles by *C. elegans* during feeding. Reproduction, as measured by brood size, was the most sensitive parameter upon both acute and long-term particle exposures. Acute exposure to the different silica particles neither affected nematode survival or brood growth at any of the tested concentrations nor reduced locomotion behaviour as measured by the tracks area formed by exposed worms. However, reduced brood size was observed after 24 h of exposure to all the different materials,

except for vanillin-functionalised MCM-41 nano, and the bare and eugenol-functionalised MCM-41 nano displayed the strongest effects. During the long-term exposure assay, minor differences between the different materials were found in the RI parameter, which almost reached complete reduction in most cases, but eugenol-functionalised resulted in higher GI percentages at higher concentrations. Overall, the eugenol-functionalised particles had the strongest effect on *C. elegans* at both exposure times. The vanillin-functionalised particles had the mildest effect on brood size after 24 h of exposure, while minor differences were observed between the bare and vanillin-functionalised materials upon 96 h of exposure. The analysis of the relation between the physico-hemical parameters of particles and toxicity on *C. elegans* indicated that functionalisation yield, zeta potential and concentration were the most important properties to affect the toxicological effects deriving from particles' exposure. Our findings suggest that the type and quantity of EOC anchored to silica surfaces are crucial for determining the toxicological effects of particles on *C. elegans,* while other properties like particle type or size did not seem to play any role. However, these materials' mechanism of action on nematodes still needs to be evaluated. The results obtained with this alternative *in vivo* model can help to anticipate potential toxic responses to new materials for human health and the environment.

Acknowledgments

The authors are grateful to the Spanish Government (Project RTI2018-101599-B-C21 (MCUI/AEI/FEDER, EU)) and the Generalitat Valenciana (grant agreement no. ACIF/2016/139) for financial support. The authors appreciate the supporting help in providing nematodes from the Caenorhabditis elegans Center (CGC), which is funded by the NIH Office of

Research Infrastructure Programs (P40 OD010440). Funding for open access charge: Universitat Politècnica de València.

References

Acosta, C., Barat, J.M., Martínez-Máñez, R., Sancenón, F., Llopis, S., González, N., Genovés, S., Ramón, D., Martorell, P., 2018. Toxicological assessment of mesoporous silica particles in the nematode Caenorhabditis elegans. Environ. Res. 166, 61–70. https://doi.org/10.1016/J.ENVRES.2018.05.018

Ahn, J.M., Eom, H.J., Yang, X., Meyer, J.N., Choi, J., 2014. Comparative toxicity of silver nanoparticles on oxidative stress and DNA damage in the nematode, Caenorhabditis elegans. Chemosphere 108, 343–352. https://doi.org/10.1016/j.chemosphere.2014.01.078

Alothman, Z., 2012. A Review: Fundamental Aspects of Silicate Mesoporous Materials. Materials (Basel). 5, 2874–2902. https://doi.org/10.3390/ma5122874

Angelstorf, J.S., Ahlf, W., von der Kammer, F., Heise, S., 2014. Impact of particle size and light exposure on the effects of TiO_2 nanoparticles on *Caenorhabditis elegans*. Environ. Toxicol. Chem. 33, 2288–2296. https://doi.org/10.1002/etc.2674

Bagheri, E., Ansari, L., Abnous, K., Taghdisi, S.M., Charbgoo, F., Ramezani, M., Alibolandi, M., 2018. Silica based hybrid materials for drug delivery and bioimaging. J. Control. Release. https://doi.org/10.1016/j.jconrel.2018.03.014

Bosch, S., Botha, T.L., Jordaan, A., Maboeta, M., Wepener, V., 2018. Sublethal effects of ionic and nanogold on the nematode caenorhabditis elegans. J. Toxicol. 2018. https://doi.org/10.1155/2018/6218193

Boyd, W.A., Cole, R.D., Anderson, G.L., Williams, P.L., 2003. The effects of metals and food availability on the behavior of Caenorhabditis elegans. Environ. Toxicol. Chem. 22, 3049–3055. https://doi.org/10.1897/02-565

Brown, S.C., Kamal, M., Nasreen, N., Baumuratov, A., Sharma, P., Antony, V.B.,

Moudgil, B.M., 2007. Influence of shape, adhension and simulated lung mechanics on amorphous silica nanoparticle toxicity. Adv. Powder Technol. 18, 69–79. https://doi.org/10.1163/156855207779768214

Buckingham, S.D., Sattelle, D.B., 2008. Strategies for automated analysis of C. elegans locomotion. Invertebr. Neurosci. 8, 121–131. https://doi.org/10.1007/s10158-008-0077-3

Diab, R., Canilho, N., Pavel, I.A., Haffner, F.B., Girardon, M., Pasc, A., 2017. Silica-based systems for oral delivery of drugs, macromolecules and cells. Adv. Colloid Interface Sci. 249, 346–362. https://doi.org/10.1016/j.cis.2017.04.005

Dong, S., Qu, M., Rui, Q., Wang, D., 2018. Combinational effect of titanium dioxide nanoparticles and nanopolystyrene particles at environmentally relevant concentrations on nematode Caenorhabditis elegans. Ecotoxicol. Environ. Saf. 161, 444–450. https://doi.org/10.1016/j.ecoenv.2018.06.021

Eisenbrand, G., Pool-Zobel, B., Baker, V., Balls, M., Blaauboer, B.J., Boobis, A., Carere, A., Kevekordes, S., Lhuguenot, J.C., Pieters, R., Kleiner, J., 2002. Methods of in vitro toxicology. Food Chem. Toxicol. https://doi.org/10.1016/S0278-6915(01)00118-1

Fang-Yen, C., Avery, L., Samuel, A.D.T., 2009. Two size-selective mechanisms specifically trap bacteria-sized food particles in Caenorhabditis elegans. Proc. Natl. Acad. Sci. 106, 20093–20096. https://doi.org/10.1073/PNAS.0904036106

Fuentes, C., Fuentes, A., Barat, J.M., Ruiz, M.J., 2021a. Relevant essential oil components: a minireview on increasing applications and potential toxicity. Toxicol. Mech. Methods 31, 1–7. https://doi.org/10.1080/15376516.2021.1940408

Fuentes, C., Ruiz-Rico, M., Fuentes, A., Barat, J.M., Ruiz, M.J., 2021b. Comparative cytotoxic study of silica materials functionalised with essential oil components in HepG2 cells. Food Chem. Toxicol. 147, 111858. https://doi.org/10.1016/j.fct.2020.111858

Fuentes, C., Ruiz-Rico, M., Fuentes, A., Ruiz, M.J., Barat, J.M., 2020. Degradation

of silica particles functionalised with essential oil components under simulated physiological conditions. J. Hazard. Mater. 399, 123120. https://doi.org/10.1016/j.jhazmat.2020.123120

Fuentes, C., Verdú, S., Fuentes, A., Ruiz, M. J., & Barat, J. M. (2022). Effects of essential oil components exposure on biological parameters of Caenorhabditis elegans. Food and Chemical Toxicology, 159, 112763. doi.org/10.1016/j.fct.2021.112763

Fueser, H., Mueller, M.T., Traunspurger, W., 2020a. Rapid ingestion and egestion of spherical microplastics by bacteria-feeding nematodes. Chemosphere 261, 128162. https://doi.org/10.1016/J.CHEMOSPHERE.2020.128162

Fueser, H., Mueller, M.T., Traunspurger, W., 2020b. Ingestion of microplastics by meiobenthic communities in small-scale microcosm experiments. Sci. Total Environ. 746, 141276. https://doi.org/10.1016/J.SCITOTENV.2020.141276

Fueser, H., Mueller, M.T., Weiss, L., Höss, S., Traunspurger, W., 2019. Ingestion of microplastics by nematodes depends on feeding strategy and buccal cavity size. Environ. Pollut. 255, 113227. https://doi.org/10.1016/J.ENVPOL.2019.113227

Fueser, H., Rauchschwalbe, M.T., Höss, S., Traunspurger, W., 2021. Food bacteria and synthetic microparticles of similar size influence pharyngeal pumping of Caenorhabditis elegans. Aquat. Toxicol. 235, 105827. https://doi.org/10.1016/J.AQUATOX.2021.105827

Gamboa, J.M., Leong, K.W., 2013. In vitro and in vivo models for the study of oral delivery of nanoparticles. Adv. Drug Deliv. Rev. https://doi.org/10.1016/j.addr.2013.01.003

Gonzalez-Moragas, L., Maurer, L.L., Harms, V.M., Meyer, J.N., Laromaine, A., Roig, A., 2017. Materials and toxicological approaches to study metal and metal-oxide nanoparticles in the model organism: Caenorhabditis elegans. Mater. Horizons. https://doi.org/10.1039/c7mh00166e

Hanna, S.K., Cooksey, G.A., Dong, S., Nelson, B.C., Mao, L., Elliott, J.T.,

Petersen, E.J., 2016. Feasibility of using a standardized: Caenorhabditis elegans toxicity test to assess nanomaterial toxicity. Environ. Sci. Nano 3, 1080–1089. https://doi.org/10.1039/c6en00105j

Hao, N., Li, Linlin, Zhang, Q., Huang, X., Meng, X., Zhang, Y., Chen, D., Tang, F., Li, Laifeng, 2012. The shape effect of PEGylated mesoporous silica nanoparticles on cellular uptake pathway in Hela cells. Microporous Mesoporous Mater. 162, 14–23. https://doi.org/10.1016/j.micromeso.2012.05.040

He, Q., Zhang, Z., Gao, F., Li, Y., Shi, J., 2011. In vivo Biodistribution and Urinary Excretion of Mesoporous Silica Nanoparticles: Effects of Particle Size and PEGylation. Small 7, 271–280. https://doi.org/10.1002/smll.201001459

Heikkilä, T., Santos, H.A., Kumar, N., Murzin, D.Y., Salonen, J., Laaksonen, T., Peltonen, L., Hirvonen, J., Lehto, V.-P., 2010. Cytotoxicity study of ordered mesoporous silica MCM-41 and SBA-15 microparticles on Caco-2 cells. Eur. J. Pharm. Biopharm. 74, 483–494. https://doi.org/10.1016/J.EJPB.2009.12.006

Hildebrand, H.F., Blanchemain, N., Mayer, G., Chai, F., Lefebvre, M., Boschin, F., 2006. Surface coatings for biological activation and functionalization of medical devices. Surf. Coatings Technol. 200, 6318–6324. https://doi.org/10.1016/j.surfcoat.2005.11.086

Hunt, P.R., 2017. The C. elegans model in toxicity testing. J. Appl. Toxicol. https://doi.org/10.1002/jat.3357

ISO, 2010. ISO 10872: 2010. Water quality—Determination of the toxic effect of sediment and soil samples on growth, fertility and reproduction of Caenorhabditis elegans (Nematoda). Int. Organ. Stand. Geneva, Switzerland. 23.

Jung, S.K., Qu, X., Aleman-Meza, B., Wang, T., Riepe, C., Liu, Z., Li, Q., Zhong, W., 2015. Multi-endpoint, high-throughput study of nanomaterial toxicity in Caenorhabditis elegans. Environ. Sci. Technol. 49, 2477–2485. https://doi.org/10.1021/es5056462

Kaletta, T., Hengartner, M.O., 2006. Finding function in novel targets: C. elegans as a model organism. Nat. Rev. Drug Discov. https://doi.org/10.1038/nrd2031

Kim, S.W., Kim, D., Jeong, S.W., An, Y.J., 2020. Size-dependent effects of polystyrene plastic particles on the nematode Caenorhabditis elegans as related to soil physicochemical properties. Environ. Pollut. 258, 113740. https://doi.org/10.1016/J.ENVPOL.2019.113740

Kumar, S., Suchiang, K., 2020. Caenorhabditis elegans: Evaluation of Nanoparticle Toxicity, in: Model Organisms to Study Biological Activities and Toxicity of Nanoparticles. Springer Singapore, pp. 333–369. https://doi.org/10.1007/978-981-15-1702-0_17

Lei, L., Wu, S., Lu, S., Liu, M., Song, Y., Fu, Z., Shi, H., Raley-Susman, K.M., He, D., 2018. Microplastic particles cause intestinal damage and other adverse effects in zebrafish Danio rerio and nematode Caenorhabditis elegans. Sci. Total Environ. 619–620, 1–8. https://doi.org/10.1016/j.scitotenv.2017.11.103

Leung, M.C.K., Williams, P.L., Benedetto, A., Au, C., Helmcke, K.J., Aschner, M., Meyer, J.N., 2008. Caenorhabditis elegans: An Emerging Model in Biomedical and Environmental Toxicology. Toxicol. Sci. 106, 5–28. https://doi.org/10.1093/toxsci/kfn121

Liberman, A., Mendez, N., Trogler, W.C., Kummel, A.C., 2014. Synthesis and surface functionalization of silica nanoparticles for nanomedicine. Surf. Sci. Rep. https://doi.org/10.1016/j.surfrep.2014.07.001

Lu, L., Zhu, Z., Hu, X., 2019. Hybrid nanocomposites modified on sensors and biosensors for the analysis of food functionality and safety. Trends Food Sci. Technol. https://doi.org/10.1016/j.tifs.2019.06.009

Ma, H., Lenz, K.A., Gao, X., Li, S., Wallis, L.K., 2019. Comparative toxicity of a food additive TiO 2 , a bulk TiO 2 , and a nano-sized P25 to a model organism the nematode C. elegans. Environ. Sci. Pollut. Res. 26, 3556–3568. https://doi.org/10.1007/s11356-018-3810-4

Maleki, A., Kettiger, H., Schoubben, A., Rosenholm, J.M., Ambrogi, V., Hamidi,

M., 2017. Mesoporous silica materials: From physico-chemical properties to enhanced dissolution of poorly water-soluble drugs. J. Control. Release. https://doi.org/10.1016/j.jconrel.2017.07.047

Pluskota, A., Horzowski, E., Bossinger, O., von Mikecz, A., 2009. In Caenorhabditis elegans Nanoparticle-Bio-Interactions Become Transparent: Silica-Nanoparticles Induce Reproductive Senescence. PLoS One 4, e6622. https://doi.org/10.1371/journal.pone.0006622

Que, D.E., Hou, W.-C., Yap Ang, M.B.M., Lin, C.-C., 2020. Toxic Effects of Hydroxyl- and Amine-functionalized Silica Nanoparticles (SiO2 and NH2-SiO2 NPs) on Caenorhabditis elegans. Aerosol Air Qual. Res. 20. https://doi.org/10.4209/aaqr.2020.04.0157

Ribes, S., Ruiz-Rico, M., Pérez-Esteve, É., Fuentes, A., Barat, J.M., 2019. Enhancing the antimicrobial activity of eugenol, carvacrol and vanillin immobilised on silica supports against Escherichia coli or Zygosaccharomyces rouxii in fruit juices by their binary combinations. LWT 113, 108326. https://doi.org/10.1016/j.lwt.2019.108326

Ribes, S., Ruiz-Rico, M., Pérez-Esteve, É., Fuentes, A., Talens, P., Martínez-Máñez, R., Barat, J.M., 2017. Eugenol and thymol immobilised on mesoporous silica-based material as an innovative antifungal system: Application in strawberry jam. Food Control 81, 181–188. https://doi.org/10.1016/J.FOODCONT.2017.06.006

Riediker, M., Zink, D., Kreyling, W., Oberdörster, G., Elder, A., Graham, U., Lynch, I., Duschl, A., Ichihara, G., Ichihara, S., Kobayashi, T., Hisanaga, N., Umezawa, M., Cheng, T.J., Handy, R., Gulumian, M., Tinkle, S., Cassee, F., 2019. Particle toxicology and health - Where are we? Part. Fibre Toxicol. https://doi.org/10.1186/s12989-019-0302-8

Ruiz-Rico, M., Pérez-Esteve, É., de la Torre, C., Jiménez-Belenguer, A.I., Quiles, A., Marcos, M.D., Martínez-Máñez, R., Barat, J.M., 2018. Improving the Antimicrobial Power of Low-Effective Antimicrobial Molecules Through Nanotechnology. J. Food Sci. 83, 2140–2147. https://doi.org/10.1111/1750-

3841.14211

Santos, H.A., Riikonen, J., Salonen, J., Mäkilä, E., Heikkilä, T., Laaksonen, T., Peltonen, L., Lehto, V.-P., Hirvonen, J., 2010. In vitro cytotoxicity of porous silicon microparticles: Effect of the particle concentration, surface chemistry and size. Acta Biomater. 6, 2721–2731. https://doi.org/10.1016/J.ACTBIO.2009.12.043

Scharf, A., Gührs, K.H., Von Mikecz, A., 2016. Anti-amyloid compounds protect from silica nanoparticle-induced neurotoxicity in the nematode C. elegans. Nanotoxicology 10, 426–435. https://doi.org/10.3109/17435390.2015.1073399

Scharf, A., Piechulek, A., Von Mikecz, A., 2013. Effect of nanoparticles on the biochemical and behavioral aging phenotype of the nematode caenorhabditis elegans. ACS Nano 7, 10695–10703. https://doi.org/10.1021/nn403443r

Schertzinger, G., Zimmermann, S., Grabner, D., Sures, B., 2017. Assessment of sublethal endpoints after chronic exposure of the nematode Caenorhabditis elegans to palladium, platinum and rhodium. Environ. Pollut. 230, 31–39. https://doi.org/10.1016/j.envpol.2017.06.040

Schindelin, J., Arganda-Carreras, I., Frise, E., Kaynig, V., Longair, M., Pietzsch, T., Preibisch, S., Rueden, C., Saalfeld, S., Schmid, B., Tinevez, J.Y., White, D.J., Hartenstein, V., Eliceiri, K., Tomancak, P., Cardona, A., 2012. Fiji: An open-source platform for biological-image analysis. Nat. Methods 9, 676–682. https://doi.org/10.1038/nmeth.2019

Stiernagle, T., 2006. Maintenance of C. elegans. WormBook. https://doi.org/10.1895/wormbook.1.101.1

Verdú, S., Ruiz-Rico, M., Perez, A.J., Barat, J.M., Talens, P., Grau, R., 2020. Toxicological implications of amplifying the antibacterial activity of gallic acid by immobilisation on silica particles: A study on C. elegans. Environ. Toxicol. Pharmacol. 80, 103492. https://doi.org/10.1016/j.etap.2020.103492

Wang, H., Wick, R.L., Xing, B., 2009. Toxicity of nanoparticulate and bulk ZnO, Al2O3 and TiO2 to the nematode Caenorhabditis elegans. Environ. Pollut. 157,

1171–1177. https://doi.org/10.1016/j.envpol.2008.11.004

Williams, D.C., Bailey, D.C., Fitsanakis, V.A., 2017. Caenorhabditis elegans as a Model to Assess Reproductive and Developmental Toxicity. Reprod. Dev. Toxicol. 303–314. https://doi.org/10.1016/B978-0-12-804239-7.00017-2

Wu, T., Xu, H., Liang, X., Tang, M., 2019. Caenorhabditis elegans as a complete model organism for biosafety assessments of nanoparticles. Chemosphere 221, 708–726. https://doi.org/10.1016/j.chemosphere.2019.01.021

Yang, Y., Xu, G., Xu, S., Chen, S., Xu, A., Wu, L., 2018. Effect of ionic strength on bioaccumulation and toxicity of silver nanoparticles in Caenorhabditis elegans. Ecotoxicol. Environ. Saf. 165, 291–298. https://doi.org/10.1016/J.ECOENV.2018.09.008

Zhang, F., You, X., Zhu, T., Gao, S., Wang, Y., Wang, R., Yu, H., Qian, B., 2020. Silica nanoparticles enhance germ cell apoptosis by inducing reactive oxygen species (ROS) formation in Caenorhabditis elegans. J. Toxicol. Sci. 45, 117–129. https://doi.org/10.2131/jts.45.117

Supplementary material

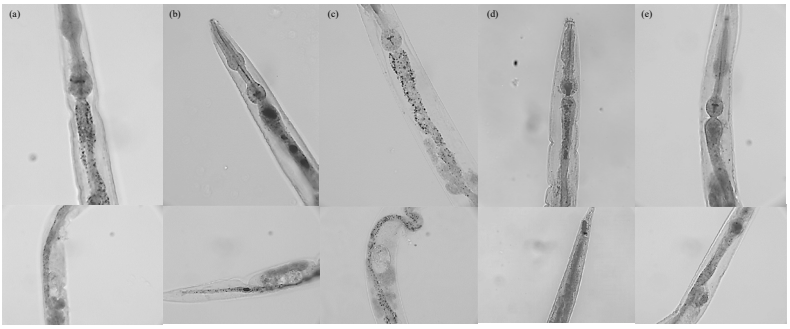

Figure S1. Representative worm micrographs (40X magnification) showing uptake and accumulation of different types of bare and EOC-functionalised silica particles along the gastrointestinal tract: (a) bare SAS; (b) bare MCM-41 micro; (c) bare MCM-41 nano; (d) eugenol MCM-41 micro; (e) vanillin MCM-41 micro.

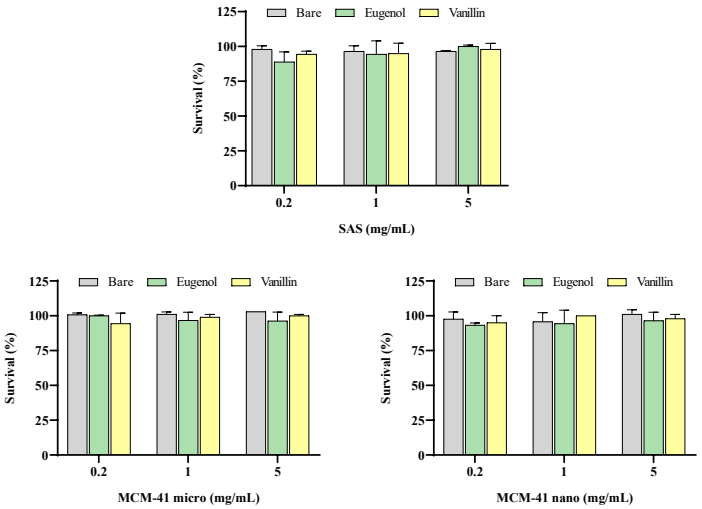

Figure S2. Survival rates of *C. elegans* exposed to 0.2, 1 and 5 mg/mL of bare and functionalised SAS, MCM-41 micro and MCM-41 nano for 24 h in M9 buffer. The different silica particles did not affect nematode survival after acute exposure.

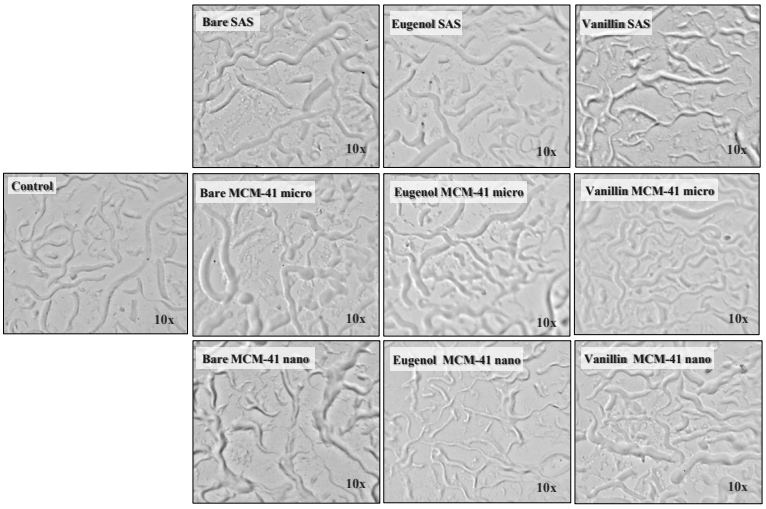

Figure S3. Tracks produced by nematodes crawling freely on a bacterial lawn in agar wells. Representative agar images from the control and the pre-exposed worms to a 1 mg/mL concentration of the different bare and functionalised silica particles for 24 h.

Table S1. Pearson correlation coefficient r values between the physico-chemical parameters of silica particles and the toxicity data in *C. elegans*.

	Con	Size	Size Dis	PZ	Yield	Larvae	Eggs	RI	GI
Conc		0.0000 (108)	-0.0016 (108)	-0.0101 (108)	0.0000 (108)	-0.1466 (108)	-0.2131 (108)	0.4655 (108)	0.4642 (108)
		1.0000	0.9867	0.9177	1.0000	0.1301	0.0268	0.0000	0.0000
Size	0.0000 (108)		0.3161 (108)	-0.0468 (108)	0.1391 (108)	-0.1258 (108)	-0.0484 (108)	0.1094 (108)	0.0471 (108)
	1.0000		0.0009	0.6302	0.1509	0.1944	0.6191	0.2598	0.6282
Size Dis	-0.0016 (108)	0.3161 (108)		-0.1948 (108)	-0.4297 (108)	0.2327 (108)	0.1165 (108)	-0.0254 (108)	0.0745 (108)
	0.9867	0.0009		0.0434	0.0000	0.0154	0.2300	0.7942	0.4437
PZ	-0.0101 (108)	-0.0468 (108)	-0.1948 (108)		0.4956 (108)	0.0422 (108)	0.3420 (108)	-0.1104 (108)	0.2685 (108)
	0.9177	0.6302	0.0434		0.0000	0.6647	0.0003	0.2553	0.0050
Yield	0.0000 (108)	0.1391 (108)	-0.4297 (108)	0.4956 (108)		-0.2941 (108)	-0.2078 (108)	-0.1721 (108)	0.3347 (108)
	1.0000	0.1509	0.0000	0.0000		0.0020	0.0309	0.0749	0.0004
Larvae	-0.1466 (108)	-0.1258 (108)	0.2327 (108)	0.0422 (108)	-0.2941 (108)		0.4816 (108)	0.0970 (108)	-0.1488 (108)
	0.1301	0.1944	0.0154	0.6647	0.0020		0.0000	0.3180	0.1244
Eggs	-0.2131 (108)	-0.0484 (108)	0.1165 (108)	0.3420 (108)	-0.2078 (108)	0.4816 (108)		-0.0015 (108)	-0.1730 (108)
	0.0268	0.6191	0.2300	0.0003	0.0309	0.0000		0.9878	0.0734
RI	0.4655 (108)	0.1094 (108)	-0.0254 (108)	-0.1104 (108)	-0.1721 (108)	0.0970 (108)	-0.0015 (108)		0.2539 (108)
	0.0000	0.2598	0.7942	0.2553	0.0749	0.3180	0.9878		0.0080
GI	0.4642 (108)	0.0471 (108)	0.0745 (108)	0.2685 (108)	0.3347 (108)	-0.1488 (108)	-0.1730 (108)	0.2539 (108)	
	0.0000	0.6282	0.4437	0.0050	0.0004	0.1244	0.0734	0.0080	

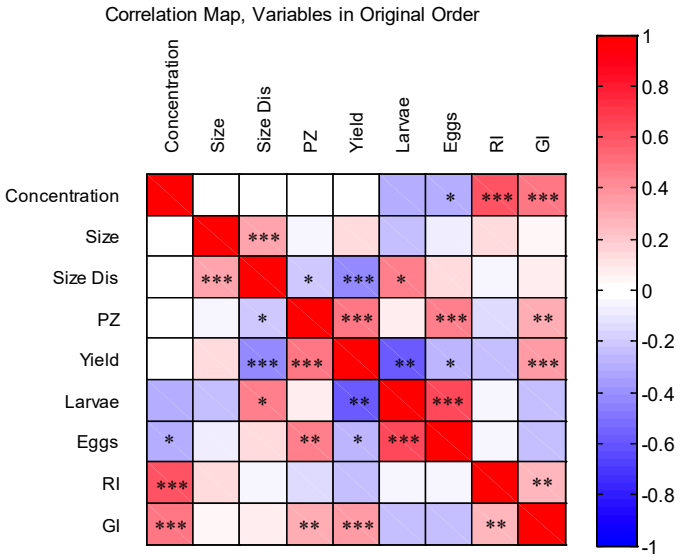

Figure S4. Pearson correlation matrix between the physico-chemical parameters of silica particles and the toxicity data in *C. elegans*. (*) $p \leq 0.05$; (**) $p \leq 0.01$; (***) $p \leq 0.01$ represent statistical significance.

General discussion

Functionalisation of silica particles with EOCs has emerged as a useful tool for enhancing EOCs' antimicrobial activity and stability. For this reason, given these new materials' promising applications for the food industry, toxicological studies must be performed to identify possible hazards for human health and the environment. In the present doctoral thesis, the potential risk deriving from oral exposure to three types of silica particles (SAS, MCM-41 microparticles, MCM-41 nanoparticles) functionalised with four different EOCs (carvacrol, eugenol, thymol, vanillin) was investigated and compared to free EOCs and pristine particles.

Multiple toxicity endpoints are required for the accurate prediction of the toxicological properties of new materials on human health and to elucidate their mechanism of action. Moreover, and according to EU legislation, following alternative methods to animal testing should apply whenever possible, to fulfil the 3Rs principles during the toxicological assessment of new compounds (European Parliament, 2010). In this thesis, three different replacement methods were used as a strategy to carry out the toxicological assessment of these new materials: simulated physiological conditions, HepG2 culture cells and the non-mammalian organism model *Caenorhabditis elegans*.

As the expected human exposure to these materials was the oral route, the first step in the toxicological assessment of particles was to study their degradation behaviour in acellular physiological fluids that mimic oral exposure conditions. After oral ingestion, cell-particles interactions and uptake may occur in the gastrointestinal tract, mainly via Peyer's patches, where the particles that cannot be eliminated can accumulate and are susceptible to be degraded by lysosomes. Accordingly, an *in vitro* digestion process was followed to simulate the conditions in the gastrointestinal tract, and artificial lysosomal fluid was used to simulate the inorganic acidic environment in the lysosomes of phagocytic cells. After exposure to both

conditions, particles' silicon dissolution rates and physico-chemical properties were characterised, such as morphology, size distribution and zeta potential. The results of this study showed that exposure to biological fluids did not modify the physico-chemical properties of any of the studied particles, but the bare MCM-41 nanoparticles' structure partially degraded during the *in vitro* digestion process. In addition, the dissolved silicon levels after being exposed to both physiological conditions differed among silica particle types, and the agglomeration state and surface area were the two main factors that determined degradation behaviour. More importantly, the results revealed that the functionalisation of silica particles with EOCs increased materials' stability under the two biological conditions, as observed by both the lower dissolution rates in the different functionalised-particle types and the preservation of the EOCs-functionalised MCM-41 nanoparticles structure compared to their bare counterparts. This effect was independent of the EOC anchored to the silica surface and the silica particle type, and was attributed to the organic compounds forming a coverage that acted as a protective barrier against enzymatic or chemical degradation.

As a result of these findings, it can be stated that functionalisation with EOCs enhances the biodurability of silica particles when exposed to physiological conditions and, thus, increases the likelihood of these materials accumulating inside the organism. At the same time however, the agglomeration state of particles did not change under the physiological conditions, which remained within the micro-sized range in all cases. Therefore, given their large size, these materials present a low risk of accumulation after oral ingestion.

Using cell cultures is a relevant tool in toxicity testing to predict the effects of hazardous compounds on human health and to elucidate their toxicological mechanisms at cellular and subcellular levels (Eisenbrand et al., 2002). Thus, as the second step, the *in vitro* toxicity assessment of materials was carried out

with a twofold objective: to predict the acute toxicological effects of the EOCs-functionalised silica particles for human health and to elucidate these new materials' toxic mechanism of action. HepG2 cells were selected for the *in vitro* toxicology studies as this cell type is a standard model for xenobiotic metabolism and toxicity studies, and displays a high degree of reproducibility.

For the *in vitro* toxicity study of the EOCs-functionalised silica particles, the cytotoxic behaviour of these new materials was first compared to that of free EOCs and pristine silica particles. In general terms, the results showed that EOCs-functionalised particles displayed a stronger cytotoxic effect than the free EOCs and pristine silica.

The four EOCs employed in this thesis (carvacrol, eugenol, thymol, vanillin) reduced cell viability in a concentration- and time-dependent manner at moderate to high concentrations as measured by the MTT assay. The most cytotoxic compounds were carvacrol and thymol, with minor differences in the IC_{50} values obtained for both components. Eugenol was approximately 3-fold less toxic than carvacrol and thymol. Vanillin, the least toxic compound against HepG2 cells, was between 6- and 7-fold less toxic than the above two monoterpenoids.

When the equivalent concentrations of the free and immobilised EOCs on silica particles' surface were compared, a milder cytotoxic effect was observed for the free compound forms independently of the analysed EOC. The three forms of pristine silica particles analysed in this thesis had a mild cytotoxic effect because only exposure to high concentrations of particles compromised cell viability. SAS had the most cytotoxic effects on HepG2, followed by MCM-41 microparticles and MCM-41 nanoparticles in that order. Indeed, no IC_{50} value for the bare MCM-41 nanoparticles was obtained within the range of the evaluated concentrations, which formed the largest agglomerates in solution despite having the smallest particle size.

By comparing the bare and the EOCs-functionalised particles, differences were found in cell viability depending on particle type, which mainly resulted from the differences in the functionalisation reaction yield. SAS functionalisation did not increase cytotoxicity in HepG2 cells, but cells were more sensitive to the functionalised than to the bare MCM-41 particles. Independently of the EOC type, the functionalised MCM-41 microparticles were the most toxic materials. Indeed, for the starting material (bare MCM-41 microparticles), cytotoxicity increased by 100-fold on average. Moreover, this cytotoxic effect was caused by the cell-particle interactions, and not by degradation products released to culture media as the extract dilution assays demonstrated. Differences still appeared according to the EOC used during the functionalisation process. Regarding carvacrol and thymol, the carvacrol- and thymol-functionalised particles were the most cytotoxic materials against HepG2 cells. Both materials exhibited a similar IC_{50} after 24 h of exposure, while a stronger cytotoxic effect was noted for the carvacrol- than for the thymol-functionalised particles when the 48-hour treatment was evaluated. As previously mentioned, eugenol was approximately 2-fold less toxic than vanillin, but only minor differences were found in the IC_{50} values of the eugenol- and vanillin MCM-41-functionalised silica after both exposure times. When comparing the yield of the functionalisation process for the different MCM-41 microparticles, the smallest amount of immobilised compound was for carvacrol and thymol, which exhibited a similar degree of functionalisation. Compared to the carvacrol- and thymol-functionalised MCM-41 microparticles, the eugenol and vanillin-functionalised counterparts employed in the cytotoxic assays presented a minimum of approximately 5-fold and 15-fold larger amount of immobilised compound, respectively. Taken together, this information suggests that the cytotoxic effect of the EOCs-functionalised silica particles depends on both the EOC type immobilised on particles' surface and the functionalisation yield achieved during the functionalisation process.

The acute oral toxicity test in rodents is a critical step for defining materials' toxicity and can serve to estimate parameters like LD_{50}, which is the dose level expected to kill 50% of the test population. LD_{50} is a crucial parameter used for hazard classification and labelling purposes. To reduce the number of animals required for an acute oral toxicity test, the Interagency Coordinating Committee on the Validation of Alternative Methods (ICCVAM) proposes a method to estimate LD_{50} values from experimental IC_{50} values. According to the proposed strategy, the estimated LD_{50} values serve to determine the starting dose for rat acute oral toxicity tests (ICCVAM, 2006). Then the calculated IC_{50} values found for the different EOCs-functionalised microparticles in HepG2 cells were used to predict the rat oral LD_{50} values by applying the regression formula for substance with no known molecular weight described by the ICCVAM (ICCVAM, 2006):

$$logLD50(mg/kg) = 0.372 * \log(\mu g/mL) + 2.024$$

Based on this model, the LD_{50} for the carvacrol- and thymol-functionalised MCM-41 microparticles was 682 mg/kg, 812 mg/kg for the eugenol-functionalised MCM-41 microparticles and 799 mg/kg for the vanillin-functionalised MCM-41 microparticles.

The Globally Harmonised System of Classification and Labelling of Chemicals (GHS) is a system developed by the United Nations for standardising and harmonising the classification and labelling of hazardous chemicals internationally (United Nations, 2019). The GHS includes five acute toxicity categories with different criteria depending on the exposure route. Oral acute toxicity category 1 ($LD_{50} \leq 5$ mg/kg bodyweight) represents the severest toxicity, while category 5 ($LD_{50} > 2{,}000$ mg/kg $\leq 5{,}000$ mg/kg) denotes a low acute toxicity hazard. According to the GHS classification, the materials evaluated in this thesis correspond to category 4 ($LD_{50} > 300$ mg/kg $\leq 2{,}000$ mg/kg), which are considered harmful if swallowed. In contrast, the

LD_{50} reported for different SAS forms in rats is > 5,000 mg/kg (Bergfeld et al., 2019), and SAS particles do not show acute toxicity according to the GHS classification criteria.

Basal cytotoxicity data can help to predict acute toxicological effects, but it should be noted here that although the assessment of basal cytotoxic endpoints measures damaged basic cellular functions and does not frequently require specialised cell functions (Stark et al., 1986), different cell types may differ in sensitivity to toxicants due to specific mechanisms of uptake and membrane interactions, signalling responses and vesicle trafficking pathways (Fruijtier-Pölloth, 2012). As a result, other cell lines should be included in future analyses for a more accurate prediction of toxic effects, such as colon adenocarcinoma cell line Caco-2, which is used as a model of the intestinal epithelium.

Different physico-chemical properties have been reported to influence the interaction of particles with biological systems and can affect the toxic potential of materials *in vitro* and *in vivo* (Heikkilä et al., 2010; Santos et al., 2010; Wu et al., 2019). Consequently, a comprehensive physico-chemical analysis of new materials is crucial during toxicity testing. This thesis characterised different materials by standard instrumental techniques to determine their shape, size, particle size distribution, zeta potential and functionalisation yield. No differences were observed between the bare and functionalised particles according to their shape or individual mean diameter size. However, changes in zeta potential and particle size distribution were found before and after the functionalisation process. In particular, the functionalisation of silica particles with the different EOCs lowered the zeta potential values, and for MCM-41 nano, hydrodynamic particle size also reduced. Our results demonstrate that the differences in cell viability between the bare and functionalised particles relied on the type of silica particles and resulted from differences in functionalisation yields. Accordingly, cationic

nature and increased hydrophobicity can be responsible for promoting a larger number of cell-particle interactions for the EOCs-functionalised silica particles, which would enhance their cytotoxic behaviour.

As the carvacrol- and thymol-functionalised MCM-41 microparticles were the most cytotoxic materials, they were used to study these particles' underlying mechanism of toxicity. Our results generally suggest that the EOCs-functionalised silica particles induced toxicity on HepG2 cells by an oxidative stress-related mechanism, which would lead to mitochondrial dysfunction and apoptosis via the mitochondrial pathway. Moreover, this effect was caused by cell-particle interactions, and not by the degradation products released to culture media as demonstrated by the extract dilution assays. Then a direct physical interaction between particles' surface and cell membranes could be responsible for inducing ROS overproduction and initiating the cascade of events that would lead to toxicity. Additionally, the mechanism of toxic action described for the functionalised particles bore similarities to the mechanism described for their constituents. However, the reported cytotoxic effects for both, EOCs and the bare MCM-41 microparticles, occurred at much higher concentrations than those found for the functionalised materials in this thesis. Some of the hypotheses for increased toxicity include: a synergistic effect given the presence of silanol groups and EOCs derivatives on the functionalised particles' surface, the high density of the EOCs susceptible to interact with cell membranes, or the incapacity of cells to metabolise immobilised components.

Employing cell cultures has been demonstrated as a useful tool for predicting the toxicity of the EOCs-functionalised particles and their constituents, and to understand these new materials' mechanism of toxicity. However, *in vitro* experiments do not provide information from the whole organism level. Hence a decision was made to study the toxicity of EOCs, the

bare silica particles and the EOCs-functionalised particles *in vivo* using *C. elegans* as an animal model.

Similar results were observed in the *in vivo* acute toxicity testing of EOCs to those obtained with HepG2 cells. All four free EOCs reduced nematode survival in a concentration-dependent manner from moderate to high concentrations of these components. Carvacrol was the most toxic compound for *C. elegans*, followed by thymol, eugenol, and lastly by vanillin. So although approximately 2 to 3-fold higher LC_{50} than IC_{50} values were detected for EOCs, the toxicity ranking was maintained between nematodes and culture cells. Moreover, when the ICCVAM regression formula to predict rat oral LD_{50} values was applied to the nematode toxicity data, a correlation was observed with the values reported in the bibliography. Exposure to sublethal carvacrol and eugenol concentrations conferred nematodes oxidative stress resistance and reduced brood size, which indicates reproductive toxicity. These results demonstrate that these components may exhibit toxic effects at the concentrations required for their bioactive properties.

As observed in the EOCs toxicity analyses, reproduction was the most sensitive parameter upon particles' acute and long-term exposure. Acute exposure to the different bare and functionalised particles neither affected nematode survival nor reduced brood growth or locomotion at any of the tested concentrations. However, brood size was reduced by all the materials, except for the vanillin-functionalised MCM-41 nanoparticles. Moreover, long-term exposure to the different particles brought about a strong inhibition in nematode growth and reproduction. In general terms, the strongest acute and long-term effects were observed for the eugenol-functionalised particles, while the vanillin-functionalised materials presented the mildest acute toxicological effects. Moreover, the relation between the physico-chemical properties of particles and the *in vivo* toxicity endpoints was studied by a multivariate statistical analysis. The results indicated that functionalisation,

zeta potential and concentration were the physico-chemical properties of particles that most affected the toxicity parameter responses evaluated in worms.

In the present doctoral thesis, the combination of alternative methods in toxicity testing, such as simulated physiological conditions, culture cells and the nematode *C. elegans,* was demonstrated as a useful strategy for assessing free EOCs, silica particles and EOCs-functionalised particles. Despite the potential toxicity of the EOCs-functionalised particles still being low, the observed increased toxicological effects compared to individual constituents make the application of these particles as filtering aids for beverages more suitable than their direct use in food matrices. However, the existing legislation on processing aids establishes that even substances that does not produce detectable residue on the final product require information on toxicokinetics, toxicology and genotoxicity. Accordingly, and togheter with other complementary studies, these new materials' genotoxic potential by using a battery of *in vitro* tests, including a bacterial reverse mutation assay and an *in vitro* micronucleus assay (EFSA, 2011), should be analysed in future studies.

Conclusions

The conclusions drawn from the different studies conducted during the present doctoral thesis are:

- Functionalisation of amorphous silica with EOCs increases particles' stability under conditions representing the human gastrointestinal tract and lysosomal fluid, as observed by both the lower dissolution rates in the different functionalised particle types and the preservation of the EOCs-functionalised MCM-41 nanoparticles structure compared to their bare counterparts.
- Although functionalisation with EOCs increases the biodurability of silica particles, the microsize of particles or their agglomerates reduces the risk of accumulation after oral ingestion and, therefore, their long-term toxicity potential.
- Acute exposure to moderate and high concentrations of EOCs reduces HepG2 viability and nematode survival. The *in vivo* assays demonstrate that sublethal concentrations to these components may induce reproductive toxicity, which suggests that they may present toxic effects at the concentrations required for their bioactive properties.
- The EOCs-functionalised particles generally exhibit a stronger toxic effect *in vitro* and *in vivo* than the free EOCs and pristine silica. Independently of EOC type, the EOCs-functionalised MCM-41 microparticles are the most cytotoxic materials.
- Our results suggest that the EOCs-functionalised particles induce toxicity on HepG2 cells by an oxidative stress-related mechanism that causes mitochondrial dysfunction and apoptosis activation via the mitochondrial pathway. Moreover, cytotoxicity is caused by direct cell-particle interactions, and not by degradation products released to culture media.
- Both the bare and EOCs-functionalised particles cause acute reproductive toxicity and inhibition in nematode growth and reproduction after long-term exposure. However, the eugenol-

functionalised particles exhibit stronger effects than the bare and vanillin-functionalised silica.

- The toxic effects of the EOCs-funtionalised silica particles observed both, *in vitro* and *in vivo,* depend on the EOC type immobilised on particles' surface and the functionalisation yield achieved during the functionalisation process. Therefore, applying standardised conditions is mandatory to guarantee the functionalisation yield obtained between reactions to extrapolate the obtained results.

References

Abbaszadeh, S., Sharifzadeh, A., Shokri, H., Khosravi, A.R., Abbaszadeh, A., 2014. Antifungal efficacy of thymol, carvacrol, eugenol and menthol as alternative agents to control the growth of food-relevant fungi. J. Mycol. Med. 24, 51–56. https://doi.org/10.1016/J.MYCMED.2014.01.063

Acosta, C., Pérez-Esteve, E., Fuenmayor, C.A., Benedetti, S., Cosio, M.S., Soto, J., Sancenón, F., Mannino, S., Barat, J., Marcos, M.D., Martínez-Máñez, R., 2014. Polymer Composites Containing Gated Mesoporous Materials for On-Command Controlled Release. ACS Appl. Mater. Interfaces 6, 6453–6460. https://doi.org/10.1021/am405939y

AESAN, 2010. Guidelines indicating the necessary documentation for the assessment of processing aids intended for use in human food.

AESAN, 2021. Aesan - Agencia Española de Seguridad Alimentaria y Nutrición [WWW Document]. AESAN. URL http://www.aesan.gob.es/en/AECOSAN/web/seguridad_alimentaria/subdetalle/coadyuvantes_tecnologicos.htm (accessed 1.19.21).

Aguilar Diaz De Leon, J., Borges, C.R., 2020. Evaluation of oxidative stress in biological samples using the thiobarbituric acid reactive substances assay. J. Vis. Exp. 2020. https://doi.org/10.3791/61122

Ahmadi, T., Bahar, S., Mohammadi Ziarani, G., Badiei, A., 2019. Formation of functionalized silica-based nanoparticles and their application for extraction and determination of Hg (II) ion in fish samples. Food Chem. 300, 125180. https://doi.org/10.1016/j.foodchem.2019.125180

Al-Naqeb, G., Ismail, M., Bagalkotkar, G., Adamu, H.A., 2010. Vanillin rich fraction regulates LDLR and HMGCR gene expression in HepG2 cells. Food Res. Int. 43, 2437–2443. https://doi.org/10.1016/j.foodres.2010.09.015

Alothman, Z., 2012. A Review: Fundamental Aspects of Silicate Mesoporous Materials. Materials (Basel). 5, 2874–2902. https://doi.org/10.3390/ma5122874

Andersen, A., 2006. Final report on the safety assessment of sodium p-Chloro-m-Cresol, p-Chloro-m-Cresol, Chlorothymol, Mixed Cresols, m-Cresol, o-Cresol,

p-Cresol, Isopropyl Cresols, Thymol, o-Cymen-5-ol, and Carvacrol. Int. J. Toxicol. 25, 29–127. https://doi.org/10.1080/10915810600716653

Andrews, D.G.H., 2019. A new method for measuring the size of nematodes using image processing. Biol. Methods Protoc. 4(1), 20. https://doi.org/10.1093/biomethods/bpz020

ASAP, 2021. Home [WWW Document]. Assoc. Synth. Amorph. Silica Prod. URL https://www.asasp.eu/ (accessed 3.29.21).

Aslantürk, Ö.S., 2018. In Vitro Cytotoxicity and Cell Viability Assays: Principles, Advantages, and Disadvantages, in: Genotoxicity - A Predictable Risk to Our Actual World. InTech. 2, 64-80. https://doi.org/10.5772/intechopen.71923

Babich, H., Stern, A., Borenfreund, E., 1993. Eugenol cytotoxicity evaluated with continuous cell lines. Toxicol. Vitr. 7, 105–109. https://doi.org/10.1016/0887-2333(93)90119-P

Bagheri, E., Ansari, L., Abnous, K., Taghdisi, S.M., Charbgoo, F., Ramezani, M., Alibolandi, M., 2018. Silica based hybrid materials for drug delivery and bioimaging. J. Control. Release. https://doi.org/10.1016/j.jconrel.2018.03.014

Bakkali, F., Averbeck, S., Averbeck, D., Idaomar, M., 2008. Biological effects of essential oils – A review. Food Chem. Toxicol. 46, 446–475. https://doi.org/10.1016/j.fct.2007.09.106

Barik, T.K., Sahu, B., Swain, V., 2008. Nanosilica - From medicine to pest control. Parasitol. Res. 103(2), 253-258https://doi.org/10.1007/s00436-008-0975-7

Ben Arfa, A., Combes, S., Preziosi-Belloy, L., Gontard, N., Chalier, P., 2006. Antimicrobial activity of carvacrol related to its chemical structure. Lett. Appl. Microbiol. 43, 149–154. https://doi.org/10.1111/j.1472-765X.2006.01938.x

Bergfeld, W.F., Belsito, D. V., Hill, R.A., Klaassen, C.D., Liebler, D.C., Marks, J.G., Shank, R.C., Slaga, T.J., Snyder, P.W., Heldreth, B., 2019. Amended Safety Assessment of Synthetically-Manufactured Amorphous Silica and Hydrated Silica as Used in Cosmetics, Cosmetic Ingredient Review. https://doi.org/10.1177/1091581820925001

Bernardos, A., Aznar, E., Coll, C., Martínez-Mañez, R., Barat, J.M., Marcos, M.D., Sancenón, F., Benito, A., Soto, J., 2008. Controlled release of vitamin B2 using mesoporous materials functionalized with amine-bearing gate-like scaffoldings. J. Control. Release 131, 181–189. https://doi.org/10.1016/J.JCONREL.2008.07.037

Bezerra, D.P., Soares, A.K.N., De Sousa, D.P., 2016. Overview of the role of vanillin on redox status and cancer development. Oxid. Med. Cell. Longev. 2016, 1–9. https://doi.org/10.1155/2016/9734816

Bikiaris, D.N., Vasileiou, A.A., 2009. Fumed Silica Reinforced Nanocomposites. In: Wang, B.Y. (ed.) Current Status and Promises in Environmental Biodegradation Research Focus, Nova Publishers, New York (Chapter 7), 189-215.

Boelsterli, U.A., 2007. Mechanistic toxicology : the molecular basis of how chemicals disrupt biological targets. CRC Press, Taylor and Francis, London, 312. https://doi.org/10.1201/9780367806293

Braun, K., Pochert, • Alexander, Beck, M., Fiedler, • Richard, Gruber, J., Lindén, M., 2016. Dissolution kinetics of mesoporous silica nanoparticles in different simulated body fluids. J. Sol-Gel Sci. Technol. 79, 319–327. https://doi.org/10.1007/s10971-016-4053-9

Brenner, S., 1974. The Genetics of Caenorhabditis elegans. Genetics 77(1), 71–94.

Brown, S.C., Kamal, M., Nasreen, N., Baumuratov, A., Sharma, P., Antony, V.B., Moudgil, B.M., 2007. Influence of shape, adhension and simulated lung mechanics on amorphous silica nanoparticle toxicity. Adv. Powder Technol. 18, 69–79. https://doi.org/10.1163/156855207779768214

Brühwiler, D., 2010. Postsynthetic functionalization of mesoporous silica. Nanoscale 2, 887. https://doi.org/10.1039/c0nr00039f

Burt, S., 2004. Essential oils: their antibacterial properties and potential applications in foods—a review. Int. J. Food Microbiol. 94, 223–253. https://doi.org/10.1016/J.IJFOODMICRO.2004.03.022

Calas, A., Uzu, G., Martins, J.M.F., Voisin, D., Spadini, L., Lacroix, T., Jaffrezo, J.-L., 2017. The importance of simulated lung fluid (SLF) extractions for a more relevant evaluation of the oxidative potential of particulate matter. Sci. Rep. 7, 11617. https://doi.org/10.1038/s41598-017-11979-3

Calo, J.R., Crandall, P.G., O'Bryan, C.A., Ricke, S.C., 2015. Essential oils as antimicrobials in food systems – A review. Food Control 54, 111–119. https://doi.org/10.1016/J.FOODCONT.2014.12.040

Chalfie, M., Tu, Y., Euskirchen, G., Ward, W.W., Prasher, D.C., 1994. Green fluorescent protein as a marker for gene expression. Science (80-.). 263, 802–805. https://doi.org/10.1126/science.8303295

Chaudhary, V., Sharma, S., 2017. An overview of ordered mesoporous material SBA-15: synthesis, functionalization and application in oxidation reactions. J. Porous Mater. 24, 741–749. https://doi.org/10.1007/s10934-016-0311-z

Cheng, W.-Y., Hsiang, C.-Y., Bau, D.-T., Chen, J.-C., Shen, W.-S., Li, C.-C., Lo, H.-Y., Wu, S.-L., Chiang, S.-Y., Ho, T.-Y., 2007. Microarray analysis of vanillin-regulated gene expression profile in human hepatocarcinoma cells. Pharmacol. Res. 56, 474–482. https://doi.org/10.1016/J.PHRS.2007.09.009

Ciappellano, S.G., Tedesco, E., Venturini, M., Benetti, F., 2016. In vitro toxicity assessment of oral nanocarriers. Adv. Drug Deliv. Rev. 106, 381-401. https://doi.org/10.1016/j.addr.2016.08.007

Clavijo, A., Kronberg, M.F., Rossen, A., Moya, A., Calvo, D., Salatino, S.E., Pagano, E.A., Morábito, J.A., Rosa Munarriz, E., 2016. The nematode Caenorhabditis elegans as an integrated toxicological tool to assess water quality and pollution. Sci. Total Environ. 569–570, 252–261. https://doi.org/10.1016/j.scitotenv.2016.06.057

Corsi, A.K., Wightman, B., Chalfie, M., 2015. A transparent window into biology: a primer on Caenorhabditis elegans. Genetics, 200(2), 387-407. https://doi.org/10.1895/wormbook.1.177.1

Crebelli, R., Dusemund, B., Galtier, P., Gilbert, J., Gott, DM, Gundert-Remy, U.,

König, J., Lambré, C., Leblanc, J-c, Mortensen, A., Mosesso, P., Parent-Massin, D., Stankovic, I., Tobback, P., Waalkens-Berendsen, I., Woutersen, R., Wright, M., Gott, D, Gürtler, R., Leblanc, JC, 2012. Guidance for submission for food additive evaluations. EFSA J. https://doi.org/10.2903/j.efsa.2012.2760

Croissant, J.G., Fatieiev, Y., Almalik, A., Khashab, N.M., 2018. Mesoporous Silica and Organosilica Nanoparticles: Physical Chemistry, Biosafety, Delivery Strategies, and Biomedical Applications. Adv. Healthc. Mater. 7(4), 1700831. https://doi.org/10.1002/adhm.201700831

D'Arcy, M.S., 2019. Cell death: a review of the major forms of apoptosis, necrosis and autophagy. Cell Biol. Int. 43, 582–592. https://doi.org/10.1002/CBIN.11137

Daneshian, M., Akbarsha, M.A., Blaauboer, B., Caloni, F., Cosson, P., Curren, R., Goldberg, A., Gruber, F., Ohl, F., Pfaller, W., Van Der Valk, J., Vinardell, P., Zurlo, J., Hartung, T., Leist, M., Hopkins Bloomberg, J., 2011. t 4 Workshop Report* A framework program for the teaching of alternative methods (replacement, reduction, refinement) to animal experimentation. ALTEX-Alternatives to animal experimentation, 28(4), 341-352.

De Meringo, A., Morscheidt, C., Thelohan, S., Tiesler, H., 1994. In vitro assessment of biodurability: Acellular systems, in: Environmental Health Perspectives. 102(suppl 5), 47–53. https://doi.org/10.1289/ehp.94102s547

De Souza, T.B., Orlandi, M., Coelho, L.F.L., Malaquias, L.C.C., Dias, A.L.T., De Carvalho, R.R., Silva, N.C., Carvalho, D.T., 2014. Synthesis and in vitro evaluation of antifungal and cytotoxic activities of eugenol glycosides. Med. Chem. Res. 23, 496–502. https://doi.org/10.1007/s00044-013-0669-2

De Vincenzi, M., Stammati, A., De Vincenzi, A., Silano, M., 2004. Constituents of aromatic plants: Carvacrol. Fitoterapia 75, 801–804. https://doi.org/10.1016/j.fitote.2004.05.002

Deavall, D.G., Martin, E.A., Horner, J.M., Roberts, R., 2012. Drug-induced oxidative stress and toxicity. Vol 2012. J. Toxicol.

https://doi.org/10.1155/2012/645460

Deb, D.D., Parimala, G., Saravana Devi, S., Chakraborty, T., 2011. Effect of thymol on peripheral blood mononuclear cell PBMC and acute promyelotic cancer cell line HL-60. Chem. Biol. Interact. 193, 97–106. https://doi.org/10.1016/J.CBI.2011.05.009

Di Giuseppe, D., 2020. Characterization of fibrous mordenite: A first step for the evaluation of its potential toxicity. Crystals 10, 1–15. https://doi.org/10.3390/cryst10090769

Diab, R., Canilho, N., Pavel, I.A., Haffner, F.B., Girardon, M., Pasc, A., 2017. Silica-based systems for oral delivery of drugs, macromolecules and cells. Adv. Colloid Interface Sci. 249, 346–362. https://doi.org/10.1016/j.cis.2017.04.005

Dimov, I., Maduro, M.F., 2019. The C. elegans intestine: organogenesis, digestion, and physiology. Cell Tissue Res. 1-14. https://doi.org/10.1007/s00441-019-03036-4

Dorman, H.J.D., Deans, S.G., 2000. Antimicrobial agents from plants: antibacterial activity of plant volatile oils. J. Appl. Microbiol. 88, 308–316. https://doi.org/10.1046/j.1365-2672.2000.00969.x

EC, 2008. Regulation (EC) no 1334/2008 of the European Parliament and of the council of 16 December 2008 on flavourings and certain food ingredients with flavouring properties for use in and on foods and amending council regulation (EEC) no 1601/91, regulations (EC. Off. J. Eur. Communities L354, 34–50.

ECETOC, J., 2006. REPORT No. 51. Synthetic amorphous silica (CAS No. 7631–86-9), European Centre for Ecotoxicology and Toxicology of Chemicals.

ECHA, 2021. European Chemicals agency [WWW Document]. URL https://echa.europa.eu/es/ (accessed 1.7.21).

EFSA Panel on Food Additives and Nutrient Sources added to Food (ANS), 2012. Guidance for submission for food additive evaluations. EFSA Journal, 10(7), 2760.

EFSA Panel on Food Additives and Nutrient Sources added to Food (ANS), 2018a. Re-evaluation of silicon dioxide (E 551) as a food additive. EFSA Journal, 16(1), e05088. https://doi.org/10.2903/j.efsa.2018.5088

EFSA Scientific Committee, 2018b. Guidance on risk assessment of the application of nanoscience and nanotechnologies in the food and feed chain: Part 1, human and animal health. EFSA journal, 16(7), e05327. https://doi.org/10.2903/j.efsa.2018.5327

EFSA, 2011. Scientific opinion on genotoxicity testing strategies applicable to food and feed safety assessment. EFSA Journal, 9(9), 2379.

Eisenbrand, G., Pool-Zobel, B., Baker, V., Balls, M., Blaauboer, B.J., Boobis, A., Carere, A., Kevekordes, S., Lhuguenot, J.C., Pieters, R., Kleiner, J., 2002. Methods of in vitro toxicology. Food Chem. Toxicol. 40(2-3), 193-236. https://doi.org/10.1016/S0278-6915(01)00118-1

Ellis, H.M., Horvitz, H.R., 1986. Genetic control of programmed cell death in the nematode C. elegans. Cell 44, 817–829. https://doi.org/10.1016/0092-8674(86)90004-8

Erkekoglu, P., Kocer Giray, B., Başaran, N., 2011. 3R Principle and Alternative Toxicity Testing Methods, J. Pharm. Sci.

EU, 2008. Regulation (EC) No 1333/2008 of the European Parliament and of the Council of 16 December 2008 on food additives (Text with EEA relevance), Official Journal of the European Union.

European Parliament, 2010. DIRECTIVE 2010/63/EU of the European Parliament and of the Council of 22 September 2010 on the protection of animals used for scientific purposes, in: DIRECTIVE 2010/63/EU of the European Parliament and of the Council of 22 September 2010 on the Protection of Animals Used for Scientific Purposes. pp. 33–78.

European Parliament, 2015. Regulation (EU) 2015/2283 of the European Parliament and of the Council of 25 November 2015 on novel foods, amending Regulation (EU) No 1169/2011 of the European Parliament and of the Council

and repealing Regulation (EC) No 258/97 of the European Parliam, Official Journal of the European Union.

Fashina, A., Antunes, E., Nyokong, T., 2013. Silica nanoparticles grafted with phthalocyanines: Photophysical properties and studies in artificial lysosomal fluid. New J. Chem. 37, 2800–2809. https://doi.org/10.1039/c3nj00439b

FDA, 2020. CFR - Code of Federal Regulations Title 21.

FDA, 2021. FDA (U.S. Food and Drug Administration, U.S. Department of Health and Human Services). Database of Select Committee on Gras Substances (SCOGS) [WWW Document]. https://doi.org/10.1201/9781420037838.ch1

Félix, M.A., Braendle, C., 2010. The natural history of Caenorhabditis elegans. Curr. Biol. 20(22), 965-969. https://doi.org/10.1016/j.cub.2010.09.050

Fire, A., Xu, S., Montgomery, M.K., Kostas, S.A., Driver, S.E., Mello, C.C., 1998. Potent and specific genetic interference by double-stranded RNA in caenorhabditis elegans. Nature 391, 806–811. https://doi.org/10.1038/35888

Fitzgerald, D.J., Stratford, M., Gasson, M.J., Ueckert, J., Bos, A., Narbad, A., 2004. Mode of antimicrobial of vanillin against Escherichia coli, Lactobacillus plantarum and Listeria innocua. J. Appl. Microbiol. 97, 104–113. https://doi.org/10.1111/j.1365-2672.2004.02275.x

Flynn, J., Mallen, S., Durack, E., O'Connor, P.M., Hudson, S.P., 2019. Mesoporous matrices for the delivery of the broad spectrum bacteriocin, nisin A. J. Colloid Interface Sci. 537, 396–406. https://doi.org/10.1016/j.jcis.2018.11.037

Frézal, L., Félix, M.A., 2015. C. elegans outside the Petri dish. Elife 2015, e05849. https://doi.org/10.7554/eLife.05849.001

Fruijtier-Pölloth, C., 2012. The toxicological mode of action and the safety of synthetic amorphous silica—A nanostructured material. Toxicology 294, 61–79. https://doi.org/10.1016/j.tox.2012.02.001

Fruijtier-Pölloth, C., 2016. The safety of nanostructured synthetic amorphous silica (SAS) as a food additive (E 551). Arch. Toxicol. 90, 2885–2916.

https://doi.org/10.1007/s00204-016-1850-4

Fuentes, C., Ruiz-Rico, M., Fuentes, A., Ruiz, M. J., Barat, J. M., 2020. Degradation of silica particles functionalised with essential oil components under simulated physiological conditions. Journal of Hazardous Materials, 399, 123120.

Fuentes, C., Ruiz-Rico, M., Fuentes, A., Barat, J.M., Ruiz, M.J., 2021. Comparative cytotoxic study of silica materials functionalised with essential oil components in HepG2 cells. Food Chem. Toxicol. 147, 111858. https://doi.org/10.1016/j.fct.2020.111858

Fujisawa, S., Atsumi, T., Kadoma, Y., Sakagami, H., 2002. Antioxidant and prooxidant action of eugenol-related compounds and their cytotoxicity. Toxicology 177, 39–54. https://doi.org/10.1016/S0300-483X(02)00194-4

Gañán, J., Morante-Zarcero, S., Pérez-Quintanilla, D., Sierra, I., 2014. Evaluation of functionalized mesoporous silicas for reverse phase high performance liquid chromatography: An application for the separation of steroids. Microchem. J. 114, 53–58. https://doi.org/10.1016/j.microc.2013.12.003

Gao, S., Chen, W., Zeng, Y., Jing, H., Zhang, N., Flavel, M., Jois, M., Han, J.D.J., Xian, B., Li, G., 2018. Classification and prediction of toxicity of chemicals using an automated phenotypic profiling of Caenorhabditis elegans. BMC Pharmacol. Toxicol. 19, 1–11. https://doi.org/10.1186/s40360-018-0208-3

García-Ríos, E., Ruiz-Rico, M., Guillamón, J.M., Pérez-Esteve, É., Barat, J.M., 2018. Improved antimicrobial activity of immobilised essential oil components against representative spoilage wine microorganisms. Food Control 94, 177–186. https://doi.org/10.1016/j.foodcont.2018.07.005

G-Biosciences, 2021. TMRE Mitochondrial Membrane Potential Assay (Cat. # 786-1313, 786-1314) [WWW Document]. URL https://www.gbiosciences.com/Bioassays/Cell_Health_Assay/Apoptosis-Assays-Accessories/TMRE_Mitochondrial_Membrane_Potential_Assay (accessed 8.20.21).

Gel, U., 2012. FITC Annexin V Apoptosis Detection Kit I. Koch-Light Lab. Colobrook 5–7.

Gonzalez-Moragas, L., Maurer, L.L., Harms, V.M., Meyer, J.N., Laromaine, A., Roig, A., 2017. Materials and toxicological approaches to study metal and metal-oxide nanoparticles in the model organism: Caenorhabditis elegans. Mater. Horizons 4(5), 719-746. https://doi.org/10.1039/c7mh00166e

Gonzalez-Moragas, L., Roig, A., Laromaine, A., 2015. C. elegans as a tool for in vivo nanoparticle assessment. Adv. Colloid Interface Sci. 219, 10–26. https://doi.org/10.1016/j.cis.2015.02.001

Goulet, F., Vachon, P., Helie, P., 2011. Evaluation of the toxicity of eugenol at anesthetic doses in African clawed frogs (Xenopus laevis). Toxicologic pathology, 39(3), 471-477.

Gualtieri, A.F., Pollastri, S., Bursi Gandolfi, N., Gualtieri, M.L., 2018. In vitro acellular dissolution of mineral fibres: A comparative study. Sci. Rep. 8, 8(1), 1-12. https://doi.org/10.1038/s41598-018-25531-4

Handbook - Introduction [WWW Document], n.d. URL https://www.wormatlas.org/hermaphrodite/introduction/mainframe.htm (accessed 12.20.20).

Hao, N., Li, Linlin, Zhang, Q., Huang, X., Meng, X., Zhang, Y., Chen, D., Tang, F., Li, Laifeng, 2012. The shape effect of PEGylated mesoporous silica nanoparticles on cellular uptake pathway in Hela cells. Microporous Mesoporous Mater. 162, 14–23. https://doi.org/10.1016/j.micromeso.2012.05.040

Hardy, A., Benford, D., Halldorsson, T., Jeger, M.J., Knutsen, H.K., More, S., Naegeli, H., Noteborn, H., Ockleford, C., Ricci, A., Rychen, G., Schlatter, J.R., Silano, V., Solecki, R., Turck, D., Younes, M., Chaudhry, Q., Cubadda, F., Gott, D., Oomen, A., Weigel, S., Karamitrou, M., Schoonjans, R., Mortensen, A., 2018. Guidance on risk assessment of the application of nanoscience and nanotechnologies in the food and feed chain: Part 1, human and animal health.

EFSA J. 16. https://doi.org/10.2903/j.efsa.2018.5327

Harrison, E., 2009. Generally Recognized as Safe Determination for Silicon Dioxide When Added Directly and/or Indirectly to Human Food, Lewis & Harrison, Washington, D. C., 1-77

He, Q., Shi, J., Zhu, M., Chen, Y., Chen, F., 2010. The three-stage in vitro degradation behavior of mesoporous silica in simulated body fluid. Microporous Mesoporous Mater. 131, 314–320. https://doi.org/10.1016/J.MICROMESO.2010.01.009

He, Q., Zhang, Z., Gao, F., Li, Y., Shi, J., 2011. In vivo Biodistribution and Urinary Excretion of Mesoporous Silica Nanoparticles: Effects of Particle Size and PEGylation. Small 7, 271–280. https://doi.org/10.1002/smll.201001459

Hedgecock, E.M., Sulston, J.E., Thomson, J.N., 1983. Mutations affecting programmed cell deaths in the nematode Caenorhabditis elegans. Science, 220(4603), 1277–1279. https://doi.org/10.1126/science.6857247

Heikkilä, T., Santos, H.A., Kumar, N., Murzin, D.Y., Salonen, J., Laaksonen, T., Peltonen, L., Hirvonen, J., Lehto, V.-P., 2010. Cytotoxicity study of ordered mesoporous silica MCM-41 and SBA-15 microparticles on Caco-2 cells. Eur. J. Pharm. Biopharm. 74, 483–494. https://doi.org/10.1016/J.EJPB.2009.12.006

Ho, K., Yazan, L.S., Ismail, N., Ismail, M., 2009. Apoptosis and cell cycle arrest of human colorectal cancer cell line HT-29 induced by vanillin. Cancer Epidemiol. 33, 155–160. https://doi.org/10.1016/J.CANEP.2009.06.003

Ho, Y.C., Huang, F.M., Chang, Y.C., 2006. Mechanisms of cytotoxicity of eugenol in human osteoblastic cells in vitro. Int. Endod. J. 39, 389–393. https://doi.org/10.1111/j.1365-2591.2006.01091.x

Hobert, O., 2013. The neuronal genome of Caenorhabditis elegans. WormBook: The Online Review of C. elegans Biology. https://doi.org/10.1895/wormbook.1.161.1

Hunt, P.R., 2017. The C. elegans model in toxicity testing. J. Appl. Toxicol. 37(1), 50-59. https://doi.org/10.1002/jat.3357

Hyldgaard, M., Mygind, T., Meyer, R.L., 2012. Essential oils in food preservation: Mode of action, synergies, and interactions with food matrix components. Front. Microbiol. 3, 1–12. https://doi.org/10.3389/fmicb.2012.00012

IARC, 1987. Silica and some silicates. IARC Monogr. Eval. Carcinog. Risk Chem. Hum. 42, 1–440.

ICCVAM, 2006. ICCVAM Test Method Evaluation Report (TMER): In Vitro Cytotoxicity Test Methods for Estimating Starting Doses For Acute Oral Systemic Toxicity Testing: NIH Publication No: 07-4519 1–334.

Izquierdo-Barba, I., Colilla, M., Manzano, M., Vallet-Regí, M., 2010. In vitro stability of SBA-15 under physiological conditions. Microporous Mesoporous Mater. 132, 442–452. https://doi.org/10.1016/J.MICROMESO.2010.03.025

Jaganathan, H., Godin, B., 2012. Biocompatibility assessment of Si-based nano- and micro-particles. Adv. Drug Deliv. Rev. 64, 1800–1819. https://doi.org/10.1016/J.ADDR.2012.05.008

JECFA, 2021. WHO | JECFA [WWW Document]. Eval. Jt. FAO/WHO Expert Comm. Food Addit. URL https://apps.who.int/food-additives-contaminants-jecfa-database/search.aspx. (accessed 3.1.21).

Kachur, K., Suntres, Z., 2020. The antibacterial properties of phenolic isomers, carvacrol and thymol. Crit. Rev. Food Sci. Nutr. 60, 3042–3053. https://doi.org/10.1080/10408398.2019.1675585

Kaletta, T., Hengartner, M.O., 2006. Finding function in novel targets: C. elegans as a model organism. Nat. Rev. Drug Discov. 5(5), 387-399. https://doi.org/10.1038/nrd2031

Kamatou, G.P., Vermaak, I., Viljoen, A.M., 2012. Eugenol—From the Remote Maluku Islands to the International Market Place: A Review of a Remarkable and Versatile Molecule. Molecules 17, 6953–6981. https://doi.org/10.3390/molecules17066953

Kandárová, H., Letaáiová, S., 2011. Alternative methods in toxicology: Pre-validated and validated methods. Interdiscip. Toxicol. 4, 107–113.

https://doi.org/10.2478/v10102-011-0018-6

Kaur, B., Chakraborty, D., 2013. Biotechnological and molecular approaches for vanillin production: A review. Appl. Biochem. Biotechnol. 169, 1353–1372. https://doi.org/10.1007/s12010-012-0066-1

Khalil, A.A., Rahman, U.U., Khan, M.R., Sahar, A., Mehmood, T., Khan, M., 2017. Essential oil eugenol: Sources, extraction techniques and nutraceutical perspectives. RSC Adv. 7, 32669–32681. https://doi.org/10.1039/c7ra04803c

Kresge, C.T., Vartuli, J.C., Roth, W.J., Leonowicz, M.E., 2004. The discovery of ExxonMobil's M41S family of mesoporous molecular sieves, in: Studies in Surface Science and Catalysis. Elsevier Inc., pp. 53–72. https://doi.org/10.1016/s0167-2991(04)80193-9

Kyriakidou, K., Brasinika, D., Trompeta, A.F.A., Bergamaschi, E., Karoussis, I.K., Charitidis, C.A., 2020. In vitro cytotoxicity assessment of pristine and carboxyl-functionalized MWCNTs. Food Chem. Toxicol. 141, 111374. https://doi.org/10.1016/j.fct.2020.111374

Larson, R., 2010. Assessing the Solubility of Silicon Dioxide Particles Using Simulated Lung Fluid. Open Toxicol. J. 4, 51–55. https://doi.org/10.2174/1874340401004010051

Lee, Jienny, Cho, J.Y., Lee, S.Y., Lee, K.W., Lee, Jongsung, Song, J.Y., 2014. Vanillin protects human keratinocyte stem cells against Ultraviolet B irradiation. Food Chem. Toxicol. 63, 30–37. https://doi.org/10.1016/j.fct.2013.10.031

Lee, R., 2005. Web resources for C. elegans studies. WormBook: The Online Review of C. elegans Biology. https://doi.org/10.1895/wormbook.1.48.1

Lei, L., Wu, S., Lu, S., Liu, M., Song, Y., Fu, Z., Shi, H., Raley-Susman, K.M., He, D., 2018. Microplastic particles cause intestinal damage and other adverse effects in zebrafish Danio rerio and nematode Caenorhabditis elegans. Sci. Total Environ. 619–620, 1–8. https://doi.org/10.1016/j.scitotenv.2017.11.103

Leung, M.C.K., Williams, P.L., Benedetto, A., Au, C., Helmcke, K.J., Aschner, M.,

Meyer, J.N., 2008. Caenorhabditis elegans: An Emerging Model in Biomedical and Environmental Toxicology. Toxicol. Sci. 106, 5–28. https://doi.org/10.1093/toxsci/kfn121

Liberman, A., Mendez, N., Trogler, W.C., Kummel, A.C., 2014. Synthesis and surface functionalization of silica nanoparticles for nanomedicine. Surf. Sci. Rep. https://doi.org/10.1016/j.surfrep.2014.07.001

Lin, Y.-S., Abadeer, N., Haynes, C.L., 2011. Stability of small mesoporous silicananoparticles in biological media. Chem. Commun. 47, 532–534. https://doi.org/10.1039/C0CC02923H

Llana-Ruiz-Cabello, M., Gutiérrez-Praena, D., Pichardo, S., Moreno, F.J., Bermúdez, J.M., Aucejo, S., Cameán, A.M., 2014a. Cytotoxicity and morphological effects induced by carvacrol and thymol on the human cell line Caco-2. Food Chem. Toxicol. 64, 281–290. https://doi.org/10.1016/j.fct.2013.12.005

Llana-Ruiz-Cabello, M., Maisanaba, S., Puerto, M., Prieto, A.I., Pichardo, S., Jos, Á., Cameán, A.M., 2014b. Evaluation of the mutagenicity and genotoxic potential of carvacrol and thymol using the Ames Salmonella test and alkaline, Endo III- and FPG-modified comet assays with the human cell line Caco-2. Food Chem. Toxicol. 72, 122–128. https://doi.org/10.1016/j.fct.2014.07.013

Llana-Ruiz-Cabello, M., Gutiérrez-Praena, D., Puerto, M., Pichardo, S., Jos, Á., Cameán, A.M., 2015. In vitro pro-oxidant/antioxidant role of carvacrol, thymol and their mixture in the intestinal Caco-2 cell line. Toxicol. Vitr. 29, 647–656. https://doi.org/10.1016/j.tiv.2015.02.006

Lu, L., Zhu, Z., Hu, X., 2019. Hybrid nanocomposites modified on sensors and biosensors for the analysis of food functionality and safety. Trends Food Sci. 90, 100-110. Technol. https://doi.org/10.1016/j.tifs.2019.06.009

Maisanaba, S., Prieto, A.I., Puerto, M., Gutiérrez-Praena, D., Demir, E., Marcos, R., Cameán, A.M., 2015. In vitro genotoxicity testing of carvacrol and thymol using the micronucleus and mouse lymphoma assays. Mutat. Res. - Genet.

Toxicol. Environ. Mutagen. 784–785, 37–44. https://doi.org/10.1016/j.mrgentox.2015.05.005

Maleki, A., Kettiger, H., Schoubben, A., Rosenholm, J.M., Ambrogi, V., Hamidi, M., 2017. Mesoporous silica materials: From physico-chemical properties to enhanced dissolution of poorly water-soluble drugs. J. Control. Release. https://doi.org/10.1016/j.jconrel.2017.07.047

Maralhas, A., Monteiro, A., Martins, C., Kranendonk, M., Laires, A., Rueff, J., Rodrigues, A.S., 2006. Genotoxicity and endoreduplication inducing activity of the food flavouring eugenol. Mutagenesis 21, 199–204. https://doi.org/10.1093/mutage/gel017

Marchese, A., Orhan, I.E., Daglia, M., Barbieri, R., Di Lorenzo, A., Nabavi, S.F., Gortzi, O., Izadi, M., Nabavi, S.M., 2016. Antibacterial and antifungal activities of thymol: A brief review of the literature. Food Chem. 210, 402–414. https://doi.org/10.1016/j.foodchem.2016.04.111

Martins, C., Doran, C., Laires, A., Rueff, J., Rodrigues, A.S., 2011. Genotoxic and apoptotic activities of the food flavourings myristicin and eugenol in AA8 and XRCC1 deficient EM9 cells. Food Chem. Toxicol. 49, 385–392. https://doi.org/10.1016/j.fct.2010.11.013

Memar, M.Y., Raei, P., Alizadeh, N., Akbari Aghdam, M., Kafil, H.S., 2017. Carvacrol and thymol. Rev. Med. Microbiol. 28, 63–68. https://doi.org/10.1097/MRM.0000000000000100

Meynen, V., Cool, P., Vansant, E.F., 2009. Verified syntheses of mesoporous materials. Microporous Mesoporous Mater. 125, 170–223. https://doi.org/10.1016/J.MICROMESO.2009.03.046

Miret, S., De Groene, E.M., Klaffke, W., 2006. Comparison of in vitro assays of cellular toxicity in the human hepatic cell line HepG2. J. Biomol. Screen. 11, 184–193. https://doi.org/10.1177/1087057105283787

Moritz, M., Geszke-Moritz, M., 2015. Mesoporous materials as multifunctional tools in biosciences: Principles and applications. Mater. Sci. Eng. C 49, 114–

151. https://doi.org/10.1016/J.MSEC.2014.12.079

Mosmann, T., 1983. Rapid colorimetric assay for cellular growth and survival: Application to proliferation and cytotoxicity assays. J. Immunol. Methods 65, 55–63. https://doi.org/10.1016/0022-1759(83)90303-4

Munerato, M.C., Sinigaglia, M., Reguly, M.L., De Andrade, H.H.R., 2005. Genotoxic effects of eugenol, isoeugenol and safrole in the wing spot test of Drosophila melanogaster. Mutat. Res. - Genet. Toxicol. Environ. Mutagen. 582, 87–94. https://doi.org/10.1016/j.mrgentox.2005.01.001

Murugadoss, S., van den Brule, S., Brassinne, F., Sebaihi, N., Mejia, J., Lucas, S., Petry, J., Godderis, L., Mast, J., Lison, D., Hoet, P.H., 2020. Is aggregated synthetic amorphous silica toxicologically relevant? Part. Fibre Toxicol. 17, 1. https://doi.org/10.1186/s12989-019-0331-3

Nagar, Y., Thakur, R.S., Parveen, T., Patel, D.K., Ram, K.R., Satish, A., 2020. Toxicity assessment of parabens in Caenorhabditis elegans. Chemosphere 246, 125730. https://doi.org/10.1016/j.chemosphere.2019.125730

Nagoor Meeran, M.F., Javed, H., Taee, H. Al, Azimullah, S., Ojha, S.K., 2017. Pharmacological properties and molecular mechanisms of thymol: Prospects for its therapeutic potential and pharmaceutical development. Front. Pharmacol. 8, 380. https://doi.org/10.3389/fphar.2017.00380

Nejad, S.M., Özgüneş, H., Başaran, N., 2017. Pharmacological and Toxicological Properties of Eugenol. Turkish J. Pharm. Sci. 14, 201–206. https://doi.org/10.4274/tjps.62207

OECD, 2016. OECD Environment, Health and Safety Publications, Series on the Safety of Manufactured Nanomaterials, No. 53. DOSSIER ON SILVER NANOPARTICLES. 1, 1–59. https://doi.org/ENV/JM/MONO(2007)10

OECD Guideline, 2018. OECD Guideline for the Testing of Chemicals – Repeated Dose 90-Oral Toxicity Study in Rodents – OECD 408 1–17.

OECD, 2018. Series on the Safety of Manufactured Nanomaterials No 86. Assessment of Biodurability of Nanomaterials and Their Surface Ligands.

Organisation for Economic Co-operation and Development (OECD), Paris, France. ENV/JM/MONO(2018).

Oliveira, C., Meurer, Y., Oliveira, M., Medeiros, W., Silva, F., Brito, A., Pontes, D., Andrade-Neto, V., 2014. Comparative Study on the Antioxidant and Anti-Toxoplasma Activities of Vanillin and Its Resorcinarene Derivative. Molecules 19, 5898–5912. https://doi.org/10.3390/molecules19055898

Otterstedt, J.-E., Brandreth, D.A., 2013. Small Particles Technology, Springer Science & Business Media.

Palić, D., Herolt, D.M., Andreasen, C.B., Menzel, B.W., Roth, J.A., 2006. Anesthetic efficacy of tricaine methanesulfonate, metomidate and eugenol: Effects on plasma cortisol concentration and neutrophil function in fathead minnows (Pimephales promelas Rafinesque, 1820). Aquaculture 254, 675–685. https://doi.org/10.1016/j.aquaculture.2005.11.004

Peña-Gómez, N., Ruiz-Rico, M., Fernández-Segovia, I., Barat, J.M., 2019a. Study of apple juice preservation by filtration through silica microparticles functionalised with essential oil components. Food Control 106, 106749. https://doi.org/10.1016/j.foodcont.2019.106749

Peña-Gómez, N., Ruiz-Rico, M., Pérez-Esteve, É., Fernández-Segovia, I., Barat, J.M., 2019b. Novel antimicrobial filtering materials based on carvacrol, eugenol, thymol and vanillin immobilized on silica microparticles for water treatment. Innov. Food Sci. Emerg. Technol. 58, 102228. https://doi.org/10.1016/j.ifset.2019.102228

Peña-Gómez, N., Ruiz-Rico, M., Pérez-Esteve, É., Fernández-Segovia, I., Barat, J.M., 2020. Microbial stabilization of craft beer by filtration through silica supports functionalized with essential oil components. LWT 117, 108626. https://doi.org/10.1016/j.lwt.2019.108626

Pérez-Esteve, É., Ruiz-Rico, M., de la Torre, C., Llorca, E., Sancenón, F., Marcos, M.D., Amorós, P., Guillem, C., Martínez-Máñez, R., Barat, J.M., 2016a. Stability of different mesoporous silica particles during an in vitro digestion.

Microporous Mesoporous Mater. 230, 196–207. https://doi.org/10.1016/J.MICROMESO.2016.05.004

Pérez-Esteve, É., Ruiz-Rico, M., de la Torre, C., Villaescusa, L.A., Sancenón, F., Marcos, M.D., Amorós, P., Martínez-Máñez, R., Barat, J.M., 2016b. Encapsulation of folic acid in different silica porous supports: A comparative study. Food Chem. 196, 66–75. https://doi.org/10.1016/J.FOODCHEM.2015.09.017

Prashar, A., Locke, I.C., Evans, C.S., 2006. Cytotoxicity of clove (Syzygium aromaticum) oil and its major components to human skin cells. Cell Prolif. 39, 241–248. https://doi.org/10.1111/j.1365-2184.2006.00384.x

Puerari, R.C., Ferrari, E., de Cezar, M.G., Gonçalves, R.A., Simioni, C., Ouriques, L.C., Vicentini, D.S., Matias, W.G., 2019. Investigation of toxicological effects of amorphous silica nanostructures with amine-functionalized surfaces on Vero cells. Chemosphere 214, 679–687. https://doi.org/10.1016/j.chemosphere.2018.09.165

Ramos, M., Beltran, A., Valdes, A., Peltzer, M.A., Jimenez, A., Garrigos, M.C., Zaikov, G.E., 2013. Carvacrol and thymol for fresh food packaging. J. Bioequivalence Bioavailab. 5, 154–160. https://doi.org/10.4172/jbb.1000151

Rampersad, S.N., 2012. Multiple Applications of Alamar Blue as an Indicator of Metabolic Function and Cellular Health in Cell Viability Bioassays. Sensors 12, 12347–12360. https://doi.org/10.3390/s120912347

Ray, P.D., Huang, B.-W., Tsuji, Y., 2012. Reactive oxygen species (ROS) homeostasis and redox regulation in cellular signaling. Cell. Signal. 24, 981. https://doi.org/10.1016/J.CELLSIG.2012.01.008

Ribes, S., Ruiz-Rico, M., Pérez-Esteve, É., Fuentes, A., Talens, P., Martínez-Máñez, R., Barat, J.M., 2017. Eugenol and thymol immobilised on mesoporous silica-based material as an innovative antifungal system: Application in strawberry jam. Food Control 81, 181–188. https://doi.org/10.1016/J.FOODCONT.2017.06.006

Ribes, S., Fuentes, A., Talens, P., Barat, J.M., 2018. Prevention of fungal spoilage in food products using natural compounds: A review. Crit. Rev. Food Sci. Nutr. 58, 2002–2016. https://doi.org/10.1080/10408398.2017.1295017

Ribes, S., Ruiz-Rico, M., Pérez-Esteve, É., Fuentes, A., Barat, J.M., 2019. Enhancing the antimicrobial activity of eugenol, carvacrol and vanillin immobilised on silica supports against Escherichia coli or Zygosaccharomyces rouxii in fruit juices by their binary combinations. LWT 113, 108326. https://doi.org/10.1016/j.lwt.2019.108326

Ribes, S., Ruiz-Rico, M., Moreno-Mesonero, L., Moreno, Y., Barat, J.M., 2020. Natural antimicrobial compounds immobilised on silica microparticles as filtering materials: Impact on the metabolic activity and bacterial viability of waterborne microorganisms. Environ. Technol. Innov. 21, 101219. https://doi.org/10.1016/j.eti.2020.101219

Rojo, L., Vazquez, B., Parra, J., Bravo, A.L., Deb, S., San Roman, J., 2006. From natural products to polymeric derivatives of "Eugenol": A new approach for preparation of dental composites and orthopedic bone cements. Biomacromolecules 7, 2751–2761. https://doi.org/10.1021/bm0603241

Ros-Lis, J. V., Bernardos, A., Pérez, É., Barat, J.M., Martínez-Máñez, R., 2018. Functionalized Silica Nanomaterials as a New Tool for New Industrial Applications, in: Impact of Nanoscience in the Food Industry. Elsevier Inc., 165–196. https://doi.org/10.1016/B978-0-12-811441-4.00007-8

Ruiz-Rico, M., Pérez-Esteve, É., Bernardos, A., Sancenón, F., Martínez-Máñez, R., Marcos, M.D., Barat, J.M., 2017. Enhanced antimicrobial activity of essential oil components immobilized on silica particles. Food Chem. 233, 228–236. https://doi.org/10.1016/J.FOODCHEM.2017.04.118

Ruiz-Rico, M., Pérez-Esteve, É., de la Torre, C., Jiménez-Belenguer, A.I., Quiles, A., Marcos, M.D., Martínez-Máñez, R., Barat, J.M., 2018. Improving the Antimicrobial Power of Low-Effective Antimicrobial Molecules Through Nanotechnology. J. Food Sci. 83, 2140–2147. https://doi.org/10.1111/1750-3841.14211

Rusell, W.M.S., Burch, R.L., 1959. The principles of humane experimental technique. Methuen.

Ruszkiewicz, J.A., Pinkas, A., Miah, M.R., Weitz, R.L., Lawes, M.J.A., Akinyemi, A.J., Ijomone, O.M., Aschner, M., 2018. C. elegans as a model in developmental neurotoxicology. Toxicol. Appl. Pharmacol. 354, 126–135. https://doi.org/10.1016/j.taap.2018.03.016

Sakamuru, S., Attene-Ramos, M.S., Xia, M., 2016. Mitochondrial membrane potential assay. Methods Mol. Biol. 1473, 17–22. https://doi.org/10.1007/978-1-4939-6346-1_2

Salehi, B., Mishra, A.P., Shukla, I., Sharifi-Rad, M., Contreras, M. del M., Segura-Carretero, A., Fathi, H., Nasrabadi, N.N., Kobarfard, F., Sharifi-Rad, J., 2018. Thymol, thyme, and other plant sources: Health and potential uses. Phyther. Res. 32, 1688–1706. https://doi.org/10.1002/ptr.6109

Santos, H.A., Riikonen, J., Salonen, J., Mäkilä, E., Heikkilä, T., Laaksonen, T., Peltonen, L., Lehto, V.-P., Hirvonen, J., 2010. In vitro cytotoxicity of porous silicon microparticles: Effect of the particle concentration, surface chemistry and size. Acta Biomater. 6, 2721–2731. https://doi.org/10.1016/J.ACTBIO.2009.12.043

Severin, I., Souton, E., Dahbi, L., Chagnon, M.C., 2017. Use of bioassays to assess hazard of food contact material extracts: State of the art. Food Chem. Toxicol. 105, 429–447. https://doi.org/10.1016/J.FCT.2017.04.046

Sharifi-Rad, M., Varoni, E.M., Iriti, M., Martorell, M., Setzer, W.N., del Mar Contreras, M., Salehi, B., Soltani-Nejad, A., Rajabi, S., Tajbakhsh, M., Sharifi-Rad, J., 2018. Carvacrol and human health: A comprehensive review. Phyther. Res. https://doi.org/10.1002/ptr.6103

Shi, J., Hua, Z., Zhang, L., 2004. Nanocomposites from ordered mesoporous materials. J. Mater. Chem. 14, 795. https://doi.org/10.1039/b315861f

SIDS, O., 2004. Synthetic amorphous silica and silicates.

Sisakhtnezhad, S., Heidari, M., Bidmeshkipour, A., 2018. Eugenol enhances

proliferation and migration of mouse bone marrow-derived mesenchymal stem cells in vitro. Environ. Toxicol. Pharmacol. 57, 166–174. https://doi.org/10.1016/j.etap.2017.12.012

Slamenová, D., Horváthová, E., Sramková, M., Marsálková, L., 2007. DNA-protective effects of two components of essential plant oils carvacrol and thymol on mammalian cells cultured in vitro. Neoplasma 54, 108–12.

Solaini, G., Sgarbi, G., Lenaz, G., Baracca, A., 2007. Evaluating Mitochondrial Membrane Potential in Cells. Biosci. Rep. 27, 11–21. https://doi.org/10.1007/S10540-007-9033-4

Stark, D.M., Shopsis, C., Borenfreund, E., Babich, H., 1986. Progress and problems in evaluating and validating alternative assays in toxicology. Food Chem. Toxicol. 24, 449–455. https://doi.org/10.1016/0278-6915(86)90091-8

Stebounova, L. V., Guio, E., Grassian, V.H., 2011. Silver nanoparticles in simulated biological media: a study of aggregation, sedimentation, and dissolution. J. Nanoparticle Res. 13, 233–244. https://doi.org/10.1007/s11051-010-0022-3

Stephens, M.L., Mak, N.S., 2013. History of the 3Rs in Toxicity Testing: From Russell and Burch to 21st Century, in: Reducing, Refining and Replacing the Use of Animals in Toxicity Testing. 19, 1. https://doi.org/10.1039/9781849737920-00001

Stiernagle, T., 2006. Maintenance of C. elegans. WormBook, 2, 51-67. https://doi.org/10.1895/wormbook.1.101.1

Stopford, W., Turner, J., Cappellini, D., Brock, T., 2003. Bioaccessibility testing of cobalt compounds. J. Environ. Monit. 5, 675–680. https://doi.org/10.1039/b302257a

Suntres, Z.E., Coccimiglio, J., Alipour, M., 2015. The Bioactivity and Toxicological Actions of Carvacrol. Crit. Rev. Food Sci. Nutr. 55, 304–318. https://doi.org/10.1080/10408398.2011.653458

Tang, B., Tong, P., Xue, K.S., Williams, P.L., Wang, J.S., Tang, L., 2019. High-

throughput assessment of toxic effects of metal mixtures of cadmium(Cd), lead(Pb), and manganese(Mn) in nematode Caenorhabditis elegans. Chemosphere 234, 232–241. https://doi.org/10.1016/j.chemosphere.2019.05.271

Tejeda-Benitez, L., Olivero-Verbel, J., 2016. Caenorhabditis elegans, a biological model for research in toxicology, in: Reviews of Environmental Contamination and Toxicology. Springer New York LLC, 237, 1-35. https://doi.org/10.1007/978-3-319-23573-8_1

The C. elegans Sequencing Consortium, 1998. Genome sequence of the nematode C. elegans: A platform for investigating biology. Science, 282(5396), 2012-2018. https://doi.org/10.1126/science.282.5396.2012

Thermo Fisher Scientific, 2019. CyQUANT™ LDH Cytotoxicity Assay Kit Product Information Sheet [WWW Document]. MAN0018500. URL https://www.thermofisher.com/document-connect/document-connect.html?url=https%3A%2F%2Fassets.thermofisher.com%2FTFS-Assets%2FLSG%2Fmanuals%2FMAN0018500_CyQUANT-LDH-Cytotoxicity-Assay-Kit_PI.pdf&title=UHJvZHVjdCBTaGVldDogQ3lRVUFOVCBMREggQ3l0b3RveGljaXR5IEF (accessed 8.11.21).

Tippayatum, P., Chonhenchob, V., 2007. Antibacterial activities of thymol, eugenol and nisin against some food spoilage bacteria. Nat. Sci. 41, 319–23.

Trewyn, B.G., Slowing, I.I., Giri, S., Chen, H.-T., Lin, S.-Y., 2007. Synthesis and Functionalization of a Mesoporous Silica Nanoparticle Based on the Sol-Gel Process and Applications in Controlled Release. https://doi.org/10.1021/ar600032u

Ultee, A., Kets, E.P.W., Smid, E.J., 1999. Mechanisms of action of carvacrol on the food-borne pathogen. Appl. Environ. Microbiol. 65, 4606–4610. https://doi.org/10.1128/aem.65.10.4606-4610.1999

Ultee, A., Smid, E.J., 2001. Influence of carvacrol on growth and toxin production

by Bacillus cereus. Int. J. Food Microbiol. 64, 373–378. https://doi.org/10.1016/S0168-1605(00)00480-3

Ündeğer, Ü., Başaran, A., Degen, G.H., Başaran, N., 2009. Antioxidant activities of major thyme ingredients and lack of (oxidative) DNA damage in V79 Chinese hamster lung fibroblast cells at low levels of carvacrol and thymol. Food Chem. Toxicol. 47, 2037–2043. https://doi.org/10.1016/j.fct.2009.05.020

United Nations, 2019. Globally Harmonized System of Classification and Labelling of Chemicals, United Nations, New York and Geneva. https://doi.org/10.14927/reeps.10.2_60

USDA, 2010. Silicon Dioxide Handling/Processing.

Utembe, W., Potgieter, K., Stefaniak, A.B., Gulumian, M., 2015. Dissolution and biodurability: Important parameters needed for risk assessment of nanomaterials. Part. Fibre Toxicol. 12, 11. https://doi.org/10.1186/s12989-015-0088-2

Wang, C., Youle, R.J., 2009. The Role of Mitochondria in Apoptosis. Annu. Rev. Genet. 43, 95. https://doi.org/10.1146/ANNUREV-GENET-102108-134850

WHO, 2009. Principles and methods for the risk assessment of chemicals in food, World Health Organization. Environmental Health Criteria, 240.

Wittkowski, P., Marx-Stoelting, P., Violet, N., Fetz, V., Schwarz, F., Oelgeschläger, M., Schönfelder, G., Vogl, S., 2019. Caenorhabditis elegans As a Promising Alternative Model for Environmental Chemical Mixture Effect Assessment - A Comparative Study. Environ. Sci. Technol. 53, 12725–12733. https://doi.org/10.1021/acs.est.9b03266

Wu, T., Xu, H., Liang, X., Tang, M., 2019. Caenorhabditis elegans as a complete model organism for biosafety assessments of nanoparticles. Chemosphere 221, 708–726. https://doi.org/10.1016/j.chemosphere.2019.01.021

Wright, S. E., Baron, D. A., Heffner, J. E., 1995. Intravenous eugenol causes hemorrhagic lung edema in rats: proposed oxidant mechanisms. The Journal of laboratory and clinical medicine, 125(2), 257-264.

Xiong, H., Pears, C., Woollard, A., 2017. An enhanced C. elegans based platform for toxicity assessment. Sci. Rep. 7, 1–11. https://doi.org/10.1038/s41598-017-10454-3

Xu, J., Zhou, F., Ji, B.P., Pei, R.S., Xu, N., 2008. The antibacterial mechanism of carvacrol and thymol against Escherichia coli. Lett. Appl. Microbiol. 47, 174–179. https://doi.org/10.1111/j.1472-765X.2008.02407.x

Yanishlieva, N. V, Marinova, E.M., Gordon, M.H., Raneva, V.G., 1999. Antioxidant activity and mechanism of action of thymol and carvacrol in two lipid systems. Food Chem. 64, 59–66. https://doi.org/10.1016/S0308-8146(98)00086-7

Yin, Q.H., Yan, F.X., Zu, X.Y., Wu, Y.H., Wu, X.P., Liao, M.C., Deng, S.W., Yin, L.L., Zhuang, Y.Z., 2012. Anti-proliferative and pro-apoptotic effect of carvacrol on human hepatocellular carcinoma cell line HepG-2. Cytotechnology 64, 43–51. https://doi.org/10.1007/s10616-011-9389-y

Yoshida, T., Yoshioka, Y., Matsuyama, K., Nakazato, Y., Tochigi, S., Hirai, T., Kondoh, S., Nagano, K., Abe, Y., Kamada, H., Tsunoda, S., Nabeshi, H., Yoshikawa, T., Tsutsumi, Y., 2012. Surface modification of amorphous nanosilica particles suppresses nanosilica-induced cytotoxicity, ROS generation, and DNA damage in various mammalian cells. Biochem. Biophys. Res. Commun. 427, 748–752. https://doi.org/10.1016/J.BBRC.2012.09.132

Younes, M., Aggett, P., Aguilar, F., Crebelli, R., Dusemund, B., Filipič, M., Frutos, M.J., Galtier, P., Gott, D., Gundert-Remy, U., Kuhnle, G.G., Leblanc, J., Lillegaard, I.T., Moldeus, P., Mortensen, A., Oskarsson, A., Stankovic, I., Waalkens-Berendsen, I., Woutersen, R.A., Wright, M., Boon, P., Chrysafidis, D., Gürtler, R., Mosesso, P., Parent-Massin, D., Tobback, P., Kovalkovicova, N., Rincon, A.M., Tard, A., Lambré, C., Lambré, C., 2018. Re-evaluation of silicon dioxide (E 551) as a food additive. EFSA J. 16. https://doi.org/10.2903/j.efsa.2018.5088

Yun, J.-W., Kim, S.-H., You, J.-R., Kim, W.H., Jang, J.-J., Min, S.-K., Kim, H.C., Chung, D.H., Jeong, J., Kang, B.-C., Che, J.-H., 2015. Comparative toxicity of

silicon dioxide, silver and iron oxide nanoparticles after repeated oral administration to rats. J. Appl. Toxicol. 35, 681–693. https://doi.org/10.1002/jat.3125

Zhang, Y., 2018. Cell toxicity mechanism and biomarker. Clin. Transl. Med. 7, 34. https://doi.org/10.1186/s40169-018-0212-7

Zorova, L.D., Popkov, V.A., Plotnikov, E.Y., Silachev, D.N., Pevzner, I.B., Jankauskas, S.S., Babenko, V.A., Zorov, S.D., Balakireva, A. V., Juhaszova, M., Sollott, S.J., Zorov, D.B., 2018. Mitochondrial membrane potential. Anal. Biochem. 552, 50–59. https://doi.org/10.1016/j.ab.2017.07.009